

THE BIOLOGICAL EFFECTS OF COMMONLY USED  
EXCIPIENTS

JOHN POLLARD

Doctor of Philosophy

ASTON UNIVERSITY

August 2016

©John Pollard, 2016

John Pollard asserts his moral right to be identified as the author of this thesis

The copy of this thesis has been supplied on condition that anyone who consults it is understood to recognise that its copyright rests with its author and that no quotation from the thesis and no information derived from it may be published without appropriate permission of acknowledgement.

Aston University

## THE BIOLOGICAL EFFECTS OF COMMONLY USED EXCIPIENTS

John Pollard

Doctor of Philosophy

August 2016

### Thesis Summary

Efflux transporters such as ABCB1 (P-gp) and ABCC2 (MRP-2) expressed on the apical membranes of epithelial cells of the intestine represent a formidable barrier for the effective delivery of a plethora of pharmaceutically relevant compounds. Excipients have attracted significant interest in their role as efflux protein inhibitors. To this end, the aim of this study was to examine the biological effects of commonly used excipients, and utilise this information in the design and manufacture of orally disintegrating tablets (ODT) using a design of experiments (DoE) approach.

The 'gold standard' model of assessing intestinal efflux modulation remains the Caco-2 Transwell® model. As this method is time and resource consuming, a novel high-throughput screening assay was developed to screen excipients for activity against the ABCB1 and ABCC2 transporters using the specific fluorescent probes rhodamine 123 (R-123) and 5(6)-carboxy-2',7'-dichlorofluorescein (CDF) respectively. Of all the excipients screened, surfactants showed the highest efficacy against ABCB1 with some materials showing lower IC<sub>50</sub> values than the established inhibitors verapamil (VER) and ciclosporin (CsA).

One of the lead candidate excipients, poloxamer 407, was incorporated into a high-dose (795 mg) and a low-dose (295 mg) paracetamol (acetaminophen, APAP) formulation at 2 % (w/w). Whilst the development of the high-dose tablets was terminated with a disintegration time of 37 s, conforming to *European Pharmacopeia* specifications, the low-dose tablets were selected for manufacture using a rotary tablet press. These final formulations had disintegration times of 9-43 s over a range of compressions (6-23 kN), providing tablets that conform to both the *European Pharmacopeia* and *United States Pharmacopeia*. Taken with a 250 mL glass of water, these tablets are capable of delivering 5.9 mg of poloxamer 407 to give a final concentration of  $2.36 \times 10^{-3}$  % (w/v), 2.7 times higher than the determined IC<sub>50</sub> value for this excipient. To investigate an additional method of incorporating surfactants into ODTs, granules containing ibuprofen were coated in a Kollicoat IR solution containing 2 % (w/v) PEG 2000, poloxamer 407 or Cremophor EL. The ODTs made from these granules by direct compression produced tablets with disintegration times below 30 seconds, showing the viability of this complementary method of propagating the surfactant content of oral dosage formulations.

Key words: Oral drug delivery, excipients, efflux transporters, kinetics, orally disintegrating tablets

### **Acknowledgements**

I would like to express my deepest appreciation to my supervisor, Professor Yvonne Perrie for her exemplary support and guidance during this project. I would also like to extend my gratitude to my associate supervisor, Professor Afzal Mohammed, for all his help and advice during both promising and more testing times. I further thank Dr Raj Badhan for his continued assistance with the pharmacokinetics. In addition, thanks must go to Mr Muhammad Kabeer Arshad for his contributions.

I would like to also thank Dr Ali Rajabi-Siahboomi, Dr Shahrzad Missaghi, Dr Manish Ghimire of Colorcon, in addition all the members of Colorcon with whom I was fortunate enough to work with.

Many thanks are moreover owed to The Biotechnology and Biological Sciences Research Council (BBSRC) for their financial support.

Last but not least I thank my friends and family for their ongoing support, in addition to my parents and foremost to my grandmother, Pamela Pollard, to whom this thesis is dedicated.

### Accepted Conference Abstracts

Abstracts awarded podium presentations are marked with an asterisk.

\* Pollard, J, Badhan, R, Siaboomi, A R, Mohammed, A, Perrie, Y (2016). Development of an Orally Disintegrating Tablet Formulation Incorporating Biologically Active Excipient. UKPharmSci, University of Strathclyde, UK.

Pollard, J, Badhan, R, Siaboomi, A R, Mohammed, A, Perrie, Y (2016). The Development of Orally Disintegrating Tablets Incorporating Biologically Active Excipients. Controlled Release Society 43<sup>rd</sup> Annual Meeting, Seattle, WA, USA.

\* Pollard, J, Badhan, R, Siaboomi, A R, Mohammed, A, Perrie, Y (2016). Utilisation of an *In Vitro* High-throughput Screening Assay in the Development of Orally Disintegrating Tablets with Enhanced Delivery Capability. UK and Ireland Controlled Release Society Annual Symposium, University of Cardiff, UK.

\* Pollard, J, Badhan, R, Siaboomi, A R, Mohammed, A, Perrie, Y (2015). High-throughput Screening of Excipients with a Biological Effect: A Kinetic Study on the Effects of Surfactants on Efflux Transporters. UKPharmSci, University of Nottingham, UK.

Pollard, J, Badhan, R, Siaboomi, A R, Mohammed, A, Perrie, Y (2015). The Role of Polyethylene Glycols on the Modulation of the Anionic ABCC2 Transporter. Controlled Release Society 42<sup>nd</sup> Annual Meeting and Exposition, Edinburgh, UK.

Pollard, J, Badhan, R, Siaboomi, A R, Mohammed, A, Perrie, Y (2015). The Inclusion of Biologically Active Excipients in Orally Disintegrating Tablets for Targeting of ABCB1 and ABCC2 Efflux Transporter Systems. UK and Ireland Controlled Release Society Workshop and Symposium, University of Nottingham, UK.

Pollard, J, Badhan, R, Siaboomi, A R, Mohammed, A, Perrie, Y (2014). A Rapid, High-throughput Method for the Screening of Commonly Used Excipients with a Biological Effect. Innovation in Encapsulation, Royal Society of Chemistry, London, UK.

Pollard, J, Badhan, R, Siaboomi, A R, Mohammed, A, Perrie, Y (2014). The Development of a High-throughput Screening Protocol for Efflux Inhibitors Amongst Commonly Used

Excipients. 1<sup>st</sup> International Congress: From Drug Discovery to Drug Delivery, Athens, Greece.

Pollard, J, Badhan, R, Siaboomi, A R, Mohammed, A, Perrie, Y (2014). The Characterisation of ODTs: Exploiting Pharmaceutical Excipients with Biological Effects. UKPharmSci, University of Hertfordshire, UK.

Pollard, J, Siaboomi, A R, Mohammed, A, Perrie, Y. (2014) Orally disintegrating Tablets: Enhancing Drug Permeation Through Formulation, UK and Ireland Controlled Release Society Annual Symposium. University College, Cork, Ireland.

Pollard, J, Siaboomi, A R, Mohammed, A, Perrie, Y (2013). The biological effects of high molecular weight PEGylated excipients commonly used in pharmaceutical formulations, UKPharmSci, Edinburgh, UK

Pollard, J, Siaboomi, A R, Mohammed, A, Perrie, Y (2013). Investigating the impact of polymer blends on drug release from polymer matrices, UKICRS Annual Symposium. University of Reading UK.

## *Table of Contents*

<b>Thesis Summary</b> .....	<b>2</b>
<b>Acknowledgements</b> .....	<b>3</b>
<b>Accepted Conference Abstracts</b> .....	<b>4</b>
<b>Table of Figures</b> .....	<b>14</b>
<b>Table of Tables</b> .....	<b>27</b>
<b>Abbreviations</b> .....	<b>30</b>
<b>1. Introduction</b> .....	<b>36</b>
1.1. The Advantages and Disadvantages of the Oral Route of Drug Administration ..	36
1.2. Drug Dissolution and the Gastrointestinal Tract .....	37
1.3. Intestinal Absorption and Transporters .....	39
1.4. The ABC Transporter Systems .....	40
1.4.1. P-glycoprotein (P-gp, ABCB1) .....	41
1.4.2. Multidrug Resistance Associated Protein family (MRP, ABCC) .....	42
1.4.3. Breast Cancer Resistance Protein (BCRP, ABCG2) .....	43
1.5. ABC-Transporter-Substrate Recognition.....	44
1.6. Commonly Utilised Models of Intestinal Absorption .....	47
1.6.1. <i>In Vivo</i> Models of the Gastrointestinal Tract.....	47
1.6.2. <i>In Vitro</i> Models of the Gastrointestinal Tract .....	50
1.6.2.1. Ussing Chamber .....	50
1.6.2.2. Everted Gut Sac.....	51
1.6.2.3. Cell Based Models.....	52
1.7. Excipient-Efflux Transporter Interactions .....	54
1.7.1. The Biological Effects of Excipients on P-gp Activity.....	55
1.7.1.1. PEGs and PEGylated Surfactants .....	55

1.7.1.2.	Natural Polymers.....	59
1.7.1.3.	Cyclodextrins.....	60
1.7.1.4.	Lipid Excipients.....	60
1.7.1.5.	Thiomers.....	60
1.7.2.	The Biological Effect of Excipients on MRP2 Activity.....	60
1.7.3.	The Biological Effects of Excipients on BCRP Activity.....	61
1.8.	Model Substrate Drugs and Fluorescent Probe Substrates.....	62
1.8.1.	Rhodamine 123 and 5 (6)-Carboxy-2',7'-dichlorofluorescein.....	62
1.8.2.	Inhibitors of P-gp Efflux.....	64
1.8.3.	Inhibitors of MRP Efflux.....	65
1.8.4.	Paracetamol.....	66
1.8.5.	Ibuprofen.....	67
1.9.	Orally Disintegrating Tablets.....	67
1.9.1.	Overview.....	67
1.9.2.	Formulation Strategies for Making ODTs.....	68
1.9.2.1.	Freeze drying.....	68
1.9.2.2.	Moulding.....	69
1.9.2.3.	Compression.....	69
1.9.3.	Role of Disintegrants in Directly Compressed ODT Systems.....	70
1.9.4.	Taste Masking.....	71
1.9.5.	Assessment of ODT Physical Characteristics.....	72
1.10.	Thesis Aim and Objectives.....	75
<b>2.</b>	<b>Materials and Methods.....</b>	<b>78</b>
2.1.	Materials.....	78
2.2.	<i>In Vitro</i> Methods for the Detection of Efflux Inhibition.....	79
2.2.1.	Initial Screening Protocol: The <i>In Vitro</i> Caco-2 Transwell® Model.....	79

2.2.1.1.	Stock Solutions .....	79
2.2.1.2.	General Cell Protocol.....	79
2.2.1.3.	Transwell® Protocol for Differentiated Caco-2 Monolayers .....	79
2.2.1.4.	Indometacin Permeability through Caco-2 Monolayers .....	80
2.2.1.5.	Apical to Basolateral Concentration-Dependent Transport of Indometacin .....	80
2.2.1.6.	Basolateral to Apical Transport of Indometacin.....	81
2.2.1.7.	Permeability of Indometacin in the Presence of the PEGylated Excipients PEG 400, PEG 8000, POLYOX™ N-10 and Poloxamer 407 .....	81
2.2.1.8.	Lucifer Yellow Transport for the Monitoring of Monolayer Integrity .....	81
2.2.1.9.	High Performance Liquid Chromatography (HPLC) Analysis of Indometacin .....	82
2.3.	High-throughput Protocol for the Detection of Materials with a Biological Effect: Development and Validation .....	82
2.3.1.	Stock Solutions .....	84
2.3.2.	General Cell Protocol.....	85
2.3.3.	Fluorescence Microscopy.....	85
2.3.4.	Cytotoxicity Measurements using the MTT Assay .....	85
2.3.5.	Cellular Accumulation of Tracer Dyes .....	85
2.3.6.	Calculation of Kinetic Parameters .....	86
2.4.	The Design, Manufacture and Production of ODTs Incorporating Biologically-Active Excipients.....	86
2.4.1.	Design of Experiments .....	87
2.4.2.	Tablet Fabrication – Single Press .....	87
2.4.3.	Tablet Fabrication – Rotary Press .....	87
2.4.4.	Physical Characterisation.....	88

2.4.4.1. Hardness .....	88
2.4.4.2. Disintegration Times .....	88
2.4.4.3. Friability .....	88
2.4.4.4. Physical Parameters.....	88
2.5. Investigation into the Incorporation of Biologically-Active Surfactants into Granule Coatings for the use in Directly Compressed ODTs.....	89
2.5.1. Preparation of Ibuprofen Granules via Wet Granulation .....	89
2.5.2. Preparation of Kollicoat IR Coating Solutions Containing Biologically-Active Excipients.....	89
2.5.3. Preparation of ODTs from Surfactant-Coated Granules.....	90
2.5.4. Powder Characteristics Testing .....	90
2.5.4.1. Bulk and Tapped Density of the Granules.....	90
2.5.4.2. Angle of Repose .....	91
2.5.5. Physical Properties of ODTs Made from Surfactant-Coated Granules.....	91
2.5.6. Statistical Analysis.....	92
<b>3. The Development and Validation of a High-Throughput Screening Assay for the Detection of Excipients with Efflux Modulation Characteristics .....</b>	<b>94</b>
3.1. Chapter Aim and Objectives .....	94
3.2. The <i>In Vitro</i> Transwell® Model.....	94
3.2.1. Examination of Test Solution Concentrations: Drug and Excipient.....	94
3.2.2. Results of <i>In Vitro</i> Screening Using the Transwell® Model.....	96
3.2.2.1. The Impact of Indometacin on Tight junction Integrity.....	96
3.2.2.2. Indometacin Concentration-Dependent Transport.....	98
3.2.2.3. Indometacin Permeability Across Caco-2 Monolayers in the Presence of PEG 400	101

3.2.2.4. Indometacin Permeability Across Caco-2 Monolayers in the Presence of PEG 8000.....	102
3.2.2.5. Indometacin Permeability Across Caco-2 Monolayers in the Presence of POLYOX.....	103
3.2.2.6. Indometacin Permeability Across Caco-2 Monolayers in the Presence of Poloxamer 407.....	105
3.2.2.7. Confirming the Increase in Indometacin Transport as Efflux Inhibition.	107
3.2.2.8. Membrane Integrity Studies: Lucifer Yellow Transport .....	108
3.3. Introduction to High-Throughput Screening .....	109
3.3.1. Evaluation of Rhodamine Concentration Range.....	109
3.3.2. Inhibition of ABCB1-Mediated Efflux.....	111
3.3.3. Method Optimisation .....	113
3.3.3.1. Effects of Growth Time on the Cellular Accumulation of R-123.....	113
3.3.3.2. Effects of Incubation Time on the Cellular Accumulation of R-123 .....	115
3.3.3.3. The Effects of Media Composition on the Cellular Viability.....	116
3.3.3.4. Effects of Media Composition on the Cellular Accumulation of R-123 ...	118
3.3.4. The Validation of the HTS Method by Evaluating the Impact of Tween 20 and Tween 80 on Caco-2 Monolayers .....	122
3.3.4.1. Cytotoxicity.....	122
3.3.4.2. The Biological Effects of Tween 20 and Tween 80 on ABCB1 Activity ....	123
3.3.5. Testing the Biological Effects of MCC, HPMC, Starch 1500 and PVAP on ABCB1-Mediated Transport .....	126
3.3.6. Conclusions of <i>In Vitro</i> Method Development and Model Selection .....	130
<b>4. A Kinetic Study on the Effects of Excipients against ABCB1- and ABCC2-Mediated Transport .....</b>	<b>134</b>
4.1. Chapter Aim and Objectives .....	134

4.2. An Examination of Inhibitors of the ABCB1 and ABCC2 Efflux Transporter Systems .....	135
4.3. An Examination of the Effects of Low Viscosity HPMCs on ABCB1- and ABCC2- Mediated Transport.....	139
4.3.1. The Effects of Low Viscosity HPMCs on Cellular Viability .....	140
4.3.2. The Effects of Low Viscosity HPMCs on ABCB1- and ABCC2-Mediated Transport .....	141
4.4. An Examination of the Effects of Polyethylene Glycols Against ABCB1- and ABCC2-Mediated Transport.....	144
4.4.1. The Effects of PEGs on Cellular Viability .....	144
4.4.2. The Effects of PEGs on ABCB1- and ABCC2-Mediated Transport.....	147
4.5. An Examination of the Effects of Poloxamers and Tweens on ABCB1- and ABCC2-Mediated Transport.....	151
4.5.1. The Effects of Poloxamers and Tweens on Cellular Viability .....	152
4.5.2. The Effects of Poloxamers and Tweens on ABCB1- and ABCC2-Mediated Transport .....	155
4.5.3. The Effects of Poloxamers and Tweens on Caco-2 Membrane Integrity .....	158
4.5.4. The Effects of Poloxamers and Tweens on Micelle Encapsulation of the Tracer Dye R-123 .....	161
4.6. An Examination of the Effects of Surfactants on ABCB1- and ABCC2-Mediated Transport .....	164
4.6.1. Effects of Surfactants on Cellular Viability .....	165
4.6.2. Effects of the Surfactants on ABCB1- and ABCC2-Mediated Efflux .....	166
4.6.3. The Effects of Surfactant Structure on Inhibition of ABCB1-Mediated Efflux.....	171
4.6.4. Conclusions of <i>In Vitro</i> Kinetic Screening using the HTS Method .....	173
<b>5. The Design and Manufacture of Orally Disintegrating Tablets with Enhanced Delivery Capability .....</b>	<b>176</b>

5.1. Chapter Aim and Objectives .....	176
5.2. Tablet Design Overview .....	176
5.3. Design of Experiments: Screening Round 1 .....	178
5.3.1. Tablet Description.....	179
5.3.2. Physical Characterisation.....	179
5.3.3. Design of Experiments Interpretation of Excipient Composition.....	183
5.4. Formulation Refinement.....	186
5.4.1. Effects of Poloxamer 407 Content on Hardness and Disintegration .....	186
5.4.2. Effects of Kollidon® Crospovidone Type on Hardness and Disintegration...190	
5.4.3. Effects of Kollidon® Crospovidone Concentration on Hardness and Disintegration .....	193
5.4.4. Effects of Ethylcellulose Concentration on Hardness and Disintegration.....	195
5.4.5. Effects of Binder Type and Further Optimisation.....	198
5.5. Design of Experiments: Screening Round 2.....	201
5.5.1. Physical Characterisation.....	201
5.5.2. Design of Experiments Interpretation of Data.....	205
5.6. Scale-up Manufacture using the Rotary Tablet Press .....	208
5.6.1. Physical Characterisation.....	209
5.6.2. Weight Variation.....	214
5.7. Evaluation of Over the Counter Orally Disintegrating Tablets .....	214
5.8. Conclusions of Tablet Design and Manufacture .....	217
<b>6. An Investigation into the Incorporation of Biologically-Active Surfactants into Ibuprofen Granule Coatings for the use in Directly Compressed .....</b>	<b>219</b>
6.1. Introduction.....	219
6.2. Evaluation of Flow Properties of Surfactant-Coated Granules.....	221
6.3. Evaluation ODTs Produced using of Surfactant-Coated Granules .....	224

6.4. Uniformity of Content.....226

6.5. Conclusion of the Investigation into Surfactant –Coated ODTs .....226

**7. Overall Conclusions.....228**

**8. References .....235**

**Appendix – MTT Toxicology Data .....259**

**Table of Figures**

- Figure 1.1. Graphical representation of the bioavailability equation. A compound undergoes liberation from its dosage form, and must survive the transition past the intestinal epithelia. The absorbed fraction,  $f_a$ , gets gradually diminished by the action of metabolism within the cell,  $f_g$ , and subsequent hepatic degradation,  $f_h$ , before systemic circulation is reached. ....38
- Figure 1.2. Intestinal absorption pathways, showing (A) paracellular, (B) transcellular passive/transporter mediated, (C) transporter mediated transcytosis, and (D) transporter mediated efflux.....40
- Figure 1.3. The crystal structure of murine P-gp. The protein consists of two bundles of six transmembrane helices. The inward facing formation results in a large internal cavity open to the cytoplasm and inner leaflet. The presumed drug binding pocket consists largely of hydrophobic and aromatic residues. The N and C terminal of the protein is coloured yellow and red respectively. NBD = nucleotide binding domain. Lipid bilayer location is shown in approximation (Protein Data Bank file 3G5U). Diagram adapted from (Aller et al., 2009). ....42
- Figure 1.4. The two-step model of substrate transport of P-gp. (A) The substrate (maroon) partitions into the bilayer into the inner leaflet. Here, it is able to enter the intramembranous substrate binding pocket. (B) ATP (yellow) interaction with the nucleotide-binding domain (NBD) causes a conformational change of the protein, exposing the substrate to the extracellular space (Protein Data Bank file 3G5U). Diagram adapted from (Aller et al., 2009). ....46
- Figure 1.5. Experimental set up of the *in situ* technique. Freshly excised intestine of the anaesthetised rat is exposed and the test compound is introduced via the syringe at a controlled rate. Samples are then collected at the desired point further down the tract to determine the degree of compound uptake. This can either be the whole intestinal tract (Doluisio model) or a 10 cm section (single pass intestinal perfusion (SPIP) model) (Barthe et al., 1999). ....49
- Figure 1.6. Intestinal perfusion technique in man. Once the balloons are inflated, the sectioned-off area of the intestine serves as a model barrier. The closed section is then rinsed in drug-free buffer, and then the drug solution added. Intestinal integrity is

measured simultaneously using the retention of a non-absorbed marker compound such as PEG 4000 (Barthe et al., 1999). .....	50
Figure 1.7. The Ussing chamber. Two transport buffers are separated by the intestinal membrane clamped in place. The electrical resistance of the membrane is constantly monitored in order to ensure membrane integrity. The test compound can then be introduced to one compartment and its ingress monitored to the other compartment (Barthe et al., 1999). .....	51
Figure 1.8. Everted gut sac model. Freshly excised gut sac is inverted over a glass rod and tied at both ends after introducing the test compound. The transport process can then be monitored by the appearance of the compound to the incubation medium (Barthe et al., 1999). .....	52
Figure 1.9. Experimental setup of Caco-2 Transwell® model. Cells are grown for 21 days to allow full differentiation. For apical to basolateral (AP to BL) transport studies, functionally analogous to mucosal to serosal transport, cells are washed in buffer and the drug-containing buffer added to the apical compartment and drug-free buffer to the basolateral compartment. Samples are then taken from the basolateral compartment at fixed intervals. For basolateral to apical (BL to AP) transport, the drug-containing solution is added to the basolateral compartment and samples taken from the apical compartment. ....	53
Figure 1.10. The chemical structures of A) rhodamine 123, B) 5(6)-carboxy-2',7'-dichlorofluorescein and C), the 5(6)-carboxy-2',7'-dichlorofluorescein premoiety 5(6)-carboxy-2',7'-dichlorofluorescein diacetate. ....	62
Figure 1.11. Schematic diagram of the uptake of the fluorescent probe substrates. The relative contribution of BCRP and MRP1 in the transport of R-123 is assumed negligible on the Caco-2 cell line. However, the influx transporter OATP cannot be excluded in the ingress of R-123 and CDF. ....	63
Figure 1.12. The chemical structure of verapamil hydrochloride, the most widely utilised form of the drug. ....	64
Figure 1.13. The chemical structure of ciclosporin. ....	65
Figure 1.14. The chemical structure of indometacin. ....	65
Figure 1.15. The chemical structure of probenecid. ....	66
Figure 1.16. The chemical structure of APAP. ....	66

Figure 1.17. The chemical structure of ibuprofen. ....	67
Figure 1.18. Overview of the disintegration equipment. Tablets are added to the cylinder whilst the basket assembly is in motion in warmed disintegration media. The time taken for the tablet to pass through the mesh is then recorded as the disintegration time. Disks, as required, are placed on top of the tablet to aid disintegration but may interfere with tablets that are gel-forming in nature (USP, 2012b).....	73
Figure 1.19. Overview of Friability Equipment. Tablets are weighed, added to the equipment and rotated at 25 rpm for 4 minutes. The tablets are then removed, brushed clean and then reweighed. Percentage friability is then calculated (USP, 2013).....	74
Figure 2.1. Graphical representation of the fluorescent HTS screening model. Once the probe has achieved ingress into the cell, the only way for it to escape is by efflux. With increased concentrations of inhibitor, this is no longer possible and the cells most inhibited retain the highest concentration of dye. This is subsequently detected by a rise in fluorescent signal. ....	83
Figure 2.2. The volume of literature concerning the biological effects of commonly used excipients against P-gp and MRP2, using the keyword search 'excipient P-gp' or 'excipient MRP2'.....	84
Figure 2.3. Graphical representation of the conversion of CDFDA to CDF. CDFDA solution is colourless, but gets converted to a cascade of fluorescent compounds by the action of intracellular esterases, chiefly CDF. ....	84
Figure 3.1. The apical to basolateral transport of IND at varying concentrations through 21-day old Caco-2 monolayers. Data is presented as mean $\pm$ SD of triplicate values. Statistical significance was analysed using two-way ANOVA followed by Dunnett's <i>post hoc</i> test annotated as follows: **** ( $p < 0.0001$ ). ....	98
Figure 3.2. Bidirectional apparent permeability coefficient data for AP-BL (clear) and BL-AP transport (blue), conducted over a range of IND concentrations, showing A) 10 $\mu$ M, B) 25 $\mu$ M, C) 50 $\mu$ M and D) 100 $\mu$ M. Data presented as $\pm$ SD ( $n = 3$ ). BL-AP transport is broadly dominant to AP-BL, suggesting the latter is influenced by efflux transporters residing on the apical membrane.....	100
Figure 3.3. The permeability of IND in the presence of PEG 400, showing A) the percentage transport and B) apparent permeability ( $P_{app}$ ) for AP-BL transport of 50 $\mu$ M IND across 21-	

day old Caco-2 monolayers either alone or with 0.1-0.5 % (v/v) PEG 400 in the apical compartment. All results are shown in triplicate. Data is presented as  $\pm$  SD. Statistical significance was analysed using two-way ANOVA followed by Dunnett's *post hoc* test annotated as follows: \*\* ( $p < 0.01$ ). .....102

Figure 3.4. The permeability of IND in the presence of PEG 8000, showing A) the percentage transport and B) apparent permeability ( $P_{app}$ ) for AP-BL transport of 50  $\mu$ M IND across 21-day old Caco-2 monolayers either alone or with 0.369-1.19 mg mL<sup>-1</sup> PEG 8000 in the apical compartment. All results are shown in triplicate. Data is presented as  $\pm$  SD. Statistical significance was analysed using two-way ANOVA followed by Dunnett's *post hoc* test annotated as follows: \*\*\*\* ( $p < 0.0001$ ). .....103

Figure 3.5. The permeability of IND in the presence of POLYOX N-10, showing A) the percentage transport and B) apparent permeability ( $P_{app}$ ) for AP-BL transport of 50  $\mu$ M IND across 21-day old Caco-2 monolayers either alone or with 0.369- 1.19 mg mL<sup>-1</sup> POLYOX in the apical compartment. All results are shown in triplicate. Data is presented as  $\pm$  SD. Statistical significance was analysed using two-way ANOVA followed by Dunnett's *post hoc* test annotated as follows: \*\* ( $p < 0.01$ ); \*\*\*\* ( $p < 0.0001$ ). .....104

Figure 3.6. The permeability of IND in the presence of poloxamer 407 showing A) the percentage transport and B) apparent permeability ( $P_{app}$ ) for AP-BL transport of 50  $\mu$ M IND across 21-day old Caco-2 monolayers either alone or with 0.63-1.9 mg mL<sup>-1</sup> poloxamer 407 in the apical compartment. All results are shown in triplicate. Data is presented as  $\pm$  SD. Statistical significance was analysed using two-way ANOVA followed by Dunnett's *post hoc* test annotated as follows: \* ( $p < 0.01$ ); \*\*\*\* ( $p < 0.0001$ ). .....106

Figure 3.7. The basolateral to apical (BL-AP) transport of IND in the presence of PEG 8000 and POLYOX N-10, showing A) the percentage drug transported and B) the permeability coefficients. Error bars refer to standard deviation ( $n = 3$ ). No statistically significant difference was observed using two-way ANOVA between all time points tested in the presence of the excipients and the control, ns ( $p > 0.05$ ). .....108

Figure 3.8. The concentration-dependent uptake of R-123 over a 4-hour period on the Caco-2 cell line. Cellular accumulation of R-123 was linear over the concentration range and time points used. Cells were incubated in DMEM-HEPES (pH 7.4) with a R-123 concentration

between 1 and 250  $\mu\text{M}$  to obtain the time points indicated. Error bars are shown as  $\pm$  SD (data pooled from 10 wells). .....110

Figure 3.9. The effects of VER and IND on R-123 accumulation. Uptake of R-123 was increased in the presence of 1-100  $\mu\text{M}$  of the ABCB1 efflux protein inhibitor VER in a concentration-dependent manner after 4 hours incubation (A) but not in the presence of the MRP family inhibitor IND until a concentration of 100  $\mu\text{M}$  (B). Data is presented as  $\pm$  SD (data pooled from 10 wells), with R-123-only control normalised to 100 %. Statistical significance was analysed using one-way ANOVA followed by Dunnett's *post hoc* test annotated as follows: \* ( $p < 0.05$ ); \*\*\*\* ( $p < 0.0001$ ). .....112

Figure 3.10. The increase in the ABCB1 substrate accumulation was confirmed using fluorescence microscopy showing 10  $\mu\text{M}$  R-123 alone (A) and with 10  $\mu\text{M}$  or 100  $\mu\text{M}$  VER (B and C respectively), leading to a concentration-dependent blockade of the ABCB1 efflux mechanism shown schematically above each image. Images are representative of cells imaged under identical conditions using 40x magnification using Caco-2 monolayers grown for 7 days in 6-well plates. ....113

Figure 3.11. Visual indication of confluence seen under light microscopy observation. Complete confluence is observed on day 3 (A), with early dome formation observed on day 4 (B). By day 14 (C), numerous domes appear with well-defined established borders although monolayers appear less smooth. Images taken on 10x magnification. ....114

Figure 3.12. The effects of growth time on the uptake of R-123 in the presence of 100  $\mu\text{M}$  VER, tested on day 5 (clear bars) and day 7 (blue bars). The increase in R-123 accumulation remains consistent following the appearance of dome structures on the monolayers on around day 5 post-seeding following treatment with 100  $\mu\text{M}$  VER. Data is shown as the percentage increase from inhibitor-free control wells  $\pm$  SD (intraday data pooled from 3 plates,  $n = 30$  wells total). Statistical significance was analysed using one-way ANOVA followed by Tukey's *post hoc* test annotated as follows: ns ( $p > 0.05$ ). .....114

Figure 3.13. The effects of pre-incubation time of VER on the cellular accumulation of R-123. Full ABCB1 blockade is achieved in less than 10 minutes pre-incubation with 100  $\mu\text{M}$  VER. Data is shown as the percentage increase from inhibitor-free control after 60 minutes uptake  $\pm$  SD (data pooled from 3 plates,  $n = 30$  wells total). Statistical significance was

- analysed using one-way ANOVA followed by Dunnett's *post hoc* test annotated as follows: ns ( $p > 0.05$ ); \*\*\*\* ( $p < 0.0001$ ). .....116
- Figure 3.14. The effects of serum on the cellular viability of monolayers of Caco-2 cells. MTT cell viability assays measured the mitochondrial activity of the cells with serum (clear bars) and without (blue bars), over a 24 hour period. Data is shown standardised against serum-containing media as 100 %  $\pm$  SD (data pooled from 3 plates for a total of 30 wells). Statistical significance was analysed using two-way ANOVA followed by Dunnett's *post hoc* test annotated as follows: \*\* ( $p < 0.01$ ); \*\*\*\* ( $p < 0.001$ ). .....118
- Figure 3.15. The effects of media composition on R-123 accumulation. Cellular uptake of R-123 alone was found to be unaffected by the presence of serum in the media composition over a 4 hour period. In the presence of serum (clear bars), the relative increase in R-123 accumulation by the action of 100  $\mu$ M VER was reduced compared to serum-free media (blue bars). Data is shown as raw relative fluorescence units (RFU) for direct comparison of uptakes  $\pm$  SD (data pooled from 3 plates,  $n = 30$ ). Statistical significance was analysed using one-way ANOVA followed by Tukey's *post hoc* test annotated as follows: ns ( $p > 0.05$ ); \*\*\*\* ( $p < 0.001$ ). .....119
- Figure 3.16. The toxicological effects of the Tweens on Caco-2 monolayers. MTT assays were performed on Caco-2 monolayers incubated with varying concentrations of Tween 80 (A) and Tween 20 (B) for 4 hours. Data expressed as the mean of percentage cell viability relative to untreated controls  $\pm$  SD ( $n = 20$  from 2 passage numbers). Statistical significance was analysed using one-way ANOVA followed by Dunnett's *post hoc* test annotated as follows: \*\* ( $p < 0.01$ ); \*\*\*\* ( $p < 0.0001$ ). Triton-X was used as a positive control at 0.05 % (v/v). .....123
- Figure 3.17. The biological effects of the Tweens on ABCB1 activity, showing (A) Tween 80 and (B) Tween 20 after 4 hours of incubation in the presence of R-123. Data is shown as the percentage increase in cellular R-123 accumulation in the presence of the Tweens versus excipient-free control wells, presented as the mean from  $n = 10$  wells  $\pm$  SD. Statistical significance was analysed using two-way ANOVA followed by Dunnett's *post hoc* test annotated as follows: ns ( $p > 0.05$ ); \*\* ( $p < 0.01$ ); \*\*\* ( $p < 0.001$ ); \*\*\*\* ( $p < 0.0001$ ). .....125
- Figure 3.18. The percentage increase in cellular accumulation of R-123 in the presence of 100  $\mu$ M VER or the excipients of choice of 4 hours, showing A) PVAP, B) HPMC, C) MCC

and D) Starch 1500. Data is presented as  $\pm$  SD (data pooled from 8 wells), with R-123-only control normalised to 100 %. Statistical significance was analysed using one-way ANOVA followed by Dunnett's *post hoc* test annotated as follows: ns ( $p > 0.05$ ); \* ( $p < 0.05$ ); \*\*\* ( $p < 0.001$ ); \*\*\*\* ( $p < 0.0001$ ). .....129

Figure 3.19. Schematic diagram of HTS protocol. Cells are grown for 5-7 days, at which point MTT is conducted on the test excipient to determine the non-toxic concentrations used. Next, a separate 96-well plate is prepared for the uptake study by carefully washing out the well, incubating with the excipient(s) before the addition of the fluorescent probe. Cells are then incubated for 2 hours prior to careful washing, lysing, and fluorescence quantification using black 96 well plates. ....132

Figure 4.1. The IC<sub>50</sub> curves of inhibitors of efflux proteins, showing activity against A) ABCB1 and B) ABCC2. Caco-2 cells were grown for 5-7 days on 96-well plates prior to experimentation. Data presented as each of a minimum of 4 replicates from 2.5  $\mu$ M initial extracellular concentration of either R-123 or CDFDA as probes of ABCB1 and ABCC2 activity, respectively. ....137

Figure 4.2. The general structure of HPMCs, with the degree of substitution of methoxyl or hydroxypropyl ( $x$ ) specific to the grade. ....139

Figure 4.3. The effects of HPMCs on cellular viability using the MTT toxicology assay, showing A) METHOCEL E3, B) METHOCEL E6, C) METHOCEL E15 and D) METHOCEL K3. Caco-2 cells were grown for 5-7 days on 96-well plates prior to experimentation. Data presented as the mean value of 6 replicates  $\pm$  SD. Statistical significance was analysed using one-way ANOVA followed by Dunnett's *post hoc* test annotated as follows: \*\* ( $p < 0.01$ ); \*\*\*\* ( $p < 0.0001$ ). ....141

Figure 4.4. The effects of HPMCs on the uptake of the ABCB1 and ABCC2 specific probes R-123 and CDF (CDFDA) respectively, showing A) METHOCEL E3, B) METHOCEL E6, C) METHOCEL E15 and D) METHOCEL K3. Caco-2 cells were grown for 5-7 days on 96-well plates prior to experimentation. Data presented as each replicate from a minimum of four data values as a function of overall R-123 or CDF (CDFDA) uptake for ABCB1 and ABCC2 respectively with initial conditions of 2.5  $\mu$ M extracellular tracer dye per well, with excipient-free control wells set to 100 % transporter activity. ....143

- Figure 4.5. The general structure of a PEG monomer, where  $n$  is the average number of repeat units, with the name of the polymer based on its average molecular weight.....144
- Figure 4.6. The effects of PEGs on cellular viability using the MTT toxicology assay, showing A) PEG 400, B) PEG 4000, C) PEG 8000, D) PEG 12000, E) PEG 20000 and F) POLYOX N-10. Caco-2 cells were grown for 5-7 days on 96-well plates prior to experimentation. Data presented as the mean value of 6 replicates  $\pm$  SD. Statistical significance was analysed using one-way ANOVA followed by Dunnett's *post hoc* test annotated as follows: \*\* ( $p < 0.01$ ); \*\*\*\* ( $p < 0.0001$ ).....146
- Figure 4.7. The effects of PEGs on the uptake of the ABCB1 and ABCC2 specific probes R-123 and CDF (CDFDA) respectively, showing A) PEG 400, B) PEG 4000, C) PEG 8000, D) PEG 12000, E) PEG 20000 and F) POLYOX N-10. Caco-2 cells were grown for 5-7 days on 96-well plates prior to experimentation. Data presented as each replicate value from a minimum of triplicate data values.....150
- Figure 4.8. The general structures of A) Poloxamers and B) Tweens. Poloxamers consist of a hydrophobic poly(propylene oxide) (PPO) core ( $y$ ) flanked by poly(ethylene oxide) (PEO) chains ( $x$  and  $z$ ), the precise composition of which give rise to the HLB of the polymer. Tweens consist of ethoxylated sorbitan esterified with fatty acids. The Tween shown is Tween 20 with a lauric acid lipophilic group, whereas Tween 80 contains an oleic acid group.....152
- Figure 4.9. Typical (A) and atypical (B) MTT profiles presented after incubation with various concentrations of A) Poloxamer 188 and B) Poloxamer 407. Caco-2 cells were grown for 7 days on the smooth plastic of 96-well plates before 4 hour exposure to the excipients and 3 hours incubation with MTT. Note the increase in formazan production for wells containing higher concentrations of poloxamer 407 shown by the increase in the purple intensity despite the same initial concentrations of MTT. Also note that the bands of the highest intensity, poloxamer 407 at 10 % (w/v), do not correspond to the highest bar on the chart. Formazan production was of such intensity that crystals typically dislodge during draining of the MTT solution prior to isopropanol addition, and so do not have a representative bar on the chart. Morphological examination of the cells under such concentrations using light microscopy clearly showed cells in distress. Data shown as mean  $\pm$  SD from a minimum of 8 replicates over 2 passage numbers. Statistical significance was

- analysed using one-way ANOVA followed by Dunnett's *post hoc* test annotated as follows:  
 \*\* ( $p < 0.01$ ); \*\*\*\* ( $p < 0.0001$ ).....154
- Figure 4.10. ABCB1 and ABCC2 modulation of the poloxamers and Tweens, showing A) Poloxamer 182, B) Poloxamer 184, C) Poloxamer 407, D) Poloxamer 335, E) Poloxamer 188, F) Tween 80 and G) Tween 20. Data presented as a function of overall R-123 uptake with initial conditions of 2.5  $\mu$ M extracellular tracer dye, with non-treated controls set to 100 % transporter activity. Data shown pooled from a minimum of 5 replicates per concentration  $\pm$  SD. ....157
- Figure 4.11. The uptake of R-123 in the absence of ATP synthesis, showing A) Poloxamer 182, B) Poloxamer 184, C) Poloxamer 407, D) Poloxamer 335, E) Poloxamer 188, F) Tween 80 and G) Tween 20. Cells were incubated in the presence of surfactants for 1 hour at 37 °C, then rinsed in ice cold KH buffer (pH 7.4) and incubated at 4 °C in the dark in the presence of 100 nM R-123. Data shown  $\pm$  SD from data pooled from 5 replicates in relation to the surfactant-free control (KH buffer only) replicates. Statistical significance was analysed using one-way ANOVA followed by Dunnett's *post hoc* test annotated as follows: ns ( $p > 0.05$ ); \* ( $p < 0.05$ ); \*\* ( $p < 0.01$ ); \*\*\*\* ( $p < 0.0001$ ).....160
- Figure 4.12. Rhodamine 123 (50 nM) was incubated for 2 hours at 37 °C in the presence of various concentrations of poloxamers and Tweens in the absence of cells in order to assess the contribution of the excipients to tracer dye quenching, showing A) Poloxamer 182, B) Poloxamer 184, C) Poloxamer 407, D) Poloxamer 335, E) Poloxamer 188, F) Tween 80 and G) Tween 20. Data presented in relation to the surfactant-free control (KH buffer only) wells  $\pm$  SD from at least 6 individual replicates. CMCs (dashed line) obtained from literature (P182 from (Tiberg et al., 1991), measured at 23 °C, P407, P335 and P184 measured at 30 °C and P188 measured at 40 °C (Alexandridis et al., 1994), Tween 80 and Tween 20 from (Patist et al., 2000) measured at 22 °C). Statistical significance was analysed using one-way ANOVA followed by Dunnett's *post hoc* test annotated as follows: \*\* ( $p < 0.01$ ).....163
- Figure 4.13. Percentage inhibition curves of various surfactants against ABCB1 showing A) Poloxamer 182, B) Span 20, C) Crovol A70, D) Etocas 29, E) Poloxamer 184, F) Etocas 40, G) Acconon C44, H) Tween 80, I) Tween 20, J) Myrj S40, K) Poloxamer 407 and L) Poloxamer 335. Sigmoidal curves were constructed from 4 different passage numbers on confluent Caco-2 monolayers grown on 96 well plates for 5-7 days and are shown pooled from a

minimum of 4 replicates per concentration. Data presented as a function of overall R-123 or CDF (CDFDA) uptake for ABCB1 and ABCC2 respectively with initial conditions of 2.5 $\mu$ M extracellular tracer dye per well, with excipient-free control wells set to 100 % transporter activity. ....	168
Figure 5.1. The results of the DoE screening approach, showing tablet hardness (clear bars) and disintegration time (blue bars) for A) low-dose and B) high-dose tablets. Whilst some low-dose formulations and all high-dose formulations were able to disintegrate in less than 3 minutes in accordance with the EP, no formulations conformed to the USP limit of 30 seconds. Data presented as mean $\pm$ SD from $n = 10$ tablets for hardness and 6 tablets for disintegration time. ....	181
Figure 5.2. Design of experiments trace plots for low-dose formulations showing A) hardness and B) disintegration, showing the impact of Starch 1500 (red), MCC (blue) and mannitol (black).....	184
Figure 5.3. Design of experiments trace plots for high-dose formulations showing A) hardness and B) disintegration, showing the impact of Starch 1500 (red), MCC (blue) and mannitol (black).....	185
Figure 5.4. The impact of poloxamer 407 on A) low-dose F5, B) low-dose F6, C) high-dose F5 and D) high-dose F6, showing hardness (clear bars) and disintegration times (blue bars). Data presented as mean $\pm$ SD from $n = 10$ tablets for hardness and 6 tablets for disintegration time. Statistical significance was analysed using one-way ANOVA followed by Dunnett's <i>post hoc</i> test annotated as follows: ns ( $p > 0.05$ ); * ( $p < 0.05$ ); **** ( $p < 0.0001$ )..	189
Figure 5.5. The structural schematic of crospovidone. ....	190
Figure 5.6. The impact changing the superdisintegrant type on A) low-dose F5, B) low-dose F6, C) high-dose F5 and D) high-dose F6, showing hardness (clear bars) and disintegration times (blue bars). Hardness and disintegration data shown as the mean from an $n$ of 10 and 6 tablets respectively $\pm$ SD. Statistical significance was analysed using one-way ANOVA followed by Dunnett's <i>post hoc</i> test annotated as follows: ns ( $p > 0.05$ ); ** ( $p < 0.01$ ); **** ( $p < 0.0001$ ). ....	192
Figure 5.7. The impact changing concentration of the superdisintegrant, Kollidon CL-F, on A) low-dose F5, B) low-dose F6, C) high-dose F5 and D) high-dose F6, showing hardness (clear bars) and disintegration times (blue bars). Hardness and disintegration data shown	

as the mean from an  $n$  of 10 and 6 tablets respectively  $\pm$  SD. Statistical significance was analysed using one-way ANOVA followed by Dunnett's *post hoc* test annotated as follows: ns ( $p > 0.05$ ); \*\* ( $p < 0.01$ ); \*\*\*\*, ( $p < 0.0001$ ). .....194

Figure 5.8. The schematic structure of ethylcellulose. ....195

Figure 5.9 The impact of ETHOCEL 7 FP concentration on A) low-dose F5, B) low-dose F6, C) high-dose F5 and D) high-dose F6, showing hardness (clear bars) and disintegration times (blue bars). Hardness and disintegration data shown as the mean of  $n = 10$  and 6 tablets respectively  $\pm$  SD. Statistical significance was analysed using one-way ANOVA followed by Dunnett's *post hoc* test annotated as follows: ns ( $p > 0.05$ ); \* ( $p < 0.05$ ); \*\*\* ( $p < 0.001$ ); \*\*\*\* ( $p < 0.0001$ ). .....197

Figure 5.10. Summary of optimisation steps for A) low-dose F5, B) low-dose F6, C) high-dose F5 and D) high-dose F6, showing the conversion of the multipurpose binder, Starch 1500, to StarCap 1500, showing hardness (clear bars) and disintegration times (blue bars), in addition to optimising P407 to 2 %. Hardness and disintegration data shown as the mean of  $n$  of 10 and 6 tablets respectively  $\pm$  SD with disintegration times annotated for clarity. Statistical significance was conducted by one-way ANOVA followed by Tukey's *post hoc* test. Statistical significance is annotated as follows: ns ( $p > 0.05$ ); \*\* ( $p < 0.01$ ); \*\*\*\* ( $p < 0.0001$ ). .....200

Figure 5.11. The results of the second round of DoE screening, showing tablet hardness (clear bars) and disintegration time (blue bars) for A) low-dose and B) high-dose tablets. Data presented as the mean of  $n = 10$  tablets for hardness and  $n = 6$  tablets for disintegration time  $\pm$  SD.....203

Figure 5.12. Design of experiments trace plots for low-dose formulations showing A) hardness and B) disintegration, showing the impact of StarCap 1500 (red), MCC (blue) and mannitol (black).....206

Figure 5.13. Design of experiments trace plots for high-dose formulations showing A) hardness and B) disintegration, showing the impact of StarCap 1500 (red), MCC (blue) and mannitol (black).....207

Figure 5.14. The formulations shown in Table 5.10 made by direct compression, showing tablet hardness (clear bars) and disintegration time (blue bars). Data presented as mean  $\pm$  SD from  $n = 10$  tablets for hardness and 6 tablets for disintegration time  $\pm$  SD. Statistical

significance was calculated using one-way ANOVA with Dunnett's <i>post hoc</i> test, annotated as follows: **** ( $p < 0.0001$ ). .....	209
Figure 5.15. The results of the physical characterisation of tablets produced by the rotary tablet press, showing tablet hardness (clear bars) and disintegration time (blue bars). Data presented as the mean of $n = 10$ tablets for hardness and $n = 6$ tablets for disintegration time $\pm$ SD. ....	210
Figure 5.16. The results of the impact of compression force on range of physical tablet attributes, showing A) ejection force, B) hardness, C) disintegration time and D) friability. Data presented as the mean of $n = 10$ tablets for hardness and friability and $n = 6$ tablets for disintegration time $\pm$ SD. ....	213
Figure 5.17. Marketed products used for comparative study, showing the biconcave shape of A) Calpol SixPlus and B) Nurofen Meltlets produced via direct compression and C) the flat faced, lyophilised Imodium Instants, and their respective unbroken blister packs. ....	215
Figure 5.18 The hardness and disintegration times of OTC formulations. Data shown as the mean of $n = 3$ tablets for disintegration and $n = 3$ tablets for hardness, $\pm$ SD. For Imodium® Instants, disintegration time was instantaneous upon contact with water. Likewise hardness was too low to be detected. OTC data is shown in comparison to the fastest disintegrating low-dose and high-dose tablets, F15 and F13 respectively, from the second round of DoE screening (shown in Figure 5.11) where data is presented as the mean of $n = 6$ tablets for disintegration time $n = 10$ tablets for hardness, $\pm$ SD. ....	216
Figure 6.1. The chemical structure of the polyvinyl alcohol-polyethylene glycol copolymer Kollicoat IR. ....	220
Figure A.1. The effects of the surfactants on cellular viability using the MTT toxicology assay, showing A) Capmul PG-8, B) Capmul MCM, C) Capmul MCM C8, D) Capmul PG-12, E) Poloxamer 182, F) Span 20, G) Arlatone TV, H) Crovol A-70, I) Etocas 29, J) Brij S-10, K) Poloxamer 184, L) Etocas 40, M) Brij CS-12, N) Acconon C-44, O) NatraGem S140, P) Acconon MC8-2, Q) Tween 80, R) Cetomacrogol 1000, S) Tween 20, T) Myrj S-40, W) Poloxamer 335, X) Myrj S-100, Y) Poloxamer 407, Z) Poloxamer 188. Caco-2 cells were grown for 5-7 days on 96-well plates prior to experimentation. Data presented as the mean value of at least 6 replicates $\pm$ SD. Statistical significance was analysed using one-way	

ANOVA followed by Dunnett's *post hoc* test with variance as follows: \* ( $p < 0.05$ ); \*\* ( $p < 0.01$ ); \*\*\* ( $p < 0.001$ ); \*\*\*\* ( $p < 0.0001$ ). .....262

## Table of Tables

Table 1.1. Overview of commonly used production techniques, marketed formulations and associated advantages and disadvantages. ....	68
Table 1.2. Overview of commonly used disintegrants and their particle size.....	70
Table 2.1. Formulation composition of ODTs used in coating trials.....	89
Table 2.2. Nomenclature of Kollicoat IR dispersions. ....	90
Table 2.3. Specifications used during the coating process. ....	90
Table 3.1. Typical PEG 400, PEG 8000, POLYOX N-10 and poloxamer 407 concentrations found in oral dosage forms. The resultant polymer concentrations used in the study assumes the oral dosage formulation is taken with a 250 mL glass of water.....	96
Table 3.2. The change in transepithelial resistance over time in the presence of drug alone or with PEG 8000.....	98
Table 3.3. Typical absorption to secretion permeability coefficients for 50 $\mu$ M IND through 21-day old Caco-2 monolayers. The higher value of the former compared to the latter is suggestive of transporter mediated efflux, demonstrated by the asymmetrical transport.	101
Table 3.4. Percentage Lucifer yellow transported after 60 minutes through 21-day old Caco-2 monolayers grown in Transwell® inserts. Data shown as the mean of triplicate values $\pm$ SD, .....	109
Table 3.5. Optimised conditions for HTS protocol. ....	120
Table 3.6. Purpose and structural formula of excipients tested (* source Handbook of Pharmaceutical Excipients, 6 <sup>th</sup> Edition).....	128
Table 3.7. A critique of the aspects of both models tested in this chapter. Media consumption per plate is based on renewal every 48 hours and includes seeding media..	131
Table 4.1. Literature IC <sub>50</sub> values of the inhibitors against those obtained from Caco-2 cells grown for 5-7 days on 96-well plates. Data of determined IC <sub>50</sub> values shows the outcome of the kinetic modelling using GraphPad Prism presented in Figure 4.1 extrapolated for 50 % transporter inhibition using the sigmoidal curve.....	138
Table 4.2. Degree of substitution and viscosity of the METHOCEL LV grade HPMCs. ....	140
Table 4.3. The range of surfactants selected for initial HTS according to the hydrophilic-lipophilic balance values. ....	152
Table 4.4. The utilisation of surfactants based on their HLB values (Griffin, 1946). ....	164

Table 4.5. The range of surfactants selected for HTS according to the hydrophilic-lipophilic balance values.....	165
Table 4.6. Physical properties and IC <sub>50</sub> values of the tested excipients. Molecular weight values were either obtained from the manufacturer or estimated from the structures, as given in the parentheses below. All other values were determined experimentally. ....	170
Table 5.1. List of excipient selected for ODT development.....	177
Table 5.2. Low-dose and high-dose formulation compositions indicated by the first round of DoE mapping using JMP 12 DoE software to optimise MCC, Starch 1500 and mannitol content within the ODT formulation.....	178
Table 5.3. Remaining physical data from both high and low-dose APAP tablet. For all datasets, <i>n</i> = 10 tablets.....	182
Table 5.4. Summary of the model statistics on the impact of the test excipients on hardness and disintegration on the low-dose formulations from the first round of DoE screening. ....	185
Table 5.5. Summary of the model statistics on the impact of the test excipients on hardness and disintegration on the high-dose formulations from the first round of DoE screening. ....	185
Table 5.6. Low-dose and high-dose formulation compositions indicated by the second round of DoE mapping using JMP 12 DoE software to optimise MCC, Starch 1500 and mannitol content (indicating the key variables in red) within the ODT formulation. ....	202
Table 5.7. Results of friability testing of the low-dose and high-dose formulations following the second round of DoE screening, showing the percentage loss of tablet mass after 100 rotations and 400 rotations. ....	204
Table 5.8. Summary of the model statistics on the impact of the test excipients on hardness and disintegration on the low-dose formulations from the second round of DoE screening. ....	207
Table 5.9. Summary of the model statistics on the impact of the test excipients on hardness and disintegration on the high-dose formulations from the second round of DoE screening. ....	207
Table 5.10. The composition of the final formulations chosen for production of the Picolla rotary tablet press indicating the key variables (red). ....	208
Table 5.11. The percentage weight loss of tablets produced by the rotary press, showing normal friability (100 rotations) and accelerated friability (500 rotations). ....	211

Table 5.12. The weight variation data of tablets produced using the rotary press. Data presented from 10 tablets per formulation. ....	214
Table 6.1. Formulation composition of ODTs used in coating trials.....	220
Table 6.2. Nomenclature of Kollicoat IR dispersions. ....	220
Table 6.3. The classification of powder flow based on angle of repose, Carr's Index and Hausner Ratio. ....	223
Table 6.4. The powder flow properties of the ODT formulations. Results are presented as mean $\pm$ SD from $n = 3$ , except moisture content.....	223
Table 6.5. The physical properties of tablets produced from the coated powders C1 (compressed at 2 metric tons) and C2-C4 (compressed at 1 metric ton). Data presented $\pm$ SD from $n = 3$ tablets (aside from friability).....	225
Table 6.6. Content uniformity of tablets ( $n = 3$ ) produced from uncoated granules and granules coated with various dispersions (C1-C4).....	226

### Abbreviations

% v/v	Percentage Volume to Volume
% w/v	Percentage Weight to Volume
ABC	ATP Binding Cassette
ABCB1	P-glycoprotein (P-gp)
ABCC2	Multidrug Resistance Transporter 2 (MRP2)
ABCG2	Breast Cancer Resistance Protein (BCRP)
ADMET	Absorption, Distribution, Metabolism, Excretion and Toxicology
ANOVA	Analysis of Variance
AP	Apical
AP-BL	Apical-to-Basolateral Transport
APAP	Acetaminophen
API	Active Pharmaceutical Ingredient
ATP	Adenosine Triphosphate
ATV	Atorvastatin
BBB	Blood Brain Barrier
BCRP	Breast Cancer Resistance Protein
BL	Basolateral
BL-AP	Basolateral-to-Apical Transport
BP	British Pharmacopoeia
BSC	Biopharmaceutics Classification System
Caco-2	Human Colonic Adenocarcinoma Cell line

CDF	5(6)-Carboxy-2',7'-Dichlorofluorescein
CDFDA	5(6)-Carboxy-2',7'-Dichlorofluorescein Diacetate
Clog <i>D</i>	Calculated Log <i>D</i>
Clog <i>P</i>	Calculated Log <i>P</i>
CMC	Critical Micelle Concentration
CNS	Central Nervous System
CsA	Ciclosporin
CYP	Cytochrome
Da	Dalton
ddH <sub>2</sub> O	Double-Distilled Water
DDIs	Drug-Drug Interactions
DMEM	Dulbecco's modified eagle medium
DMSO	Dimethyl Sulfoxide
EP	European Pharmacopoeia
FBS	Foetal Bovine Serum
FDA	Food and Drug Administration
GIT	Gastrointestinal Tract
HBA	Hydrogen Bond Acceptor
HBD	Hydrogen Bond Donor
HBSS	Hank's Balanced Salt Solution
HEPES	4-(2-hydroxyethyl)-1-piperazineethanesulfonic acid
HLB	Hydrophilic-Lipophilic Balance

HPLC	High Performance Liquid Chromatography
HPMC	Hydroxypropyl Methylcellulose
HTS	High-Throughput Screening
IND	Indometacin
IV	Intravenous
KH	Krebs-Henseleit Buffer
$K_m$	Michaelis-Menten Kinetics
LDH	Lactate Dehydrogenase
$\log D$	Logarithm of the distribution coefficient
$\log P$	Logarithm of the partition coefficient
LY	Lucifer Yellow
MCC	Microcrystalline Cellulose
MDCK	Madin-Darby canine kidney cell line
MDR	Multi-Drug Resistance
MRP	Multidrug Resistance-Associated protein
MT	Metric Ton
MTT	3-[4,5-dimethylthiazol-2-yl]-2,5- diphenyltetrazolium bromide
MW	Molecular Weight
NBD	Nucleotide-Binding Domain
NCE	New Chemical Entity
NEAA	Non-Essential Amino Acids
NSAID	Non-Steroidal Anti-Inflammatory Drugs

OATP	Organic Anion-Transporting Polypeptide
ODT	Orally Disintegrating Tablet
OTC	Over the Counter
PAMAM	Poly(amidoamine), a class of dendrimer
$P_{app}$	Apparent Permeability
PBD	Probenecid
PBS	Phosphate Buffered Saline
PD	Pharmacodynamics
PDB	Protein Data Bank
PE	Polyethylene
$P_{eff}$	Effective Permeability
PEG	Polyethylene Glycol
PEO	Polyethylene Oxide
PK	Pharmacokinetics
PO	Propylene Oxide
PVAP	Polyvinyl Acetate Phthalate
PVP	Polyvinylpyrrolidone
QbD	Quality by Design
R-123	Rhodamine 123 (6-amino-9-(2-methoxycarbonylphenyl)xanthen-3-ylidene] azanium chloride)
RFU	Relative Fluorescence Units
RSD	Relative Standard Deviation

SAR	Structure-Activity Relationship
SD	Standard Deviation
SPIP	Single Pass Intestinal Perfusion
TDI	Time-Dependent Inhibition
TEER	Transepithelial Electrical Resistance
TPGS	d- $\alpha$ -Tocopheryl polyethylene glycol 1000 succinate
TPSA	Topological Polar Surface Area
USP	United States Pharmacopoeia
VER	Verapamil
ZO-1	Zonula occludens-1 tight junction protein

## Chapter 1

### Introduction

## 1. Introduction

### 1.1. The Advantages and Disadvantages of the Oral Route of Drug Administration

The ease of administration and increased patient compliance rank highly among the multitude of reasons why oral delivery is still the preferred route of administration for many pharmaceutical products today, despite advances in transmucosal, transdermal and even pulmonary delivery systems, amongst others. Oral drug formulations have been estimated to account for 90 % of all medicines, with further growth expected as the market develops (Gabor et al., 2010).

As such, absorption following oral administration has been subject to intense study in order to optimise the amount of material that is able to reach the systemic circulation. Unlike a drug delivered directly into the circulatory system via the *intravenous* route, which will reach 100 % bioavailability, pharmaceutical compounds taken via the oral route must pass a series of barriers in order to reach the systemic circulation. The intestinal wall, particularly the jejunum, represents the final obstacle before the compound is able to enter the body, coinciding with the greatest concentration in expression of the major ABC-binding cassette transporters such as P-glycoprotein (P-gp, ABCB1) and the multidrug resistance protein (MRP2, ABCC2) (Taipalensuu et al., 2001). These transporters are expressed on the apical membranes of cells of the intestinal epithelium and act to expel drugs back into the intestinal lumen. The substrate promiscuity of P-gp is well known, and collectively efflux transporters pose a challenge to efficient drug delivery via the oral route of administration. Beyond the role of limiting bioavailability of drugs taken via the oral route, up-regulation of efflux transporters is one mechanism by which neoplastic cells become refractory to treatments (Ling, 1987).

Whilst inhibitors of efflux proteins exist, they are limited by the high concentrations required, which often impart their own toxic effects. Recent advances in the field of excipient-drug interactions have revealed a diverse range of materials which are able to overcome efflux, either by increasing the uptake of test substrates across intestinal barriers *in vitro* or *in vivo*, or by sensitising refractory tumours to treatments. Such excipients

already have FDA approval, are currently in use and accepted, and can be incorporated in oral dosage forms using existing fabrication techniques.

## 1.2. Drug Dissolution and the Gastrointestinal Tract

Upon ingestion of a tablet, the active material must be liberated from the dosage form for absorption to occur, and one of the rate-limiting steps in the effective oral delivery of any pharmaceutical compound is the rate of dissolution. This is described by the Noyes-Whitney equation, shown in Equation 1.1,

$$\frac{dW}{dt} = \frac{A \cdot D}{h} \cdot \left( C_s - \frac{X_d}{V} \right) \quad \text{Equation 1.1}$$

where  $dW/dt$  is the rate of dissolution,  $A$  is the surface area available for dissolution,  $D$  is the diffusional coefficient,  $h$  is the thickness of the boundary layer,  $X_d$  is the amount of drug dissolved,  $V$  is the volume of the dissolution media, and  $C_s$  is the solubility of the compound. From this equation, it is possible to ascertain how the dissolution rate of a compound can be enhanced, even those with limited solubility, such as decreasing particle size, optimising wettability, decreasing the thickness of the boundary layer and ensuring as close to sink conditions as possible can all be seen as ways to increase the rate of dissolution.

Once it has undergone dissolution, the active compound must reach the absorbing membrane, the intestinal epithelium. To achieve this, the drug must pass safely through the acidic content of the stomach and the digestive enzymes of the stomach and small intestine. The reported pH of the stomach varies between reports but has been shown in the rested state to be 2.8 for females and 2.2 for males (Feldman and Barnett, 1991). This increases following ingestion of a meal owing to the buffering capacity of food, but is normalised after 3-4 hours by the secretion of gastric fluid (Go, 1976). Many weakly acidic drugs, such as acetaminophen, are poorly absorbed by the stomach and greatly absorbed in the small intestine (Heading et al., 1973). As such, the rate of uptake is greatly related to the rate of gastric emptying. The rate of gastric emptying can be affected by many factors. Alcohol and some drugs are known to increase the rate of emptying (Kaufman and Kaye,

1979), whilst other factors such as opiate analgesics can decrease the rate of emptying (Nimmo et al., 1975). Once the small intestine has been reached, the drug faces a series of challenging barriers in order to pass through to the desired site of action (Figure 1.1). This process can be summarised using Equation 1.2 to describe the amount of drug that is able to reach systemic circulation, otherwise known as bioavailability ( $F$ ),

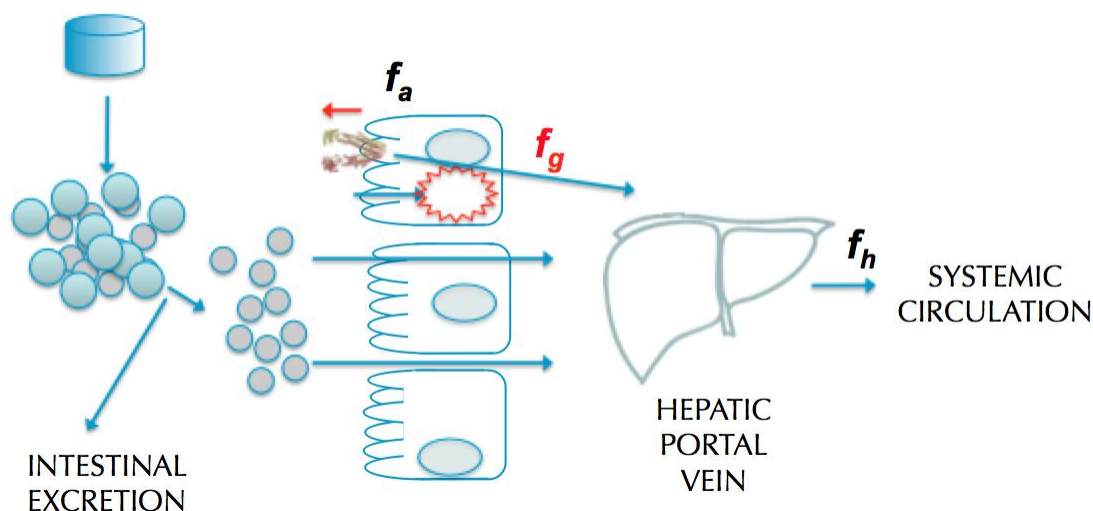


Figure 1.1. Graphical representation of the bioavailability equation. A compound undergoes liberation from its dosage form, and must survive the transition past the intestinal epithelia. The absorbed fraction,  $f_a$ , gets gradually diminished by the action of metabolism within the cell,  $f_g$ , and subsequent hepatic degradation,  $f_h$ , before systemic circulation is reached.

$$F = F_a F_g F_h \quad \text{Equation 1.2}$$

where  $F_a$  is the fraction of drug which is absorbed,  $F_g$  is the fraction able to survive gut metabolism and  $F_h$  is the fraction able to escape hepatic metabolism (Pond and Tozer, 1984). It can be seen from this equation that a drug given by the intravenous (IV) route escapes these obstructions entirely, yet as discussed this route of administration is not favoured outside of a clinical setting. Collectively, the steps outlined in Figure 1.1 and Equation 1.2 are known as the first pass metabolism. Some drugs, such as oxycodone, diazepam and methadone, survive well to the systemic circulation, with oral bioavailability values of 60-87 % (Poyhia et al., 1992, Poyhia et al., 1993), 97 % (Palm et al., 1997) and 85 %

(Dale et al., 2002), respectively. Other drugs, such as morphine and cocaine, have poor bioavailability values of around 30 % or less as a result of pre-systemic metabolism (Säwe, 1986, Fattinger et al., 2000).

### **1.3. Intestinal Absorption and Transporters**

A layer of mucosa covers the intestinal epithelial membrane through which a drug must penetrate. However, this is generally not a rate-limiting step in absorption (Aungst, 2012, Fagerholm and Lennernäs, 1995). The intestinal epithelium may be considered the gatekeeper of substrate uptake, with nutrient and xenobiotic ingress occurring through a series of complex processes (Figure 1.2), with the specific type of uptake based on several physiochemical properties of the compound in question. The paracellular hypothesis describes the passive movement of the drug through the monolayer via intracellular tight junctions. Primarily, molecular weight/size and flexibility of geometric structure will influence the extent of paracellular passage, whilst solubility, chemical composition and charge distribution are further considerations (Aungst, 2012, Goole et al., 2010, Artursson et al., 1993b). The tight junction macromolecular complex provides this barrier function and is the rate-limiting structure to large and/or charged compounds, yet allows ingress to small uncharged compounds (Figure 1.2a). A major component of the tight junction complex is Zonula occludens (ZO-1), which act by directly binding actin cytoplasmic filaments to the transmembrane protein occludens, and so form cell-cell interfaces. Here, they play a cardinal role in the exclusion of macromolecules by the paracellular route, effectively sealing the apical plasma membranes of the intestinal lumen (Van Itallie et al., 2009). Transcellular transport of lipophilic molecules can occur through the lipid bilayer, or by membrane bound proteins on the apical side (Figure 1.2b), or by transcytosis (Figure 1.2c) (Goole et al., 2010, Le Ferrec et al., 2001). However, not all transport is absorptive e.g. apical to basolateral. A further consideration of drug transport is that of efflux, whereby xenobiotics are expelled back into the intestinal lumen (Figure 1.2d).

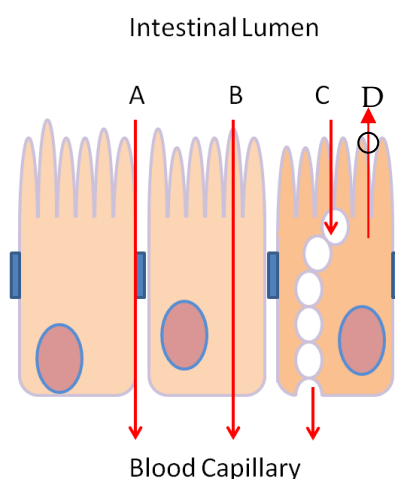


Figure 1.2. Intestinal absorption pathways, showing (A) paracellular, (B) transcellular passive/transporter mediated, (C) transporter mediated transcytosis, and (D) transporter mediated efflux.

#### 1.4. The ABC Transporter Systems

In addition to acting as an instrument of absorption, the intestine must also act as a barrier to xenobiotics, bacteria and other harmful substances. In order to protect specific tissues and the body as a whole, the GI tract employs a number of transporters, known as efflux transporters, to expel unwanted substances back to the intestinal lumen and prevent them from reaching systemic circulation. The purpose of such efflux transporters is believed to be in protecting the body from environmental toxins. The most widely reported information is on the adenosine triphosphate (ATP)-binding cassette (ABC) transporters due to being heavily implicated in the development of multidrug resistance (MDR) in cancer cells, where they are over-expressed. ABC proteins involved in drug resistance chiefly include P-glycoprotein (P-gp, ABCB1), multidrug resistance protein 1 (MRP1, ABCC1), multidrug resistance protein 2 (MRP2, ABCC2) and breast cancer resistance protein (BCRP, ABCG2). These proteins have overlapping specificity, and collectively transport a vast range of diverse compounds.

#### 1.4.1. P-glycoprotein (P-gp. ABCB1)

P-glycoprotein (Figure 1.3) was the first of the ABC transporters to be characterised and a founding member of the ABC superfamily alongside MRP1. The transporter was first discovered after a 170,000 Da protein was isolated from the cell surface of Chinese hamster ovary cells which were resistant to colchicine and a plethora of amphiphilic drugs. Owing to its effects on permeability, this protein was named P-glycoprotein (Juliano and Ling, 1976). This protein has since been found in a whole range of tissues, and the influence on pharmacokinetics and pharmacodynamics (PK/PD) are widespread: absorption by expelling xenobiotics back into the intestinal lumen; distribution by preventing entry through the blood brain barrier (BBB); xenobiotic metabolism due to the protein being affiliated to cytochrome P450 (CYP); P-gp lining the renal tubes will influence excretion (Mizuno et al., 2003, Goole et al., 2010). P-gp shows remarkable levels of broad poly-specificity, and is capable of compound recognition from 220 Da (cimetidine) to 1202 (ciclosporin), and even up to 4000 Da in the case of  $\beta$ -amyloid (Pan et al., 1994, Goldberg et al., 1988, Lam et al., 2001). The only real common feature of substrates of P-gp is hydrophobicity, and membrane partitioning is believed to be the initial step in protein-substrate interaction.

Beyond the role of resistance in cancer cells, the transporter has been implicated in resistance to other drugs. Western blot analysis has shown that brain P-gp was increased 2-fold in rats chronically treated with morphine, a P-gp substrate (Löscher and Potschka, 2005). P-gp homologues have also been implicated in the spread of treatment resistant pathogenic bacteria, fungi and parasites (Alcantara et al., 2013, Xu et al., 1998, Cowman, 1991, Gibbons et al., 2003, Poole, 2005), and, as such, P-gp can be seen at the centre of some of the deadliest diseases on the planet.

This transporter is coded for by the *MDR1* gene in humans (*mdr1a* in rats and other organisms) (Schuetz et al., 1998), and is known from human genome nomenclature as ABCB1. However, in the GI tract, distribution is not even: the terminal ileum has the highest expression, approximately 4 times that of the duodenum and twice as high as the colonic regions (Zimmermann et al., 2005), although inter-person variability is observed. The impact of ABCB1 on drug uptake is also compounded by the co-expression and co-

localisation of the transporter with metabolic enzymes, particularly cytochrome P450 (CYP) 3A4, the major phase I metabolising enzyme (Wacher et al., 1995). CYP3A4 accounts for 30 % of human hepatic microsomal cytochromes (Shimada et al., 1994) and is the most numerous of the enteric cytochromes (Zhang et al., 1999). Additionally, ABCB1 and CYP3A4 have known substrate recognition overlap suggesting likely synergism between the two (Wacher et al., 1995), making the presence of these proteins a further issue for concern in effective oral drug delivery.

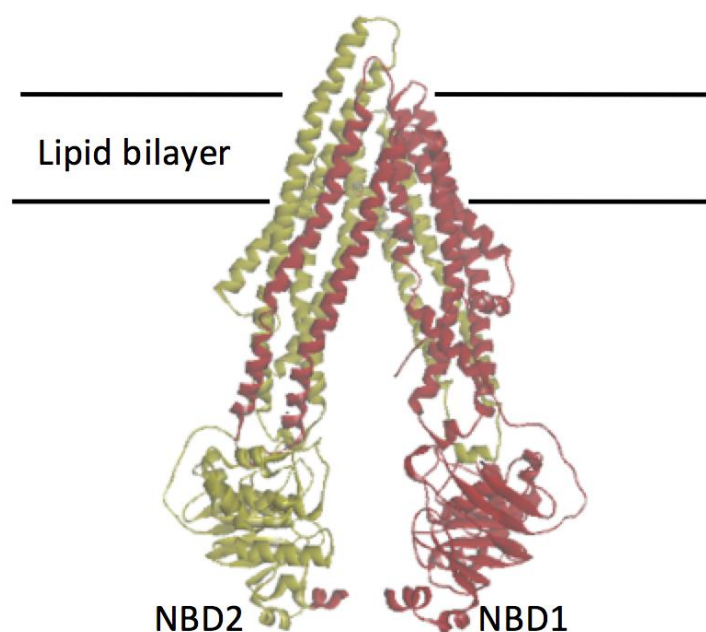


Figure 1.3. The crystal structure of murine P-gp. The protein consists of two bundles of six transmembrane helices. The inward facing formation results in a large internal cavity open to the cytoplasm and inner leaflet. The presumed drug binding pocket consists largely of hydrophobic and aromatic residues. The N and C terminal of the protein is coloured yellow and red respectively. NBD = nucleotide binding domain. Lipid bilayer location is shown in approximation (Protein Data Bank file 3G5U). Diagram adapted from (Aller et al., 2009).

#### 1.4.2. Multidrug Resistance Associated Protein family (MRP, ABCC)

The multidrug resistance protein 1 (MRP1/ABCC1) was first identified due to its overexpression in small cell lung cancer (SCLC) resistance (Cole et al., 1992) where *MRP* mRNA expression in treatment-resistance cell lines was shown to be 25 times higher than non-resistant parental cell lines (Zaman et al., 1993). Alongside P-gp, MRP1 was first of the ABC transporter families to be discovered, but only displays around 15 % amino acid

homology to P-gp (Cole et al., 1992). The MRP isoforms transport both uncharged hydrophobic in addition to anionic conjugates.

Interestingly, Zaman *et al* (1993) were to conclude that the overexpression of *MRP* did not account for all forms of non-P-gp MDR. Since then, it has emerged that MRP has several known isoforms (MRP1-MRP7), some of which overlap in terms of substrate specificity but differ in tissue expression. MRP1 is only known to be expressed in the proliferative cells at the enterocyte renewal sites of the murine model, where it is suspected to be involved in xenobiotic protection of this layer (Peng et al., 1999) and is unlikely to participate in the absorption process from the small intestine. In terms of affecting drug absorption, the second isoform of MRP, MRP2 (ABCC2), is perhaps the most important of the MRP isoforms, as it was first shown to be expressed on the apical border of the small intestine of both the rat (Mottino et al., 2000) and rabbit (Van Aubel et al., 2000) models. In a comprehensive human subject study, various parts of the intestine were sampled for the presence of expression of MRP1-MRP5, in addition to MDR1. In the duodenum, the rank of expression was seen MRP3 >> MDR1 > MRP2 (Zimmermann et al., 2005). However abundant, MRP3 is known as a bile salt transporter (Hirohashi et al., 2000) and although it is known to transport chemotherapeutic drugs, such as vinblastine and methotrexate (Hirohashi et al., 1999, Kool et al., 1999), expression of MRP3 is basolateral and, therefore, unlikely to impact drug bioavailability. Much like P-gp, MRP2 also displays site-specific expression, being almost non-existent in the upper ileum, with the highest concentration in the duodenum and disappearing once more in all segments of the colon (Zimmermann et al., 2005). Just as co-localisation of P-gp and CYP3A suggests close cooperation of the two, MRP2 is often co-expressed with conjugating enzymes which essentially provide for exportation the conjugated metabolites (Cao et al., 2006).

#### **1.4.3. Breast Cancer Resistance Protein (BCRP, ABCG2)**

Breast cancer resistance protein (BCRP) takes its namesake from the MC-7 human breast carcinoma cells from which it was first discovered, after cells became refractory to mitoxantrone, doxorubicin, and daunorubicin treatment, and this was demonstrated not to be caused by P-gp or MRP1 (Doyle et al., 1998). Later, the murine homologue of the transporter was found on the apical membranes of the small intestine in mice (Jonker et al.,

2000), leading to the possibility of pharmacokinetic intervention during human oral drug delivery. Indeed, BCRP expression as well as MRP2 expression have been shown to be higher than that of MRP1 in the human jejunum (Taipalensuu et al., 2001).

The specific inhibitor of BCRP, GF120918, has been used to demonstrate the role of this transporter in limiting the uptake of some drugs taken orally. In both wild type and P-gp deficient mice, GF120918 increased the oral uptake of topotecan, a known substrate of BCRP, by six-fold in the former and nine-fold in the latter, respectively (Jonker et al., 2000). In the human subject, the same inhibitor led to an increase in topotecan plasma levels from 40 % to 97 % (Kruijtzter et al., 2002).

### 1.5. ABC-Transporter-Substrate Recognition

Given the implications of efflux transporters on drug target engagement at the desired dose, the study of structure-activity relationships (SAR) that improve biological activity has become a focal point. A typical 'Rule of 5' (RO5) that describes 90% of orally active drugs to navigate through stage II clinical trials is shown as (a) molecular weight < 500 Da; (b) lipophilicity ( $\log P$ ) or the calculated 1-octanol-water partition ( $\text{Clog}P$ ) < 5; (c) the number of hydrogen bond donors, OH and NH count to be < 5; and (d) the hydrogen bond acceptor (HBA), O and N count to be < 10 (Lipinski et al., 1997). The fundamental RO5 can be expanded using a holistic approach to define the physicochemical properties required by a compound to be an ABC-transporter substrate, in particular a substrate of P-gp.

With regards to CNS exposure, six physicochemical properties have been defined which effect P-gp efflux by comparing 108 diverse drug candidates with 119 marketed drug candidates (Wager et al., 2010). These are  $\text{Clog}P$ ,  $\text{Clog}D_{7.4}$ , molecular weight, topological polar surface area (TPSA), number of hydrogen bond donors (HBDs), and most basic centre ( $pK_a$ , log of the acidic dissociation constant). An analysis of over 1000 structurally diverse compounds showed that compounds with a  $\text{Clog}P < 4.0$  and with a TPSA between  $40\text{-}80\text{\AA}^2$  were more likely to circumvent P-gp efflux (Raub, 2006). In an additional study by the same group of over 2000 compounds, structures with a TPSA <  $60\text{\AA}^2$  with a  $pK_a < 8.0$  were much more likely to be identified as non-P-gp substrates (Desai et al., 2012). Increasing passive permeability was also noted as a method of avoiding P-gp efflux.

Two models have been proposed for the mechanism of efflux action. The simplest is known as the pore model and assumes the protein is expelled from the cell by a protein channel. However, the most popular paradigm is known as the “hydrophobic vacuum cleaner” model (Raviv et al., 1990). Here, the substrate is able to partition the bilayer as it enters the inner leaflet of the membrane (Figure 1.4). It is then taken up into the internal binding site, at which point the affinity of the nucleotide binding sites for ATP increases. Following ATP binding, a conformational change of the protein presents the substrate to the outer leaflet or extracellular space, sterically occluding access to the inner leaflet. ATP hydrolysis then returns the protein to the original configuration. This model is supported by X-ray crystallography, demonstrating that P-gp has binding sites located at an internal cavity located within the transmembrane section, indicating substrate acquisition occurs here (Aller et al., 2009). According to the two-step model of substrate binding, P-gp binds its substrate in the cytosolic membrane leaflet. As such, a compound rapidly diffusing across a membrane will evade P-gp efflux. Indeed, an increase in TPSA, HBD and HBA will serve to reduce the passive permeability of a compound and thus increase its chances of interactions with an efflux transporter. The dominant role of TPSA, HBD and HBA is supported by an *in vitro* permeability study of 4176 compounds (Hitchcock et al., 2012). Of these, 52% of compounds with a TPSA > 90 Å<sup>2</sup> were categorised as substrates of P-gp, but only 14% with TPSA < 70 Å<sup>2</sup> were substrate. For HBD count, 57% of compounds with > 2 HBDs were categorised as P-gp substrates, with only 9% with no HBD being considered substrates. ClogP had little influence on P-gp efflux within the range of drug-likeness (Hitchcock et al., 2012).

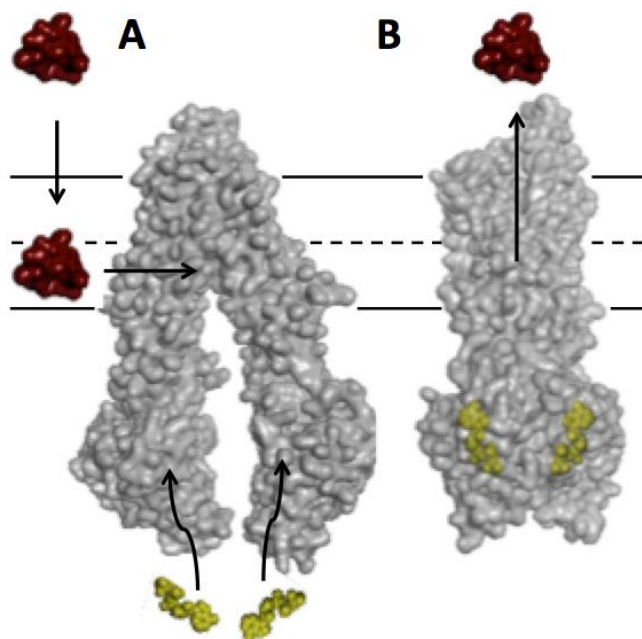


Figure 1.4. The two-step model of substrate transport of P-gp. (A) The substrate (maroon) partitions into the bilayer into the inner leaflet. Here, it is able to enter the intramembranous substrate binding pocket. (B) ATP (yellow) interaction with the nucleotide-binding domain (NBD) causes a conformational change of the protein, exposing the substrate to the extracellular space (Protein Data Bank file 3G5U). Diagram adapted from (Aller et al., 2009).

The inhibition specificities of P-gp, BCRP and MRP2 have been shown to be highly overlapping. A study testing the inhibition properties of 122 structurally diverse drugs on P-gp, BCRP and MRP2 revealed 23 transporter-specific inhibitors and 19 overlapping multi-specific inhibitors (Matsson et al., 2009). General inhibitors were found, on average, to be more lipophilic (median  $\log D_{7.4} = 4.5$ ) and aromatic than specific inhibitors, or non-inhibitors. According to the two-step model of substrate interaction with P-gp (Aller et al., 2009), discussed above, the ligand partitioning into the plasma membrane allows the inhibitors to bind to an intramembranous site. As most of the homology between the ABC transporters is found in the nucleotide-binding domain (NBD), the authors suggest that the non-lipophilic, negatively charged, multi-specific compounds in this study (silymarin and quercetin,  $\log D_{7.4} = 1.5$  and  $1.0$ , respectively) might interact with the transporters in a similar manner to the negatively charged phosphate moiety in ATP (Matsson et al., 2009). Binding site differences between transporters may also play a role in specificity, as BCRP-specific inhibitors generally contained more nitrogen atoms than P-gp specific inhibitors, suggesting hydrogen bond  $\pi$ - $\pi$  or  $\pi$ -cation interactions may be important for BCRP

binding (Matsson et al., 2009). In contrast, P-gp inhibitors contained more carbonyl oxygen, which are less likely to participate in hydrogen bond formation, consistent with the hydrogen bond acceptor patterns of P-gp substrates already discussed. The low lipophilicity of BCRP and MRP2 inhibitors is suggestive of a less important role of plasma membrane partitioning for these transporters, and that the substrate binding sites for these transporters lies within a cytosolic location, in contrast to P-gp (Aller et al., 2009). The true distinction between ABC-transporter substrate recognition and inhibitor recognition remains to be further determined, as ABC-transporters belong to a diverse group of membrane-bound proteins, many of which are currently lacking structural information (Klepsch and Ecker, 2010). Current information is, therefore, based on examination of known substrates and inhibitors.

## 1.6. Commonly Utilised Models of Intestinal Absorption

Of cardinal importance in drug development and formulation is to have a predictive model for the absorption of the compound in man. By definition, any biological model has its limitations in terms of the overall similarity to the *in vivo* tissue to which it should replicate. This includes, but is not restricted to, representative physiology, metabolic enzymes and efflux transporters. As such, there are a number of models which are available to drug delivery scientists who wish to replicate faithfully the transport that occurs at the site of the majority of drug uptake.

### 1.6.1. *In Vivo* Models of the Gastrointestinal Tract

The *in vivo* method of modelling has many advantages, coupling the presence of a mucus layer with a functional circulatory system. Aside from human voluntary trials, the *rattus* model is perhaps the most popular ahead of the canine model. Not only does this latter model represent something of a moral dilemma for using *canis familiaris*, from a purely scientific perspective the canine model is often cited as being an overestimation of the model of metabolism in comparison to the human model. One study comparing the fraction absorbed in dog and man only found an  $r^2$  correlation value of 0.512 (Chiou et al., 2000). The same authors previously found a much better correlation, with an  $r^2$  value of 0.975, between human and rat bioavailability (Chiou and Barve, 1998). In a study examining compounds with varying mechanisms of uptake (P-gp-mediated, organic cation

transporter-mediated, and passive diffusion), it was found that overall fraction absorbed of all compounds was closely correlated ( $r^2 = 0.8$ ) (Cao et al., 2006) despite moderate ( $r^2 = 0.56$ ) correlation in transporter expression. Despite having a quicker intestinal transit time, some drug uptake profiles in dogs appears more complete, often associated with larger villi compared humans in addition to increased canine bile secretion, which could aid solubilisation of poorly water-soluble compounds (Kararli, 1995). It is also not possible to delineate the different mechanisms of absorption and identity of rate limiting steps. As such, *in vivo* testing has to be carefully considered.

An extension of the *in vivo* modelling system is the *in situ* model of the small intestine (Figure 1.5), which offers the advantages of using living tissue coupled with the mucus layer and a live blood flow to the tissues in question. Typically, an animal has been surgically manipulated under the influence of an anaesthetic to display the mucosal fascia. The disappearance of drug from the intestinal lumen is then monitored as a measure of drug absorption. Generally, the *in situ* model is validated using different marker compounds such as PEG 4000, mannitol and D-glucose, usually radiolabelled, in order to assess how the volume of drug solution changes in response to water absorption, and to monitor intestinal viability in a similar manner to TEER values for *in vitro* monolayers, discussed later. However, the choice of anaesthetic used is critical, as it has been shown to have a strong influence on intestinal absorption (Yuasa et al., 1993). This model has two main variations. The Doluisio method utilises the whole small intestine of the rat (Doluisio et al., 1969), whereas the single pass intestinal perfusion (SPIP) utilises just a single 10 cm section of the intestine, typically the jejunum (Amidon et al., 1988). Both have shown excellent correlation to the effective permeability ( $P_{\text{eff}}$ ) of both passively absorbed and carrier mediated transport. In a recent study, both variations of the technique were shown to have an  $r^2$  value of 0.93 (Lozoya-Agullo et al., 2015).



Figure 1.5. Experimental set up of the *in situ* technique. Freshly excised intestine of the anaesthetised rat is exposed and the test compound is introduced via the syringe at a controlled rate. Samples are then collected at the desired point further down the tract to determine the degree of compound uptake. This can either be the whole intestinal tract (Doluisio model) or a 10 cm section (single pass intestinal perfusion (SPIP) model) (Barthe et al., 1999).

Of course, there exists a method of testing absorption on the human subject as well. In its most advanced form developed by Lennernäs *et al* (Figure 1.6), the intestinal perfusion method involves using a multichannel sterile tube which is able to inflate two balloons in order to section off a 10 cm section of the intestine (Lennernäs et al., 1992). Introduced orally after local anaesthetic, the sectioned off segment of intestine is exposed to the free drug perfusate. Owing to its technical complexity and reliance on human volunteers, this technique is not suitable for widespread usage, but has shown good correlation to pharmacokinetic studies including Biopharmaceutics Classification System (BCS) prediction and correlation of carrier mediated transport (Lennernäs, 1997).



Figure 1.6. Intestinal perfusion technique in man. Once the balloons are inflated, the sectioned-off area of the intestine serves as a model barrier. The closed section is then rinsed in drug-free buffer, and then the drug solution added. Intestinal integrity is measured simultaneously using the retention of a non-absorbed marker compound such as PEG 4000 (Barthe et al., 1999).

## 1.6.2. *In Vitro* Models of the Gastrointestinal Tract

### 1.6.2.1. Ussing Chamber

The Ussing chamber model (Figure 1.7) is still a mainstay of transport studies through semipermeable biological membranes, with its origins dating back over 60 years (Ussing and Zerahn, 1951). In the format of intestinal transport, a small sheet of enteric tissue is clamped between two buffer-containing chambers, which are oxygenated to aid sample viability. The test compound is then added to the donor compartment and ingress is monitored in the receiver compartment, analogous to mucosal to serosal transport. However, bidirectional transport is also possible. An advantage of the system is that it can be used for transport studies on special tissues of the GI tract. Just like TEER, electrical resistance is used to monitor the viability of the tissue sample – a short circuit indicating the integrity of the barrier (Yeh et al., 1994). As with all models, the Ussing chamber is disadvantaged by the limitations of the tissue from which the membrane was sourced.



Figure 1.7. The Ussing chamber. Two transport buffers are separated by the intestinal membrane clamped in place. The electrical resistance of the membrane is constantly monitored in order to ensure membrane integrity. The test compound can then be introduced to one compartment and its ingress monitored to the other compartment (Barthe et al., 1999).

#### 1.6.2.2. Everted Gut Sac

Just like the Ussing chamber, the everted gut sac model (Figure 1.8) is still a popular model despite the older vintage (Wilson and Wiseman, 1954). Unlike the Ussing method however, the whole of the rat intestinal tract can be used. This is excised from starved rats and transferred to oxygenated media and everted using a glass rod. Individual parts are then sectioned off with a silk suture. Whilst visual inspection and monitoring of glucose and amino acid consumption ensure viability of the sample, the test solution is then incubated with the sac for various amounts of time. As the full array of efflux transporters are present in the sample, it is possible to get kinetic data relating to this type of transport as well, and for screening for potential efflux inhibitors, which may be drugs or excipients (Barthe et al., 1998, Hubbard et al., 2015). The model can be used to examine site-specific transport depending on which part of the sac was sectioned off. Once more, such a model follows the limitations of the animal tissue from which the tissue was derived.



Figure 1.8. Everted gut sac model. Freshly excised gut sac is inverted over a glass rod and tied at both ends after introducing the test compound. The transport process can then be monitored by the appearance of the compound to the incubation medium (Barthe et al., 1999).

### 1.6.2.3. Cell Based Models

Cell based models not only reduce the burden of animal research, they are relatively simple to produce and, when grown in specifically designed plastic inserts, have well developed protocols for ease of data analysis. Due to the non-proliferative nature of small intestinal epithelial cells, the most widely accepted *in vitro* model remains cell lines of colonic origin. From these, the polarised and differentiated human adenocarcinoma (Caco-2) cells are known to express microvilli and enzymatic components resembling those of the intestinal epithelium (Wilson et al., 1990). However, this model is also not without its limitations. Cytochrome P450 and its isoforms, the enzymatic barrier to oral absorption and part of the first-pass effect, is weakly expressed in comparison to the levels observed *in vivo*, although this can be addressed using vector transfection (Hu et al., 1999). The expression of ABCB1 is also higher than that of the human colon (Englund et al., 2006). Therefore, the interpretation of Caco-2 data requires careful consideration, and studies have shown huge differences in inter-laboratory variability among data sets, with discrepancies often attributed to different culture conditions and the selection of varying cells from a heterogeneous subpopulation of cells (Walter and Kissel, 1995), amongst others. Despite these drawbacks, the Caco-2 cell line is highly regarded as the *in vitro* 'gold standard' model for drug absorption across the small intestine and remains in widespread usage, most commonly when seeded in Transwell® inserts, whereby cells are grown to full differentiation over a three week period on these semipermeable polycarbonate membranes (Figure 1.9).

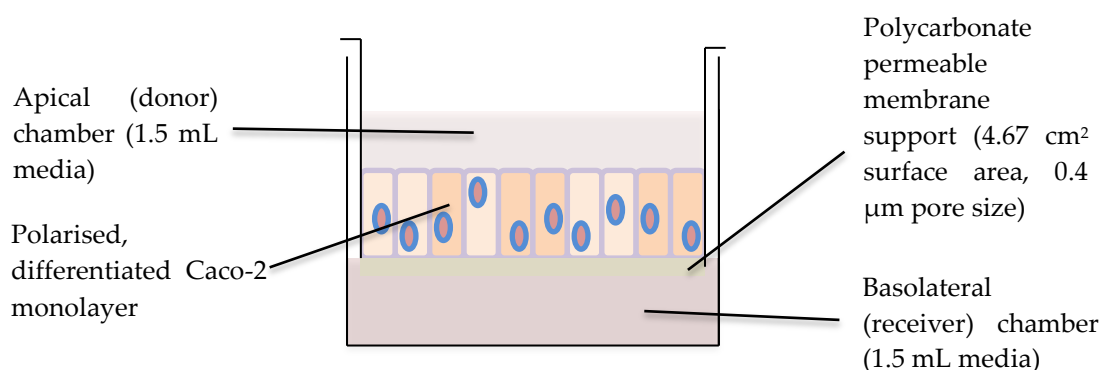


Figure 1.9. Experimental setup of Caco-2 Transwell® model. Cells are grown for 21 days to allow full differentiation. For apical to basolateral (AP to BL) transport studies, functionally analogous to mucosal to serosal transport, cells are washed in buffer and the drug-containing buffer added to the apical compartment and drug-free buffer to the basolateral compartment. Samples are then taken from the basolateral compartment at fixed intervals. For basolateral to apical (BL to AP) transport, the drug-containing solution is added to the basolateral compartment and samples taken from the apical compartment.

Following full differentiation, epithelial integrity is measured indirectly using transepithelial electrical resistance (TEER); that is, the resistance of an electrical current passed across the monolayer. By short-circuiting the membrane, interference of electrical current generated by ion transport is negligible and, therefore, follows that an increase in TEER correlated to monolayer integrity, and so a decrease in paracellular transport. By sampling the basolateral media, the progress of compound transport can be monitored and the apparent permeability coefficient ( $P_{app}$ ) calculated using Equation 1.3,

$$P_{app} = \frac{dQ}{dt} (AC_0)^{-1} \quad \text{Equation 1.3.}$$

where  $dQ/dt$  is the rate of appearance of the test compound on the basolateral side ( $\text{ng s}^{-1}$ ),  $C_0$  is the initial concentration on the apical side ( $\text{mg mL}^{-1}$ ) and  $A$  is the surface area of the monolayer ( $\text{cm}^2$ ).  $P_{app}$  has units of  $\text{cm s}^{-1}$ . Apparent permeability coefficients data obtained from Caco-2 cells have been shown to correlate to those of the human intestine (Irvine et al., 1999, Wilson et al., 1990).

A development of the Caco-2 model can be seen in the numerous subclones of the parental cell line that can also be selected for various characteristics after exposure to various compounds or early to late passage numbers. Most notably, the TC-7 subclones were selected for increased taurocholic acid transport (Caro et al., 1995). These subclones displayed higher growth rates, and higher expression of phase II metabolic enzymes, such as UDP-glucuronyltransferases, which are known to be deficient in the parental cell line. Despite functional analysis of the P-gp substrate ciclosporin transport demonstrating lower levels of this transporter, both cell lines demonstrated correlation between absorption in humans and  $P_{app}$  values *in vitro* (Grès et al., 1998).

Madin Darby canine kidney cells (MDCK), isolated by Madin & Darby (Gaush et al., 1966), rose to prominence in the field of viral research for decades in the literature, in addition to their nominal role in renal transport experiments. This cell line is heterogeneous and comes in two strains: the 'tight' epithelium MDCK I and the leaky epithelium MDCK II (Richardson et al., 1981). Later, this cell line was harnessed as a molecular barrier model for compounds of pharmaceutical interest (Cho et al., 1989), and now frequently appears in literature as such, favoured for the much shorter amount of time required in order to reach confluence compared to the 3 week growth time of Caco-2. As with the Caco-2 model, MDCK cells form polarised epithelium with brush borders and tight junctions when grown on semi permeable membranes. Despite the absence of P-gp in MDCK cells, viral transfection has been used successfully to transfer the *MDR1* gene product to the monolayers, allowing the apical expression of this transporter (Pastan et al., 1988). These are known in the literature as MDCK-MDR1 cells. Likewise, comparative research can be conducted following MRP2 and BCRP transfection, known as MDCK-MRP2 and MDCK-BCRP cells, respectively.

### 1.7. Excipient-Efflux Transporter Interactions

It has been reported that P-gp function is dependent on the maintenance of the lipid-protein interface (Callaghan et al., 1997). By increasing the water content of the membrane proteins, surfactants may interfere with the function of P-gp (Dudeja et al., 1995). Surfactants are capable of interacting with lipid bilayers and disrupting hydrogen or ionic bonding, or may insert themselves into the bilayer itself. Because of this, a large number of

surfactants have been reported to exhibit efflux transporter inhibition. However, the other ABC transporters are more deeply-embedded within the lipid membrane, allowing for a more robust function in the face of surfactant interaction (Batrakova et al., 2004). As such, the volume of literature regarding excipients with a biological effect against P-gp is, under the circumstances, considerably asymmetric when compared to that of other ABC transporters. Moreover, the latter discovery of the other ABC transporters may have produced a lag in the discovery of suitable probe substrates.

### **1.7.1. The Biological Effects of Excipients on P-gp Activity**

#### **1.7.1.1. PEGs and PEGylated Surfactants**

Polyethylene glycols (PEGs), synthetic polyethers, are amphiphilic water-soluble polymers available in a plethora of molecular weights, which are well tolerated *in vivo*. As such, PEGs and PEGylated excipients have an illustrious role in pharmaceutical formulations as plasticisers in film coating (Okhamafe and York, 1985), putative lubricants (Al-Nasassrah et al., 1998), binder augmentation (although a poor binder *per se* (Elgindy et al., 1988)), and solubility and dissolution enhancing agents in the form of solid dispersions (Geneidi et al., 1981). Lower molecular weight PEGs, such as PEG 400, are liquid, and become more solid as a function of the molecular weight, becoming waxy at 1000 Daltons (PEG 1000) and crystalline powders over 4000 Daltons (PEG 4000). Over 100,000 Daltons, the nomenclature changes to poly(ethylene) oxide (PEO). The ether bond of PEG is extremely useful in solubilising poorly soluble entities, and PEGs are often found as the hydrophilic moieties of a number of surfactants.

The paradigm of the biological effect of PEGylated excipients first appeared in the literature regarding the reversal multiple drug resistant (MDR), the phenomenon in which solid tumour cells become refractory in nature by the up-regulation of the *MDR1* gene encoding P-glycoprotein (Ueda et al., 1987). Polyethyloxlated castor oil, Cremophor EL, was shown to sensitise the MDR cell lines R100 and K562 to the chemotherapeutic drug daunorubicin (Woodcock et al., 1990). The study was later expanded using mouse P388 MDR tumour cells using the surfactants Cremophor EL, Tween 80 and Solutol HS15,

further demonstrating the efflux inhibition effects of the polyethoxylated moiety. As the implications of P-gp inhibition of PEGylated excipients became clear, further groups began testing such excipients on the absorptive tissues of the intestine. Initial *in vitro* studies on rat jejunal tissues showed the efficacy of PEGs and Pluronic P85 on increasing the serosal to mucosal (s to m) transport of the P-gp substrate digoxin (Johnson et al., 2002b). Studies during the same year established the Caco-2 cell line as a model for demonstrating the effects of excipients against P-gp, with PEG 300 (Hugger et al., 2002a), and in a later study with PEG 300, Cremophor EL and Tween 80 using the Caco-2 and MDCK-MDR1 cell line (Hugger et al., 2002b). The study found that 20 % (v/v) PEG 300 was able to completely inhibit P-gp efflux transport of Caco-2 monolayers using the P-gp –substrate anti-cancer drugs doxorubicin and taxol (Hugger et al., 2002a). In the follow-up study, the same team then used *MDR1* transfected Madin Darby Canine Kidney (MDCK-MDR1) cell line, and found that PEG 300 (20 % v/v) was again enough to achieve complete P-gp inhibition (Hugger et al., 2002b). Using the *in vitro* everted gut sac model and *in vivo* improved single pass perfusion model studies, PEG 400 has been shown to increase the permeability of the lipophilic compound ganciclovir in the range of 0.1 – 1 % (w/v). Furthermore, no regional differences were observed, and the effect was not dose-dependent (Li et al., 2011b). The role of PEG 400 as a permeability enhancer has been further supported by another study examining the role of the polymer in digoxin efflux and verapamil (VER) metabolism to test for the inhibition of cytochrome P540 3A (CYP3A) using rat jejunal tissue (Johnson et al., 2002b). The study showed that the presence of PEG 400 between 1 % and 20 % (w/v) was enough to inhibit serosal to mucosal transport of digoxin between 47 % to 64 %, respectively, and VER metabolism by 54 % to 100 %, respectively. In an extended study using a broad range of PEGs and PEGylated compounds further demonstrated the role of these compounds as efflux inhibitors. PEGs 400, 2000, 20000, monooleate, monostearate and monolaurate, in the range 0.1 – 20 % (w/v), were all shown to inhibit the efflux of the P-gp substrate rhodamine 123 (R-123) across rat intestinal membranes (Shen et al., 2006). Lipid nanocapsules, developed as a drug delivery device, have been shown to increase the level of cytotoxicity of the anticancer drug etoposide in C6, F98 and 9L glioma cell lines with increased retention of the cytotoxic compounds (Lamprecht and Benoit, 2006). A component of these lipid nanocapsules was polyethylene glycol-660-hydrostearate,

previously demonstrated as a P-gp inhibitor (Coon et al., 1991, Buckingham et al., 1995), and the phenomenon of overcoming MDR was believed to be attributed to the polymer in this case.

PEGylated surfactants were amongst the first of the excipients known to have efflux-inhibiting effects, and the mode of action is often multifaceted. Using 0.0025 – 0.01 % Tween 20 increased the sensitivity of MDR cells for a range of anticancer drugs, with specific increased accumulation of doxorubicin. RT-PCR analysis confirmed that low concentrations of Tween 20 could down-regulate the expression of P-gp in HepG2/R cells, effectively reversing MDR (Yang et al., 2012). A further study showed that Tween 20, Tween 80, Myrj 52 and Brij 30 could increase the intracellular accumulation of epirubicin in Caco-2 cells, whilst decreasing basolateral to apical efflux, and increased the mucosal to serosal absorption in rat jejunum and ileum (Lo, 2003). This study also found that the optimal hydrophilic to lipophilic balance of the compounds for increased uptake was in the range 10-17, and the optimal inhibition was observed for compounds containing polyethylene chains and intermediate chain length fatty acids and fatty alcohols.

The transport of taxol has been examined in the presence of the PEGylated surfactants Cremophor EL 35 and Tween 80 at 0.1 % (v/v) and 0.05 % (v/v), respectively, using both the Caco-2 and MDCK-MDR1 cell lines (Hugger et al., 2002b). Both excipients were inactive as inhibitors of P-gp in MDCK-MDR1 cells and only partial inhibitors of P-gp in Caco-2 cells in the concentrations used. The difference in activity was suggested to be because of the differences in the interactions of the surfactants with the different cell membranes. However, Cremophor EL 35 and Tween 80 have been shown to be full inhibitors of P-gp using ganciclovir as the P-gp substrate during *in vitro* everted gut sac and *in situ* improved perfusion model experiments, using a higher concentration range than in the previous study (0.1-1 % w/v) (Li et al., 2011b). Numerous other findings have demonstrated the inhibition of P-gp by Cremophor EL 35 (Shono et al., 2004, Rege et al., 2002, Cornaire et al., 2004) and Tween 80 (Shono et al., 2004, Li-Blatter et al., 2009, Rege et al., 2002).

Poloxamers, triblock copolymers also known as Pluronic, have also shown inhibition activity towards efflux transporters. This effect was first demonstrated using Pluronic P85 (Alakhov et al., 1996), and since then these materials have been comprehensively studied

for the structure/function relationship to P-gp inhibition. Using bovine brain microvessel endothelial cell line (BBMECs), poloxamers of differing hydrophilic-lipophilic balance (HLB) values were tested for efficacy against the efflux transporter (Batrakova et al., 2003). It was found that poloxamers with a propylene oxide between 30-60 units had the greatest impact on efflux inhibition. The most efficacious of the materials had a HLB value below 20. Poloxamers within this range showed strong membrane fluidisation tendencies alongside reduction in ATPase activity. The efficacy of poloxamers is attributed to the monomers, as activity is known to decrease after the critical micelle concentration (CMC) has been reached (Miller et al., 1997).

The amphiphilic surfactant D- $\alpha$ -tocophyheryl polyethylene glycol succinate (TPGS) has been demonstrated as a reversal agent of MDR in P-gp expressing (MDR1 transfected) G185 cells. These cells are typically resistant to the cytotoxic drugs doxorubicin, vinblastine, colchicine and paclitaxel by 27-135 fold. TPGS increased the sensitivity of G185 cells to these compounds, whilst decreasing basolateral to apical permeation in a concentration-dependent manner. This concentration was well below the critical micelle concentration of TPGS (0.02% w/w); it was suggested that this was not the method of inhibition of P-gp (Dintaman and Silverman, 1999). In agreement with this, a similar study using amprenavir, a HIV protease inhibitor and P-gp substrate, TPGS could inhibit the efflux action of P-gp to the same extent as P-gp inhibitors, such as verapamil (Yu et al., 1999). In another study, the different chain lengths of TPGS were synthesised to examine their inhibitory effects on R-123 efflux; whilst TPGS-1000 showed optimal inhibition, chain lengths between 238 and 3400 also showed notable potency as inhibitors of P-gp, with the results following Weibull distribution. Interestingly, the degradation products of TPGS-1000, vitamin E, vitamin E succinate and PEG 1000 had no effect on R-123 efflux at the concentrations used (Collnot et al., 2006). Inhibition of P-gp by TPGS has been suggested to occur by membrane rigidisation (Rege et al., 2002).

Dendrimers, also known as dendritic polymers, are multi-branched excipients that can be used as a polymeric carrier. Emanating from a central core, the branches have the potential to be functionalised or conjugated to a desired compound. The biological effects of dendrimers was first demonstrated by conjugating the P-gp substrate propranolol to

Generation 3 (G3) polyamidoamine (PAMAM) dendrimers, which resulted in an increase in the apical to basolateral transport of the drug through Caco-2 monolayers (D'Emanuele et al., 2004). In another study using the same material conjugated to paclitaxel, permeability through Caco-2 monolayers was improved 12-fold, with the basolateral to apical transport being statistically higher in the first instance, implicating the role of P-gp in paclitaxel transport (Teow et al., 2013). Conjugated to doxorubicin, G3 PAMAM has also been shown to increase the cellular accumulation of the drug in brain capillary endothelial cells (BCECs), whilst also increasing the uptake of the drug 6-fold in the *in vivo* murine model across the blood brain barrier (Cui et al., 2009).

Generation 3.5 (G3.5) and Generation 4 (G4) dendrimers were able to increase the oral uptake of the P-gp substrate camptothecin in the murine model (Sadekar et al., 2013). Interestingly the transport of mannitol was not increased, suggesting that tight junction modulation was not a significant mechanism. In contrast, dendrimers have been shown to be able to reversibly modulate tight junctions, shown by ZO-1 staining (Liu and Chiu, 2013). In another study, dendrimer G3.5 transport in Caco-2 cells was shown to be dynamin-dependent and clathrin-dependent, indicative of receptor-mediated endocytosis for transepithelial transport (Goldberg et al., 2010). In a more recent study, PEGylated Generation 5 PAMAM (G5 PEG) modified nanoliposome was used to increase the oral uptake of probucol in the *in vivo* murine model (Ma et al., 2015). In the same study, the increase was shown to be related to P-gp on the Caco-2 model, but independent of caveolae endocytosis pathway by transfecting and up-regulating expression of Caveolin 1 (Cav-1), a protein crucial to the maintenance and structure of the caveolae. These up-regulated cells showed no change in transport of probucol-G5 PEG compared to non-transfected cells. Furthermore, the transport of dendrimers through monolayers has not been shown to be temperature dependent, indicating that the polymers themselves are not P-gp substrates (El-Sayed et al., 2003).

#### **1.7.1.2. Natural Polymers**

In the only study of natural polymers on the inhibition of efflux transporters, the anionic xantham gum and gellan, and sodium alginates flavivam and ascophyllum have been

shown to accumulate the P-gp substrates vinblastine and doxorubicin in the everted gut sac model (Carreno-Gomez and Duncan, 2002).

#### **1.7.1.3. Cyclodextrins**

Cyclodextrins, enzymatically modified starches, have the ability to form inclusion bodies which increases the solubility of lipophilic drugs (Goole et al., 2010). The most potent compound of the class at forming these inclusion bodies is 2, 6-di-0-methyl- $\beta$ -cyclodextrin (DM- $\beta$ -CyD). This compound has shown a strong ability to inhibit the efflux capacity of P-gp, and thus increase the apical to basolateral permeation of 2P,7P-bis(2-carboxyethyl)-5(6)-carboxyfluorescein (BCECF), a P-gp and MRP2 substrate. Furthermore, DM- $\beta$ -CyD was demonstrated to remove MRP2 and P-gp from the apical membrane into the buffer, whilst decreasing the level of cholesterol in the membrane (Yunomae et al., 2003). The same compound was also shown to increase the oral bioavailability of the poorly water-soluble drug ciclosporin by inhibiting these efflux transporters (Oda et al., 2004).

#### **1.7.1.4. Lipid Excipients**

Few studies have been conducted on the biological effect of lipid excipients. Peceol and Gelucire 44/14 have been shown to be able to inhibit P-gp at concentrations below 0.5 % (v/v) to a comparable level to that of verapamil, a known P-gp inhibitor, in Caco-2 monolayers. Using Western blot, it was revealed that this inhibition was by reduced down-regulation of *MRD1* gene expression (Sachs-Barrable et al., 2007).

#### **1.7.1.5. Thiomers**

Thiomers are surfactants that utilise the thiol component of their structure in much the same way the PEGylated moiety, and these polymers can also have a biological effect. Interestingly, these materials have been shown to have higher efficacy in comparison to Pluronic P85 (Greindl et al., 2009), one of the most potent modulators of P-gp mediated transport (Batrakova et al., 2003). The functional efficacy of thiomers is related to molecular mass and degree of thiolation (Grabovac et al., 2015).

### **1.7.2. The Biological Effect of Excipients on MRP2 Activity**

Although the effects of many excipients on the P-gp transporter are now well established in the literature, the same cannot be said for their effect on MRP2. The first mention in

literature appears in a study comparing several non-ionic surfactants on their propensity to inhibit efflux of the probe substrates of P-gp (rhodamine 123, R-123) and MRP2 (5-chloromethylfluorecein, CMF) using the transfected MDCK cell line (Bogman et al., 2003). Although this study provides perhaps one of the first attempts at pharmacokinetic categorisation of the effects of excipients against these transporters, the authors acknowledge that cellular damage may have been a contributing factor to the damage of intracellular esterase, known to convert the prodrug CMFDA into the fluorescent compounds, and prevented the establishment of data relating to ABCCC2 transporter system. Another group demonstrated the efficacy of Cremophor EL and PEG 2000 on the ABCC2 transport system on the Caco-2 cell line (Li et al., 2013a), later expanding the study to include Cremophor RH and poloxamer 407 (Li et al., 2014b). Additionally, thiolated poly(acrylic) acid-cysteine polymers have been shown to have a biological effect against MRP2 mediated transport (Greindl et al., 2009). Taken together, these studies are the extent of the knowledge of biological effects of PEGylated excipients on the MRP2.

### **1.7.3. The Biological Effects of Excipients on BCRP Activity**

Information on the biological effects of these excipients against BCRP has an equally sparse footing in the literature as those against MRP2, and is dominated by a single group. Yamagata *et al* tested the effects of Pluronic P85 and Tween 20 on the mouse model (Yamagata et al., 2007b). In the presence of both excipients, the bioavailability of topotecan was increased in wild type mice but not BCRP knockout mice. In the same set of experiments, the mucosal to serosal absorptive transport was monitored in everted mouse ileum; once more uptake was only increased in wild type ileum and not those of the BCRP knockouts (Yamagata et al., 2007b). Using MDCKII-BCRP cells, Tween 20 and Pluronic P85 were shown to reversibly modulate the transport of the BCRP substrate mitoxantrone. Interestingly, the effects of P85 diminished at high substrate concentration, implying that the mechanism of action of this excipient may be competitive; the same result was not seen for Tween 20, which was believed to be non-competitive or mixed type (Yamagata et al., 2009). The excipient set was then diversified to a number of different surfactants, and it was found that Cremophor EL, Span 20, Brij 30, in addition to P85 and Tween 20, were able to increase the uptake of mitoxantrone in MDCKII-BCRP cells. Interestingly, intracellular ATP levels were not altered (Yamagata et al., 2007a).

## 1.8. Model Substrate Drugs and Fluorescent Probe Substrates

In order to develop an assay to study the efflux transporters, consideration must be taken to known substrates and the specificity of each. In this respect, fluorescent molecules that are probes of efflux transporters are held in high merit for their ability to aid high-throughput, without the need for lengthy analytical techniques, such as High Performance Liquid Chromatography (HPLC). Similarly, any assay screening for efflux inhibition must first be validated against known modulators of the transporters of interest.

### 1.8.1. Rhodamine 123 and 5 (6)-Carboxy-2',7'-dichlorofluorescein

The P-gp substrate rhodamine 123 (R-123, Figure 1.10a) and the MRP2 substrate 5(6)-carboxy-2',7'-dichlorofluorescein (CDF, Figure 1.10b), are both widely employed to probe activity of their respective efflux transporters. R-123 is able to enter the cell via direct diffusion across membranes, whereas, CDF is unable to directly cross membranes and so is used for assay studies as the promoiety 5(6)-carboxy-2',7'-dichlorofluorescein diacetate (CDFDA, Figure 1.10c), which is freely able to diffuse across membranes. Once inside the cell, this prodrug is converted to a highly fluorescent array of compounds, chiefly CDF, which can only escape the cell via the MRP2 transporter (Zamek-Gliszczyński et al., 2003). It is the innate fluorescence of these two entities that helps facilitate rapid high-throughput screening of P-gp and MRP2 transporter activity.

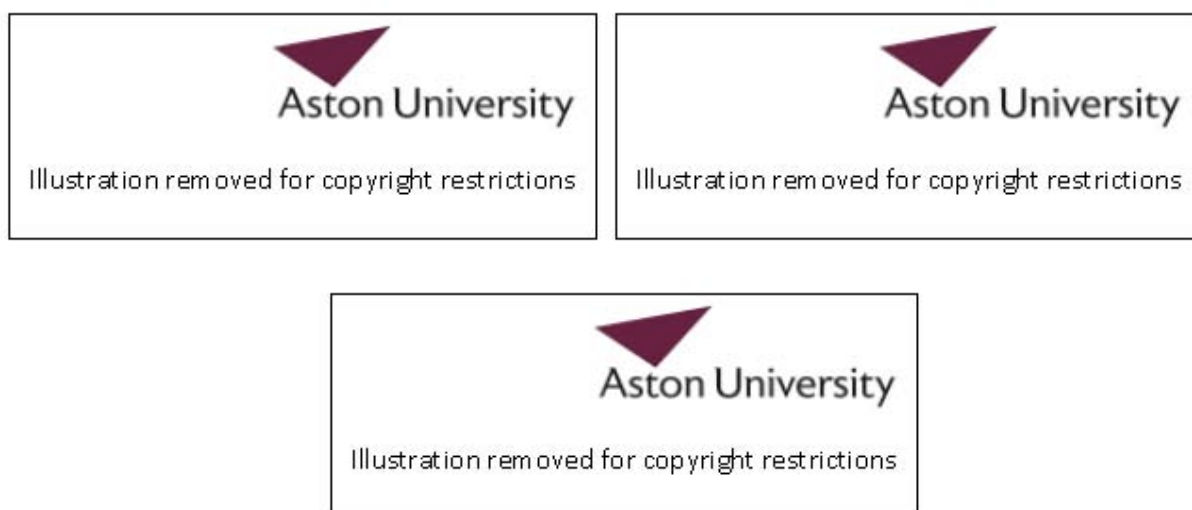


Figure 1.10. The chemical structures of A) rhodamine 123, B) 5(6)-carboxy-2',7'-dichlorofluorescein and C), the 5(6)-carboxy-2',7'-dichlorofluorescein promoiety 5(6)-carboxy-2',7'-dichlorofluorescein diacetate.

At low concentrations, the uptake of R-123 has been shown to be a saturable process that can be inhibited by the organic anion-transport (Oat)1a4 substrates digoxin, quinine, amongst others, in the rat model. Oat1a4 is orthologous to human OATP1A2, suggesting the potential of active uptake of the fluorescent probe (Annaert and Brouwer, 2005). CDF also appears to be a substrate of Oatp1 transporter system (Zamek-Gliszczyński et al., 2003). However, the contribution of Oat transporters as a whole on fluorescent dye transport is negligible. The Michaelis-Menten constant ( $K_m$ ) for Oatp-mediated transport of R-123 is 0.3  $\mu\text{M}$ , with a  $V_{\text{max}}$  of 6.8  $\mu\text{M}$  (Annaert and Brouwer, 2005). For P-gp-mediated active transport, the  $K_m$  is 17.5  $\mu\text{M}$  and the  $V_{\text{max}}$  is 20.4  $\mu\text{M}$  (Forster et al., 2012).

At higher concentrations, the uptake of R-123 is by passive diffusion. As an amphiphilic molecule, R-123 is able to traverse the lipid bilayer by rare inversions known as 'flip flop' events. R-123 excluded by P-gp is free to continuously re-enter the cell by a process in which the hydrophobic elements of the compound initially bind to the acidic head groups of the phospholipids. The efflux of R-123 by P-gp is mediated by pairs of the probe binding simultaneously to the protein (Wang et al., 2006). Although MRP1 has been suggested to have a role in R-123 transport (Daoud et al., 2000), expression of this efflux transporter is low on the Caco-2 cell line (Prime-Chapman et al., 2004), suggesting a negligible contribution of the transporter, and hence specificity of the probe to P-gp. Only mutated BCRP is capable of transporting R-123 whilst the wild-type BCRP cannot (Honjo et al., 2001). A summary of the transport of these probes is presented in Figure 1.11.

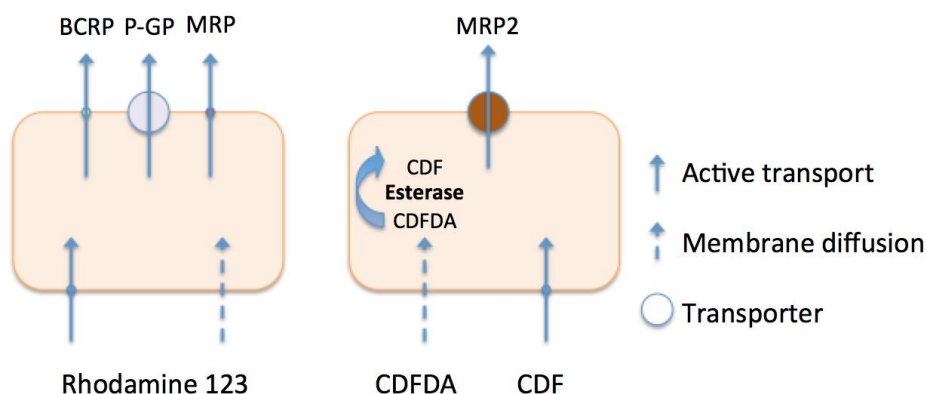


Figure 1.11. Schematic diagram of the uptake of the fluorescent probe substrates. The relative contribution of BCRP and MRP1 in the transport of R-123 is assumed negligible on the Caco-2 cell line. However, the influx transporter OATP cannot be excluded in the ingress of R-123 and CDF.

### 1.8.2. Inhibitors of P-gp Efflux

Verapamil (VER, Figure 1.12) is an L-type calcium channel blocker used in the treatment of hypertension. The ability of this drug to overcome MDR was first noticed in the 1980s (Tsuruo et al., 1981). However, this drug proved useless as an inhibitor *in vivo* due to the unacceptable levels of toxicity attributed to the high serum levels required to achieve efflux inhibition. From the potential usage in efflux assays, VER is one of the most commonly used inhibitors of P-gp in the literature (Burton et al., 1993). Used in conjunction with R-123, VER is a powerful tool for assessing the P-gp functionality of a cell line. VER is a known substrate of P-gp, but is able to traverse the cell membrane rapidly with an apparent permeability ( $P_{app}$ ) value of  $12.6 \times 10^{-6} \text{ cm s}^{-1}$  (Pauli-Magnus et al., 2000), which is able to quickly saturate the transporter and render it ineffective at the transport of other compounds. VER has been shown to be a non-competitive inhibitor, suggesting that P-gp has separate binding sites for both R-123 and VER (Wang et al., 2006).



Figure 1.12. The chemical structure of verapamil hydrochloride, the most widely utilised form of the drug.

Ciclosporin (CsA, Figure 1.13) is an immunosuppressant drug commonly used to prevent allograft rejection after transplant. Much like VER, CsA has long been known as an inhibitor of MDR (Slater et al., 1986) yet failed to translate into the clinical setting due to toxicity issues. CsA, like VER, interferes with substrate-recognition by second-site binding (Tamai and Safa, 1991), yet CsA is a better inhibitor of taxol and colchicine resistance, whereas VER is a superior inhibitor of vinblastine and daunorubicin transport, all P-gp substrates (Cardarelli et al., 1995), suggesting subtle but different affinities in binding site. The multi-faceted transport of P-gp gets even more convoluted by the fact both VER and

CsA are competitive inhibitors of each other, implying a common binding site, or sites (Naito and Tsuruo, 1989).



Figure 1.13. The chemical structure of ciclosporin.

### 1.8.3. Inhibitors of MRP Efflux

Indometacin (IND, Figure 1.14) is a member of the non-steroidal anti-inflammatory (NSAID) group of drugs. Although IND contains two carbonyl groups of the carboxylic and amine moieties which are polar and therefore capable of hydrogen bonding, the large nature of the molecule and the hydrophobic ring system makes IND practically insoluble in water. Under the BCS, indometacin is a class II compound, meaning that it has low solubility but high permeability (Löbenberg and Amidon, 2000).



Figure 1.14. The chemical structure of indometacin.

In addition to being a model Class II compound, IND and probenecid (PBD), a uricosuric and renal tubular transport blocking agent (Figure 1.15), are known inhibitors of organic anion transporters such as the MRP family of efflux proteins (Holló et al., 1996, Feller et al., 1995). Moreover, the degree of expression of the various MRPs has been discussed, and the relative efflux contribution of each is negligible when compared to the higher expression profiles of the MRP2 transporter on the Caco-2 cell line.



Figure 1.15. The chemical structure of probenecid.

#### 1.8.4. Paracetamol

Paracetamol, also known as acetaminophen (APAP, Figure 1.16), is an analgesic typically used to treat pain and pyrexia. APAP is a poor choice as an efflux substrate as it is not a well-defined ABCB1 or ABCC2 substrate, and is able to rapidly cross the membrane with a  $P_{app}$  value of  $23.7-100 \times 10^{-6} \text{ cm s}^{-1}$  (Yamashita et al., 2000, Irvine et al., 1999) on the Caco-2 model. Additionally, APAP has roughly 80 % fraction absorbed in humans (Irvine et al., 1999). However, owing to its low toxicity, APAP is commonly used in early phase tablet formulation development.



Figure 1.16. The chemical structure of APAP.

### 1.8.5. Ibuprofen

Ibuprofen (Figure 1.17) is another member of the NSAID group of drugs. The uptake of ibuprofen is almost complete in humans, with the fraction absorbed around 95 % (Zhao et al., 2001). Furthermore, ibuprofen has a  $P_{app}$  value between  $5.64\text{-}6.98 \times 10^{-5} \text{ cm s}^{-1}$ , and is not described as a substrate for efflux (Faassen et al., 2003, Hellinger et al., 2010). However, the drug is known for its high degree of cohesion, resulting in poor flow properties as well as bad compaction (Rasenack and Müller, 2002), in addition to having a bitter taste (Gryczke et al., 2011). Therefore, ibuprofen is an excellent candidate as a model drug for coating trials.



Figure 1.17. The chemical structure of ibuprofen.

## 1.9. Orally Disintegrating Tablets

### 1.9.1. Overview

The Noyes-Whitney equation describes how surface area, amongst other factors, can be optimised to increase the rate of drug dissolution, and therefore absorption. One strategy to rapidly increase surface area, and thereby accelerate dissolution and enhance drug uptake, is to formulate an orally disintegrating tablet (ODT) (Shangraw et al., 1980). As ODTs require no water for administration, they are easy to administer and are ideal dosage formulations for medical conditions where severe nausea and vomiting is common, such as migraines, where an ordinary dosage formulation may be partially or completely expelled. Additionally, faced with the extreme cost and length of time taken to take a new chemical entity (NCE) to the market, many companies have considered new methods of administration of old drugs, which can combine recent advances in excipient or manufacturing technologies, coupled with extension of patent life.

One major application of the ODT is for patients with difficulty swallowing. Dysphagia is a common condition prevalent in around 35 % of the population in general and an additional 40 % of geriatric patients, and often, tablet size and taste play a role in tablet acceptance (Sastry et al., 2000). Recent progress has been made on ODTs which have the ability to disintegrate within the oral cavity, without access to water. Such formulations have even been shown to increase bioavailability of the drug by increasing the rate of dissolution on human trials (Ahmed and Hassan, 2007).

### 1.9.2. Formulation Strategies for Making ODTs

Three general techniques exist for the production of ODTs currently on the market (Table 1.1). These are:

- Freeze Drying
- Moulding
- Direct Compression

Table 1.1. Overview of commonly used production techniques, marketed formulations and associated advantages and disadvantages.

<i>Production Technique</i>	<i>Marketed Example</i>	<i>Advantages</i>	<i>Disadvantages</i>
Freeze-drying	Imodium® Instants - 2mg Loperamide hydrochloride	Immediate Dissolution	Incompatible with water soluble drugs Poor hardness
Moulding	Ralivia FlashDose® - 50 mg Tramadol	Fast Dissolution	High production costs Low strength
Direct Compression	Nurofen® Meltlets - 200 mg ibuprofen	Standard Equipment Low production cost	Disintegration and porosity reliant upon excipient choice

#### 1.9.2.1. Freeze drying

Freeze-drying, known also as lyophilisation, is one of the most common techniques. In this method, the formulation is frozen below -18 °C, and decreased pressure removes the solvent from a frozen solution containing infrastructure-forming excipients (Nail and Gatlin, 1993). The resulting dosage forms are highly porous with a large surface area,

allowing rapid dissolution and disintegration. This technique is particularly useful for heat-sensitive APIs. Zydis<sup>®</sup> was the first of the freeze-dried ODTs, and the system favours drugs with low water solubility or complete insolubility as they are reluctant to form eutectic mixtures during the freezing process (Seager, 1998). Although disintegration times are regarded as excellent, freeze-dried ODTs are often fragile, requiring specialised packaging that adds to the manufacturing costs (Chang et al., 2000). However, the bulking agent can reach a glassy state, which can also be imparted on to the API to form amorphous drug.

### **1.9.2.2. Moulding**

Moulded ODTs can be prepared in two ways. Compression moulding as the name suggests, involves compressing a powder mixture that has been softened with a solvent (typically water or ethanol). The second variation on this technique involves dissolving the drug in a molten matrix, known as heat moulding. The outcome of both techniques is a solid dispersion. The drug in these dosage formulations can remain in discrete particles or microparticles. If the drug is completely dissolved in the matrix, it is known as a solid solution, although it can also exist partially dissolved in the carrier. As these tablets are much less compact compared to compressed tablets, they have favourable porosity characteristics. Conversely, moulded tablets suffer from poor mechanical strength, although this can be addressed by adding binders such as sucrose, acacia or polyvinylpyrrolidone to the solvent phase (Chang et al., 2000).

### **1.9.2.3. Compression**

Whilst freeze-drying and moulding are effective in porosity forming, fast disintegrating tablets, the technology remains expensive and time consuming, requiring special equipment. Tablets made by freeze drying often exhibit poor mechanical strength. Therefore, direct compression is the most commonly used manufacture method for ODTs as it utilises existing techniques and excipients with a low number of processing steps, whilst allowing high API doses to be incorporated. For directly compressed tablets, disintegration is largely based on the choice of disintegrant(s).

### 1.9.3. Role of Disintegrants in Directly Compressed ODT Systems

The role of disintegrant excipients is to break the tablet upon contact with water. The ingress of water is essential for overcoming the binding properties of the tablet. This is typically achieved by wicking or swelling (Kornblum and Stoopak, 1973). Disintegrants are generally water-insoluble components, and ideally swelling does not lead to gel formation that may impede the access of water to the tablet.

Several main disintegrants and the veritable ‘superdisintegrants’ exist on the market (Table 1.2). Crospovidone (cross-linked polyvinylpyrrolidone), is commonly known by the marketed name Kollidon, produced by BASF, and come in a range of particle sizes. Polyplasdone is also crospovidone produced by ISP. Ac-Di-Sol is composed of cross-linked carboxymethylcellulose, and Primojel is composed of cross-linked carboxymethylation (Quadir and Kolter, 2006).

Table 1.2. Overview of commonly used disintegrants and their particle size.

<i>Disintegrant</i>	<i>Brand</i>	<i>Particle Size (<math>\mu\text{m}</math>)</i>
Crospovidone	Kollidon CL	110-130
	Kollidon CL-F	20-40
	Kollidon CL-SF	10-30
	Kollidon CL-M	3-10
	Polyplasdone XL	100-130
	Polyplasdone XL-10	30-50
Croscarmellose sodium	Ac-Di-Sol	49
Sodium Starch Glycolate	Primojel	41

For direct compression, the choice of disintegrant depends upon the formulation and preparation techniques. Crospovidone has been used at 2.5-8 % (w/w) (Okuda et al., 2012), 5 % (w/w) (Mishra et al., 2006) and 7 % (w/w) (Shu et al., 2002). In one study, it was found that increasing the level of crospovidone from 4 to 12 % (w/w) had no impact upon disintegration time ( $p > 0.05$ ), although wetting time increased significantly ( $p < 0.05$ ) with increased levels (Okuda et al., 2012). At 3 % (w/w), crospovidone of various grades (Kollidon CL, CL SF, CL M and CL F) were found to be superior to croscarmellose sodium and microcrystalline cellulose, with disintegration times under 30 seconds in comparable

formulations (Amelian and Winnicka, 2012). More recently, crospovidone has been optimised at 4 % to produce satisfactory tablets for a disintegration time of 33 seconds for directly compressed tablets of montelukast sodium (Usmani et al., 2015). However, in another study, croscarmellose sodium was found to be superior to crospovidone as well as sodium starch glycolate (Amrutkar et al., 2007), highlighting the importance of disintegrant selection in formulation evaluation.

Microcrystalline cellulose (MCC) is semi-depolymerised cellulose commonly used as an excipient under the brand names Emcocel, Vivacel, and more commonly Avicel. MCC is the most common of the cellulose-based excipients, and exhibits good binding properties owing to its plastic deformation under pressure that occur through hydrogen bonding to adjacent MCC particles (Al-Khattawi and Mohammed, 2013). Using direct compression, MCC and low-substituted hydroxypropyl cellulose (L-HPC) used as disintegrants have shown quick disintegration time in the ratio 8:2-9:1 (Watanabe et al., 1995). This study demonstrated the feasibility of using MCC for ODTs, and remains one of the earliest examples in literature. Tablets containing Avicel PH-101 grade have been shown to exhibit superior hardness although with slower disintegration time compared to Avicel PH-102 when made under direct compression (Lahdenpää et al., 1997). As such, PH-102 grade is generally favoured due to flow properties. Tablets produced using this grade of MCC have been shown to be sensitive to magnesium stearate content up to 1 %, although not significantly. Disintegration time was unaffected by the presence of the lubricant (Mitrevej et al., 1996). In orally disintegrating tablets, MCC has been shown to have a gritty mouth feel, and this can be eliminated using fine particle size PH-M (Ishikawa et al., 2001). Further micronisation of MCC is possible; PH-M-06, with a lower particle size of 7 µm, was found to be superior to PH-102 in terms of mouth feel.

#### **1.9.4. Taste Masking**

Taste masking is also an important factor in ODT development. In one study, 90 % of paediatricians have reported that taste was a major barrier in patient compliance (Milne and Bruss, 2008). As ODTs rapidly disintegrate, they deliver the active substance directly to the tongue and, therefore, the taste buds, making taste masking an important issue for the formulation. Several techniques have been employed for taste masking purposes, including

but not limited to complexation (Dinge and Nagarsenker, 2008), hot melt extrusion (Gryczke et al., 2011), microencapsulation and traditional sweeteners. Of the latter, sugar-based materials are highly favoured as they are highly soluble in water, so dissolve quickly in saliva. Mannitol is one of the most common of the sugars used in this process and is known for its pleasant taste and cool mouth feel. Similarly, aspartame and citric acid are commonly used, as are other recognised flavours such as lemon and strawberry. Those extreme tastes that cannot be covered using sweeteners require encapsulation to ensure the drug does not undergo dissolution in proximity to the tongue. However, the choice of taste masking is important as not to interfere with the existing tablet dynamics, such as disintegration time, and the amount of additional taste-masking materials must be kept low to prevent excess gains in tablet weight and size.

#### **1.9.5. Assessment of ODT Physical Characteristics**

The time taken for a tablet to disintegrate underlies the ODT formulation process. The disintegration test is designed to mimic the conditions of the mouth, and the FDA recommends a disintegration time of 30 seconds or less based on the USP disintegration test (McLaughlin et al., 2009). Using USP 30 apparatus (Figure 1.18) the tablet is placed in the disintegration tube within the basket assembly and the time for the tablet to pass through the mesh is recorded whilst the basket is raised and lowered. The disintegration medium is held at  $37 \pm 2$  °C.



Figure 1.18. Overview of the disintegration equipment. Tablets are added to the cylinder whilst the basket assembly is in motion in warmed disintegration media. The time taken for the tablet to pass through the mesh is then recorded as the disintegration time. Disks, as required, are placed on top of the tablet to aid disintegration but may interfere with tablets that are gel-forming in nature (USP, 2012b).

Hardness is an important characteristic for production, post-production processing such as coating, and maintaining a consistent dissolution profile. Typically hardness is conducted by crushing the tablet diametrically between two metal plungers on equipment which has been routinely calibrated (USP, 2012c). If the tablet is too hard, it may not undergo desired disintegration or drug dissolution; conversely a tablet too low in hardness will not survive processing. However, no restrictions are placed on hardness acceptably that must be established during the tablet formulating stage.

Friability is a measure of tablet strength and indicates how a tablet may behave during processes and transport post-manufacture. The USP standard test is 100 revolutions in a friabilator at 25 RPM (Figure 1.19).



Figure 1.19. Overview of Friability Equipment. Tablets are weighed, added to the equipment and rotated at 25 rpm for 4 minutes. The tablets are then removed, brushed clean and then reweighed. Percentage friability is then calculated (USP, 2013).

Tablets are weighed before and after the procedure and the friability, expressed as a percentage, is calculated based on Equation 1.4,

$$F = 100. \left( \frac{1 - w}{w_0} \right) \quad \text{Equation 1.4}$$

where  $F$  is the percentage friability,  $w_0$  is the collective weight of the tablets before testing and  $w$  is the weight of the collective tablets after testing. For ODTs, friability regulations follow the 1 % recommended for all non-coated tablets produced via direct compression (USP, 2013).

### 1.10. Thesis Aim and Objectives

Due to the role in limiting the ingress of compounds through epithelial barriers, the collective efflux transporter system is of interest from the pharmacodynamic and pharmacokinetic perspectives in anticipating the behaviour of a drug *in vivo*. The interaction of commonly used excipients with intestinal efflux transporters has come under increasing attention, as formulation scientists seek innovative ways to improve the absorption of pharmaceutical compounds displaying low bioavailability. Whilst literature is already enriched with keynote examples of materials that have a biological effect, few are quantified or appropriately modelled, allowing scope for augmentation of existing knowledge whilst exploring the vast quantities of materials still awaiting evaluation. Combining the information provided by Noyes-Whitney (Equation 1.1), whereby an increase in surface area (e.g. rapid disintegration times) can increase the rate of dissolution, and the bioavailability formula (Equation 1.2) showing how an increase in any fraction propagates through the equation to result in an increase in overall bioavailability, indicates how a superior oral dosage formulation can be produced.

The review of the existing literature reveals an extensive yet disparate list of excipients that elicit an effect against the ABC efflux transporters, chiefly P-gp. Such information is rarely quantified in the kinetic terms that could be of use to a formulation scientist wishing to increase the bioavailability of drugs that fall victim to efflux.

As such, the central aim of this thesis is to develop and validate a high-throughput screening assay to detect and quantify the effects of commonly used excipients against the ABCB1 and ABCC2 efflux transporter systems, and to utilise this knowledge to design and manufacture an oral dosage platform with the capability to achieve enhanced delivery of drugs with poor bioavailability. In order to achieve this, a number of objectives must be met.

- The first is the development and validation an *in vitro* high-throughput screening assay using the Caco-2 model for the detection of commonly used excipients with a biological effect against ABCB1 and ABCC2. The development of such an assay requires careful consideration of the types of model drugs and probes. The

specificity and kinetics of the probes needs to be carefully considered, in addition to their routes of ingress through the model.

- The second objective is the additional development of modelling techniques, which can quantify this data in such a way to predict the quantity of material needed in order to elicit such a desired effect, whilst establishing a framework from which the data can be compared to known inhibitors of the efflux transporters. This objective requires the careful consideration of commonly used inhibitors of the respective efflux transporters.
- The third and final objective is the design and manufacture of an ODT delivery system incorporating the theoretical content of biologically active material in order to elicit the appropriate biological effect *in vivo*. Once more, the challenges in developing an ODT must first be understood if this objective is to be achieved.

## **Chapter 2**

### Materials and Methods

## 2. Materials and Methods

### 2.1. Materials

Caco-2 cells were purchased from Public Health England and used at passage numbers 49-55. L-Glutamine, Foetal Calf Serum (FBS), Hank's Balanced Salt Solution (HBSS), Penicillin-Streptomycin, Dulbecco's modified Eagle's medium (DMEM), and non-essential amino acids (NEAA) were purchased from BioSera (East Sussex, UK). 0.5 % trypsin-EDTA, indometacin (IND), Lucifer yellow (LY), rhodamine 123 (R-123), 5(6)-carboxy-2',7'-dichlorofluorescein diacetate (CDFDA), MTT, Pluronic® F127 (poloxamer 407), Tween® 80, Tween® 20, PEG 400, PEG 4000, PEG 8000, PEG 12000 and PEG 20000 were purchased from Sigma Aldrich (Dorset, UK). Capmul® MCM, Capmul® MCM C8-2, Capmul® PG-12, Capmul® PG-8, Acconon® C-44 and Acconon® MC-8 were a kind gift from ABITECH Corporation (Columbus, USA). Poloxamer 182, Span 20, Arlatone TV, Crovol A-70, Etocas 29, Brij S-10, poloxamer 184, Etocas 40, Brij CS-12, Acconon C-44, NatraGem S140, Acconon MC8-2, Cetomacrogol 1000, Myrj S-40, poloxamer 335, Myrj S-100 and poloxamer 188 were kind gifts from Croda (Goole, UK). Crospovidone Kollidon® CL, CL-F, CL-SF and CL-M were a kind gift from BASF (Ludwigshafen, Germany). Microcrystalline cellulose (MCC) Avicel® PH-102 was purchased from FMC (Cork, Ireland). Mannogem® 2080 mannitol was a kind gift from SPI Pharma (Lewes, USA). Granular acetaminophen (APAP) Compap™ PVP3 was obtained from Mallinckrodt Pharmaceuticals (Dublin, Ireland). Poloxamer 407 and ETHOCEL™ Ethylcellulose 7 FP were obtained from DOW (Midland, USA). Compritol® 888 ATO was a kind gift from Gattefossé (Saint-Priest, France). Kollicoat IR was obtained from BASF (Alabama, USA). POLYOX™ N-10, Starch 1500® and StarCap 1500® were obtained from Colorcon (Harleysville, USA). In order to compare the tablets to existing marketed formulations, Nurofen® Meltlets (Reckitt Benckiser), Calpol® SixPlus Fast Melts (McNeil Products Ltd) and Imodium® Instant (McNeil Products Ltd) were purchased over the counter.

## **2.2. *In Vitro* Methods for the Detection of Efflux Inhibition**

### **2.2.1. Initial Screening Protocol: The *In Vitro* Caco-2 Transwell® Model**

The Caco-2 model is well known for being the 'gold standard' workhorse of cell based *in vitro* drug transport. With this in mind, the project started with the development of a protocol for using the Transwell® model. This model takes 21 days for full differentiation, and is both time and resource heavy. In addition, there are multiple routes by which a molecule can pass through the monolayer, and consequently the model has to be carefully validated and cellular damage excluded from data.

#### **2.2.1.1. Stock Solutions**

As IND concentrations as high as 500 µM has previously been shown to lead to consistent and reproducible damage to Caco-2 monolayer integrity (Tang et al., 1993), the drug concentration for all studies was kept at or below 100 µM. Drug stock solution was prepared overnight in HBSS the absence of solvents prior to experimentation and filtered. The excipient solutions were made up fresh before use.

#### **2.2.1.2. General Cell Protocol**

Due to the non-proliferative nature of small intestinal epithelial cells, the most widely accepted *in vitro* model remains cell lines of colonic origin. From these, polarised and differentiated adenocarcinoma (Caco-2) cells are highly regarded as the *in vitro* 'gold standard' as a model for the small intestine, expressing microvilli and enzymatic components resembling those of the intestinal epithelium (Wilson et al., 1990). Caco-2 cells from frozen stock were grown in 75 cm<sup>2</sup> (T75) vented flasks at 37 °C in 5 % CO<sub>2</sub> with 90 % relative humidity in Dulbecco's modified Eagle's medium (DMEM) supplemented with 10 % foetal bovine serum (FBS), 1 % non-essential amino acids (NEAA), 2 mM L-glutamine and 1 % penicillin-streptomycin (pen-strep). Media was renewed every 48 hours.

#### **2.2.1.3. Transwell® Protocol for Differentiated Caco-2 Monolayers**

The cells were harvested after reaching 80 – 90 % confluency within the T75 flasks, the optimal level for enhanced P-gp expression in long term cultures (Anderle et al., 1998) using trypsin-EDTA (3 mL, 0.5 % trypsin w/v). The basolateral compartment of each insert was filled with 2.5 mL of media and allowed to equilibrate in the incubator whilst the cells

were being split. These cells were then seeded onto the apical fascia of six well Transwell® inserts (0.4 µm pore size, 24 mm diameter), to a density of  $2 \times 10^5$  cells per well. Cell media was replaced every 48 hours (1.5 mL apical, 2.5 mL basolateral).

#### **2.2.1.4. Indometacin Permeability through Caco-2 Monolayers**

In order to study the transport of IND as a probe substrate, its transport *in vitro* must be carefully examined. After 21-25 days post-seeding, confluence was confirmed by ensuring the transepithelial electrical resistance (TEER) values exceeded  $400 \Omega \cdot \text{cm}^2$  (in practice, all monolayers initially exceeded  $500 \Omega \cdot \text{cm}^2$ ) adjusted for membrane resistance, using a Millicell® ERS device (Millipore, MA, USA) before and after each study, previously demonstrated to correlate with the formation of established tight junctions, established in fresh DMEM (pH 7.4 at 37 °C). To exclude the influence of a pH gradient on the passive transport of IND (pH hypothesis) all apical and basolateral solutions were buffered using 25 mM HEPES (pH 7.4 at 37 °C).

#### **2.2.1.5. Apical to Basolateral Concentration-Dependent Transport of Indometacin**

As a transport protein, P-gp is governed by Michaelis-Menten kinetics. The key parameters to determining the substrate concentration are the  $V_{\text{max}}$ , the maximum output of the system, and Michaelis-Menten constant ( $K_m$ ), the substrate concentration required to achieve the rate of half of  $V_{\text{max}}$ . In order to obtain excellent detectability, the IND concentration must be sufficiently high, yet not as high as to saturate the transporter. Above the  $K_m$ , any efflux inhibition will be more difficult to detect as transporter is effectively fully inhibited and the drug is able to pass through the monolayer without ATP-driven repulsion back to the apical compartment of the Transwell®. At higher concentrations still, toxicity imparted by the drug may occur. As such, the movement of drug from the apical to basolateral (AP-BL) chambers was examined over a drug concentration range from 10 – 100 µM. Cells were twice washed in HBSS to remove FCS and incubated for 30 minutes in fresh HBSS. The Transwell® inserts were then randomised to new clusters in fresh 6-well plates and DMEM-HEPES was added to the basolateral receiver compartment (2.5 mL). The medium containing the drug was added to the apical side (1.52 mL) to initiate the experiment, and the initial apical concentration was determined by sampling 200 µL from the apical well, functionally analogous to the intestinal lumen. The cells were then incubated at 37 °C on an

orbital shaker with 100 RPM rotation to ensure agitation of the cell-drug boundary layer. Sample aliquots (200  $\mu\text{L}$ ) were taken at set time intervals from the basolateral compartments, to be replaced by an equal volume of pre-warmed drug-free DMEM-HEPES.

#### **2.2.1.6. Basolateral to Apical Transport of Indometacin**

The ratio of the  $P_{\text{app}}$  values in the basolateral to apical (BL-AP) and apical to basolateral (AP-BL) gives an indication as to the degree of efflux a drug is subjected to. This is known as the efflux ratio. For BL-AP concentration-dependent uptake studies, various concentrations of drug-containing DMEM-HEPES (10-100  $\mu\text{M}$ ) were added to the basolateral compartment. The experiments were initiated by adding fresh DMEM-HEPES to the apical compartment. This was sampled at discrete time points and replaced using fresh DMEM-HEPES.

#### **2.2.1.7. Permeability of Indometacin in the Presence of the PEGylated Excipients PEG 400, PEG 8000, POLYOX™ N-10 and Poloxamer 407**

As P-gp resides on the apical compartment of intestinal cells, any excipients that inhibit this efflux transporter will increase the permeability in the apical to basolateral (AP-BL) direction of transport. The AP-BL permeability of IND in the presence of various concentrations of the respective excipients, representing intestinal lumen to blood capillary transport in the presence of clinically-significant concentrations of excipients, were conducted as described by adding the respective amount of polymer within the drug-containing DMEM-HEPES to the apical well and sampling the basolateral at the same discrete time points. Results were tested in triplicate. As the influence of P-gp is restricted to the apical membrane of the Caco-2 cells, the effects of excipients which are efflux inhibitors should not increase IND permeability in the basolateral to apical (BL-AP) direction of transport. To test this, the transport studies were conducted in the BL-AP direction by adding the same concentrations of the drug and polymer to the basolateral compartment as described, and monitoring drug ingress at the apical compartment.

#### **2.2.1.8. Lucifer Yellow Transport for the Monitoring of Monolayer Integrity**

As indometacin is being examined as an efflux substrate, any increase in permeability must exclude the possibility of transporter system bypass by simple modification of the

paracellular route or loss of membrane integrity. Whilst this mechanism may provide a way for a molecule to escape efflux and so increase its permeability, the focus of the investigation is to examine materials which are able to modulate these transporters directly. As such, the AP-BL flux of Lucifer yellow (LY), a small compound that undergoes paracellular transport but which is not a P-gp substrate, was tested in the AP-BL direction by replacing IND with 100  $\mu\text{M}$  of the compound in the presence of the highest concentration (1.19  $\text{mg mL}^{-1}$ ) of either PEG 8000 or POLYOX N-10. Preliminary spectrophotometer results indicated that LY and DMEM, specifically the pH indicator phenol red of DMEM, exhibited the same absorbance bands. As such, the serum-free media was exchanged with HBSS. Transwell® inserts were washed in warm buffer and the test solutions added. The cells were then placed in the incubator for 60 minutes with shaking at 100 RPM. During this time, a calibration curve was established using LY in HBSS by pipetting 200  $\mu\text{L}$  of test solution in triplicate to a black 96-well plate. Fluorescence was measured using a Unicam Helios 96-well plate reader (excitation  $\lambda$  428 nm, emission  $\lambda$  540 nm). After 60 minutes, 200  $\mu\text{L}$  of HBSS was taken from the receiver compartment of the Transwell® and pipetted on to a clean black 96-well plate for reading.

#### **2.2.1.9. High Performance Liquid Chromatography (HPLC) Analysis of Indometacin**

Samples were analysed by HPLC, obtained using a Shimadzu LC2010AHT HPLC system with autosampler (Shimadzu Corporation, Kyoto, Japan). Separation was performed using Phenomenex Gemini C18 (150 X 4.6 mm, 5  $\mu\text{m}$ ) analytical column maintained at 19 ° C, with detection at 264 nm. Elution was conducted using an isocratic method with a binary phase consisting of acetonitrile and double distilled water with 0.2 % TFA (50:50, v/v), with a flow rate of 1.2  $\text{mL min}^{-1}$ . The apparent permeability coefficient ( $P_{\text{app}}$ ) was then calculated using Equation 1.3.

### **2.3. High-throughput Protocol for the Detection of Materials with a Biological Effect: Development and Validation**

The slow turnover rate of data from the Transwell® model prompted an overhaul in the approach to *in vitro* screening. Indometacin requires time-consuming analytical processing on the HPLC to produce data. Additionally, the high amount of time and resources taken to produce a single 6-well Transwell® is out of all proportion to the data which it is able to

yield. As such, attention was turned to the development of a high-throughput (HTS) screening protocol. Keeping the Caco-2 platform, the format was redesigned to maximise throughput by the addition of high-affinity fluorescent probes, which can be analysed and quantified in seconds. Growth time was also scrutinised in order to yield the maximum amount of data possible with the shortest amount of time and resources. In principle, this technique follows the ingress of fluorescent components into the cells. Once inside, the rise in fluorescent signal of inhibited cells is consistent with efflux inhibition (Figure 2.1).

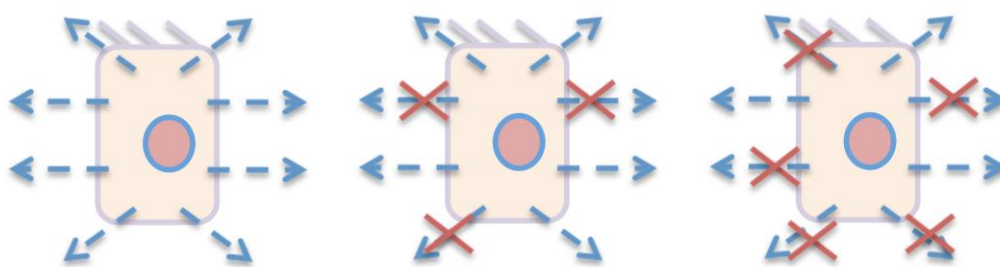


Figure 2.1. Graphical representation of the fluorescent HTS screening model. Once the probe has achieved ingress into the cell, the only way for it to escape is by efflux. With increased concentrations of inhibitor, this is no longer possible and the cells most inhibited retain the highest concentration of dye. This is subsequently detected by a rise in fluorescent signal.

During the early phase of development of this assay, it became apparent that the volume of literature concerning the effects of excipients against MRP2 was vastly under studied. The scale of this disparity is highlighted in Figure 2.2. Several reasons are possible for this knowledge gap; the MRP transporters have been more recently implicated in MDR than the veritable P-gp, and the role of effluxing medicinal compound in the intestine is also subordinate to that of P-gp in terms of substrate diversity. Furthermore, suitable fluorescent probes took time to develop which could be used in HTS. In order to address this, a specific probe of this transporter was incorporated into the HTS assay, 5(6)-carboxy-2',7'-dichlorofluorescein diacetate (CDFDA), which gets converted to 5(6)-carboxy-2',7'-dichlorofluorescein (CDF) within the cells (Figure 2.3). With this novel probe, the intention was to complement the existing literature using a novel HTS platform validated for the detection of inhibitors against P-gp and MRP2.

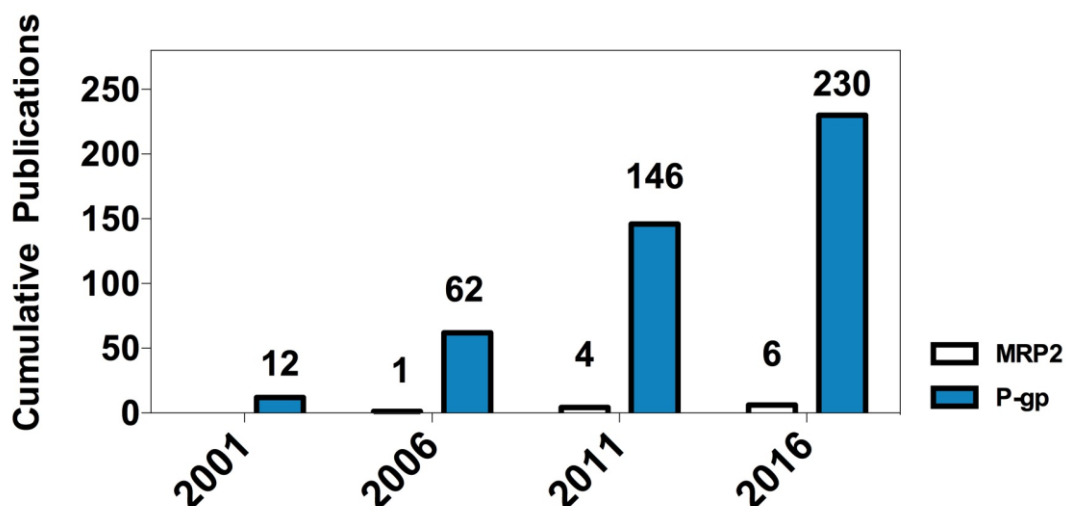


Figure 2.2. The volume of literature concerning the biological effects of commonly used excipients against P-gp and MRP2, using the keyword search ‘excipient P-gp’ or ‘excipient MRP2’.



Figure 2.3. Graphical representation of the conversion of CDFDA to CDF. CDFDA solution is colourless, but gets converted to a cascade of fluorescent compounds by the action of intracellular esterases, chiefly CDF.

### 2.3.1. Stock Solutions

Stock solutions of excipients were made in fresh Krebs-Henseleit (KH) buffer (118 mM NaCl, 4.7 mM KCl, 1.2 mM MgSO<sub>4</sub>, 1.25 mM CaCl<sub>2</sub>, 1.2 mM KH<sub>2</sub>PO<sub>4</sub>, 25 mM NaHCO<sub>3</sub>, 11 mM glucose) to a final concentration of 10 % (w/v). Fluorescent probes were made to 20 μM in DMSO and stored at -80 °C until use. Experimental usage of DMSO never exceeded 0.0125 % (v/v), which was not considered to have a significant impact on the study.

### 2.3.2. General Cell Protocol

Caco-2 cells obtained from Public Health England were grown from a 25 cm<sup>2</sup> (T25) vented flasks at 37 °C in 5 % CO<sub>2</sub> with 90 % relative humidity in DMEM supplemented with 20 % foetal bovine serum (FBS) for seeding media or 10 % FBS for growth media, 1 % non-essential amino acids (NEAA) and 2 mM L-glutamine and in the absence of antibiotics. Media was renewed every 48 hours, and experiments were always conducted within 24 hours of feeding.

### 2.3.3. Fluorescence Microscopy

Cells were seeded in 6 well plates to a density of 4 x 10<sup>4</sup> cells per well and grown for 7 days, with media changed every 48 hours. On the day of the study, cells were washed in HBSS and incubated for 1 hour using 10 or 100 µM verapamil (VER). R-123 was then added to a final concentration of 10 µM and incubated for 60 minutes prior to imaging (Leica DMI 4000B) using the excitation wavelength 485 nm and emission at 585 nm.

### 2.3.4. Cytotoxicity Measurements using the MTT Assay

To determine a non-toxic concentration range to use for testing of the excipients, mitochondrial activity was measured by the reduction of MTT (3-[4,5-dimethylthiazol-2-yl]-2,5-diphenyltetrazolium bromide; thiazolyl blue) to the insoluble product formazan. Culture media of confluent 96 well plates was exchanged for 200 µL test solution containing increasing concentrations of the excipient or drug solutions and incubated for 4 hours in order to encompass an incubation period longer than operational exposure time of the cells during assay conditions. The wells were then emptied and refilled using 100 µL of 0.5 mg mL<sup>-1</sup> MTT and incubated for 3 hours. The formazan was then dissolved using 100 µL of 0.1 N HCl in isopropanol and absorbance then read at 570 nm. Non-treated control wells were set to 100 % viability.

### 2.3.5. Cellular Accumulation of Tracer Dyes

At 90 % confluence, cells were split from a T75 and centrifuged for 5 minutes at 1440 RPM for 5 minutes. Cells were re-suspended in warm media and redistributed to a density of 4 x 10<sup>4</sup> cells per well in clear 96 well plates and grown for up to 7 days. Confluence was confirmed using light microscopy. Monolayers were washed twice using KH (pH 7.4) and left to equilibrate for up to 30 minutes. The wells were then refilled using 200 µL KH buffer

containing the excipient of study over a logarithmic concentration range. Following 30 minutes pre-incubation with the selected excipient or inhibitor, the wells were emptied and refilled with the same concentrations of excipient or inhibitors which had been well mixed with 2.5  $\mu\text{M}$  of either R-123 or CDFDA. This step was necessary in order to negate the influence of excipient viscosity acting to prevent dye ingress. Following 2 hours incubation with the transporter probes, the cells were washed 3 times using ice-cold water and snap-frozen at  $-80\text{ }^{\circ}\text{C}$  for 5 minutes or overnight. Cells were then lysed in double distilled water under refrigeration and the lysate was transferred to black 96-well plates for fluorescence reading (ex 485, em 535). In order to assess the degree of membrane damage imparted by the excipients, the 7-day old monolayers grown in 96-well plates were incubated with excipient for 2 hours at  $37\text{ }^{\circ}\text{C}$  as previously described. The cells were then washed and cooled to  $4\text{ }^{\circ}\text{C}$  in order to arrest all ATP-driven processes (e.g. efflux) after which the cells were exposed to 100 nM R-123 for 30 minutes. Cells were then washed and lysed as previously described.

#### **2.3.6. Calculation of Kinetic Parameters**

In order to quantify the biological effects of excipients, half of the maximal inhibitory concentration ( $\text{IC}_{50}$ ) values, the concentration of the tested compound which is able to reduce transporter activity by 50 %, were calculated using non-linear regression of GraphPad Prism Software (Version 6.0) to 95 % confidence. Data was normalised against control (non-treated cells), which were set to 100 % efflux activity. These  $\text{IC}_{50}$  values were then used for direct comparison to known inhibitors of efflux transporters.

#### **2.4. The Design, Manufacture and Production of ODTs Incorporating Biologically-Active Excipients**

Having developed and validated a HTS assay for the detection of excipients that could modulate efflux-mediated transport, the confluence of the *in vitro* screening was the design and manufacture of an ODT tablet that takes advantage of this knowledge in order to achieve enhanced drug delivery capability. The following work was completed as part of a 6-month placement at the Colorcon facility in Dartford, UK. Here, two alternative ODT platforms were created, a 'low-dose' 295 mg tablet and a 'high-dose' 795 mg dosage form. The model drug at this stage was intended to be atorvastatin, which is a substrate of both

P-gp and MRP2, and has limited bioavailability. This drug comes in a 10 mg, 20 mg, 40 mg and 80 mg tablet strength. However, owing to the safety considerations of using this drug in an industrial pharmaceutical laboratory, paracetamol (acetaminophen, APAP) was chosen as an early stage formulation alternative API to be converted to atorvastatin at the late stage of development. The high-dose ODT was developed as a stand-alone dosage formulation with the sole purpose of loading APAP.

#### **2.4.1. Design of Experiments**

A Design of Experiments (DoE) approach was used to evaluate the impact of various multi-purpose excipients on the physical characteristics of the tablets using JMP 12 software. This initially examined the impact of various Starch 1500, mannitol and MCC content on tablet hardness, disintegration times, tablet friability, tablet thickness, tablet width, and tablet weight. However, only the hardness and disintegration times were affected by the filler composition. Later, StarCap 1500 was examined *in lieu* of Starch 1500.

#### **2.4.2. Tablet Fabrication – Single Press**

Materials were combined and mechanically mixed in a tumbler for 5 minutes in the absence of the lubricant. Batch size for single compression was 40 g. The lubricant glyceryl behenate (Compritol® 888 ATO) was then added and the mixture shaken for a further minute. Tablets were made by direct compression by adding the 295 mg of low-dose mixed to a 10 mm die using normal convex geometry or 795 mg of high-dose powder to a 13 mm die with flat faced tooling. Compression was achieved at 1 MT using an Atlas Auto T8 with no dwell time.

#### **2.4.3. Tablet Fabrication – Rotary Press**

Materials were combined and mechanically mixed for 15 minutes in the absence of the lubricant using Pharmatech Omogenizator rotary mixer at 22 RPM. Batch size for rotary compression was 1 kg. Compritol® 888 ATO was then added and the mixture shaken for a further 5 minutes. Tablets were made by direct compression by adding the 295 mg of low-dose mixed to a 10 mm die using convex geometry. Compression was conducted at 0.6, 1.2, 1.8 and 2.3 MT using a 10-station rotary press (Picolla, Riva) with a turret rotation at 25 RPM. However, only 5 of the 10 die positions in the turret were fitted, the remaining left blank.

#### 2.4.4. Physical Characterisation

##### 2.4.4.1. Hardness

Hardness is an industrial consideration for the production of the tablet, subsequent processing, transport, and in maintaining a consistent dissolution profile. If the tablet is too hard, it may not undergo desired disintegration or drug dissolution; conversely a tablet too low in hardness will not survive processing. Hardness was tested using the 4M hardness testing equipment (Thun, Switzerland) using 10 randomly selected tablets, with data displayed as the mean  $\pm$  SD.

##### 2.4.4.2. Disintegration Times

Disintegration time is of central importance to the development phase of an ODT, and is regulated to 180 s according to the *European Pharmacopeia* (European Pharmacopeia, 2009) and 30 seconds according to the *United States Pharmacopeia* (McLaughlin et al., 2009). It is described as the time for a tablet to completely pass through a mesh with an aperture size of 0.60-0.655 mm. Disintegration was conducted at 37 °C using Erweka TT3 dissolution testing equipment in 900 mL distilled water (Frankfurt, Germany) according to the guidelines outlined in the USP (USP, 2012b). During initial disintegration testing, tablets were observed to stick to the plastic disc inserts covering each tube. Consequently discs were excluded. Data are reported as the mean disintegration times of 6 tablets  $\pm$  SD.

##### 2.4.4.3. Friability

Similar to hardness, friability is another consideration that will predict the likely survival of tablet integrity following manufacture. Friability was conducted according to the USP (USP, 2013). Ten pre-weighed tablets were rotated at 25 RPM for 4 minutes using F2 rotation equipment (Sotax, Basel, Switzerland). Tablets were then dusted off and reweighed and the percentage loss of weight was calculated. Extended friability testing was then conducted using an additional 400 rotations, followed by dusting and reweighing. In both cases, data is reported as the percentage loss of mass.

##### 2.4.4.4. Physical Parameters

Monitoring changes in the tablet composition during manufacture ensures consistency within the batch and that it conforms to USP regulations on weight variation. Tablet

thickness and width were both tested on digital callipers, and weight was determined by weighing dusted tablets immediately after compression. Data is reported as the mean of 10 tablets  $\pm$  SD.

## 2.5. Investigation into the Incorporation of Biologically-Active Surfactants into Granule Coatings for the use in Directly Compressed ODTs

### 2.5.1. Preparation of Ibuprofen Granules via Wet Granulation

Ibuprofen granule formulations were produced according to Table 2.1 to a 120 g batch size. This was then mixed with 25 mL of distilled water and the subsequent wet mass extrusion sieved through a 710  $\mu$ m mesh. The granules were then spread evenly on a steel tray and dried at 60 °C for two hours in the oven until a moisture range of 5-7 % was achieved, measured using a Sartorius Thermo control infrared moisture balance.

Table 2.1. Formulation composition of ODTs used in coating trials.

<i>Excipient</i>	<i>Percentage Content (%)</i>	<i>Mass (g)</i>
Starch 1500	8.68	10.42
MCC	17.37	20.84
Mannitol	28.95	34.74
Crospovidone	4.50	5.40
Magnesium stearate	0.50	0.60
Ibuprofen	40.00	48.00
Total	100.00	120

### 2.5.2. Preparation of Kollicoat IR Coating Solutions Containing Biologically-Active Excipients

The Kollicoat IR (BASF) coatings were made according to Table 2.2 by dissolving the appropriate amount of excipient in 100 mL of distilled water using a magnetic stirrer. The ibuprofen granules were then coated in 20 g batches using the ERWEKA AR 403 DKE coating pan using a 2 mL min<sup>-1</sup> spray rate at 200 rpm for 15 minutes with further conditions outlined in Table 2.3. The granules were then dried for an additional 5 minutes.

Table 2.2. Nomenclature of Kollicoat IR dispersions.

<i>Coating dispersions</i>	<i>Coating</i>
Uncoated	C0
10 % (w/v) Kollicoat IR	C1
10 % (w/v) Kollicoat IR + 2 % (w/v) PEG 2000	C2
10 % (w/v) Kollicoat IR + 2 % (w/v) Poloxamer 407	C3
10 % (w/v) Kollicoat IR + 2 % (w/v) Cremophor EL	C4

Table 2.3. Specifications used during the coating process.

Batch size	20 g
Pan speed	200 rpm
Inlet air temperature	60 °C
Outlet air temperature	40 – 45 °C
Atomizing air pressure	2 - 3 bar
Pattern air pressure	1–1.75 bar
Distance Bed-Nozzle	20 cm
Spraying rate	2mL min <sup>-1</sup>
Processing time	15 min and 30 min

### 2.5.3. Preparation of ODTs from Surfactant-Coated Granules

Magnesium stearate was then added to a total of 0.5 % (w/w) and thoroughly mixed. The granules were then made into 500 mg tablets using a Specac Atlas press at 1 ton for most formulations and 2 tons for some chosen batches, both with 6 seconds compression time.

### 2.5.4. Powder Characteristics Testing

#### 2.5.4.1. Bulk and Tapped Density of the Granules

Bulk and tapped density were measured using 10 g of granules slowly poured through a wide neck funnel into a 50 mL measuring cylinder attached to a Sotax TD2 tap density tester. The occupied volume was recorded as the bulk volume. Following 250 taps, a second reading was taken of the consolidated volume, recorded as the tapped density. Results were recorded in triplicate. Bulk and tapped density values were then used to calculate the compressibility and Hausner ratio according to Equation 2.1 and Equation 2.2, respectively:

$$\text{Compressibility Index} = 100 \cdot \left( \frac{P_{\text{tapped}} - P_{\text{bulk}}}{P_{\text{tapped}}} \right) \quad \text{Equation 2.1.}$$

$$\text{Hausner Ratio} = \left( \frac{P_{\text{tapped}}}{P_{\text{bulk}}} \right) \quad \text{Equation 2.2.}$$

#### 2.5.4.2. Angle of Repose

The angle of repose was calculated by draining 10g of granules through a funnel held 5cm above the platform. The radius ( $r$ ) and height ( $h$ ) of the resulting cone was measured order to calculate the angle of repose according to Equation 2.3:

$$\text{Angle of Repose} = \tan(\alpha) \left( \frac{\text{Height}}{0.5 \text{ Base}} \right) \quad \text{Equation 2.3.}$$

#### 2.5.5. Physical Properties of ODTs Made from Surfactant-Coated Granules

Tablet hardness and disintegration testing was conducted as previously described in sections 2.4.4.1 and 2.4.4.2, respectively, conducted in triplicate. Friability was conducted as described in section 2.4.4.3. For uniformity of content, three tablets from each batch were chosen at random and crushed using a pestle and mortar. The resulting powder was transferred to 500 mL of accurately weighed phosphate buffer (pH 7.2). The solution was inverted several times until the crushed tablet completely dissolved, and 1 mL of solution was tested for absorbance in the UV spectrometer at 264 nm using phosphate buffer as a blank between readings. According to the *United States Pharmacopeia* (USP, 2011), all 10 tested tablets must contain 85% - 115% of the drug content in comparison to the mean amount of Ibuprofen with an RSD below 6 % of the mean.

### 2.5.6. Statistical Analysis

All data sets were assessed for significance using analysis of variance (ANOVA) with a predetermined alpha value of 0.05 on GraphPad Prism software (version 6.0) with Dunnett's or Tukey's Multiple Comparison Post-test for one-way and two-way ANOVA. In all figures using statistics, the error bars depict standard deviation.

### **Chapter 3**

The Development and Validation of a High-Throughput Screening Assay for the  
Detection of Excipients with Efflux Modulation Characteristics

### **3. The Development and Validation of a High-Throughput Screening Assay for the Detection of Excipients with Efflux Modulation Characteristics**

#### **3.1. Chapter Aim and Objectives**

Polarised and differentiated adenocarcinoma (Caco-2) cells are highly regarded as the *in vitro* 'gold standard' model for the small intestine, expressing microvilli and enzymatic components resembling those of the intestinal epithelium (Wilson et al., 1990). To the formulation scientist wishing to use the Caco-2 cell line, there are a number of options as to the precise nature of the model itself. Of the potential model choices, cells grown on Transwell® inserts are commonly used after 21 days growth time. This method is typically low-throughput owing to the lengthy growth time, and additional time is required for post-experiment HPLC analytics. High-throughput processing is becoming increasingly common as a method to produce data at a faster rate and lower cost, often utilising recent advances in fluorescent probes in order to maximise output and, therefore, data processing. The aim of this study was to establish a working Transwell® model and evaluate the transport of the key probe substrate indometacin (IND) and examine the transport of this compound in the presence of PEGylated excipients. PEGs, both as stand-alone materials or as the hydrophilic chains of larger and more complex compounds, maintain an illustrious role in the pharmaceutical industry, and the biological effects of PEGylated excipients has been well studied since first appearing in the literature regarding the reversal multiple drug resistance (MDR) (Ueda et al., 1987). Moreover, this early phase of experimentation was used to evaluate whether throughput could be streamlined for screening excipients with the ability to inhibit efflux-mediated transport by evaluating other potential screening protocols.

#### **3.2. The *In Vitro* Transwell® Model**

##### **3.2.1. Examination of Test Solution Concentrations: Drug and Excipient**

As IND concentrations as high as 500  $\mu\text{M}$  has previously been shown to lead to consistent and reproducible damage to Caco-2 monolayer integrity (Tang et al., 1993), the drug concentration for all studies was kept below 100  $\mu\text{M}$ . A drug stock solution was prepared overnight prior to experimentation, which was subsequently filtered and to which various

amounts of polymer were added to achieve the concentrations shown in Table 3.1. The PEG 8000 and POLYOX concentrations were selected on the assumption of a 350 mg oral dosage form with a polymer content up to 85 % (w/v), and taken with a 250 mL glass of water on an empty stomach. Whilst the concentration of PEG 400 used in liquid dosage forms is at least 17 % (v/v) (Strickley, 2004), such high concentrations were found to be toxic to the Transwell® inserts during initial studies, with TEER values dropping well below 400  $\Omega$ .cm<sup>2</sup> (results not shown). Concentrations have been found in literature as high as 20% (v/v) for the closely related PEG 300; however, the osmotic pressure was stabilised in the *in vitro* model by using an equal concentration of PEG 300 on both sides of the membrane and the authors acknowledge that this is proof of principle rather than a true model of *in vivo* condition (Hugger et al., 2002a). As such, the maximum concentration of PEG 400 used was 0.5 % (v/v) (Table 3.1). Poloxamer 407 has been shown to be a satisfactory lubricant for tablets made by direct compression at 1 % (w/w) (Muzíková et al., 2012), and has been used as high as 19 % in formulations designed for photodynamic therapy via the administration of a thermosetting gel for the putative treatment of Barrett's oesophagus using an oral dosage form (Bourre et al., 2002). As such, this latter concentration was used for testing (Table 3.1).

Table 3.1. Typical PEG 400, PEG 8000, POLYOX N-10 and poloxamer 407 concentrations found in oral dosage forms. The resultant polymer concentrations used in the study assumes the oral dosage formulation is taken with a 250 mL glass of water.

<i>Percentage Polymer</i>		<i>Polymer Quantity in Dosage Form</i>		<i>Concentration used in Study</i>
Control	0	0	0	0
PEG 400	6.8	0.7 mL	0.10 (% v/v) <sup>a</sup>	
	10.2	1.0 mL	0.25 (% v/v) <sup>a</sup>	
	13.6	1.4 mL	0.50 (% v/v) <sup>a</sup>	
	17.0	1.7 mL		
PEG 8000	28.3	99.1 mg <sup>b</sup>	0.40 mg mL <sup>-1</sup>	
	56.6	198.1 mg <sup>b</sup>	0.79 mg mL <sup>-1</sup>	
	85.0	297.5 mg <sup>b</sup>	1.19 mg mL <sup>-1</sup>	
POLYOX N-10	28.3	99.1 mg <sup>b</sup>	0.40 mg mL <sup>-1</sup>	
	56.6	198.1 mg <sup>b</sup>	0.79 mg mL <sup>-1</sup>	
	85.0	297.5 mg <sup>b</sup>	1.19 mg mL <sup>-1</sup>	
Poloxamer 407	6.3	0.63 mg <sup>c</sup>	0.63 mg mL <sup>-1</sup>	
	12.7	1.27 mg <sup>c</sup>	0.91 mg mL <sup>-1</sup>	
	19.0	1.90 mg <sup>c</sup>	1.90 mg mL <sup>-1</sup>	

<sup>a</sup> Percentage (v/v) adjusted to lower toxicology;

<sup>b</sup> Assumes 350 mg tablet;

<sup>c</sup> Assumes 10 mL liquid dosage form.

### 3.2.2. Results of *In Vitro* Screening Using the Transwell® Model

#### 3.2.2.1. The Impact of Indometacin on Tight junction Integrity

The paracellular hypothesis describes the passive movement of the drug through the monolayer via intracellular tight junctions. The tight junction macromolecular complex provides this barrier function and is the rate-limiting structure. A major component of this structure is the Zonula occludens (ZO-1), which act by directly binding actin cytoplasmic filaments to the transmembrane protein occludens, and so form cell-cell interfaces. Here, they play a cardinal role in the exclusion of macromolecules by the paracellular route, effectively sealing the apical plasma membranes of the intestinal lumen (Van Itallie et al., 2009). IND is a non-steroidal anti-inflammatory drug (NSAID) used for the treatment of chronic inflammatory diseases. Like all drugs of this category, IND may lead to the development of gastric mucosal injury, where a plethora of individual pathologies may develop. The loss of mucosal integrity, gastric mucosal bleeding, inhibition of cell renewal

and the loss of inherent antioxidant defence has for a long time been linked to the inherent ability of NSAIDs to inhibit cyclooxygenase (COX) (Rainsford and Willis, 1982). This enzyme is necessary for the production of a group of the lipid compounds known as prostaglandins, which have a role in the regulation of inflammation, and therefore are considered protective (Rainsford and Willis, 1982). Furthermore, oxidative stress, particularly mitochondrial oxidative stress (MOS), also plays a pivotal role in NSAID-induced gastric damage (Mahmud et al., 1996). Here, the uncoupling of oxidative phosphorylation leads to a decrease in cellular ATP/ADP and a subsequent loss of membrane potential (Mahmud et al., 1996). The opening of permeability transition pores ultimately releases cytochromes from the intra-mitochondrial space and into the cytoplasm – a hallmark of apoptosis. Oxidative stress has also been shown to lead to the disassembly of tight junction proteins, particularly ZO-1 via tubulin oxidation (Banan et al., 2003). The depletion of ATP in MDCK cells was shown to alter the distribution of ZO-1, leading to the formation of insoluble complexes, which were unable to interact with the cytoskeletal proteins of the cytoplasm (Wagner et al., 2008). ATP depletion has also been shown to decrease in ZO-1 and occludin expression in Caco-2 cells (Carrasco-Pozo et al., 2013).

It follows, therefore, that in order to use Caco-2 cells as a model for the permeability of drugs through the human intestine, a concentration of IND must be found which is both detectable at each time point by the chosen analytical method, whilst leaving membrane integrity intact. Epithelial integrity can be measured indirectly using transepithelial electrical resistance (TEER), that is, the resistance of an electrical current passed across the monolayer. By short-circuiting the membrane, interference of electrical current generated by ion transport is negligible and therefore follows that an increase in TEER correlated to monolayer integrity, and so a decrease in paracellular transport. By monitoring the value before and after the permeability study in fresh DMEM growth media (37 °C), TEER was measured as accurately as possible to ensure membrane integrity was held throughout the experiment. Over the range of IND tested (10-100  $\mu\text{M}$ ), TEER values were maintained over 400  $\Omega\cdot\text{cm}^2$ , showing the ability of the membrane to maintain acceptable levels of barrier function in the presence of higher drug concentrations. Typical TEER values are presented in Table 3.2. Naturally, any disturbance to the monolayer, such as those conducted as part of the permeability study including twice washing with buffer and the absence of serum

for over 60 minutes, will lead to minor decreases in TEER. Although a decrease in the extent of TEER degradation is seen in the presence of the polymeric excipient, this is not significant ( $p > 0.05$ ).

Table 3.2. The change in transepithelial resistance over time in the presence of drug alone or with PEG 8000.

TEER Before ( $\Omega.cm^2$ )		TEER After ( $\Omega.cm^2$ )		Percentage Decrease (%)	
Control <sup>a</sup>	Drug and Excipient <sup>b</sup>	Control <sup>a</sup>	Drug and Excipient <sup>b</sup>	Control <sup>a</sup>	Drug and Excipient <sup>b</sup>
531.0 $\pm$ 20.7	534.0 $\pm$ 22.5	454.0 $\pm$ 43.1	508.7 $\pm$ 7.51	14.6 $\pm$ 5.6	4.6 $\pm$ 5.27

<sup>a</sup>10  $\mu$ M IND

<sup>b</sup>10  $\mu$ M IND with 1.19 mg mL<sup>-1</sup> PEG 8000

### 3.2.2.2. Indometacin Concentration-Dependent Transport

Based on the results shown in Table 3.2, in which the tight junction integrity was maintained, the next stage was to investigate the concentration-dependent uptake of IND in the apical to basolateral direction without the excipients being present. The percentage of drug recovered from the basolateral compartment over 60 minutes is shown in Figure 3.1. After 60 minutes, the percentage recovery for 100  $\mu$ M initial concentration of IND was significantly higher ( $p < 0.0001$ ) than for 50  $\mu$ M initial concentration, indicating that the efflux transporter has become saturated and can no longer efficiently transport the drug because the  $K_m$  value has been reached or surpassed once the system has reached equilibrium. Although initial permeability studies in the presence of polymer were conducted using 10  $\mu$ M, these results show that higher drug marker concentrations of up to 50  $\mu$ M could be used.

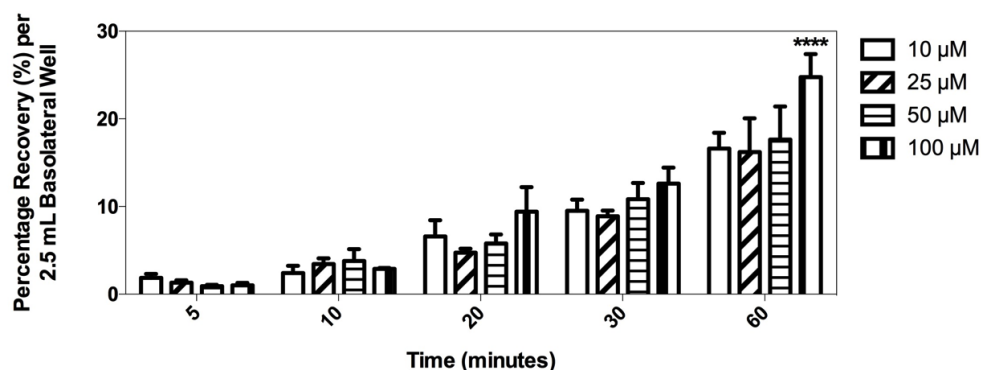


Figure 3.1. The apical to basolateral transport of IND at varying concentrations through 21-day old Caco-2 monolayers. Data is presented as mean  $\pm$  SD of triplicate values. Statistical significance was analysed using two-way ANOVA followed by Dunnett's *post hoc* test annotated as follows: \*\*\*\* ( $p < 0.0001$ ).

Plotting the permeability coefficients of AP-BL direction against BL-AP can reveal the manner of transport through which a compound is able to move through a monolayer: if the coefficients are of equal value, paracellular transport is indicated; asymmetrically superior transport in the AP-BL direction suggests carrier mediated transport, whilst asymmetrically dominant in the BL-AP direction is indicative of carrier mediated efflux. Figure 3.2 shows the data from Figure 3.1 represented as apparent permeability plotted alongside the apparent permeability data conducted using the same concentrations measured in the BL to AP direction, and Table 3.3 shows the  $P_{app}$  values obtained as a ratio of the two pathways for 50  $\mu\text{M}$  drug as a typical example. The results demonstrate that permeability is dominant in the BL-AP direction, indicating possible carrier-mediated efflux associated transport. The higher  $P_{app}$  values seen at higher concentrations of the drug at 100  $\mu\text{M}$  in the AP-BL direction ( $2.2 \times 10^{-5} \text{ cm s}^{-1}$  after 60 minutes compared to  $1.6 \times 10^{-5} \text{ cm s}^{-1}$ ,  $1.4 \times 10^{-5} \text{ cm s}^{-1}$  and  $1.5 \times 10^{-5} \text{ cm s}^{-1}$  for 50, 25 and 10  $\mu\text{M}$ , respectively) may be indicative of the drug concentration exceeding the functional capacity of the transporter in terms of efflux transporter saturation, supporting the data from Figure 3.1.

As efflux proteins such as ABCB1 reside on the apical membranes of epithelial cells, the ratio of the AP-BL and BL-AP permeability coefficients shows to what extent these transporters influence drug absorption. The examination of the transport of IND (Figure 3.2), indeed, shows that the apparent permeability is higher in the BL-AP direction, indicating that the travel in the absorptive direction is influenced by the action of efflux transporters. Despite this, the efflux ratio between these directions of travel does not exceed 2. As such, the efflux ratios that we obtained leave the transport of IND in a state of contention. Efflux ratio values above 1.2 or 1.5 indicate that the compound is a substrate of efflux transporters (Lentz et al., 2000, Polli et al., 2001). Additionally, the speed at which a compound transits the membrane must also be considered. Any rapidly-transiting compound can overcome the effects of efflux transporters by bypassing them (Polli et al., 2001). Verapamil (VER) is a well-known substrate of ABCB1, but is able to traverse the cell membrane quickly that it is able to quickly saturate the transporter with a  $P_{app}$  value of  $1.7 \times 10^{-5}$  measured on the Caco-2 monolayer (Westerhout et al., 2014). Naturally, not all compounds that transit so fast will become inhibitors. Over the course of the experiments examining the transport of IND through Caco-2 monolayers,  $P_{app}$  values between 2.18-2.59

$\times 10^{-5} \text{ cm s}^{-1}$  were recorded, in agreement with existing literature between  $1.5 \times 10^{-5}$  and  $2.0 \times 10^{-5} \text{ cm s}^{-1}$  on the Caco-2 monolayer (ElShaer et al., 2014, Mandagere et al., 2002). Using the recently outlined definition of high-permeability as compounds with a  $P_{app}$  value of  $1.6 \times 10^{-5} \text{ cm s}^{-1}$  and over (Kim et al., 2006), both our calculated IND value and the reported VER value consider both of these compounds highly permeable. In contrast, well-studied ABCB1 substrate compounds have much higher efflux ratios than those reported for IND on the Caco-2 cell line, such as digoxin between 15-18 (Hughes and Crowe, 2010, Stephens et al., 2001, Mease et al., 2012), paclitaxel between 23-391 (Mease et al., 2012, Hughes and Crowe, 2010) and rhodamine 123 with a value around 10 (Troutman and Thakker, 2003, Sachs-Barrable et al., 2007). In conclusion, IND could well be a substrate of ABCB1 with an already exceptional ability to cross membranes, rendering the action of efflux transporters redundant.

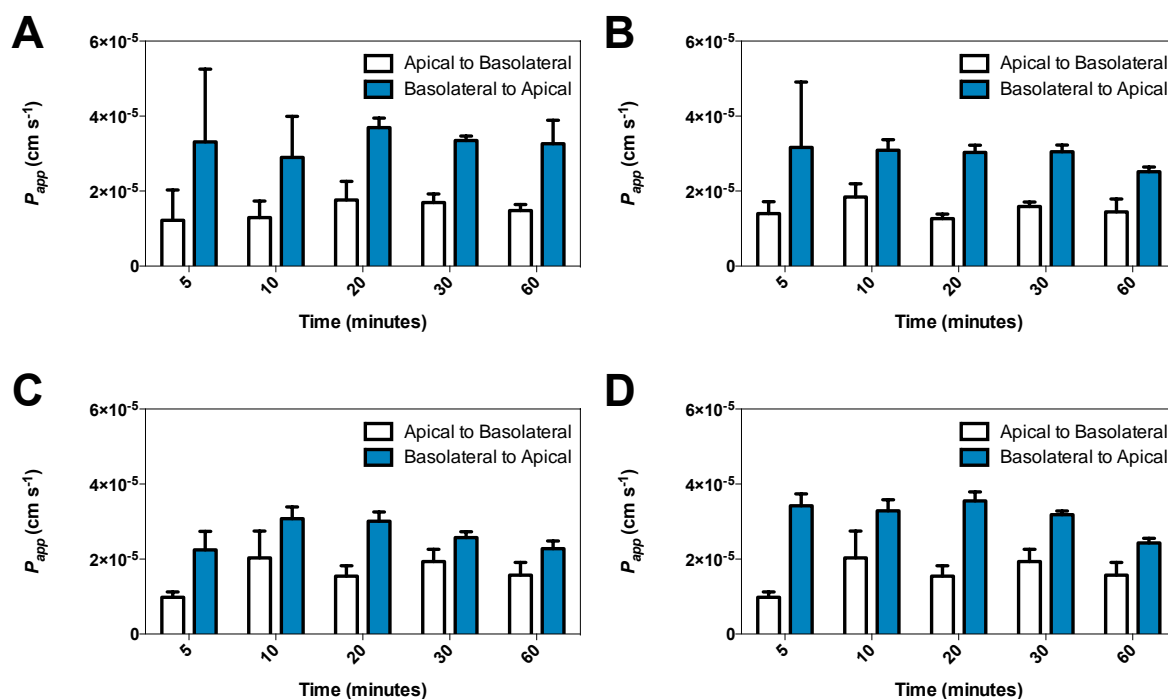


Figure 3.2. Bidirectional apparent permeability coefficient data for AP-BL (clear) and BL-AP transport (blue), conducted over a range of IND concentrations, showing A) 10  $\mu\text{M}$ , B) 25  $\mu\text{M}$ , C) 50  $\mu\text{M}$  and D) 100  $\mu\text{M}$ . Data presented as  $\pm$  SD ( $n = 3$ ). BL-AP transport is broadly dominant to AP-BL, suggesting the latter is influenced by efflux transporters residing on the apical membrane.

Table 3.3. Typical absorption to secretion permeability coefficients for 50  $\mu$ M IND through 21-day old Caco-2 monolayers. The higher value of the former compared to the latter is suggestive of transporter mediated efflux, demonstrated by the asymmetrical transport.

Time (minutes)	$P_{app} (cm\ s^{-1}) \times 10^{-5}$					Efflux Ratio ( $P_{app\ BL \rightarrow AP} / P_{app\ AP \rightarrow BL}$ )
	$P_{app\ AP \rightarrow BL}$		$P_{app\ BL \rightarrow AP}$			
5	2.87	$\pm$ 0.15	3.42	$\pm$ 0.50		1.19
10	3.09	$\pm$ 0.74	3.94	$\pm$ 0.35		1.28
20	2.13	$\pm$ 0.28	3.73	$\pm$ 0.29		1.75
30	2.37	$\pm$ 0.34	3.36	$\pm$ 0.21		1.42
60	1.82	$\pm$ 0.34	2.89	$\pm$ 0.24		1.59

### 3.2.2.3. Indometacin Permeability Across Caco-2 Monolayers in the Presence of PEG 400

PEG 400 is the lowest molecular weight material tested during the Transwell® studies and comes as a liquid at room temperature. The results of the permeability studies of IND across the Caco-2 monolayer in the presence of PEG 400 are shown in Figure 3.3. At high concentrations of this excipient, a statistically significant ( $p < 0.01$ ) increase in the percentage of IND recovered is observed at 0.5 % (v/v). When PEG 400 was used below this concentration the percentage recovery of IND decreased when compared to drug alone - this is of interest, as literature supports the paradigm of PEG 400 as a permeability enhancer (Shen et al., 2006), in addition to being able to inhibit the efflux of digoxin, a P-gp substrate, *in vitro* (Johnson et al., 2002a). Both of these studies were conducted using rat jejunal tissue, although previous studies have used PEG 300 at similar concentrations to those shown herein, also using the Caco-2 cell line (Hugger et al., 2002a). Therefore, it is possible that the formation of PEG 400 micelles is having an inhibitory effect. As a large compound, absorption of PEG 400 is less than 0.5 % *in vivo* (Hugger et al., 2002a), and any micelle formation may not only prevent cellular efflux of the drug, but prevent permeability from the AP-BL membrane. The CMC of PEG 400 in the transport media has yet to be experimentally determined, although decreasing the concentration range below 0.5 % (v/v) did lead to a statistically significant ( $p > 0.05$ ) decrease in uptake after 60 minutes for 0.5 % (v/v) PEG 400 (Figure 3.3).

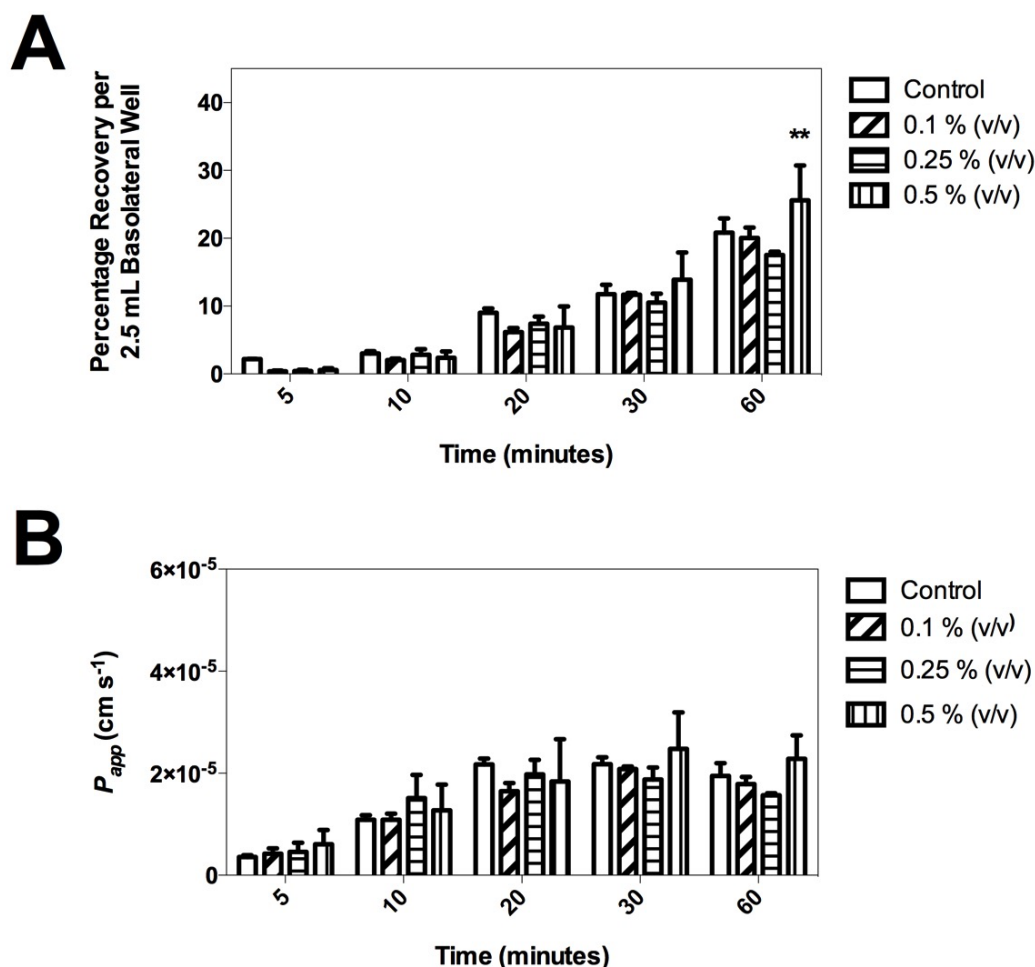


Figure 3.3. The permeability of IND in the presence of PEG 400, showing A) the percentage transport and B) apparent permeability ( $P_{app}$ ) for AP-BL transport of 50  $\mu\text{M}$  IND across 21-day old Caco-2 monolayers either alone or with 0.1-0.5 % (v/v) PEG 400 in the apical compartment. All results are shown in triplicate. Data is presented as  $\pm$  SD. Statistical significance was analysed using two-way ANOVA followed by Dunnett's *post hoc* test annotated as follows: \*\* ( $p < 0.01$ ).

#### 3.2.2.4. Indometacin Permeability Across Caco-2 Monolayers in the Presence of PEG 8000

PEG 8000 is the second lowest molecular weight material tested during the Transwell® transport studies and is a waxy material at room temperature. The results of the permeability studies of IND across the Caco-2 monolayer in the presence of PEG 8000 are shown in Figure 3.4. Both the percentage transport and apparent permeability of IND increased significantly ( $p < 0.0001$ ) for all concentrations tested, although this only occurs after 60 minutes, the final time point tested in this study. PEG 8000 has been shown to increase ABCB1 substrate permeability using IND and Caco-2 monolayers (Khan et al., 2011). This study showed a profound increase in IND transport with a 2.8-fold increase in

permeability in the presence of PEG 8000. During the study conducted herein, an enhancement in transport of IND in the highest concentration of PEG 8000 (1.19 mg mL<sup>-1</sup>) was only 1.33-fold after 60 minutes.

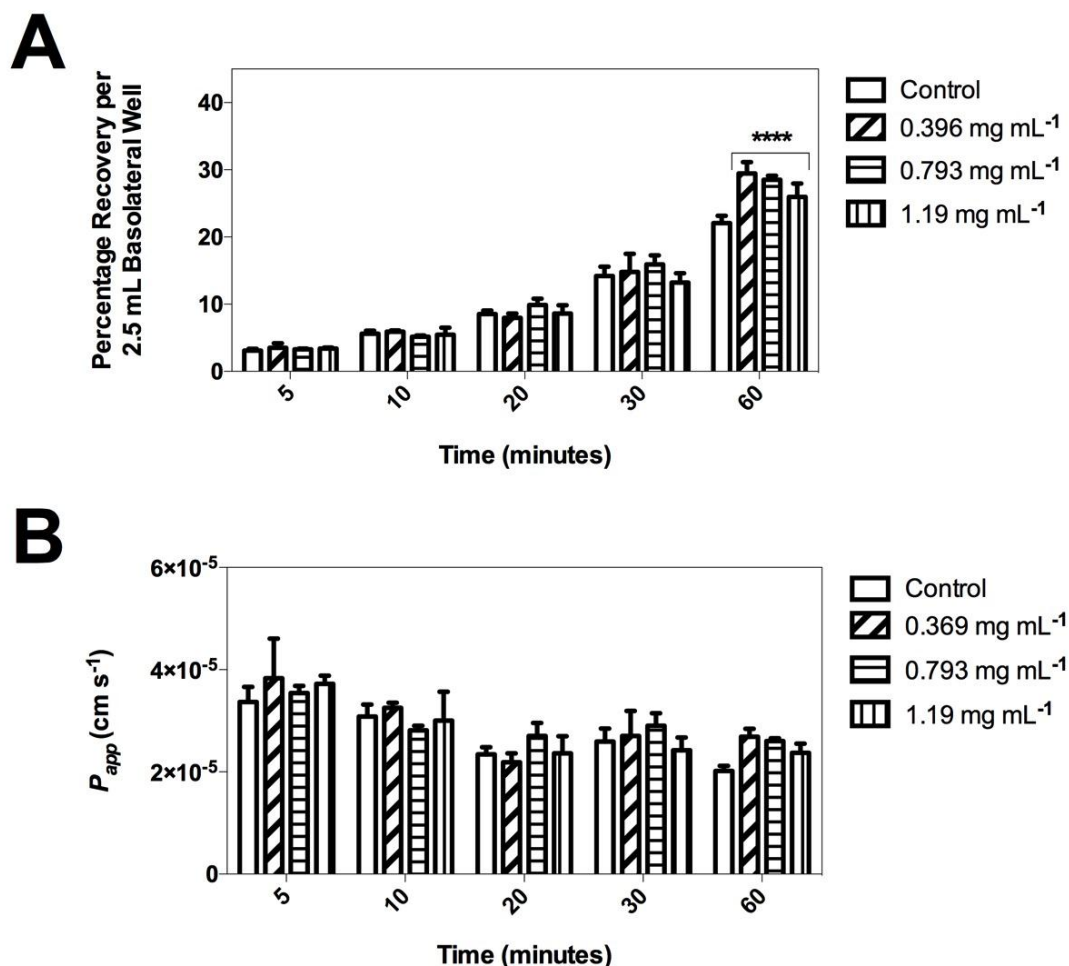


Figure 3.4. The permeability of IND in the presence of PEG 8000, showing A) the percentage transport and B) apparent permeability ( $P_{app}$ ) for AP-BL transport of 50  $\mu$ M IND across 21-day old Caco-2 monolayers either alone or with 0.369-1.19 mg mL<sup>-1</sup> PEG 8000 in the apical compartment. All results are shown in triplicate. Data is presented as  $\pm$  SD. Statistical significance was analysed using two-way ANOVA followed by Dunnett's *post hoc* test annotated as follows: \*\*\*\* ( $p < 0.0001$ ).

### 3.2.2.5. Indometacin Permeability Across Caco-2 Monolayers in the Presence of POLYOX

Higher molecular weight PEGs over 20,000 Da are known as polyethylene oxides (PEOs). POLYOX N-10 is a PEO with a molecular weight around 100,000 Da. This excipient was selected for study as a contrast to the smaller molecular weight PEGs. The results of the permeability studies of IND across the Caco-2 monolayer in the presence of POLYOX N-10

are shown in Figure 3.5. After 60 minutes, both the percentage transport and apparent permeability of IND increased significantly ( $p < 0.01$ ) in the presence of POLYOX after only 10 minutes, increasing in significance after 60 minutes ( $p < 0.0001$ ), although this increase is once more observed at the higher concentrations used, indicating the low efficacy of POLYOX as permeability enhancer.

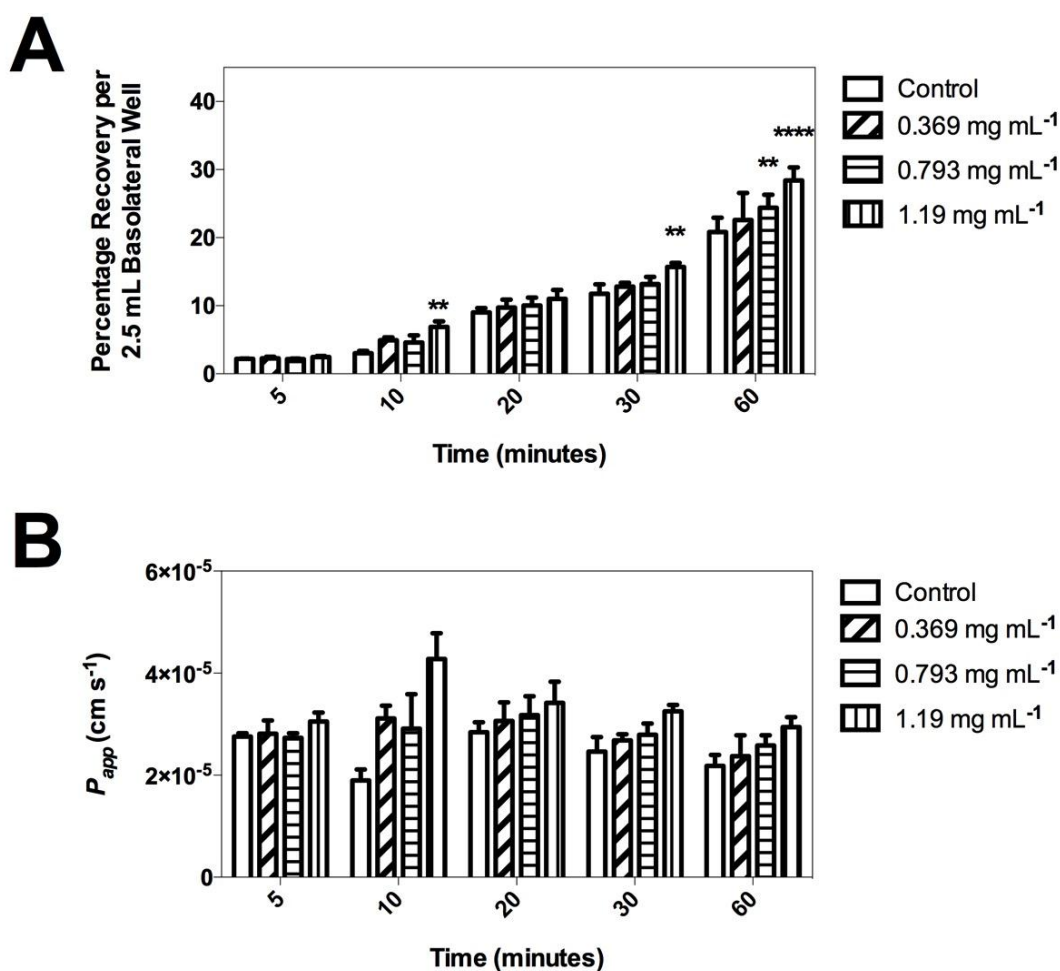


Figure 3.5. The permeability of IND in the presence of POLYOX N-10, showing A) the percentage transport and B) apparent permeability ( $P_{app}$ ) for AP-BL transport of 50  $\mu\text{M}$  IND across 21-day old Caco-2 monolayers either alone or with 0.369- 1.19  $\text{mg mL}^{-1}$  POLYOX in the apical compartment. All results are shown in triplicate. Data is presented as  $\pm$  SD. Statistical significance was analysed using two-way ANOVA followed by Dunnett's *post hoc* test annotated as follows: \*\* ( $p < 0.01$ ); \*\*\*\* ( $p < 0.0001$ ).

### 3.2.2.6. Indometacin Permeability Across Caco-2 Monolayers in the Presence of Poloxamer 407

Poloxamer 407 (P407) is an amphiphilic excipient commonly used as a surfactant with a HLB value of 22, and is a soft and waxy material at room temperature. The effects of P407 on IND transport across the Caco-2 monolayer is presented in Figure 3.6. The presence of this material lead to a profound increase in the rate of transport of IND, becoming significant at the highest concentration (1.9 mg mL<sup>-1</sup>) after just 10 minutes ( $p < 0.05$ ), becoming extremely significant after 30 minutes for all concentrations tested ( $p < 0.0001$ ). The possible reasoning for such an increase could be attributed to the mode of action previously suggested for these two different polymers in their respective action against the efflux transporters. PEGs have been reported to lead to an increase in membrane fluidity, and so disrupting the sensitivity to P-gp substrates acting in the inner leaflet of the membrane. Kabanov *et al* conducted an extensive study on poloxamers of various molecular weights and hydrophilic-lipophilic balance values (Kabanov et al., 2002). In this study using bovine brain microvascular endothelial cells (BBMECs), lipophilic poloxamers with propylene oxide (PO) lengths of 30-60 units, coupled with a HLB < 20, were the most effective of the P-gp inhibitors. Poloxamer 407 has a HLB of 22, with a PO length around 67, putting these parameters close to the ideal. The precise mechanism is multifaceted, and appears to be a combination of decreasing the affinity of P-gp for ATP, membrane fluidisation and endocytosis of P-gp substrates into the cell by micelle activity when used above the CMC (Kabanov et al., 2002). The efficacy of poloxamer 407 in inhibiting P-gp has been reported using the Caco-2 model and the rat gut sac (Guan et al., 2011). Moreover the potential of poloxamers, and surfactants in general, for high efficacy in terms of P-gp inhibition is highly intriguing, and warrants extensive investigation.

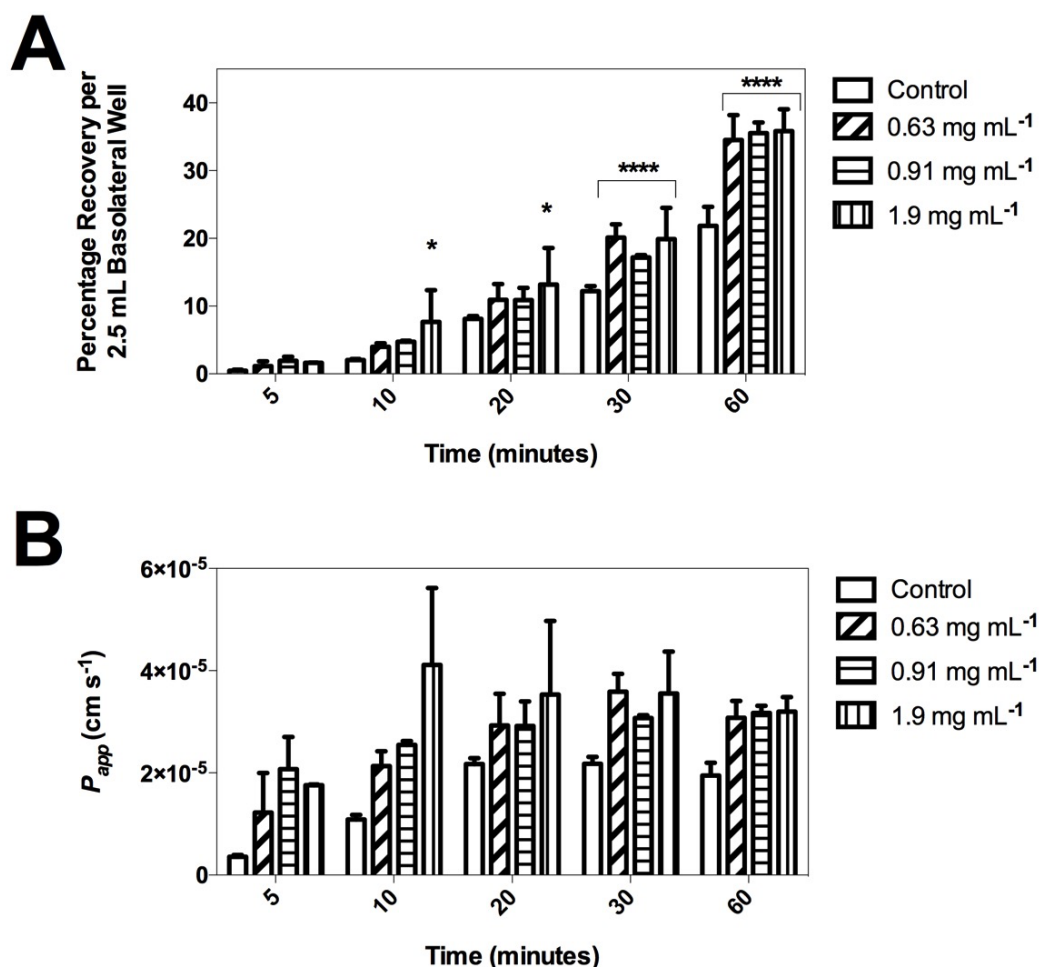


Figure 3.6. The permeability of IND in the presence of poloxamer 407 showing A) the percentage transport and B) apparent permeability ( $P_{app}$ ) for AP-BL transport of 50  $\mu\text{M}$  IND across 21-day old Caco-2 monolayers either alone or with 0.63-1.9  $\text{mg mL}^{-1}$  poloxamer 407 in the apical compartment. All results are shown in triplicate. Data is presented as  $\pm$  SD. Statistical significance was analysed using two-way ANOVA followed by Dunnett's *post hoc* test annotated as follows: \* ( $p < 0.01$ ); \*\*\*\* ( $p < 0.0001$ ).

Interestingly, the  $P_{app}$  values vary considerably over the first 2 time points (5 and 10 minutes) between 0.36 - 3.37  $\text{cm s}^{-1}$ , highlighting the difficulty in washing cells, adding test solutions before cells dry out, initiating the experiment and then sampling the first data points and replacing the subtracted media in the opening minutes of the experiment. More consistent values are obtained at 20 minutes, with  $P_{app}$  values between 2.18 - 2.59  $\times 10^{-5}$   $\text{cm s}^{-1}$  for control wells.

### 3.2.2.7. Confirming the Increase in Indometacin Transport as Efflux Inhibition

As the action of efflux transporters is contrary to that of the absorptive route, any movement of compounds arriving at the apical fascia from the basolateral compartment is unlikely to have its movement impeded by this mechanism. Whilst the mechanism of action of poloxamer 407 is well understood and the efflux inhibition properties of PEG 400 not fully elucidated using the Transwell® model herein, the two compounds which demonstrated clear efficacy were chosen for further study: PEG 8000 and POLYOX N-10. The data presented in Figure 3.7 shows the BL-AP transport of IND with the presence of 1.19 mg mL<sup>-1</sup> of either PEG 8000 or POLYOX in the basolateral compartment. The results showed no significant ( $p > 0.05$ ) difference between the percentages of drug transported when the polymers are present compared to drug transport alone. From this, it can be seen that the excipients only change the apparent permeability in the AP-BL direction of travel, indicating that the effects noted in Figure 3.4 and Figure 3.5 were isolated to the apical membrane and crucially to the fascia expressing the efflux transporters. It is by this process that the increase in IND transport can be attributed to apical efflux modulation and not by a non-specific mechanism such as tight junction modulation.

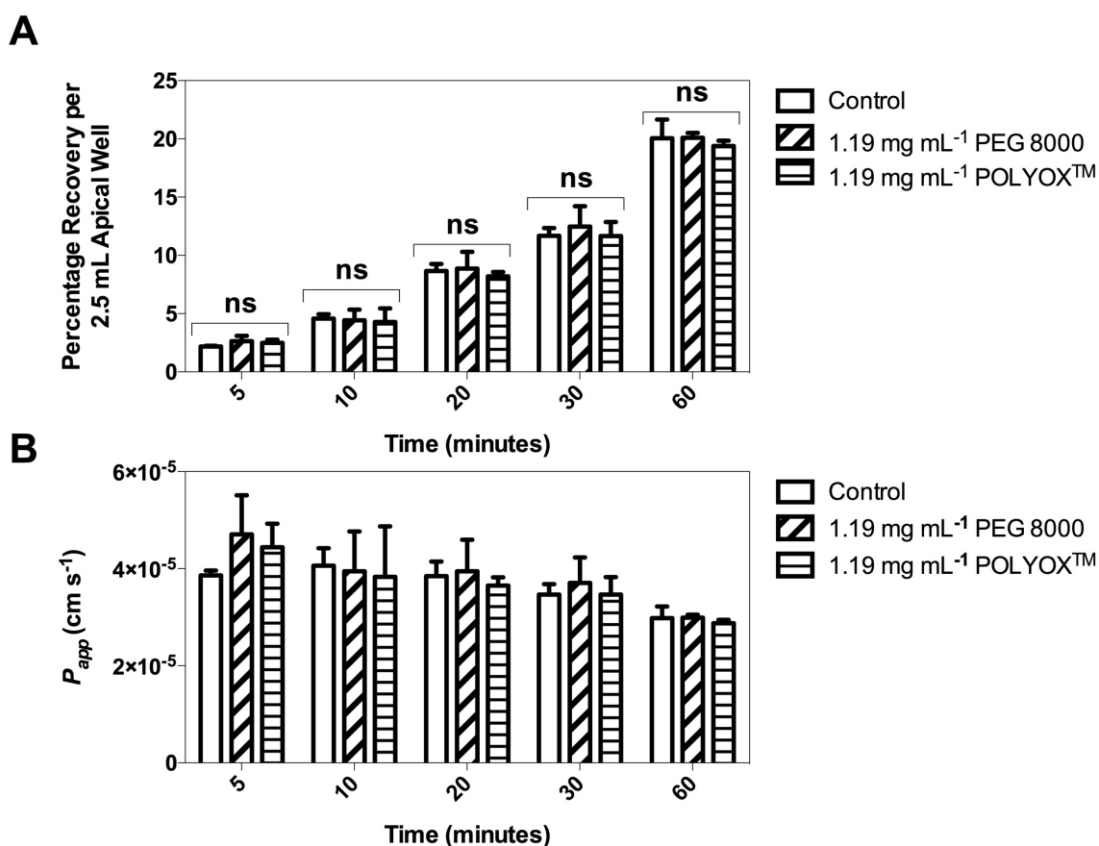


Figure 3.7. The basolateral to apical (BL-AP) transport of IND in the presence of PEG 8000 and POLYOX N-10, showing A) the percentage drug transported and B) the permeability coefficients. Error bars refer to standard deviation ( $n = 3$ ). No statistically significant difference was observed using two-way ANOVA between all time points tested in the presence of the excipients and the control, ns ( $p > 0.05$ ).

### 3.2.2.8. Membrane Integrity Studies: Lucifer Yellow Transport

Lucifer yellow (LY) is a non-P-gp substrate and is poorly transported through monolayers, making it an ideal marker for loss of membrane integrity. Therefore the AP-BL flux of LY across the Caco-2 cell monolayer was determined in the absence or presence of the highest polymeric concentrations to test for possible modulation of the paracellular pathway (Table 3.4). The results show that neither polymer had a statistically significant impact ( $p > 0.05$ ) on LY transport, with total recovery between 0.1 and 0.4 % (Table 3.4) and, hence, do not alter this pathway in Caco-2 monolayers. In an *in vivo* study, the surfactant Labrasol was able to increase the transport of LY in rat ileum at 0.1 % (Lin et al., 2007). In a study of the Caco-2 cell line, a number of nanoparticulates based on trimethylchitosan (TMC) were found to increase the permeability of LY, therefore demonstrating their propensity to open tight junction complexes (Sandri et al., 2007). Both of these studies highlight the importance

of monitoring tight junction integrity as any increase in the paracellular route may give identical results to efflux transporter inhibition.

Table 3.4. Percentage Lucifer yellow transported after 60 minutes through 21-day old Caco-2 monolayers grown in Transwell® inserts. Data shown as the mean of triplicate values  $\pm$  SD,

<i>Lucifer Yellow Transport (%)</i>	
Control	0.02 $\pm$ 0.02
PEG 8000	0.36 $\pm$ 0.56
POLYOX	0.13 $\pm$ 0.23
IND	3.30 $\pm$ 4.32

### 3.3. Introduction to High-Throughput Screening

Whilst the Transwell® model is an incredibly powerful tool for evaluating the transport of drugs through intestinal monolayers, the process suffers from slow growth rates, which can limit throughput. As such, the next stage was to use the same Caco-2 platform to develop a high-throughput screening (HTS) assay with the aim of reducing growth time to 7 days or less and increase scalability in contrast to the cumbersome Transwell® model. The fluorescent dye rhodamine 123 (R-123) has been used extensively in methodologies as a high-affinity ABCB1-mediated dye (Tapiero et al., 1984). The experimental premise of the method follows that of the bioavailability equation (Equation 1.2). As a fluorescent entity, the amount of R-123 that is retained in the cell is a function of the activity of the ABCB1 transporter and it follows that  $F_g$ , the fraction of R-123 in the cell, can be quantified as a measure of the efficacy of an efflux transporter inhibitor. Following method development and optimisation of conditions, the protocol was validated using two commonly used excipients, Tween 20 and Tween 80, both polyethylene derivatives commonly used in the pharmaceutical industry and have long been known as inhibitors of efflux mediated by P-gp.

#### 3.3.1. Evaluation of Rhodamine Concentration Range

The fluorescent probe R-123 at various concentrations was investigated in order to find a concentration of R-123 that is easily detected using the fluorescent plate reader, yet is low enough not to overwhelm ABCB1-mediated efflux. To this end, the cellular uptake of R-123 in concentrations between 1 - 250  $\mu$ M was assessed over a 4-hour period (Figure 3.8). The

uptake of R-123 was linear over the range tested ( $r^2 = 0.998$ ). For method optimisation, 5  $\mu\text{M}$  R-123 was chosen as this concentration is below the reported  $K_m$  value of the probe (7.2 - 17.5  $\mu\text{M}$  in ABCB1-expressing cells (Forster et al., 2012, Wang et al., 2006, Shapiro and Ling, 1997)). Moreover, this concentration is well within the detectability limit of the equipment. Above this concentration, the efflux transporter will quickly become saturated and any inhibition properties of the drug or excipient will be masked.

Whilst the use of R-123 as an efflux substrate was the focus of the current study, at low concentrations the uptake of this probe has been shown to be a saturable process that can be inhibited by the substrates of Oat1a4 (orthologous to human OATP1A2) such as digoxin and quinine, amongst others, in the rat model (Annaert and Brouwer, 2005). At higher concentrations, the uptake of the probe is by passive diffusion. As an amphiphilic molecule, R-123 is able to traverse the lipid bilayer by rare inversions known as 'flip flop' events. R-123 excluded by ABCB1 is free to continuously re-enter the cell by a process in which the hydrophobic elements of the compound initially bind to the acidic head groups of the phospholipids (Eytan et al., 1997). Therefore, highest level screening sensitivity (signal to noise ratio) will occur during the lowest reasonably detectable concentration of the dye and much below the saturation limit of the efflux transporter.

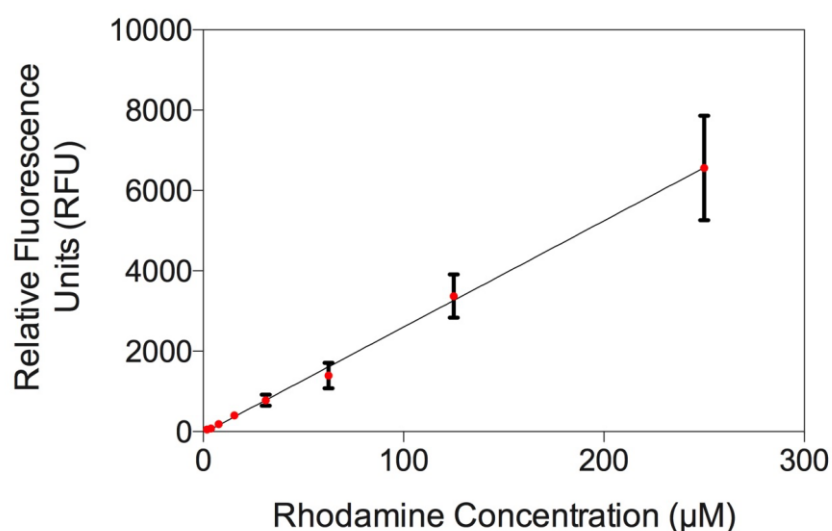


Figure 3.8. The concentration-dependent uptake of R-123 over a 4-hour period on the Caco-2 cell line. Cellular accumulation of R-123 was linear over the concentration range and time points used. Cells were incubated in DMEM-HEPES (pH 7.4) with a R-123 concentration between 1 and 250  $\mu\text{M}$  to obtain the time points indicated. Error bars are shown as  $\pm$  SD (data pooled from 10 wells).

### 3.3.2. Inhibition of ABCB1-Mediated Efflux

The efflux ability of ABCB1 in the presence of a potential inhibitor was assessed by the extent of accumulation of R-123 in the Caco-2 cells grown for 5-7 days on clear plastic 96-well plates by incubating the cells with R-123 in the presence of varying concentrations of the ABCB1 inhibitor VER (Figure 3.9), which was selected due to the high frequency of citations making use of its inhibition properties (Aller et al., 2009, Profit et al., 1999, Yumoto et al., 1999, Varma and Panchagnula, 2005). The results in Figure 3.9A demonstrate that the addition of the inhibitor leads to a concentration-dependent increase in fluorescent signal consistent with that of increased R-123 accumulation in accordance with previous studies on the Caco-2 cell line (Perloff et al., 2003, Wang et al., 2006, Shapiro and Ling, 1997). The introduction of the efflux inhibitor leads to a statistically significant increase in accumulation R-123 as low as 1  $\mu\text{M}$  of VER ( $p < 0.05$ ). Further evidence supporting the blockade of the ABCB1 efflux transporter was observed visually using fluorescence microscopy, with increased intensity in the presence of VER indicative of increased R-123 accumulation compared to control wells (Figure 3.10).

The efflux of R-123 by ABCB1 is mediated by pairs of the probe binding simultaneously to the protein. The efflux inhibition by VER is non-competitive, suggesting that ABCB1 has separate binding sites for R-123 and VER, and further elucidating the broad-specificity of this transporter (Wang et al., 2006). Although the multidrug resistance protein 1 (MRP1) has been suggested to have a role in R-123 transport (Daoud et al., 2000), expression of this efflux transporter is low on the Caco-2 cell line (Prime-Chapman et al., 2004), suggesting a negligible contribution of the transporter in this model. Indeed, no significant increase was observed in the accumulation of R-123 in the presence of the MRP inhibitor IND at low concentrations (Figure 3.9B), although becoming statistically significant at 100  $\mu\text{M}$ . This is most likely attributed to IND as a low-affinity substrate of ABCB1 as established during the Transwell® model experiments at this exact concentration (Figure 3.1). Therefore, 100  $\mu\text{M}$  of VER was chosen to be incorporated into the screening model as an excipient-free positive control due to the high degree of statistical significance versus non-treated controls, and shown to be approaching the maximum levels of inhibition of the ABCB1 transporter on the Caco-2 cell line (Burton et al., 1993). Further kinetic data could not be obtained for VER beyond 100  $\mu\text{M}$  at this stage due to the limitations of the MTT toxicology study currently

employed. As an efflux inhibitor, VER may increase the uptake of MTT in the same manner to which it increases R-123 uptake, an artefact which has previously been reported (Vellonen et al., 2004).

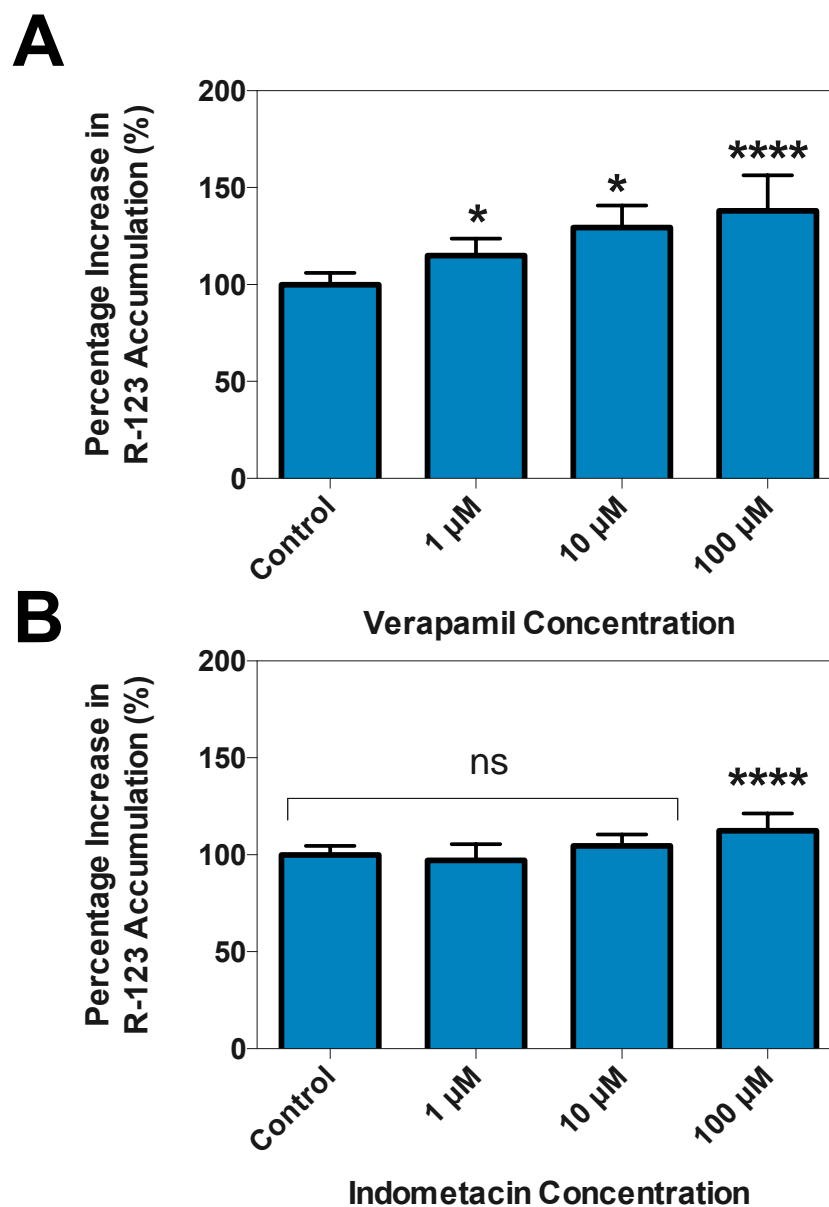


Figure 3.9. The effects of VER and IND on R-123 accumulation. Uptake of R-123 was increased in the presence of 1-100  $\mu\text{M}$  of the ABCB1 efflux protein inhibitor VER in a concentration-dependent manner after 4 hours incubation (A) but not in the presence of the MRP family inhibitor IND until a concentration of 100  $\mu\text{M}$  (B). Data is presented as  $\pm$  SD (data pooled from 10 wells), with R-123-only control normalised to 100 %. Statistical significance was analysed using one-way ANOVA followed by Dunnett's *post hoc* test annotated as follows: \* ( $p < 0.05$ ); \*\*\*\* ( $p < 0.0001$ ).

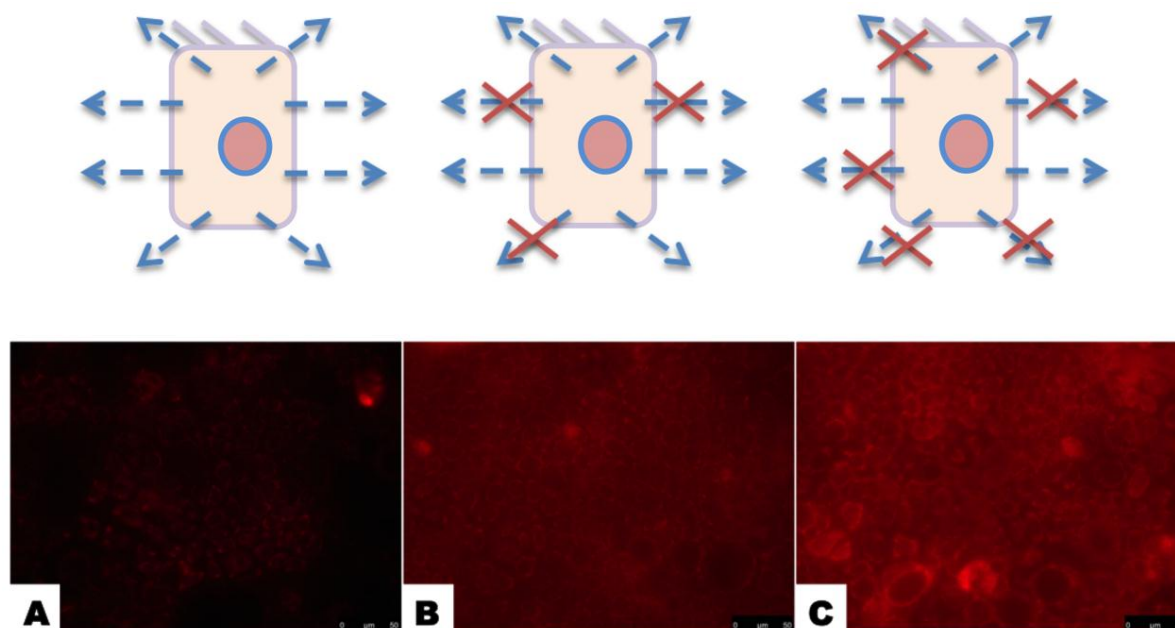


Figure 3.10. The increase in the ABCB1 substrate accumulation was confirmed using fluorescence microscopy showing 10  $\mu\text{M}$  R-123 alone (A) and with 10  $\mu\text{M}$  or 100  $\mu\text{M}$  VER (B and C respectively), leading to a concentration-dependent blockade of the ABCB1 efflux mechanism shown schematically above each image. Images are representative of cells imaged under identical conditions using 40x magnification using Caco-2 monolayers grown for 7 days in 6-well plates.

### 3.3.3. Method Optimisation

#### 3.3.3.1. Effects of Growth Time on the Cellular Accumulation of R-123

The optimisation of growth conditions is crucial in order to support reproducible R-123 uptake over a short time frame for true HTS conditions. For this purpose, cellular uptake of R-123 was tested periodically post seeding on Caco-2 cells grown for 5-7 days on clear plastic 96-well plates by incubating the cells. Dome structures, indicative of solute transport accumulation underneath a monolayer of cells grown on smooth plastic, were used as a guide to the degree of confluence, which first appear between day 4-5 and were present up to day 14 (Figure 3.11). The results of inter-day testing of the uptake of R-123 in the presence/absence of 100  $\mu\text{M}$  VER showed no statistical significance between days 5 and day 7 ( $p > 0.05$ ), with ABCB1 inhibition increasing intracellular R-123 accumulation between 134 to 147% (Figure 3.12). These results confirmed that studies could be undertaken reproducibly within this 3-day window. Caco-2 cells are well known to fully differentiate after 21 days growth post seeding, although this requires the presence of a porous material, such as the apical fascia of a Transwell® insert. When grown on the

smooth plastic of the 96-well plate, membrane becomes weak during washing steps for monolayers over 8 days old, presumably due to the high proliferation rates of the cell line resulting in net reduction in monolayer adhesion to the limited surface of the smooth plastic.

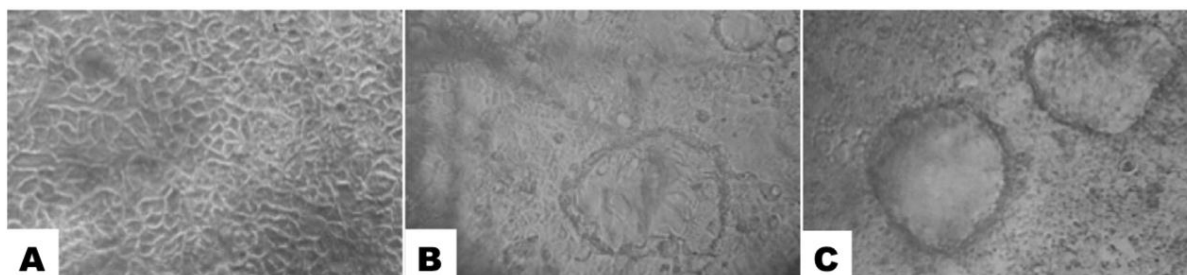


Figure 3.11. Visual indication of confluence seen under light microscopy observation. Complete confluence is observed on day 3 (A), with early dome formation observed on day 4 (B). By day 14 (C), numerous domes appear with well-defined established borders although monolayers appear less smooth. Images taken on 10x magnification.

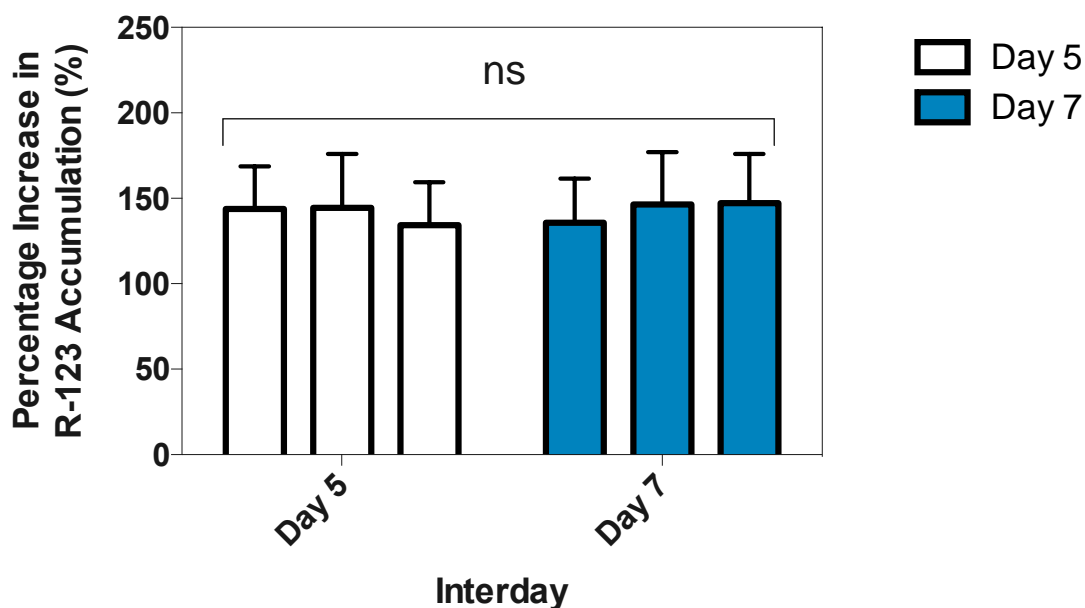


Figure 3.12. The effects of growth time on the uptake of R-123 in the presence of 100  $\mu\text{M}$  VER, tested on day 5 (clear bars) and day 7 (blue bars). The increase in R-123 accumulation remains consistent following the appearance of dome structures on the monolayers on around day 5 post-seeding following treatment with 100  $\mu\text{M}$  VER. Data is shown as the percentage increase from inhibitor-free control wells  $\pm$  SD (intraday data pooled from 3 plates,  $n = 30$  wells total). Statistical significance was analysed using one-way ANOVA followed by Tukey's *post hoc* test annotated as follows: ns ( $p > 0.05$ ).

### 3.3.3.2. Effects of Incubation Time on the Cellular Accumulation of R-123

Pre-incubation of inhibitors prior to the addition of the transporter functionality probe, fluorescent or otherwise, is highly recommended as a means of blockading the transporter system and so increasing the sensitivity of the assay for time-dependent inhibition (TDI) assays (Huang et al., 2007). In 2009, 47 % of companies screening for inhibition pre-incubated inhibitors before conducting  $IC_{50}$  values (Grimm et al., 2009). Therefore, the optimal incubation time the ABCB1 modulator VER was tested over 60 minutes (Figure 3.13). From these studies, it is shown that VER is able to traverse the cell membrane quickly, and has a  $P_{app}$  value of  $12.6 \times 10^{-6} \text{ cm s}^{-1}$  (Pauli-Magnus et al., 2000). A statistically significant ABCB1 blockade is observed after only 10 minutes pre-incubation ( $p < 0.0001$ ), leading to an increase R-123 accumulation to 146 % of the control value via transporter inhibition (Figure 3.13). No statistical difference was observed in the increase in accumulation of R-123 following further pre-incubation up to 60 minutes ( $p > 0.05$ ). As such, the membrane-permeable VER is able to quickly saturate the efflux transporter on opposing binding sites to R-123. As it is unable to exclude this concentration of VER, the inhibited ABCB1 transporter is further unable to efflux R-123 out of the cell, leading to an increase in fluorescent signal consistent with increased cellular accumulation of the fluorescent probe compared to non-treated control.

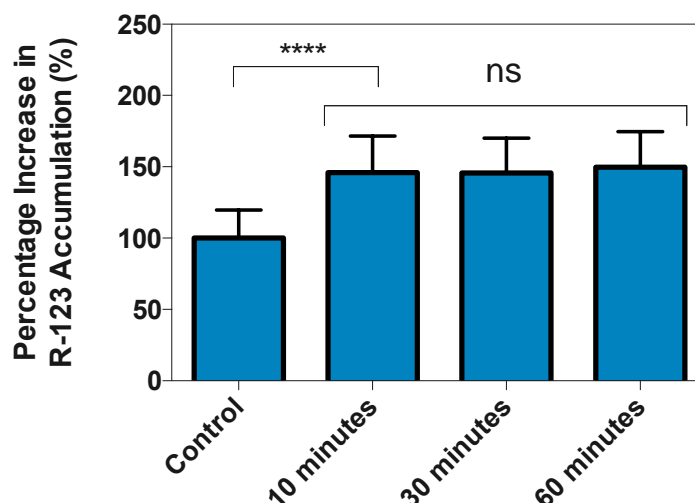


Figure 3.13. The effects of pre-incubation time of VER on the cellular accumulation of R-123. Full ABCB1 blockade is achieved in less than 10 minutes pre-incubation with 100  $\mu$ M VER. Data is shown as the percentage increase from inhibitor-free control after 60 minutes uptake  $\pm$  SD (data pooled from 3 plates,  $n = 30$  wells total). Statistical significance was analysed using one-way ANOVA followed by Dunnett's *post hoc* test annotated as follows: ns ( $p > 0.05$ ); \*\*\*\* ( $p < 0.0001$ ).

### 3.3.3.3. The Effects of Media Composition on the Cellular Viability

The binding of drugs to plasma proteins, such as albumin, is known to alter drug disposition; moreover, it is the concentration of unbound drug rather than the total concentration of drug that is responsible for its effects (Benet et al., 1996). For this reason, initial short-term R-123 uptake studies ( $\leq 4$  hours) excluded serum from the DMEM composition. To evaluate the true inhibition properties of certain excipients, extended studies ( $4 \geq$  hours) may be necessary in order to measure subtle biological effects that would be masked using short-term studies. To this end, the MTT toxicology assay was employed to test the effects of media composition on cellular viability over a 24-hour period. The MTT assay is the established method for evaluating mitochondrial dehydrogenase activity by the conversion of MTT to the insoluble formazan, which is a strong indicator of the overall viability of a cellular population. HBSS alone had a dramatic impact on the monolayers, which came off during final processing after 4 hours and so was excluded from further studies. As such, the composition of DMEM as a transport media with or without serum became the focus of investigation, and the results are presented in Figure 3.14. Interestingly, apparent mitochondrial activity increased significantly in serum-free DMEM to 190 % formazan production (compared to serum treated controls set to 100

% viability) after only 10 minutes incubation ( $p < 0.0001$ ). Over a 24-hour period, this trend continues (Figure 3.14)

Whilst *de novo* synthesis of elements essential to cellular activity such as cholesterol from acetyl-CoA (Garcia-Ruiz et al., 2009) in lieu of readily available proteins present in the media containing serum may account for the differences in mitochondrial activity over 24 hours, the difference in viability over a 10 minute period suggests this explanation to be unlikely. Moreover, the differences observed in relative viability in the presence or absence of serum is most likely attributed to protein binding by MTT itself, which limits the availability to the cells. In a previous study, it was observed that 10 % serum was enough to reduce MTT absorbance readings by as much as 50 %, similar to the present study (Huang et al., 2004). This is supported by the statistical difference between cells treated with MTT after 10 minutes versus those treated after 4 hours ( $p < 0.01$ ) and after 24 hours ( $p < 0.0001$ ), at which point the composition of the media was likely to have changed due to partial serum depletion by the time MTT was added to initiate the assay (Figure 3.14). In the absence of serum, the adhesion of the monolayers to the smooth plastic was observed to be weaker (data not shown).

The data presented in Figure 3.14 indicates that this platform can, if necessary, be extended for uptake over a 24-hour period when stabilised in serum-containing media. However, in addition to extending the time of the assay, the physiological implications of a 24-hour study are difficult to justify in the context of enhancing drug delivery. If they are able to escape metabolism and excretion by the body, a systemically circulating compound *in vivo* may last for extended periods of time in which to have a biological effect against efflux transporters. Although oral formulations are typically dosed to a steady state, and so repeated exposure to the same excipient is to be expected, only the active ingredient of the formulation is likely to be absorbed through the intestinal membrane to reach systemic stability when drug clearance is accounted for, with the pharmaceutical excipient unlikely to last more than 4 hours in transit in the gastrointestinal tract. This would suggest that any biological effects must become apparent within the first few hours of contact when the excipient is in contact with the intestinal membrane where the efflux transporters reside. Indeed, the uptake of radiolabelled molecules such as PEG 400 has been used to

demonstrate that the paracellular permeability of compounds with a molecular weight above 500 is limited in both Caco-2 monolayers and rat ileum (Artursson et al., 1993a). This molecular weight is much below the weight of many of the putative excipients being considered for testing. Therefore, whilst the possibility of a serum-stabilised extended study over a 24-hour period is achievable, a more time-efficient 4-hour assay time was selected for the R-123 screening assay.

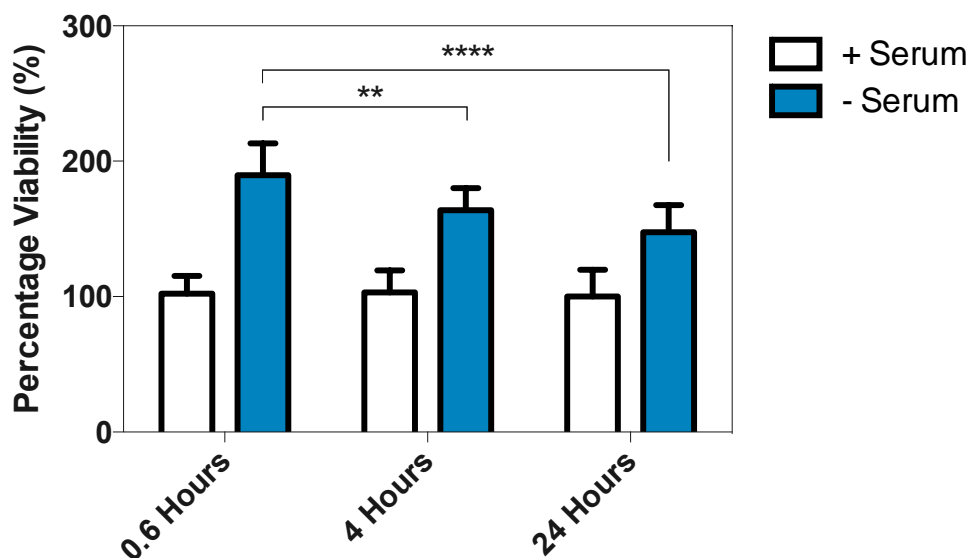


Figure 3.14. The effects of serum on the cellular viability of monolayers of Caco-2 cells. MTT cell viability assays measured the mitochondrial activity of the cells with serum (clear bars) and without (blue bars), over a 24 hour period. Data is shown standardised against serum-containing media as 100 %  $\pm$  SD (data pooled from 3 plates for a total of 30 wells). Statistical significance was analysed using two-way ANOVA followed by Dunnett's *post hoc* test annotated as follows: \*\* ( $p < 0.01$ ); \*\*\*\* ( $p < 0.001$ ).

#### 3.3.3.4. Effects of Media Composition on the Cellular Accumulation of R-123

Having established cellular viability over a 4-hour period in media both with and without serum, the impact of serum on the transport of R-123 alone and in the presence of 100  $\mu$ M VER was examined. The results are presented in (Figure 3.15). At the 4-hour time point, the cellular uptake of R-123 alone in serum-containing and serum-free media showed no significant ( $p > 0.05$ ) difference between the two, with the cell lysate showing relative fluorescent unit (RFU) values of 41 and 39 respectively (Figure 3.15). This suggests the propensity of the amphiphilic R-123 to interact with the serum proteins is limited and an almost identical amount of probe reaches the cells under both conditions. In the presence of 100  $\mu$ M VER, statistically significant differences were seen in R-123 cellular uptake between

the serum-containing and serum-free media ( $p < 0.0001$ ) from 97 RFU to 118 RFU, respectively (Figure 3.15), attributed to the high degree of protein binding of this drug. An *in vivo* human study has suggested around 90 % of circulating VER is bound to plasma proteins (Keefe et al., 1981), possibly accounting for the reduced bioavailability in the model and so decreased percentage of inhibition of the ABCB1 protein. At the site of drug delivery in the small intestines, a similar effect will be apparent due to the presence of bile and dietary proteins. Despite this, the increase in R-123 accumulation in the presence of VER in serum-containing media was still significant in the context of serum-containing controls, so this variable was chosen to stabilise cultures up to 4 hours. A summary of further assay conditions for the HTS away protocol and the rationale behind them are displayed in Table 3.5.

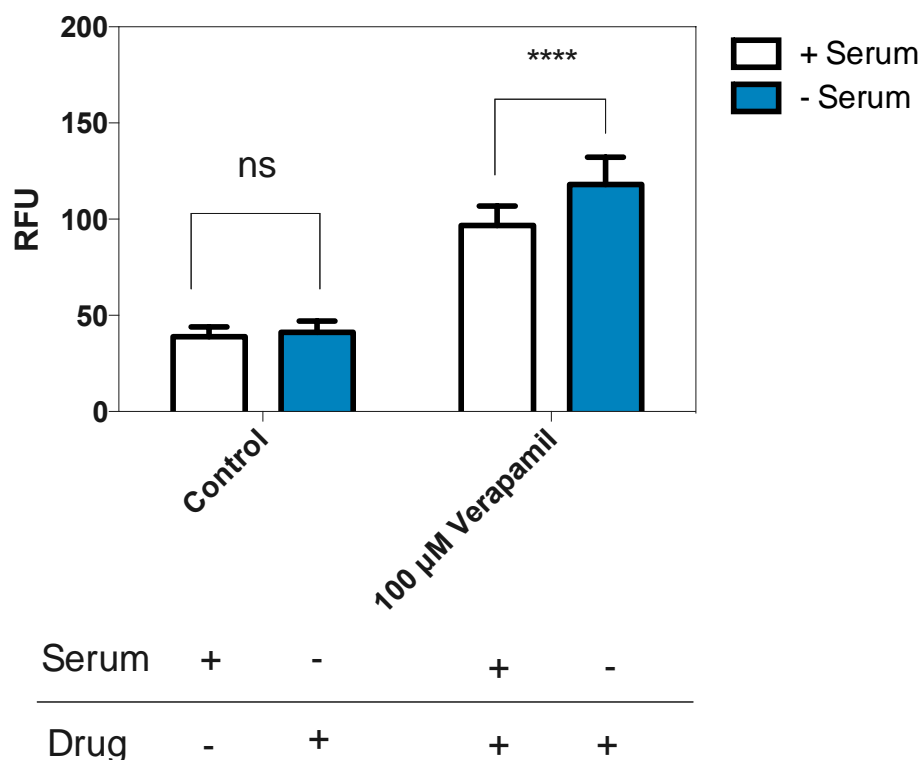


Figure 3.15. The effects of media composition on R-123 accumulation. Cellular uptake of R-123 alone was found to be unaffected by the presence of serum in the media composition over a 4 hour period. In the presence of serum (clear bars), the relative increase in R-123 accumulation by the action of 100 µM VER was reduced compared to serum-free media (blue bars). Data is shown as raw relative fluorescence units (RFU) for direct comparison of uptakes  $\pm$  SD (data pooled from 3 plates,  $n = 30$ ). Statistical significance was analysed using one-way ANOVA followed by Tukey's *post hoc* test annotated as follows: ns ( $p > 0.05$ ); \*\*\*\* ( $p < 0.001$ ).

Table 3.5. Optimised conditions for HTS protocol.

<i>Variable</i>	<i>Options</i>	<i>Chosen</i>	<i>Rationale</i>
Culture Plate	96-well plate 12-well plate 6-well plate	96-well plates	<ul style="list-style-type: none"> <li>• Low cost</li> <li>• Increased well number for higher concentration variation and increased chance of positive hit, higher <math>n</math> number for increased significance</li> </ul>
Inhibitor concentration	1 - 100 $\mu$ M	100 $\mu$ M	<ul style="list-style-type: none"> <li>• Most statistically significant concentration against non-treated control (<math>p &lt; 0.001</math>) (Figure 3.9)</li> </ul>
Cell growth time	2-14 days	7 days	<ul style="list-style-type: none"> <li>• Excellent differentiation between positive and negative controls between days 5-7 (Figure 3.12)</li> <li>• Cells require 21-day growth period on filters for complete differentiation (Wilson et al., 1990)</li> <li>• Monolayers became fragile to washing step after 7 days</li> </ul>
R-123 concentration	1 - 250 $\mu$ M	5 $\mu$ M	<ul style="list-style-type: none"> <li>• Excellent detectability below reported <math>K_m</math> of ABCB1 (Forster et al., 2012, Wang et al., 2006, Shapiro and Ling, 1997)</li> </ul>
Inhibitor Preincubation time	10-60 minutes	10 minutes	<ul style="list-style-type: none"> <li>• No significant difference (<math>p &gt; 0.05</math>) between amount of R-123 increase over 10-60 minutes (Figure 3.13)</li> </ul>

Transport Buffer	± Serum	+ Serum	<ul style="list-style-type: none"> <li>• Maintains cellular viability over extended periods</li> <li>• Significant (<math>p &lt; 0.0001</math>) increase in R-123 uptake using 100 <math>\mu\text{M}</math> VER (Figure 3.14 and Figure 3.15)</li> </ul>
Lysis buffer	HBSS PBS dH <sub>2</sub> O	dH <sub>2</sub> O	<ul style="list-style-type: none"> <li>• No expense on buffer</li> <li>• No autofluorescence (data not shown)</li> </ul>
Lysis time	15 minutes – 24 hours	15 minutes	<ul style="list-style-type: none"> <li>• Faster turnaround time for truly HTS condition</li> <li>• Less chance of R-123 degradation by lysate components</li> </ul>
Lysis conditions	Fridge (4-5 °C) Bench top (16 °C) Orbital shaker (ambient)	Orbital shaker	<ul style="list-style-type: none"> <li>• Evaluation of various lysis conditions demonstrated the superiority orbital shaker for reduced evaporation and quicker monolayer destruction</li> <li>• Plates left overnight in the fridge were found to have intact monolayers (data not shown)</li> </ul>

### **3.3.4. The Validation of the HTS Method by Evaluating the Impact of Tween 20 and Tween 80 on Caco-2 Monolayers**

#### **3.3.4.1. Cytotoxicity**

As the Caco-2 monolayer is utilised as a model for the human intestine, treatment concentrations have to be scaled appropriately. As such, MTT toxicology studies are commonly used to indicate the non-toxic parameters of test solutions by monitoring mitochondrial activity. The conversion of MTT to formazan produces an insoluble product that can be measured and quantified in relation to non-treated cells. The main toxic effects of drugs tend to be mitochondrial damage (Chresta et al., 1996). However, Tweens, as surfactants, will have an additional high propensity to interact with the lipid membranes of the cells of the monolayer, and in doing so may impart cellular toxicity. The cellular viability of the Caco-2 monolayers in the presence of different concentrations of Tween 20 and Tween 80 over 4 hours is presented in Figure 3.16. Both Tween 20 and Tween 80 showed a statistically significant reduction in cell viability on the Caco-2 cells at 1 % (v/v) ( $p < 0.01$ ) with reductions to 26 % and 89 % viability, respectively. For this reason, a concentration range between 0.01 - 0.1 % (v/v) was chosen for uptake studies in the presence of R-123, as this concentration range showed no significant change in cellular viability ( $p > 0.05$ ).

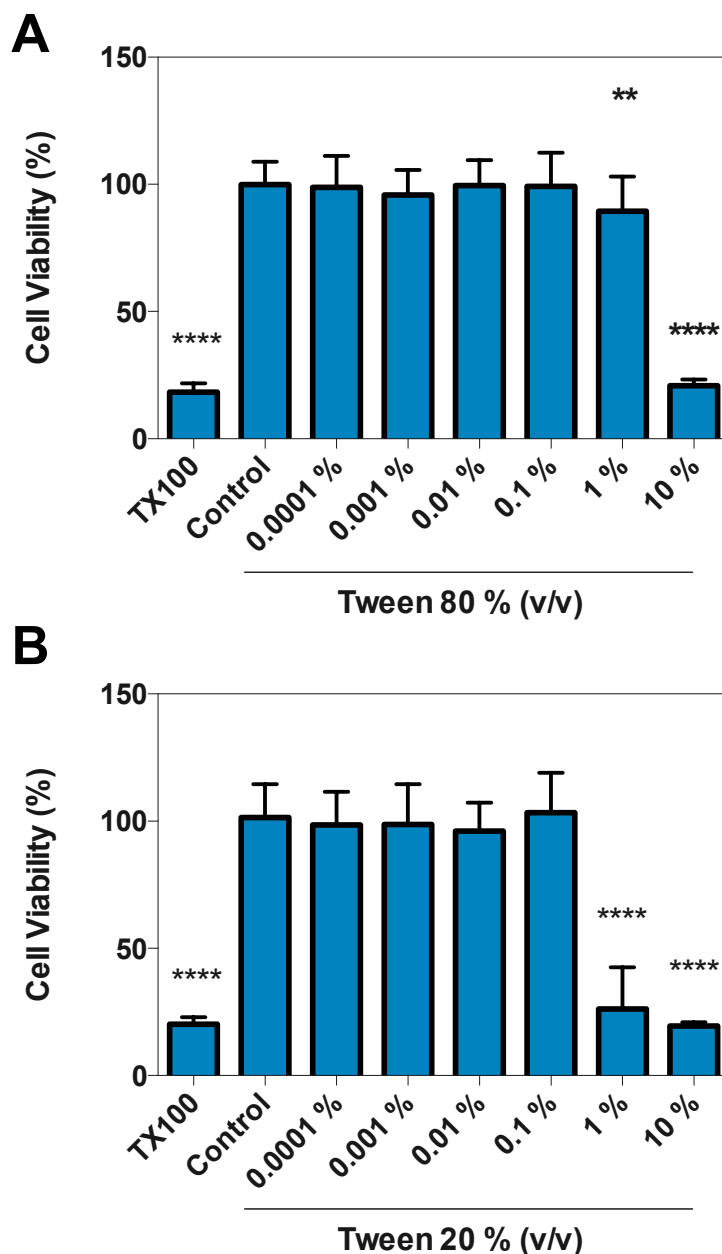


Figure 3.16. The toxicological effects of the Tweens on Caco-2 monolayers. MTT assays were performed on Caco-2 monolayers incubated with varying concentrations of Tween 80 (A) and Tween 20 (B) for 4 hours. Data expressed as the mean of percentage cell viability relative to untreated controls  $\pm$  SD ( $n = 20$  from 2 passage numbers). Statistical significance was analysed using one-way ANOVA followed by Dunnett's *post hoc* test annotated as follows: \*\* ( $p < 0.01$ ); \*\*\*\* ( $p < 0.0001$ ). Triton-X was used as a positive control at 0.05 % (v/v).

### 3.3.4.2. The Biological Effects of Tween 20 and Tween 80 on ABCB1 Activity

In order to validate the developed HTS platform, the well-known inhibitors of ABCB1-mediated transport, Tween 20 and Tween 80, were tested for their ability to inhibit ABCB1-mediated efflux of R-123. The results are presented in Figure 3.17. Over 4 hours, all

treatments showed statistically significant increases in the accumulation of R-123 ( $p < 0.05$ ). At the lowest concentration of Tween 20 and 80 (0.01 % v/v), statistical significance is observed after 120 minutes ( $p < 0.0001$ ), and 60 minutes ( $p < 0.001$ ) respectively. At 0.05 % and 0.1 % (v/v), Tween 20 increases R-123 accumulation rapidly, becoming statistically significant after 10 minutes ( $p < 0.001$  and  $0.0001$  respectively). Tween 20 has the most dramatic overall impact on the increase in accumulation: after 4 hours, the uptake in the presence of Tween 20 reached  $522.7 \pm 98.7$  % of non-treated control, whereas Tween 80 increased uptake by  $264.8 \pm 48$  % (Figure 3.17).

As a high-affinity substrate of the ABCB1 transporter system, any increase in the accumulation of R-123 can be attributed to the decrease in ABCB1-mediated efflux. As the activity of this efflux transporter decreases, the R-123 that enters the cell remains, leading to a rise in fluorescent signal compared to that of non-treated controls. Surfactants such as Tweens have been well studied for their ability to modulate ABCB1 through the altered fluidity of the lipid membrane, and so were chosen to validate the screening protocol, and the ability of a surfactant molecule to alter membrane fluidity is dependent upon the hydrophilic to lipophilic balance (HLB) (Buckingham et al., 1995). The large differences in the inhibition properties of the two Tweens cannot be explained in terms of the HLB values of the compounds, both of which are similar (16.7 and 15 for Tweens 20 and 80, respectively (Wade and Weller, 1994)). This suggests that their propensity for interacting with the lipid bilayer, and so disrupt the microviscosity of the membrane through their respective hydrophobic regions, is not only similar, but optimal (Lo, 2003). Structurally, the two Tweens have a large degree of homogeneity, and differ only in the side chain length: Tween 80 has a larger oleic acid side chain, whereas Tween 20 has a smaller lauric acid side chain. This is reflected in the molecular weights of the two compounds ( $1310 \text{ gmol}^{-1}$  for Tween 80 versus  $1228 \text{ gmol}^{-1}$  for Tween 20), and may explain why Tween 20 may have better lipid association by having less steric hindrance, and so resulting in enhanced membrane disruption when compared to Tween 80. Tweens may use several other mechanisms to modulate ABCB1, such as inhibiting protein kinase C (PKC) activity, thereby reducing the phosphorylation of the protein and resulting in a modulating effect (Komarov et al., 1996). Additionally, Tween 80 has been shown to non-competitively inhibit substrate binding to ABCB1 (Yamazaki et al., 2000). The degree of efflux inhibition

may suggest that the Tweens mode of action is multi-factorial, involving a number of mechanisms for the blockade of ABCB1. Both Tween 20 and Tween 80 appear in the literature multiple times as P-gp inhibitors (Hugger et al., 2002b, Lo, 2003, Shono et al., 2004, Li et al., 2011b), validating the dose-dependent increase in R-123 in the presence of these excipients as inhibition of ABCB1-mediated efflux.

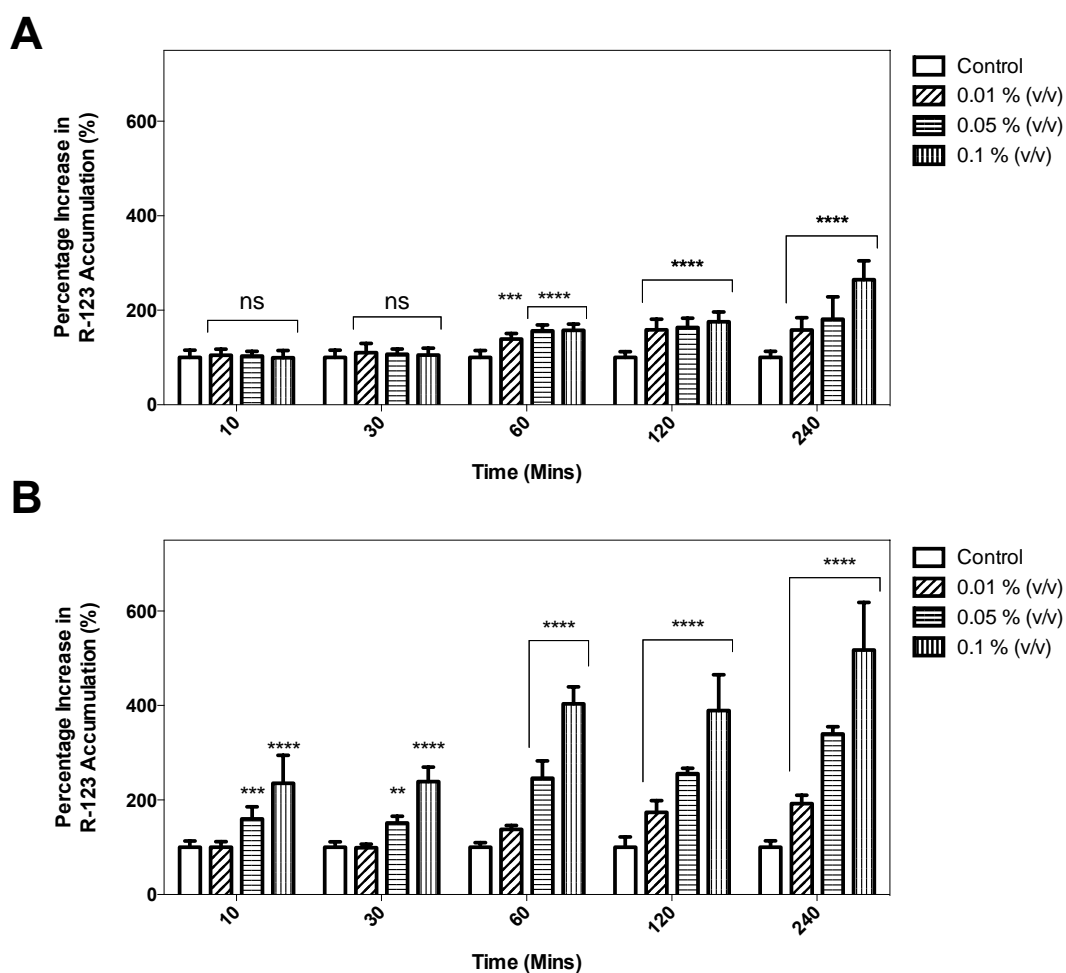


Figure 3.17. The biological effects of the Tweens on ABCB1 activity, showing (A) Tween 80 and (B) Tween 20 after 4 hours of incubation in the presence of R-123. Data is shown as the percentage increase in cellular R-123 accumulation in the presence of the Tweens versus excipient-free control wells, presented as the mean from  $n = 10$  wells  $\pm$  SD. Statistical significance was analysed using two-way ANOVA followed by Dunnett's *post hoc* test annotated as follows: ns ( $p > 0.05$ ); \*\* ( $p < 0.01$ ); \*\*\* ( $p < 0.001$ ); \*\*\*\* ( $p < 0.0001$ ).

### 3.3.5. Testing the Biological Effects of MCC, HPMC, Starch 1500 and PVAP on ABCB1-Mediated Transport

Once the assay was established and validated, the next stage was to test previously uncharacterised excipients. In order to boost throughput, the cellular accumulation of 5  $\mu\text{M}$  R-123 was examined over a 2-hour assay time. The excipients of choice were microcrystalline cellulose (MCC), Starch 1500, polyvinyl acetate phthalate (PVAP) and hydroxypropyl methylcellulose (HPMC) (Table 3.6). Although these excipients are not PEGylated, literature contains examples of compounds which have shown activity against transporters without having this moiety, such as lipid excipients which decrease expression of ABCB1 (Sachs-Barrable et al., 2007), and polycarbophil which is believed to increase oral bioavailability of paclitaxel by inhibition of this protein (Föger et al., 2008). Both MCC and HPMC are cellulose derived, whereas Starch 1500 is a polymer of amylose and branched amylopectin and PVAP consists of various repeating units of acetyl and phthalyl. Of these, only HPMC was soluble under ambient conditions at 10 mg mL<sup>-1</sup>. All other excipients tested produced suspensions at pH 7.4 (the physiological enteric pH used for *in vitro* studies), and test solutions were prepared as such. Co-solvents were not used due to concerns regarding cellular viability. As the only soluble excipient with a well-known lack of toxicity, HPMC was used to a final concentration of 10 mg mL<sup>-1</sup>, whereas all other excipients were used at 2.5 mg mL<sup>-1</sup> in order to minimise the amount of precipitate present in each of the wells.

The results of the efflux studies (Figure 3.18) demonstrate that MCC had no significant impact on efflux ( $p > 0.05$ ). However, PVAP significantly *decreased* uptake of R-123 ( $p < 0.0001$ ) between 65-59 % of the control wells in a concentration-dependent manner. Starch 1500 showed an increase in a concentration-dependent manner between 111-212 % of the control wells. Likewise, HPMC showed a concentration-dependent increase over the range tested ( $p < 0.001$ ) between 117 – 148 % of the control wells. The increase seen for Starch 1500 and HPMC is most likely not attributed to the inhibition of ABCB1 (Figure 3.18b and Figure 3.18d). HPMC is a well-known mucoadhesive, and at higher concentrations HPMC films could be seen covering the cells within each well (data not shown). During the wash phase of the experiments, this film could not be removed without prior removal of cell

monolayer, an issue likely compounded by the ice-cold wash increasing the viscosity of the excipient. Likewise, Starch 1500 particles were also visible on the cell monolayer surface which again could not be removed. Such factors are a limitation to the model, and highlight the need for increasing the diversity of the concentration ranges used over logarithmic dilution range in order to overcome such issues. The significant decrease in cellular R-123 accumulation seen by PVAP (Figure 3.18a) is most likely attributed to the decrease in pH observed over the course of the 4-hour experiment as individual particles of PVAP underwent dissolution, notably decreasing the pH of the transport media beyond the buffering capacity of the HEPES, and effectively reversing the pH gradient of the assay.

Table 3.6. Purpose and structural formula of excipients tested (\* source Handbook of Pharmaceutical Excipients, 6<sup>th</sup> Edition)

<i>Excipient</i>	<i>Purpose</i>	<i>Appearance upon dissolution in PBS (pH 7.4)</i>	<i>Structural Formula*</i>
Microcrystalline cellulose (MCC)	Disintegrant	Suspension	 <p>Aston University</p> <p>Illustration removed for copyright restrictions</p>
Starch 1500	Binder/Disintegrant	Suspension	 <p>Aston University</p> <p>Illustration removed for copyright restrictions</p>
Polyvinyl Acetate Phthalate (PVAP)	Enteric release coating polymer	Suspension	 <p>Aston University</p> <p>Illustration removed for copyright restrictions</p>
Hydroxypropyl methylcellulose (HPMC)	Extended release polymer	Clear viscous liquid	 <p>Aston University</p> <p>Illustration removed for copyright restrictions</p>

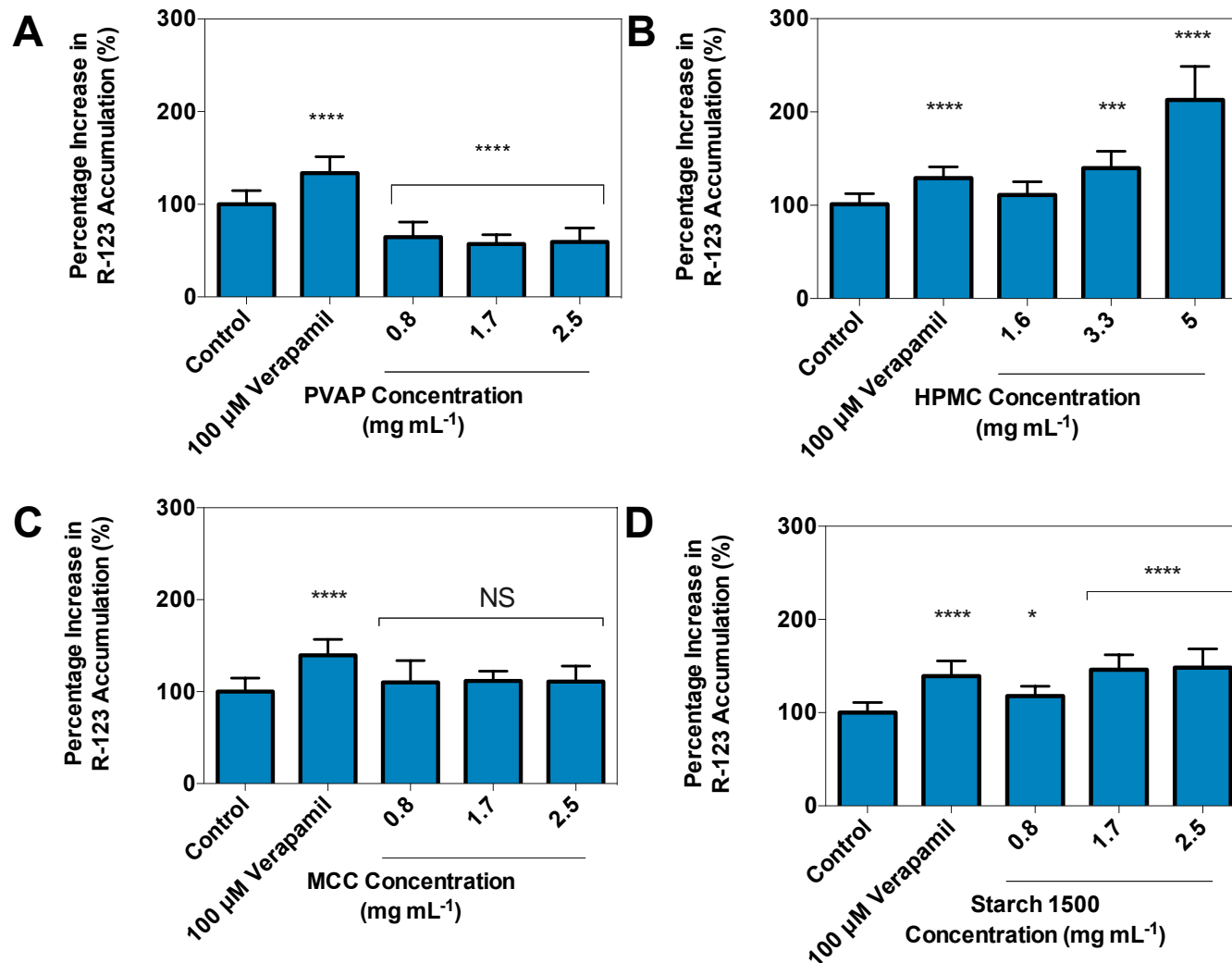


Figure 3.18. The percentage increase in cellular accumulation of R-123 in the presence of 100 µM VER or the excipients of choice of 4 hours, showing A) PVAP, B) HPMC, C) MCC and D) Starch 1500. Data is presented as  $\pm$  SD (data pooled from 8 wells), with R-123-only control normalised to 100 %. Statistical significance was analysed using one-way ANOVA followed by Dunnett's *post hoc* test annotated as follows: ns ( $p > 0.05$ ); \* ( $p < 0.05$ ); \*\*\* ( $p < 0.001$ ); \*\*\*\* ( $p < 0.0001$ ).

### 3.3.6. Conclusions of *In Vitro* Method Development and Model Selection

Using an optimised protocol, the non-ionic excipients Tween 20 and Tween 80 were tested for their biological effect against the ABCB1 transporter below their cytotoxic concentrations. The results of this study validate the HTS platform against existing literature examining the biological effects of surfactants. Of course, every model has positive and negative attributes and a fair criticism of both types evaluated are displayed in Table 3.7. Owing to the multi-purpose nature of the 96-well plate format, the reduction in the time and resources necessary to obtain data, and the high-throughput potential of the platform, this method was chosen for future development over the Transwell® model. The final HTS protocol is outlined in Figure 3.19.

During the platform development, literature searches showed the existence of a fluorescent probe of the MRP2 transporter: 5(6)-carboxy-2',7'-dichlorofluorescein. This probe is unable to cross membranes of cells, so is added to transport media in diacetate form which is able to freely diffuse to the cytoplasm where it gets converted to the fluorescent species. Although ABCC2 is a well-characterised efflux protein, little is known about the effects of excipients against its function. The addition of this new fluorescent entity to the HTS protocol presented in this chapter had the potential to address this.

Finally, a critical evaluation of the HTS platform in its current form also highlights the lack of quantification of the inhibition data. From data obtained on excipients as inhibitors of efflux transports in this chapter, no reference point can be used to link the materials in order of efficacy, or the quantity required to elicit appropriate efflux inhibition *in vivo*. This data is of critical value if the information is to be utilised in order to enhance oral dosage formulations, as it indicates the minimal quantity of material required in a potential dosage form. As such, the following chapter will focus on the kinetic analysis of excipients by highlighting the amount required to reduce transporter activity by 50 % - the IC<sub>50</sub> value.

Table 3.7. A critique of the aspects of both models tested in this chapter. Media consumption per plate is based on renewal every 48 hours and includes seeding media.

<i>Model</i>	<i>Positives</i>	<i>Negatives</i>
6-Well Transwell®	<ul style="list-style-type: none"> <li>• Considered the 'gold standard' of <i>in vitro</i> drug transport assays</li> <li>• Full differentiation</li> <li>• Established tight junctions</li> <li>• Polarised transport can be explored</li> <li>• Drug transport can be used to estimate human absorption</li> </ul>	<ul style="list-style-type: none"> <li>• Slow 21-day growth time</li> <li>• Slow time to analyse data</li> <li>• Transporter probe substrate requires careful evaluation</li> <li>• 264 mL media to get a single 6-well plate to maturation</li> <li>• Low <i>n</i> number</li> <li>• High unit cost</li> </ul>
96-Well Plate	<ul style="list-style-type: none"> <li>• 77 mL to get one 96-well plate to maturation</li> <li>• Probe specificity can easily be established</li> <li>• High-throughput, fast analysis</li> <li>• Multi-purpose platform, can easily be used for fluorescent probe uptake as well as MTT or morphological studies etc. without modification</li> <li>• High <i>n</i> number possible</li> <li>• Data easily manipulated to gain PK data</li> <li>• Low unit cost</li> </ul>	<ul style="list-style-type: none"> <li>• Poor estimation of mode of transport due to 2D monolayer, e.g. does not account for paracellular route</li> <li>• Only partial differentiation</li> <li>• Only absorptive (apical to intracellular) transport can be observed</li> <li>• Monolayer fragility over time</li> </ul>

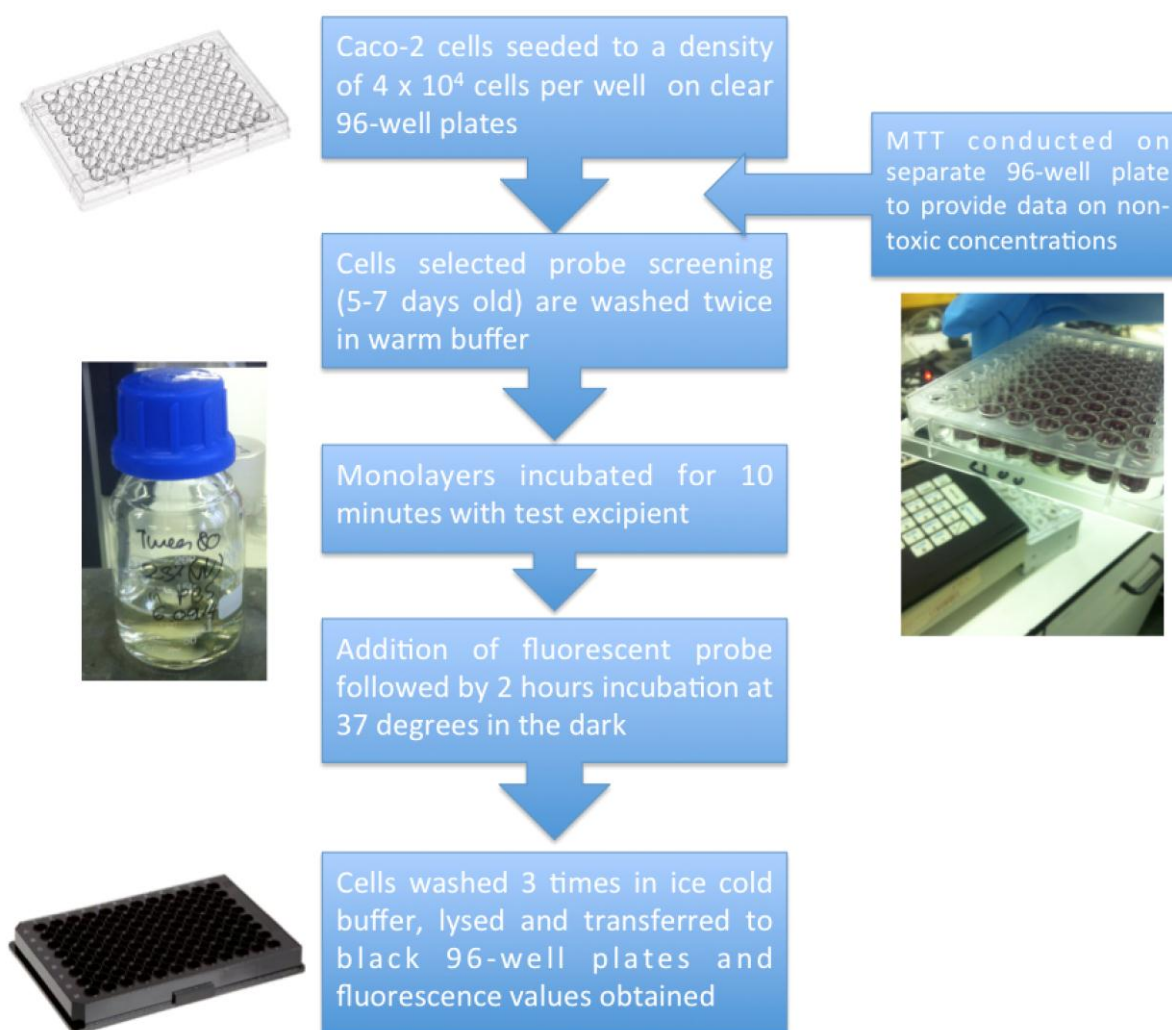


Figure 3.19. Schematic diagram of HTS protocol. Cells are grown for 5-7 days, at which point MTT is conducted on the test excipient to determine the non-toxic concentrations used. Next, a separate 96-well plate is prepared for the uptake study by carefully washing out the well, incubating with the excipient(s) before the addition of the fluorescent probe. Cells are then incubated for 2 hours prior to careful washing, lysing, and fluorescence quantification using black 96 well plates.

## **Chapter 4**

### **A Kinetic Study on the Effects of Excipients Against ABCB1- and ABCC2-Mediated Transport**

## 4. A Kinetic Study on the Effects of Excipients against ABCB1- and ABCC2-Mediated Transport

### 4.1. Chapter Aim and Objectives

Intestinal efflux transporters are of pharmacodynamic and pharmacokinetic interest for anticipating drug behaviour *in vivo*. The existing literature on this subject reveals an extensive list of excipients that elicit effects against ABC efflux transporters — most notably ABCB1. However, such information is rarely quantified in pharmacokinetic terms, thereby making the process of optimising oral formulations for increasing efflux prone drug bioavailability challenging. Therefore, the aim of the work presented in this chapter was to identify excipients of high efficacy which are inhibitors of the ABCB1 and ABCC2 efflux transporter systems, and quantify this data in a way that can be pragmatic from the formulation perspective. In order to do this, a number of objectives needed to be met:

- The first objective was to obtain kinetic data relating to the established ABCB1 inhibitors verapamil (VER) and ciclosporin (CsA) and the ABCC2 inhibitors indometacin (IND) and probenecid (PBD), in order to assess the function of these transporters on the cell line within the framework of existing literature and also to act as a reference point for the efficacy of excipients found to be inhibitors.
- As the overall aim of the project was to produce an oral dosage form capable of enhanced delivery, the second objective was to screen a plethora of excipients using the HTS assay that could be used as tablet components. These excipients were coating agents, polymeric carriers and a broad range of surfactants.
- The final objective was to identify and delineate any non-specific effects of the excipients that are not mechanisms related to transporter inhibition, such as membrane damage and toxicology, which may otherwise give false inhibition data.

In order to rank the ability of the excipients to inhibit the ABCB1 and ABCC2 efflux transporters, the data were presented in a pharmacokinetic format by elucidating the amount of excipient required to reduce the transporter activity by 50 %, the IC<sub>50</sub> value. This approach allowed the excipients to be directly compared in terms of their efficacy, as well as a direct comparison to the established inhibitors of efflux.

#### 4.2. An Examination of Inhibitors of the ABCB1 and ABCC2 Efflux Transporter Systems

In order to initially establish the functional activity of the transporters, established inhibitors of the efflux transporters were tested in conjunction with the fluorescent probes in order to obtain their IC<sub>50</sub> values, as outlined in the materials and methods section (Section 2.3). The results shown in Figure 4.1 demonstrate that the inhibitors of both ABCB1 (VER and CsA) and ABCC2 (IND and PBD) follow a dose-dependent response (non-linear regression curves), allowing IC<sub>50</sub> values to 95 % confidence to be calculated (Table 4.1). The ABCB1 inhibitors VER and CsA give IC<sub>50</sub> values of 4.08 and 1.16 μM, respectively, with the ABCC2 inhibitors IND and PBD giving IC<sub>50</sub> values of 38.08 and 68.08 μM, respectively. Compared to established literature (Table 4.1), the derived IC<sub>50</sub> data for the ABCB1 inhibitors aligns well with the published range. For the inhibitors of ABCC2, the derived IC<sub>50</sub> value for IND also aligns well with published literature, although the derived value for PBD is an order of magnitude lower than the published values (Table 4.1). However, comparative literature IC<sub>50</sub> values for IND and PBD as inhibitors of ABCC2-mediated efflux are limited, despite their prevalence in the literature as common modulators of this transporter. In this respect, the study by Heridi-Szabo *et al* was used to derive two further IC<sub>50</sub> values from the K<sub>i</sub> values given (Heredi-Szabo et al., 2008). These K<sub>i</sub> values were converted to IC<sub>50</sub> values using the Cheng-Prusoff equation (Yung-Chi and Prusoff, 1973) shown in Equation 4.1,

$$K_i = \frac{IC_{50}}{1 + \frac{[S]}{K_m}} \quad \text{Equation 4.1}$$

where K<sub>i</sub> is the inhibitor affinity, the IC<sub>50</sub> is the concentration of inhibitor that inhibits 50% of the transport, [S] is the concentration of the substrate, and K<sub>m</sub> is the substrate affinity.

From the published values collected in Table 4.1 (Rautio et al., 2006, Wang et al., 2001, Perloff et al., 2002, Tamai and Safa, 1991, Colombo et al., 2012, El-Sheikh et al., 2007, Dahan and Amidon, 2010, Heredi-Szabo et al., 2008, Förster et al., 2008), it is apparent that the variation in the cell line or vesicle type used to determine the  $IC_{50}$  has minimal impact upon the  $IC_{50}$  value obtained, as each inhibitor falls within a tight range of values. Moreover, the type of probe used has a notable impact: Rautio *et al* used the Caco-2 platform in the Transwell® format, and evaluated the  $IC_{50}$  values of VER using multiple probe substrates (Rautio et al., 2006). The inhibition  $IC_{50}$  value of VER was found to be below 11  $\mu$ M when digoxin and prazosin were used as probe substrates, between 17  $\mu$ M and 34  $\mu$ M when colchicine and vinblastine were used as probe substrates, and 60.9  $\mu$ M when calcein-AM was used as a probe substrate (Rautio et al., 2006). As P-gp has known multiple binding sites (Shapiro et al., 1999, Wang et al., 2001), Rautio *et al* attributed the broad range of inhibition  $IC_{50}$  values to the different inhibitors exerting their effects on different binding sites within the transporter (Rautio et al., 2006). Taken together, the data present in Figure 4.1 and Table 4.1 confirm the functionality of the ABCB1 and ABCC2 transporter systems on the cell line by using the combination of specific fluorescent probes with established inhibitors, subsequently validating the method and providing a foundation for translating this work on drug-drug interactions (DDIs) to excipient-drug interactions (EDIs).

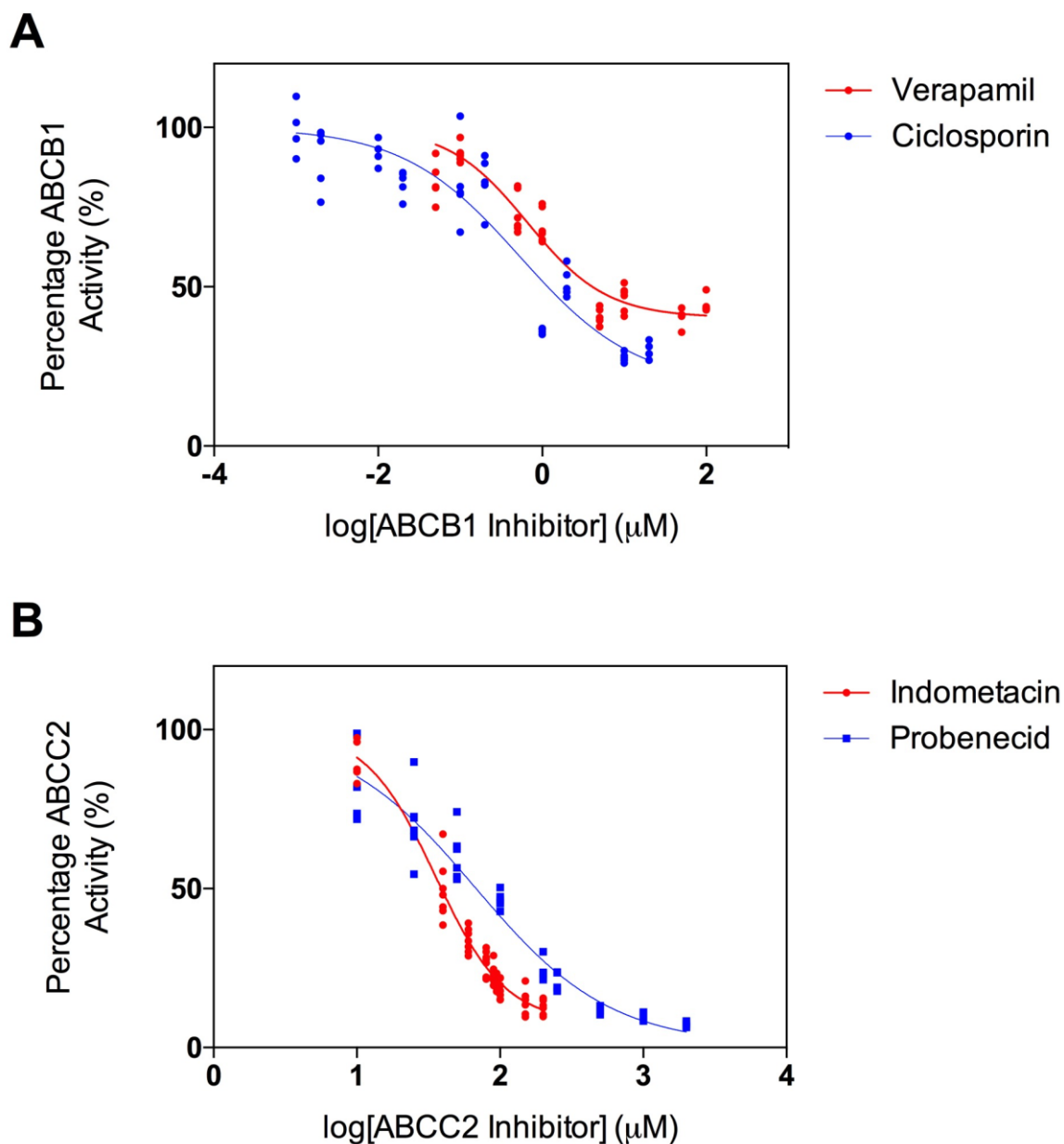


Figure 4.1. The  $\text{IC}_{50}$  curves of inhibitors of efflux proteins, showing activity against A) ABCB1 and B) ABCC2. Caco-2 cells were grown for 5-7 days on 96-well plates prior to experimentation. Data presented as each of a minimum of 4 replicates from 2.5  $\mu\text{M}$  initial extracellular concentration of either R-123 or CDFDA as probes of ABCB1 and ABCC2 activity, respectively.

Table 4.1. Literature IC<sub>50</sub> values of the inhibitors against those obtained from Caco-2 cells grown for 5-7 days on 96-well plates. Data of determined IC<sub>50</sub> values shows the outcome of the kinetic modelling using GraphPad Prism presented in Figure 4.1 extrapolated for 50 % transporter inhibition using the sigmoidal curve.

<i>Drug</i>	<i>Structure</i>	<i>Transporter Action</i>	<i>Reported IC<sub>50</sub> (μM)</i>	<i>Mean Determined Value (μM)</i>	<i>Determined Upper Value (μM)</i>	<i>Determined Lower Value (μM)</i>	
Verapamil		ABCB1/P-gp	1.18 - 60.9	(Rautio et al., 2006) <sup>a</sup>	4.08	7.44	2.36
			4.2	(Wang et al., 2001) <sup>b</sup>			
			6.5	(Perloff et al., 2002) <sup>c</sup>			
Ciclosporin		ABCB1/P-gp	0.5	(Tamai and Safa, 1991) <sup>d</sup>	1.16	1.936	0.72
	1.4		(Wang et al., 2001) <sup>b</sup>				
	0.74-2.22		(Rautio et al., 2006) <sup>a</sup>				
Indometacin	ABCC2/MRP2	25	(Colombo et al., 2012) <sup>e</sup>	38.99	41.4	36.31	
		46	(El-Sheikh et al., 2007) <sup>e</sup>				
		75.1	(Dahan and Amidon, 2010) <sup>c</sup>				
		99	(Heredi-Szabo et al., 2008) <sup>e</sup>				
Probenecid	ABCC2/MRP2	130	(Colombo et al., 2012) <sup>e</sup>	68.08	77.27	60	
		812	(Heredi-Szabo et al., 2008) <sup>e</sup>				
		814.8	(Förster et al., 2008) <sup>f</sup>				

<sup>a</sup>MDCKII-MDR1

<sup>b</sup>MDR1-NIH3T3-G185

<sup>c</sup>Caco-2

<sup>d</sup>Vincristine-resistant Chinese Hamster Lung Cells

<sup>e</sup>MRP2 Membrane Vesicles

<sup>f</sup>MDCK-ABCC2

### 4.3. An Examination of the Effects of Low Viscosity HPMCs on ABCB1- and ABCC2-Mediated Transport

Having achieved the first of objectives of this chapter by establishing the functionality of the ABCB1 and ABCC2 transporter systems, the next stage was to utilise this assay to common excipients which are efflux inhibitors, and to model these in a pharmacokinetic manner. To undertake this, hydroxypropyl methylcellulose (HPMC) was selected in the first stage of the studies. HPMC is a semi-synthetic polymer system consisting of partly *O*-methylated cellulose (Figure 4.2). High-viscosity HPMCs are frequently used in the tablet binder role, film coating and as an extended release matrix, whereas the low-viscosity HPMCs are favoured for coatings. As one known limitation of this high-throughput screening assay is viscosity, especially in those excipients that are able to impart mucoadhesion to the cell surface, the HPMCs chosen for evaluation were of the METHOCEL LV (low viscosity) type, outlined in Table 4.2. Of these, METHOCEL “E” grades are favoured for all coatings, whereas the “K” grades are recommended only for sugar coating (DOW, 2002). METHOCEL K grades have poorer flow properties compared to E grades with a higher degree of long, fibrous particles than the METHOCEL “E” grades (DOW, 2000).



Figure 4.2. The general structure of HPMCs, with the degree of substitution of methoxyl or hydroxypropyl ( $x$ ) specific to the grade.

Table 4.2. Degree of substitution and viscosity of the METHOCEL LV grade HPMCs.

<i>HPMC Grade</i>	<i>Methoxyl Content (%)</i>	<i>Hydroxypropyl Content (%)</i>	<i>Viscosity (mPa.s)</i>
METHOCEL E3 LV	28-30	7-12	2.4-3.6
METHOCEL E6 LV	28-30	7-12	5-7
METHOCEL E15 LV	28-30	7-12	12-18
METHOCEL K3 LV	19-24	7-12	2.4-3.6

#### 4.3.1. The Effects of Low Viscosity HPMCs on Cellular Viability

In order to evaluate the toxicological impact of the HPMCs against the Caco-2 cell line, the MTT assay was used to probe the mitochondrial vitality under a range of polymer concentrations. The results of the toxicological screening are presented in Figure 4.3. These materials were well tolerated in the *in vitro* cell model at concentrations as high as 0.01 % (w/v). At higher HPMC concentrations, a small but significant ( $p < 0.05$ ) reduction in apparent viability of approximately 10 to 20 % was observed (Figure 4.3). This apparent reduction in the viability of the monolayer may be attributed to residual mucoadhesion of these grades masking MTT ingress into the cells, as visual examination confirmed monolayer integrity was otherwise uninterrupted (results not shown).

On the Caco-2 cell line, HPMC K4M and HPMC K100 have been shown to have  $IC_{50}$  toxicology values of 7.69 and 13.57 mg mL<sup>-1</sup>, respectively, with the toxicology found to be related to molecular weight, with the higher molecular weight (HPMC K4M) showing significantly ( $p < 0.05$ ) higher toxicity (Li et al., 2013a). The viscosity of HPMC has been shown to be connected to molecular weight (DOW, 2000), with K100 and K4M having viscosities of 100, 000 mPa·s and 4000 mPa·s respectively at 2 % (w/v). The HPMCs tested in the present study have much lower molecular weight values (Table 4.2) and consequently would be expected to impart much lower toxicities. HPMCs are regarded as safe excipients (Burdock, 2007) and have been used up to 20 mg mL<sup>-1</sup> on both the HepG2 and Fa2N4 cell lines (Tompkins et al., 2010). As such, 0.1 % (w/v) was selected as an upper limit for efflux probe uptake studies, similar to a concentration used previously on the Caco-2 cell line grown in the Transwell® format (Rege et al., 2001).

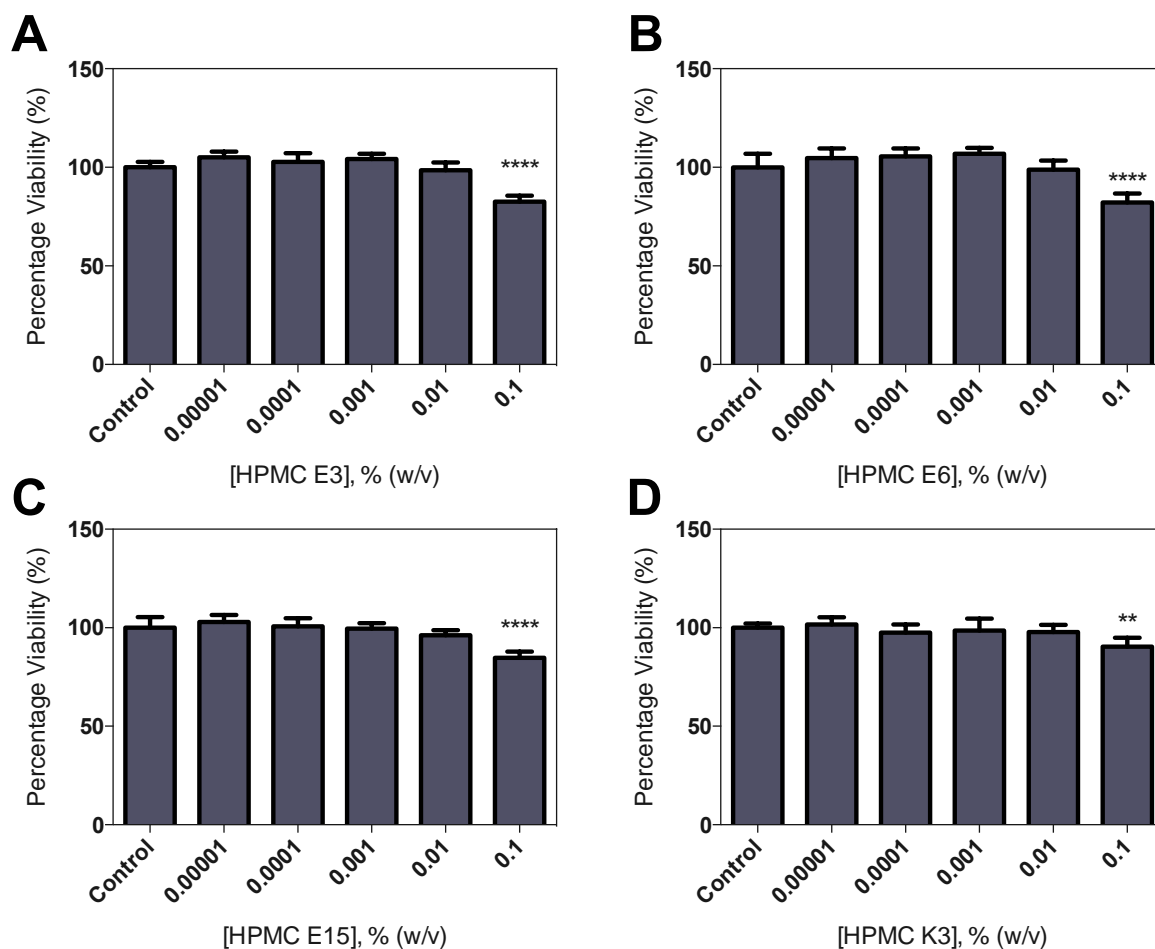


Figure 4.3. The effects of HPMCs on cellular viability using the MTT toxicology assay, showing A) METHOCEL E3, B) METHOCEL E6, C) METHOCEL E15 and D) METHOCEL K3. Caco-2 cells were grown for 5-7 days on 96-well plates prior to experimentation. Data presented as the mean value of 6 replicates  $\pm$  SD. Statistical significance was analysed using one-way ANOVA followed by Dunnett's *post hoc* test annotated as follows: \*\* ( $p < 0.01$ ); \*\*\*\* ( $p < 0.0001$ ).

#### 4.3.2. The Effects of Low Viscosity HPMCs on ABCB1- and ABCC2-Mediated Transport

Having established that the low-viscosity HPMCs are non-toxic to the Caco-2 cell line at or below 0.1 % (w/v), the next stage of investigation was to examine the impact of these excipients on ABCB1- and ABCC2-mediated efflux. The results of the screening study are presented in Figure 4.4. Over the concentrations tested, no significant ( $p > 0.05$ ) impact upon either transporter activity could be seen, and fluorescent signal remained stable for each test solution relative to control (Figure 4.4). Therefore, the data does not fit the non-linear sigmoidal regression line shown in Figure 4.1. Although the other materials in this

study have much lower viscosity than the HPMCs, and therefore less likely to alter the diffusional path of the tracer probes used, the wide concentration range used in this study should have negated the possibility of such interference on probe uptake. Therefore, it can be concluded that the low viscosity HPMCs have no efflux modulating capacity.

HPMC is frequently used as a matrix excipient in a number of formulation studies, and has been examined individually as an inhibitor of P-gp. Similar to the findings in Fig 4.4, using the Caco-2 Transwell® model, 0.012 % (w/v) HPMC E5 Premium LV has been shown to have no significant impact upon the apical to basolateral transport of the three P-gp substrate drugs atenolol, ranitidine and acyclovir (Rege et al., 2001). During the testing of a binary solid dispersion (SD) containing Solutol HS-15 and HPMC 2910, analogous to HPMC METHOCEL 'E' grade, the latter material individually showed no significant ( $p > 0.05$ ) impact upon the uptake of R-123 in ovarian NCI/ADR-RES cells overexpressing P-gp (Han and Lee, 2011). Furthermore, as part of a wider screening of a number of excipients on the rat everted gut sac model, HPMC had no significant ( $p > 0.05$ ) impact upon the transport of the P-gp substrate domperidone (Al-Mohizea et al., 2014). During the development of a hot-melt formulation of propranolol contained in a HPMC-Gelucire® 44/14, 0.0128 % (w/v) HPMC Premium K100 was excluded as a P-gp inhibitor whilst Gelucire was shown to have inhibitory properties on the Caco-2 Transwell® model (Mehuys et al., 2005). Indeed, the HPMCs do not contain the structure expected of an inhibitor of efflux, such as a hydrophobic core and hydrophilic extensions. Therefore, the data presented herein are in agreement with existing literature.

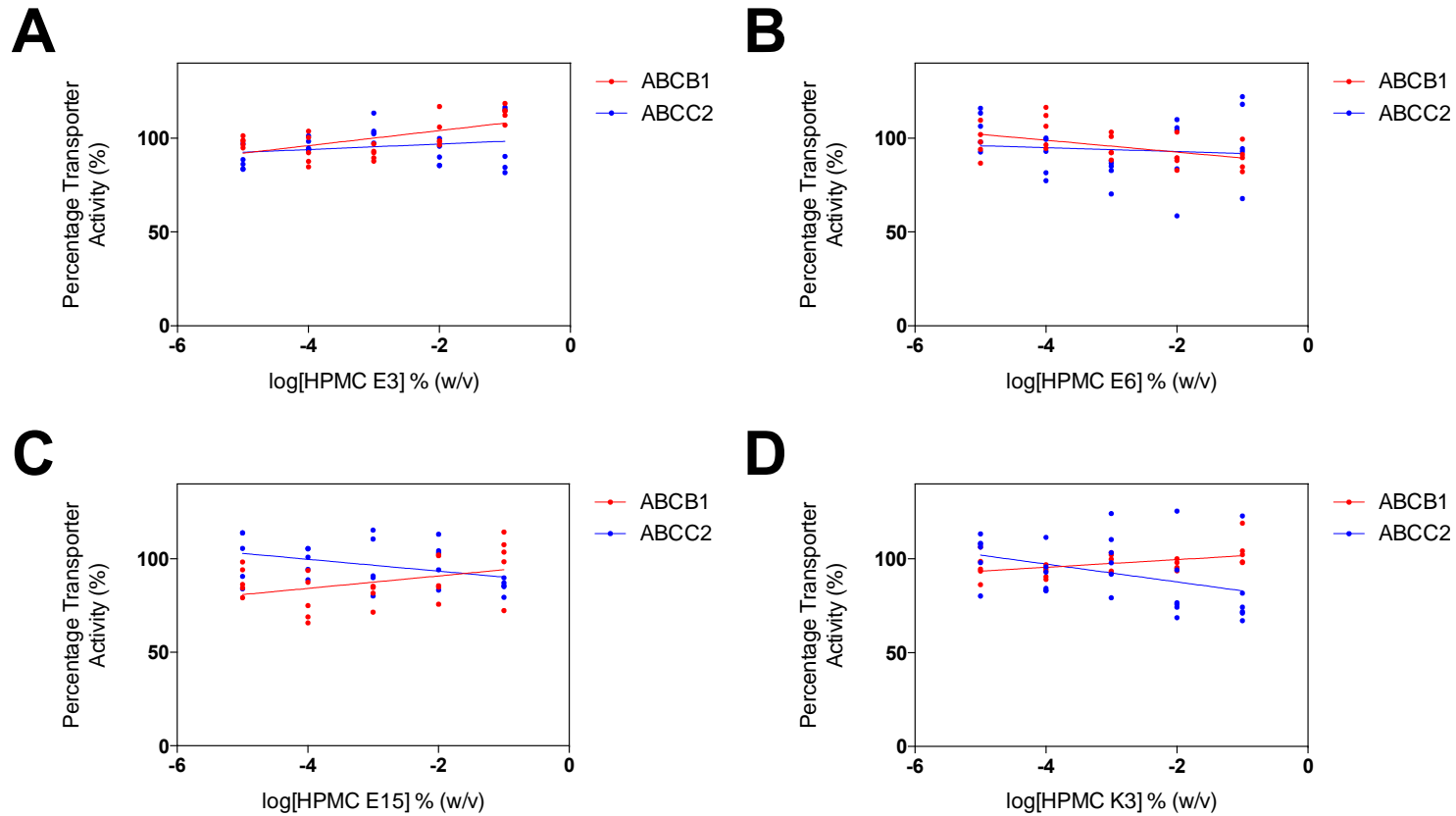


Figure 4.4. The effects of HPMCs on the uptake of the ABCB1 and ABCC2 specific probes R-123 and CDF (CDFDA) respectively, showing A) METHOCEL E3, B) METHOCEL E6, C) METHOCEL E15 and D) METHOCEL K3. Caco-2 cells were grown for 5-7 days on 96-well plates prior to experimentation. Data presented as each replicate from a minimum of four data values as a function of overall R-123 or CDF (CDFDA) uptake for ABCB1 and ABCC2 respectively with initial conditions of 2.5  $\mu$ M extracellular tracer dye per well, with excipient-free control wells set to 100 % transporter activity.

#### 4.4. An Examination of the Effects of Polyethylene Glycols Against ABCB1- and ABCC2-Mediated Transport

In Chapter 3, PEG 8000 and POLYOX N-10, a PEO, were shown to increase the rate of IND transport through Caco-2 monolayers grown in the Transwell® format (Figure 3.4 and Figure 3.5). In order to examine the impact of polymeric molecular weight on the efflux inhibition, the PEGs were re-examined using the HTS assay. Polyethylene glycols (PEGs), both as stand-alone materials and as the hydrophilic chains of larger and more complex compounds, are ubiquitous within the pharmaceutical industry, and the biological effects of PEGylated excipients were amongst the first to be implicated in the reversal of multiple drug resistance (MDR) (Ueda et al., 1987). PEGs are linear hydrophilic polymers consisting of repeating monomer units (Figure 4.5). They are generally well tolerated *in vivo*, used as an excipient in a variety of roles from water-miscible plasticisers, solvents to suspension agents (Rowe et al., 2009). PEGs over 20 kDa are known as polyethylene oxides.



Figure 4.5. The general structure of a PEG monomer, where  $n$  is the average number of repeat units, with the name of the polymer based on its average molecular weight.

##### 4.4.1. The Effects of PEGs on Cellular Viability

PEGs as excipients are well known for their low toxicity, regardless of their route of administration (Rowe et al., 2009). However, in order to assess the level of toxicity of the PEGs to the Caco-2 cell line, the MTT assay was used to measure mitochondrial activity. The results are presented in Figure 4.6. Apparent viability decreased with increasing PEG concentrations with the exception of PEG 400. For the remaining PEGs, apparent viability decreased significantly ( $p < 0.0001$ ) at 10 % (w/v), with additional decreases seen at 1 % (w/v) PEG 8000 and POLYOX ( $p < 0.01$ ). Even at 10 % (w/v) for all the PEGs tested,

monolayer integrity was confirmed using light microscopy (results not shown). Therefore, the decrease in apparent viability is most likely attributed to the reduction in thermodynamic activity in the extracellular space owing to the increased viscosity at higher PEG concentrations, thereby limiting the availability of MTT. A similar effect has been noted in a study examining the permeability of carbamazepine through rabbit intestine (Riad and Sawchuk, 1991). In this study, the permeability of the drug was found to decrease proportionally to the concentration of PEG 400 used as a cosolvent, essentially limiting the bioavailability of the drug (Riad and Sawchuk, 1991).

PEGs 400, and 20000 have been used as high as 20 % (w/v) on the rat model (Shen et al., 2006), and PEG 300 as high as 20 % (v/v) on the Caco-2 Transwell® model without loss of TEER (Hugger et al., 2002a, Hugger et al., 2002b), albeit present on both sides of the monolayer to equilibrate osmolality. In order to comply with the Transwell® study using IND presented in Chapter 3 (Figure 3.3-3.5), 1 % (w/v) was chosen as an upper concentration limit to encompass the previous inhibition range.

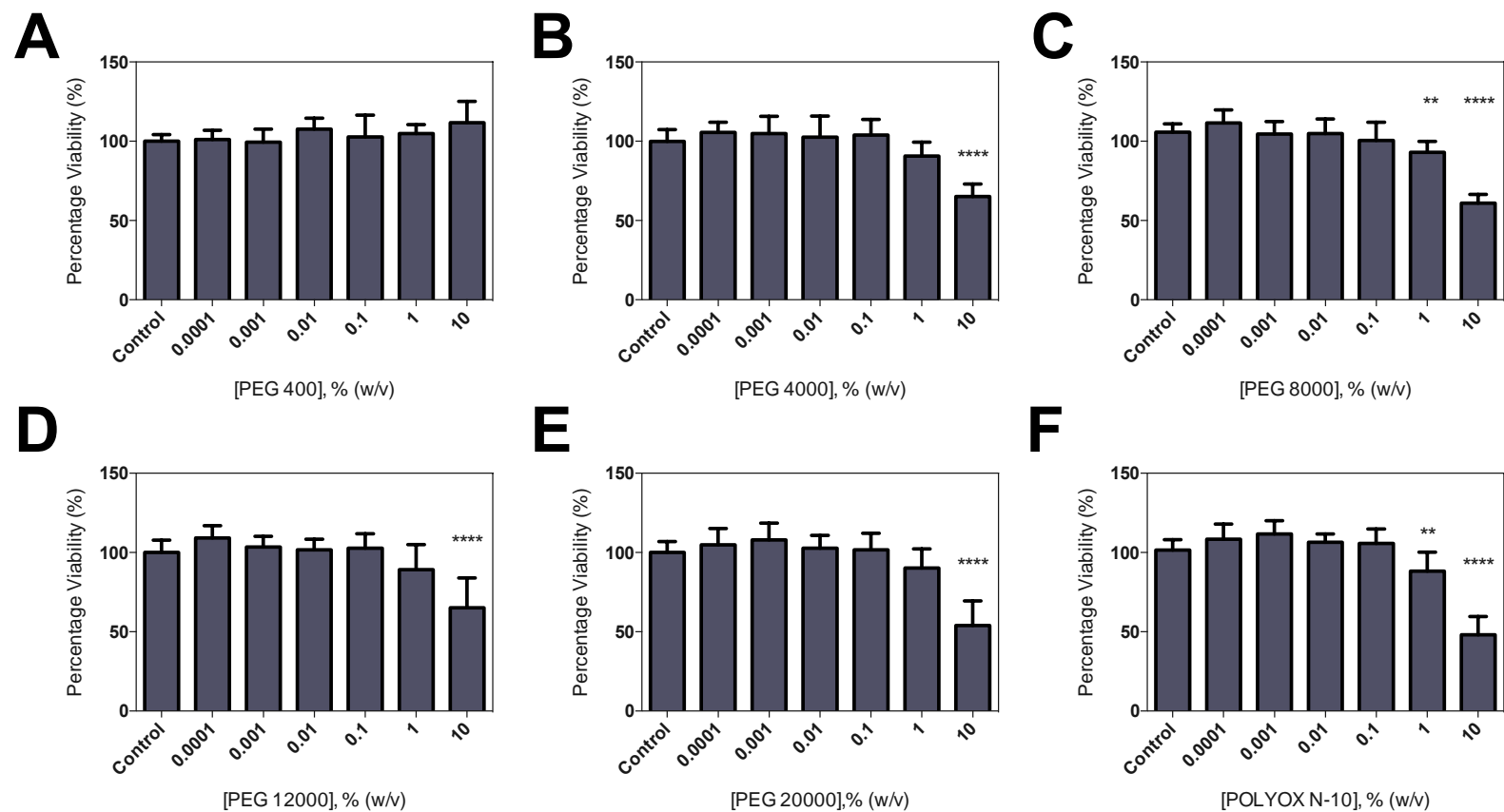


Figure 4.6. The effects of PEGs on cellular viability using the MTT toxicology assay, showing A) PEG 400, B) PEG 4000, C) PEG 8000, D) PEG 12000, E) PEG 20000 and F) POLYOX N-10. Caco-2 cells were grown for 5-7 days on 96-well plates prior to experimentation. Data presented as the mean value of 6 replicates  $\pm$  SD. Statistical significance was analysed using one-way ANOVA followed by Dunnett's *post hoc* test annotated as follows: \*\* ( $p < 0.01$ ); \*\*\*\* ( $p < 0.0001$ ).

#### 4.4.2. The Effects of PEGs on ABCB1- and ABCC2-Mediated Transport

Using the HTS protocol developed in Chapter 3, PEGs of various molecular weights were examined for their effects against ABCB1- and ABCC2-mediated efflux. The results are presented in Figure 4.7. Over the concentration range tested, none of the PEGs had a significant ( $p > 0.05$ ) impact upon the intracellular accumulation of either of the fluorescent probes, and do not fit the non-linear sigmoidal regression line shown by the established inhibitors in Figure 4.1. The PEG concentration range was chosen to exceed the previous concentration used in the Transwell® study in order to anticipate the lower plateau of an  $IC_{50}$  curve. In Chapter 3, PEG 8000 and POLYOX N-10, a PEO, were shown to increase the rate of IND transport in the apical to basolateral direction of transport at 0.0119 % (w/v) (Figure 3.4 and Figure 3.5), but not in the basolateral to apical direction (Figure 3.7). This is indicative of efflux transporter modulation, either directly through membrane fluidisation or by bypassing the transporter by the opening of tight junctions and enhancing the paracellular route. In the present study, concentrations of up to 1 % (w/v) were unable to generate an  $IC_{50}$  curve. At concentrations above this, the viscosity began to impact probe mobility (Riad and Sawchuk, 1991) (Figure 4.6).

PEGs were amongst the first excipients identified as inhibitors of efflux, and have been studied extensively. In an extended *in vitro* and *in situ* study, Qi Shen *et al* examined the effects of PEG 400, 2000 and 20000 (Shen *et al.*, 2006). The excipients and concentrations chosen herein encompassed this range intentionally, albeit with a different outcome. In the study by Shen *et al*, R-123 was also used as a P-gp substrate using the rat model, and the PEGs were used at concentrations up to 20 % (w/v) with the majority of inhibition ( $p < 0.01$ ) occurring below 1 % (w/v) for PEG 400 and PEG 20000 (Shen *et al.*, 2006). Whilst specific, R-123 is well known as an intracellular marker – actually a mitochondrial stain – and has poor passive diffusional capability through monolayers (Störmer *et al.*, 2001). The increase in uptake seen with these PEGs could well be attributed to increased drug transport via another route such as passive diffusion via tight junctions.

In a separate series of studies, Hugger *et al* was able to demonstrate the efficacy of PEG 300 on the Caco-2 Transwell® model, but only at higher concentrations up to 20 % (v/v), a concentration affected by viscosity on our study (Hugger *et al.*, 2002a, Hugger *et al.*,

2002b). Another study has concluded no significant ( $p > 0.05$ ) efficacy of PEG 1000 as stand-alone inhibitor of P-gp at the same concentration that TPGS 1000 was able to elicit an effect (0.005 % (w/v) (Collnot et al., 2006). Although low in toxicity, PEGs are high in viscosity in higher concentrations, making them difficult materials to work with for the HTS assay. Higher concentrations of PEGs will no doubt impact upon the speed of delivery with concentrations of the PEGs at or over 0.1 % (w/v) *decreased* the cellular uptake of the dyes compared to the non-treated controls, most probably attributed to altered diffusional paths of the probes by the increased viscosity of the polymers at these concentrations and so reduction in thermodynamic activity (Riad and Sawchuk, 1991). A study using the Caco-2 Transwell® model has shown that PEG 400 was able to decrease the permeability of the P-gp substrates atenolol, ranitidine and acyclovir at 1.5 % (w/v), similar to the concentration used herein, interpreted as the immobilisation of the drugs by high viscosity (Rege et al., 2001). In the study herein, the focus of the assay was direct efflux inhibition since the modulation of the paracellular route cannot be detected and this strength of the HTS model is also its weakness: any material which is high in viscosity may slow down dye ingress by altering the diffusional path and/or creating a mucoadhesive gel that favours retention of the dye into the extracellular space. Therefore, the most intriguing detail between the data presented herein and that of the literature is the exact format of the model used. Whilst the Caco-2 platform is a well-established model of intestinal absorption, most work on the inhibition properties of PEGs focuses on the Transwell® format where the 3-dimensional aspect of the model may work in the favour of proponents of PEGs as efflux inhibitors. In the HTS protocol designed and validated in the previous chapter, only intracellular accumulation of dye by direct inhibition of efflux can be detected, whereas the Transwell® format allows the possibility of other modes of efflux avoidance, such as the opening of tight junctions, and so allowing the bypass of efflux entirely. However, most groups working on this would establish that tight junctions remain intact during the experiments, either by measuring membrane resistance or using a poor paracellular marker such as mannitol to assess monolayer integrity. These methods are a good guide to monolayer integrity, but by no means infallible. Our previous work on Transwell® model demonstrated the difficulty in obtaining stable TEER values before and after experimentation. Even the effects of the buffer in use played a role in the value, as well as

temperature and the age of the media (results not shown). In our previous studies, fresh serum-containing media was always used to measure TEER before and after each study, requiring cells to be washed and refilled after each experiment. Modulation to the paracellular route by the opening of tight junction has been shown to be transient on the Caco-2 cell line (Anderberg et al., 1992, Lindhardt and Bechgaard, 2003). Therefore, the interpretation of the data is that the permeability enhancing effects of PEGs appears model-dependent.

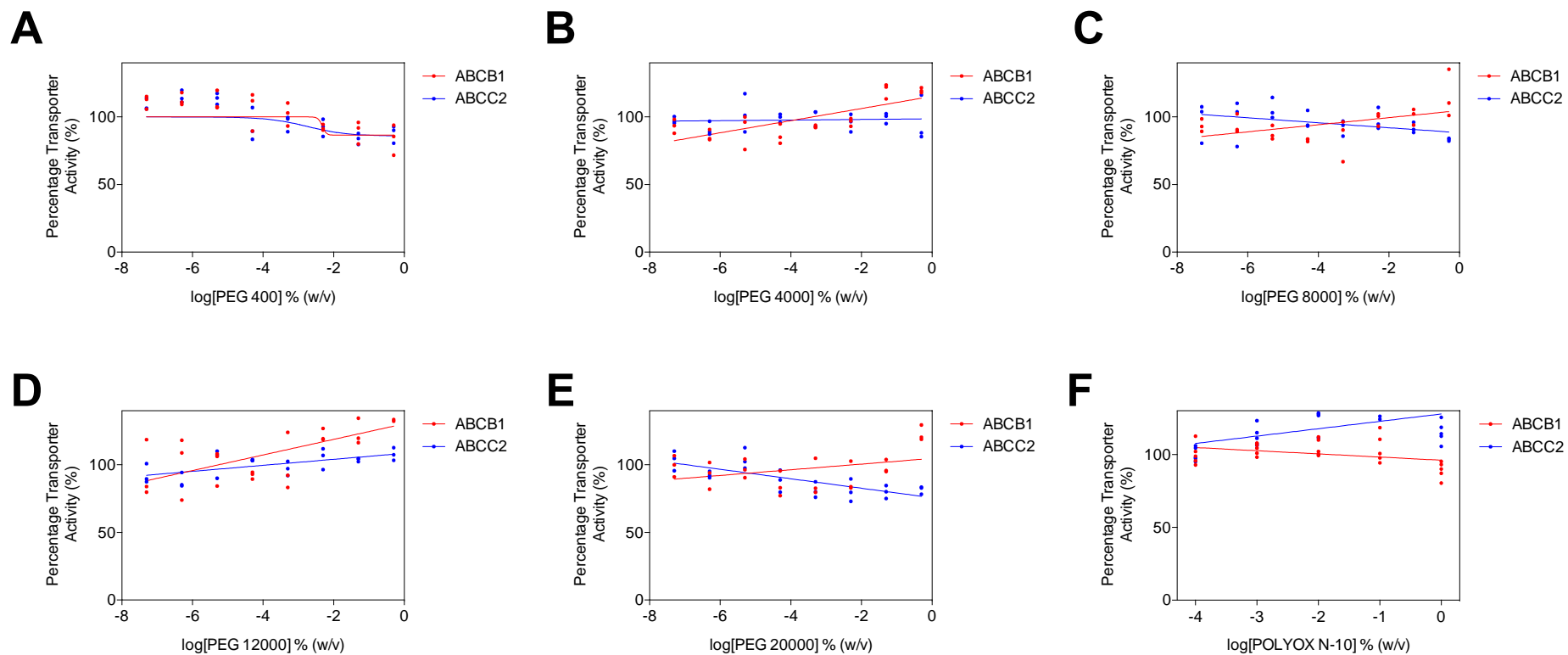


Figure 4.7. The effects of PEGs on the uptake of the ABCB1 and ABCC2 specific probes R-123 and CDF (CDFDA) respectively, showing A) PEG 400, B) PEG 4000, C) PEG 8000, D) PEG 12000, E) PEG 20000 and F) POLYOX N-10. Caco-2 cells were grown for 5-7 days on 96-well plates prior to experimentation. Data presented as each replicate value from a minimum of triplicate data values.

#### **4.5. An Examination of the Effects of Poloxamers and Tweens on ABCB1- and ABCC2-Mediated Transport**

The screening of PEGs over a range of molecular weights showed a lack of inhibition properties against the ABCB1 and ABCC2 transporter systems. PEGs are hydrophilic polymers, which may have a limited propensity to interact with cell membranes where the efflux transporters are expressed. As such, excipients of a more complex composition were examined which have a higher propensity for interacting with the membranes of cells. Poloxamers and Tweens are non-ionic amphiphilic surfactants commonly used as excipients (Figure 4.8). Poloxamers are triblock copolymers consisting of a hydrophobic core of poly(propylene oxide)(PPO) flanked on either side by hydrophilic chains of poly(ethylene oxide) (PEO). These molecules can be precisely customised to give rise to a plethora of hydrophilic-lipophilic balance (HLB) values and molecular weights by optimising the precise PPO to PEO chain length. Due to the broad specificity of poloxamers of various types, they are used as emulsifiers, gelling agents, tablet coatings and wetting agents (Rowe et al., 2009). Tweens, also known as polysorbates, consist of sorbitan core from which chains of PE and a lipophilic chain emanate. The most common Tweens used as excipients are Tween 20 and Tween 80, containing lauric and oleic lipophilic groups, respectively. Both of these Tweens contain 20 units of PEO, making them favourably hydrophilic and suitable for emulsification, solubilisation and wetting agents. (Rowe et al., 2009). As these excipients present a broad range of HLB values, molecular weights and structures (Table 4.3), the poloxamers and Tweens were chosen for HTS for activity against the ABCB1 and ABCC2 transporter system.

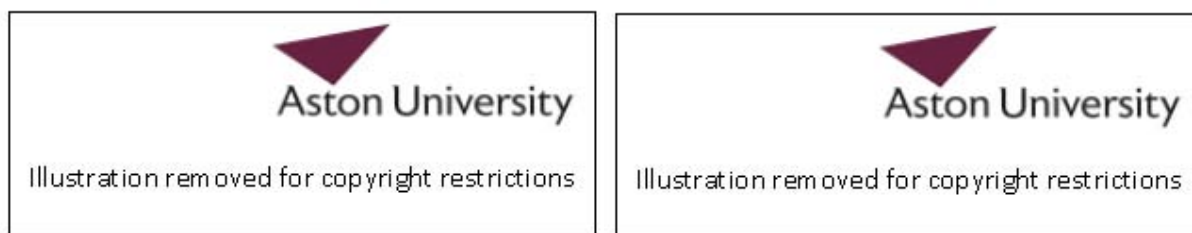


Figure 4.8. The general structures of A) Poloxamers and B) Tweens. Poloxamers consist of a hydrophobic poly(propylene oxide) (PPO) core ( $y$ ) flanked by poly(ethylene oxide) (PEO) chains ( $x$  and  $z$ ), the precise composition of which give rise to the HLB of the polymer. Tweens consist of ethoxylated sorbitan esterified with fatty acids. The Tween shown is Tween 20 with a lauric acid lipophilic group, whereas Tween 80 contains an oleic acid group.

Table 4.3. The range of surfactants selected for initial HTS according to the hydrophilic-lipophilic balance values.

<i>Excipient</i>	<i>HLB</i>	<i>Molecular Weight</i>	<i>State</i>
Poloxamer 182	7.0	2500	Liquid
Poloxamer 184	13.0	2900	Liquid
Tween 80	15.0	1310	Liquid
Tween 20	16.7	1128	Liquid
Poloxamer 335	18.0	6500	Solid
Poloxamer 407	22.0	12500	Solid
Poloxamer 188	29.0	8400	Solid

#### 4.5.1. The Effects of Poloxamers and Tweens on Cellular Viability

Surfactants have a high propensity to interact with a lipid bilayer, and in doing can eventually breach the cell membrane and cause loss of cellular viability. As such, the first investigation into the biological effect of excipients must be to delineate direct efflux inhibition from toxic and/or non-specific mechanisms. Therefore, the MTT assay was used in order to assess the cellular viability in relation to non-treated control cells (Figure 4.9).

Most materials tested for toxicology using the MTT assay will display a 'step down' profile e.g. the cellular viability decreases as a function of concentration of test excipient, resulting in a reduction in formazan production and, therefore, a reduction in percentage viability in relation to the non-treated control. Interestingly, an artefact possibly unique to the Caco-2 cell line was noticed during the MTT assays. Some materials gave statistically significant ( $p$

< 0.05) increases in apparent cellular viability owing to intense bands of formazan formed in cells treated by higher concentrations of certain excipients (Figure 4.9). Poloxamers 184, 335 and 407 all displayed these increases (Figure A.1k, Figure A.1w, and Figure A.1y of the appendix, respectively). Poloxamer 182 also displayed stronger purple bands of formazan in higher concentrations but these crystals dislodged during draining of the MTT prior to the addition of the isopropanol solvent, and so these bands are not represented on the graph (Figure 1.Ae of the appendix). This information is difficult to interpret and the effects were observed over two independent passage numbers. This is most likely attributed to the efflux inhibition properties of these compounds – MTT as a classic ‘toxin’ may well be an apparent efflux substrate, most likely of ABCB1 or another undetermined transporter cascade. Whilst the interference to the MTT assay by other endotoxins has been noted before with regards to certain drugs which are known inhibitors of efflux transporters (Vellonen et al., 2004), this is the first time this phenomenon has been observed in relation to excipients. Moreover, this effect serves as an early indication as to the efficacy of the materials for efflux inhibition. As such, the MTT toxicology assay cannot be taken at *prima facie*, and must be used in concert with a working knowledge of the novel aspects of the Caco-2 cell line and its associated morphology over different experimental conditions.

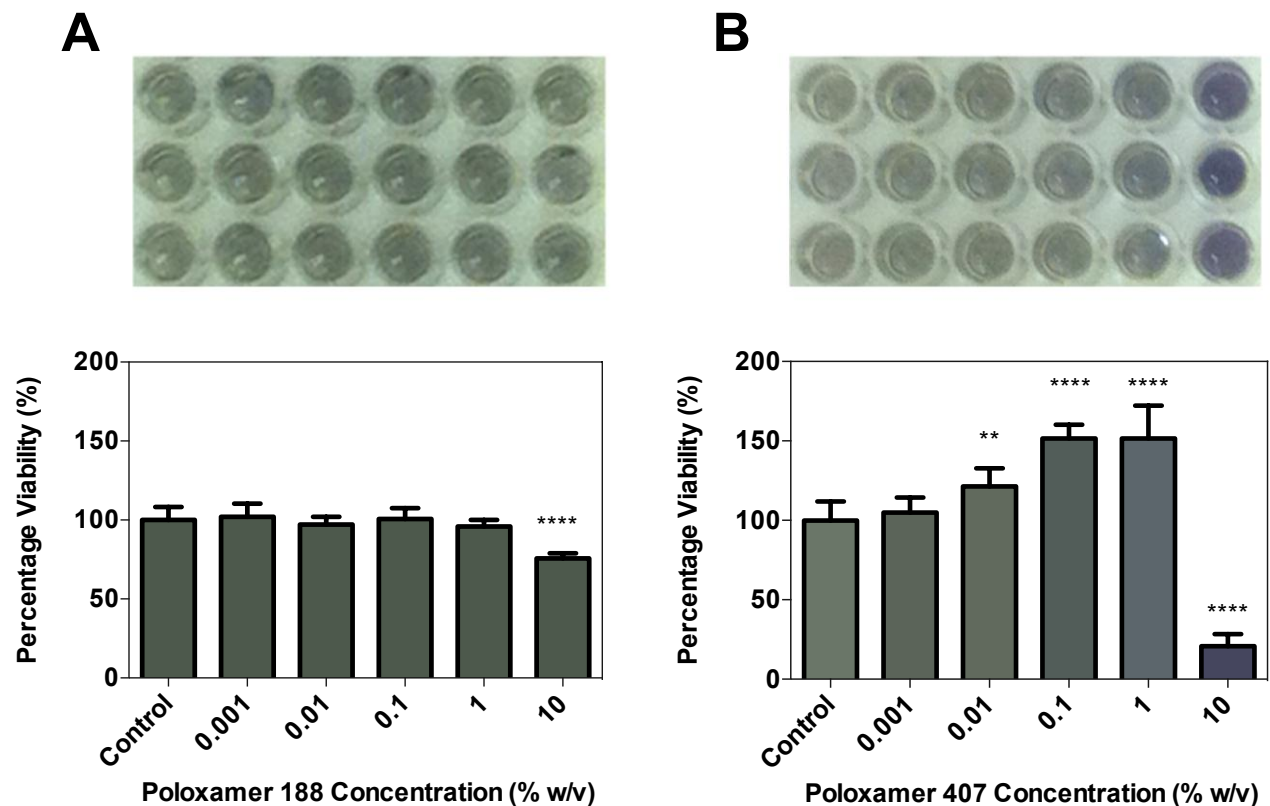


Figure 4.9. Typical (A) and atypical (B) MTT profiles presented after incubation with various concentrations of A) Poloxamer 188 and B) Poloxamer 407. Caco-2 cells were grown for 7 days on the smooth plastic of 96-well plates before 4 hour exposure to the excipients and 3 hours incubation with MTT. Note the increase in formazan production for wells containing higher concentrations of poloxamer 407 shown by the increase in the purple intensity despite the same initial concentrations of MTT. Also note that the bands of the highest intensity, poloxamer 407 at 10 % (w/v), do not correspond to the highest bar on the chart. Formazan production was of such intensity that crystals typically dislodge during draining of the MTT solution prior to isopropanol addition, and so do not have a representative bar on the chart. Morphological examination of the cells under such concentrations using light microscopy clearly showed cells in distress. Data shown as mean  $\pm$  SD from a minimum of 8 replicates over 2 passage numbers. Statistical significance was analysed using one-way ANOVA followed by Dunnett's *post hoc* test annotated as follows: \*\* ( $p < 0.01$ ); \*\*\*\* ( $p < 0.0001$ ).

#### 4.5.2. The Effects of Poloxamers and Tweens on ABCB1- and ABCC2-Mediated Transport

Using the HTS method, poloxamers and Tweens were tested for activity against ABCB1- and ABCC2-mediated transport. Contrary to PEGs, the biological effects of the poloxamers and Tweens were on the whole profound. Both of the Tweens and 4 out of the 5 poloxamers tested yielded data from which  $IC_{50}$  values could be determined for ABCB1 inhibition with over 95 % confidence (Figure 4.10). Particularly with the use of surfactants such as poloxamers and Tweens, no single unifying mechanism of inhibition appears to exist and is most likely a multi-faceted process. Membrane fluidisation is thought to be the cardinal mechanism for inhibition (Sinicrope et al., 1992). During this study, we have taken care to eliminate the effects of interference of membrane damage within the limits of viability, so we are able to exclude the possibility of severe loss of integrity as a major form of probe ingress. It has long been known that membrane fluidisation is a fundamental factor in efflux inhibition due to the sensitivity of ABC transporters such as P-gp to their microenvironment (Sinicrope et al., 1992), in particular P-gp ATPase activity (Regev et al., 1999). A comparable study examined Pluronic L85 (poloxamer 235), similar in HLB to poloxamer 184 and 335 used in this study, as an efflux inhibitor of P-gp, MRP1 and MRP2 (Batrakova et al., 2004). Using porcine kidney epithelial cells overexpressing these transporters, the degree of ATPase inhibition was observed in the order  $MRP1 < MRP2 \ll P\text{-gp}$ , attributed to conformation changes of the transporter via membrane fluidisation and/or steric hindrance of drug-binding sites by P85 side chains. This difference in the degree of inhibition is similar to the results in Figure 4.10. Whilst Batrakova *et al* suggest that MRP structures may be more robust and resilient to alterations in fluidisation, they also suggest that the differences in the overall structures between P-gp and the MRP isoforms may also play a significant role by having a binding site which is inaccessible to the long side chains of poloxamers. This could explain why none of our excipients yielded sufficient inhibition data to give an  $IC_{50}$  value for ABCC2 inhibition (Figure 4.10).

The differences in the biological effects of the PEGs and poloxamers may give us some insight into the structure/function relationship of efflux inhibitors. PEGs constitute the hydrophilic elements of the poloxamers, which are found flanking the hydrophobic core. From our data, it would be apparent that membrane interaction and subsequent

fluidisation requires the prerequisite of both hydrophilic and hydrophobic elements. More intriguingly, closer examination of our current data set would identify a trend in the efficacy of the poloxamers as ABCB1 inhibitors. This trend appears to show that not only is the hydrophobic and lipophilic composition necessary, there is also an optimum. PEGs are entirely hydrophilic and gave no IC<sub>50</sub> data in this model (Figure 4.7). Likewise, poloxamer 188, with a HLB of 29, had no significant impact either (Figure 4.10). Clearly more information would be needed to examine this trend, but it is entirely plausible that a compound should possess hydrophilic and lipophilic elements in the correct composition in order to impart specific levels of fluidisation upon the cell membrane. Hydrophilic compounds may not interact with cell membranes at all, whereas a highly lipophilic compound may in fact lead to membrane reinforcement and a subsequent increase in membrane rigidity (Batrakova et al., 2003). The relationship between these two properties may not be linear, but parabolic in nature, and warrants further exploration over a greater range of compounds.

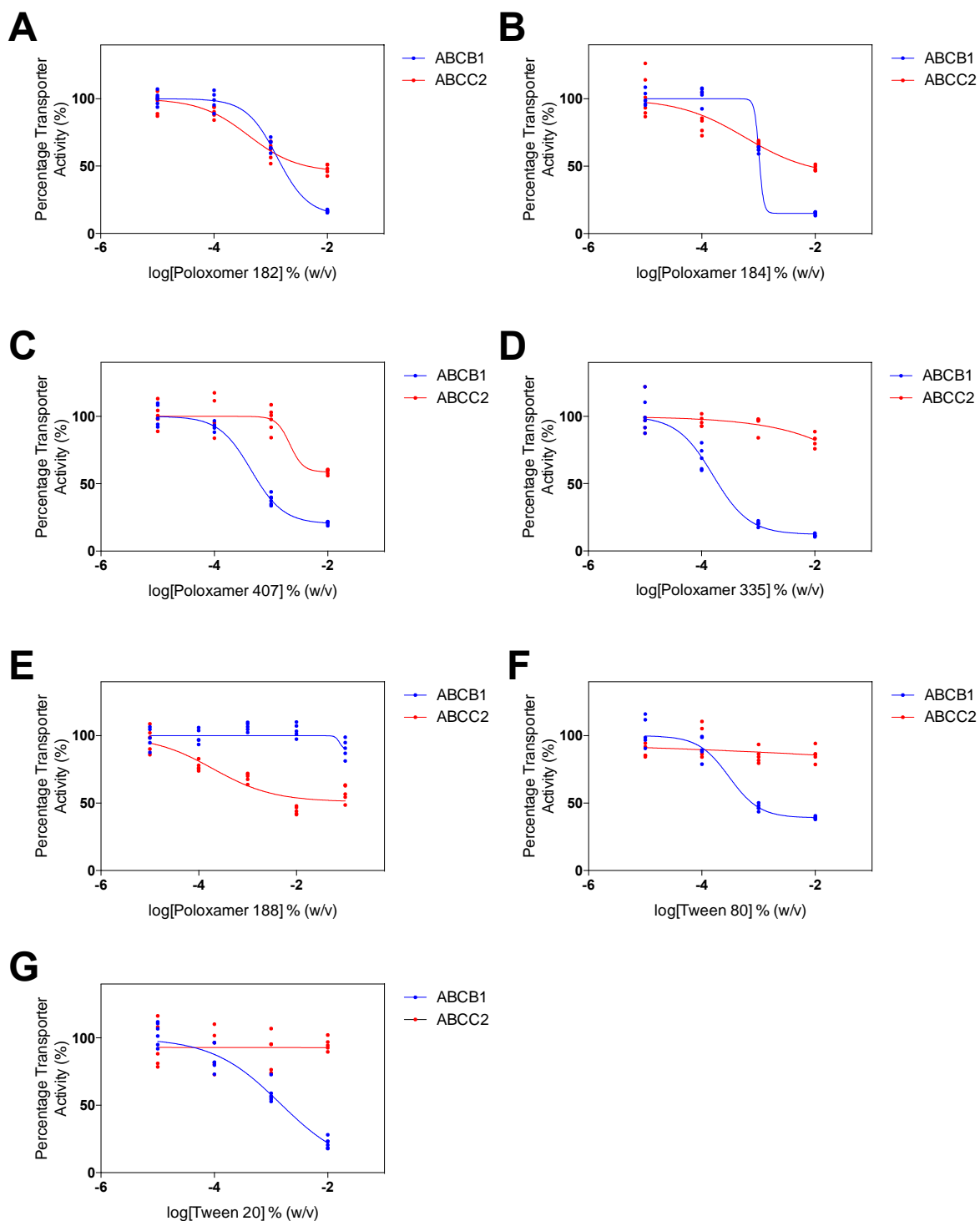


Figure 4.10. ABCB1 and ABCC2 modulation of the poloxamers and Tweens, showing A) Poloxamer 182, B) Poloxamer 184, C) Poloxamer 407, D) Poloxamer 335, E) Poloxamer 188, F) Tween 80 and G) Tween 20. Data presented as a function of overall R-123 uptake with initial conditions of 2.5  $\mu$ M extracellular tracer dye, with non-treated controls set to 100 % transporter activity. Data shown pooled from a minimum of 5 replicates per concentration  $\pm$  SD.

#### 4.5.3. The Effects of Poloxamers and Tweens on Caco-2 Membrane Integrity

As mentioned, surfactants by their nature are able to interact with cell membranes, and it is through this mechanism that potential damage could occur by which extracellular R-123 may enter the cell, bypassing efflux. Therefore to assess the level of membrane damage, the cells were incubated at 37 °C for 1 hour in the presence of the excipients and without tracer dye. The plate was then removed and placed at 4 °C. R-123 was then added to the cells. The results are presented in Figure 4.11. At this temperature, all ATP-driven processes, including efflux, should be inhibited and drug entry into the cells is a result of the cell membrane damage.

From these results in Figure 4.11, it is shown that for all 7 surfactants tested at concentrations below 0.01 % (w/v), no significant ( $p > 0.05$ ) increase in R-123 uptake was observed. This confirms that the increase in probe uptake seen in Figure 4.10 is connected to an ATP-driven process and not the result of surfactant-induced membrane damage. The central objective of this chapter was to screen for excipients that inhibit efflux transporters, and this required delineation on non-transporter related mechanisms of the excipients which could impact the accuracy of screening assay. Surfactant-induced damage could increase the 'leakiness' of the cell membrane and provide additional route of tracer dye ingress, which did occur at concentrations above 0.01 % (w/v). Above these concentrations, the surfactants promoted membrane damage, leading to a rise in fluorescent signal, as more R-123 was able to achieve cellular ingress, and/or severe morphological damage (Figure 4.11).

Surfactant-induced toxicity is dependent upon the ability to partition the cell membrane and the aqueous phase. The rate-limiting step in surfactant membrane partitioning is the formation of a free area in the membrane surface with sufficient room for amphiphile addition (Sampaio et al., 2005). Confluent epithelial cells, such as the polarised Caco-2 cell line, have a highly ordered membrane with defined tight junctions, making them less prone to surfactant-induced cell damage than non-polarised cells, such as the HeLa cell line, which have less ordered membrane structures (Inácio et al., 2011).

In order to delineate the effects of surfactant-induced membrane damage from inhibition of efflux transport, Bogman *et al* used two otherwise identical cell lines (P388), one which

expressed P-gp and the other which had no P-gp expression (Bogman et al., 2003). At lower concentrations, the surfactants were able to increase the uptake of R-123 only for cells expressing P-gp which the authors attributed to efflux inhibition, but at higher surfactant concentrations, the cellular uptake of R-123 was also increased for the cells which did not express P-gp which the authors attributed to membrane damage (Bogman et al., 2003). In another investigation examining the role of Tweens as permeability enhancers using the Caco-2 cell line, it was found that higher surfactants concentrations above the critical micelle concentration (CMC) were able to solubilise membrane components rather than the membrane itself, with severe damage occurring at higher concentrations similar to those seen in Figure 4.11 (Dimitrijevic et al., 2000). Indeed, Tween 80 has been shown to damage cell membranes at higher concentrations (Ujhelyi et al., 2012, Roohinejad et al., 2014). Using both MTT in addition to measuring the activity of the cytoplasmic enzyme lactate dehydrogenase (LDH) in the extracellular medium as an evaluation of membrane integrity, it was observed that concentrations of non-ionic surfactants close to the CMC cause acute toxicity in Caco-2 cells (Inácio et al., 2011). Below the CMC, no toxicity was recorded suggesting membrane destruction as the mode of toxicity (Inácio et al., 2011). However, cationic surfactants were able to impart toxicity well below their CMC values (Inácio et al., 2011).

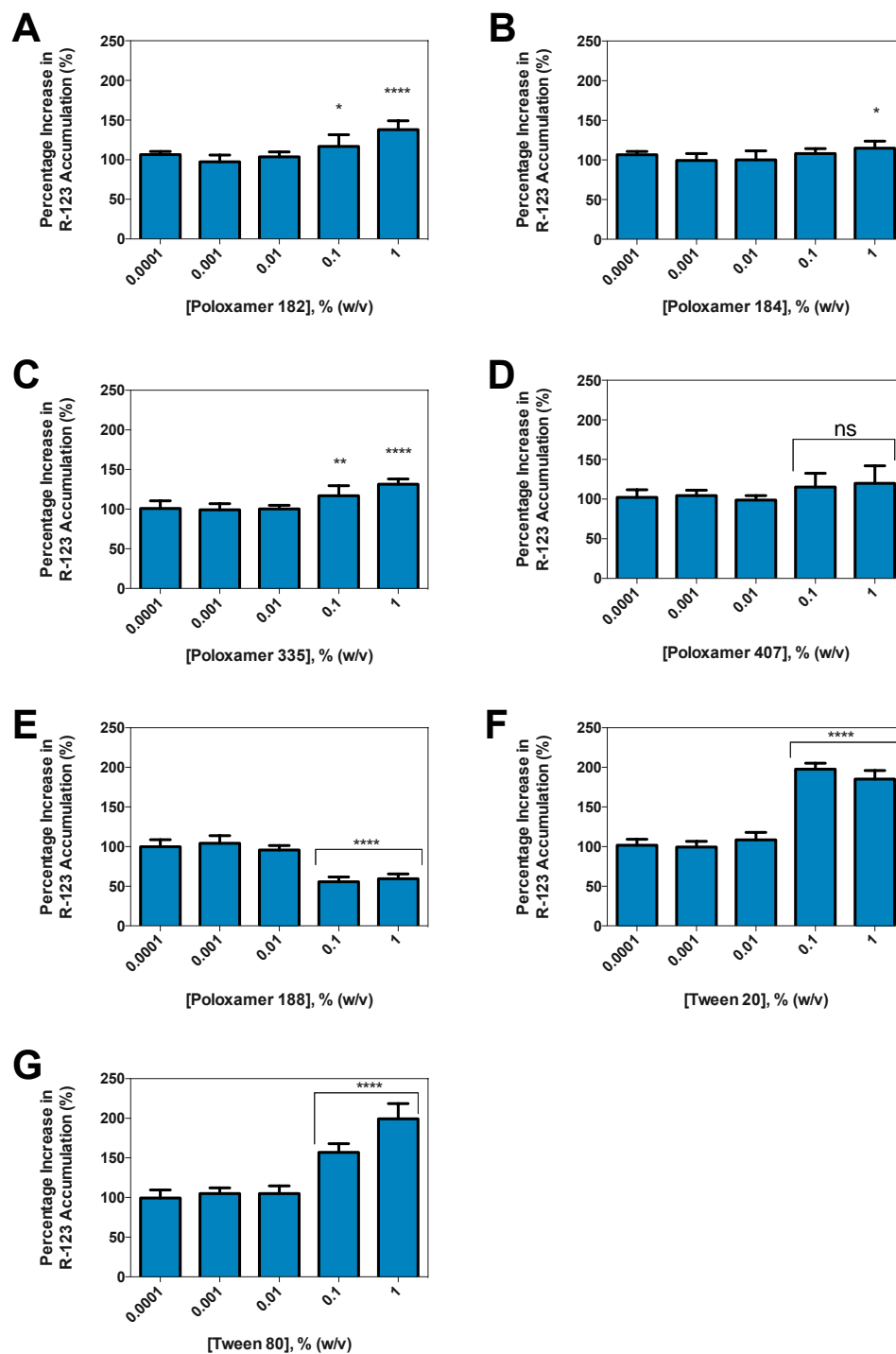


Figure 4.11. The uptake of R-123 in the absence of ATP synthesis, showing A) Poloxamer 182, B) Poloxamer 184, C) Poloxamer 407, D) Poloxamer 335, E) Poloxamer 188, F) Tween 80 and G) Tween 20. Cells were incubated in the presence of surfactants for 1 hour at 37 °C, then rinsed in ice cold KH buffer (pH 7.4) and incubated at 4 °C in the dark in the presence of 100 nM R-123. Data shown  $\pm$  SD from data pooled from 5 replicates in relation to the surfactant-free control (KH buffer only) replicates. Statistical significance was analysed using one-way ANOVA followed by Dunnett's *post hoc* test annotated as follows: ns ( $p > 0.05$ ); \* ( $p < 0.05$ ); \*\* ( $p < 0.01$ ); \*\*\*\* ( $p < 0.0001$ ).

#### 4.5.4. The Effects of Poloxamers and Tweens on Micelle Encapsulation of the Tracer Dye R-123

Alongside toxicity, the role of quenching was also examined to remove the possibility of contrived inhibition data via the encapsulation of dye into micelles and/or implicate a method of bypassing efflux transporters by delivering the tracer probe safely through the cell membrane by endocytosis. As such, the poloxamers and Tweens were examined for encapsulation by studying the phenomenon of quenching using R-123 as the tracer probe in the absence of cells. The results are presented in Figure 4.12.

Poloxamers had no significant ( $p > 0.05$ ) influence on the fluorescence intensity of R-123 up to 10 % (w/v) at or above their reported CMC values, and the data best fits linear regression (Figure 4.12). In contrast, the Tween 20 and Tween 80 both showed a decrease in fluorescence intensity, becoming significant ( $p < 0.01$ ) at 0.1 % (w/v) and 0.5 % (w/v) respectively in relation to the control wells containing only KH buffer (Figure 4.12). This reduction is most likely attributed to micelle formation, since this reduction in fluorescence intensity only occurs at concentrations above the CMC (Figure 4.12).

In a similar study to the present one, Bogman *et al* tested the ability of various surfactants to quench the fluorescent probes R-123 and CDF (Bogman et al., 2003). It was found that poloxamer 188 did not quench either fluorescent marker, but Tween 80 was able to quench both, but only above its CMC (Bogman et al., 2003) similar to the data presented in Figure 4.12. Interestingly, it was noticed that the apparent CMC of Tween 80 was about 10-fold higher in the presence of cells, attributed to the defection of Tween monomers to cell membrane partitioning, and so reducing the free monomers in the supernatant (Bogman et al., 2003). This could suggest that many of the published CMC values may be underestimates when cells are factored into the assay.

It is interesting to note that this quenching effect occurs much beyond the CMC values reported in literature. The values obtained from published literature are generally conducted at a lower temperature than those in present study, where biological conditions were simulated by using an incubator at 5 % CO<sub>2</sub> at 37°C, except for the study by Alexandridis *et al* who used a higher temperature to induce poloxamer 188 CMC formation

(Alexandridis et al., 1994). It would be expected that the elevated temperature used in this study would aid the formation of the micelles of non-ionic surfactants, although this may be offset by the 'shift' in the CMC owing to loss of monomer to membrane partitioning (Bogman et al., 2003). Furthermore, the CMC values quoted within the literature are conducted in distilled water, whilst the data obtained herein used KH buffer to replicate as closely as possible the conditions of the uptake assay. As all of the surfactants used are non-ionic, the presence of electrolytes such as sodium chloride in solution should not impact CMC formation (Acharya et al., 1997). The quenching of R-123 at higher concentrations of Tweens was only around 10 % in relation to non-treated controls at the highest concentrations of surfactant (Figure 4.12). In general, given that the amphiphilic marker R-123 appears to have poor micelle association suggests their contribution to the fluorescent probe transport is negligible in this assay (Figure 4.12).

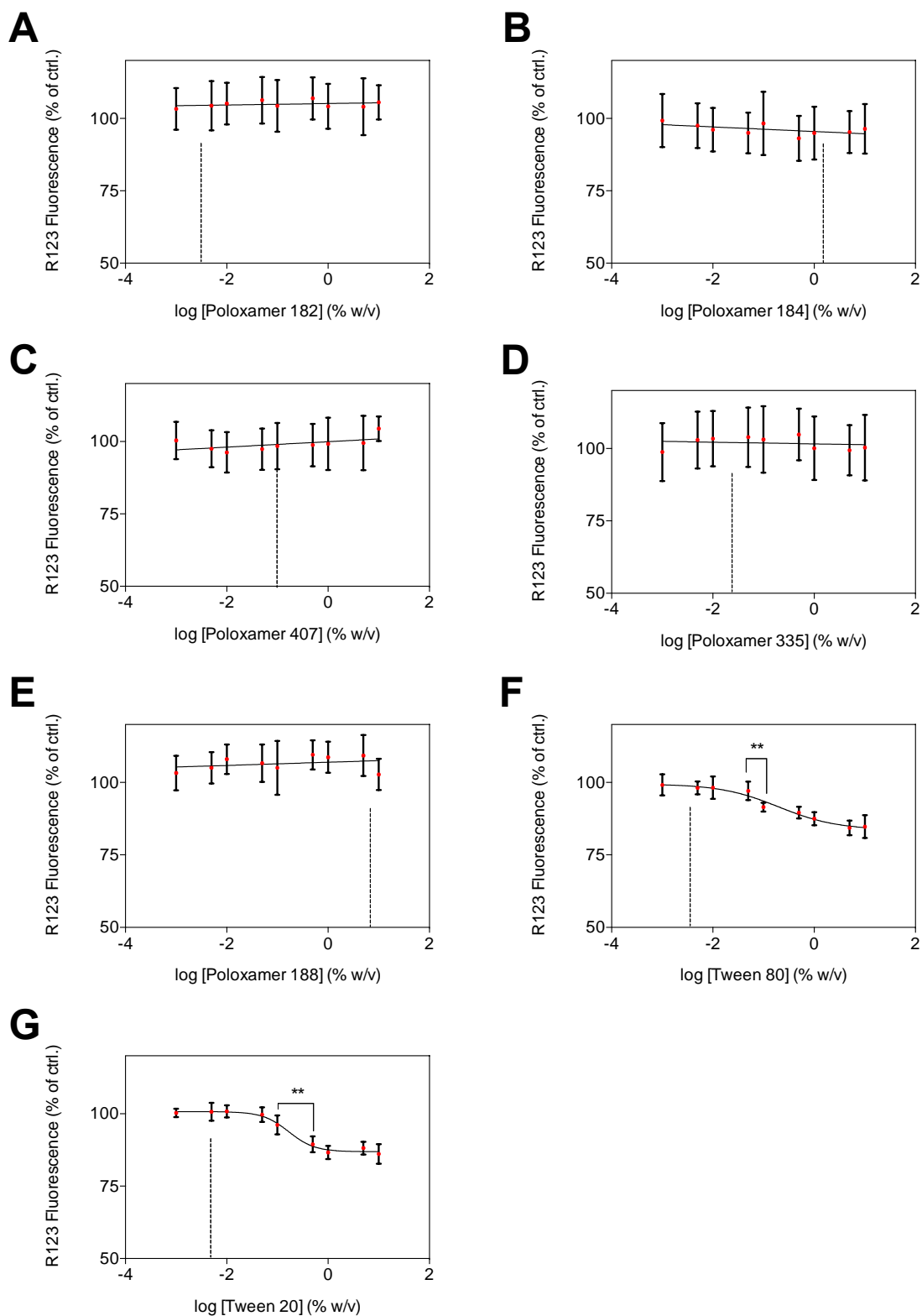


Figure 4.12. Rhodamine 123 (50 nM) was incubated for 2 hours at 37 °C in the presence of various concentrations of poloxamers and Tweens in the absence of cells in order to assess the contribution of the excipients to tracer dye quenching, showing A) Poloxamer 182, B) Poloxamer 184, C) Poloxamer 407, D) Poloxamer 335, E) Poloxamer 188, F) Tween 80 and G) Tween 20. Data presented in relation to the surfactant-free control (KH buffer only) wells  $\pm$  SD from at least 6 individual replicates. CMCs (dashed line) obtained from literature (P182 from (Tiberg et al., 1991), measured at 23 °C, P407, P335 and P184 measured at 30 °C and P188 measured at 40 °C (Alexandridis et al., 1994), Tween 80 and Tween 20 from (Patist et al., 2000) measured at 22 °C). Statistical significance was analysed using one-way ANOVA followed by Dunnett's *post hoc* test annotated as follows: \*\* ( $p < 0.01$ ).

#### 4.6. An Examination of the Effects of Surfactants on ABCB1- and ABCC2-Mediated Transport

In the previous section, a small cross section of surfactants was examined for their efflux inhibition properties. This screening found 5 inhibitors of the ABCB1 efflux transporter. Surfactants are often categorised according to their use (Table 4.4), ranging from water-oil emulsifying agents at low HLB values to solubilising agents in the higher HLB range (Griffin, 1946). In order to expand on the study of poloxamers and Tweens, additional surfactants were obtained incorporating a wider range of HLB values from lipophilic molecules with a HLB of 4.5 to hydrophilic molecules with a HLB of 29 (Table 4.5). These excipients were specifically chosen for variations in structure and molecular weights, and were evaluated for their impact on ABCB1- and ABCC2-mediated transport.

Table 4.4. The utilisation of surfactants based on their HLB values (Griffin, 1946).

<i>HLB</i>	<i>Use</i>
4-7	Water-oil
7-9	Wetting agents
8-18	Oil-water
13-15	Detergents
15-18	Solubilising agents

Table 4.5. The range of surfactants selected for HTS according to the hydrophilic-lipophilic balance values.

<i>Excipient</i>	<i>HLB</i>
Capmul PG-12	5.0
Capmul MCM	5.5
Capmul MCM C8	5.5
Capmul PG-8	6.0
Poloxamer 182	7.0
Span 20	8.6
Arlatone TV	9.0
Crovol A-70	10.0
Etocas 29	11.7
Brij S-10	12.4
Poloxamer 184	13.0
Etocas 40	13.0
Brij CS-12	13.4
Acconon C-44	13.5
NatraGem S140	14.0
Acconon MC8-2	14.5
Tween 80	15.0
Cetomacrogol 1000	15.7
Tween 20	16.7
Myrj S-40	16.7
Poloxamer 335	18.0
Myrj S-100	18.8
Poloxamer 407	22.0
Poloxamer 188	29.0

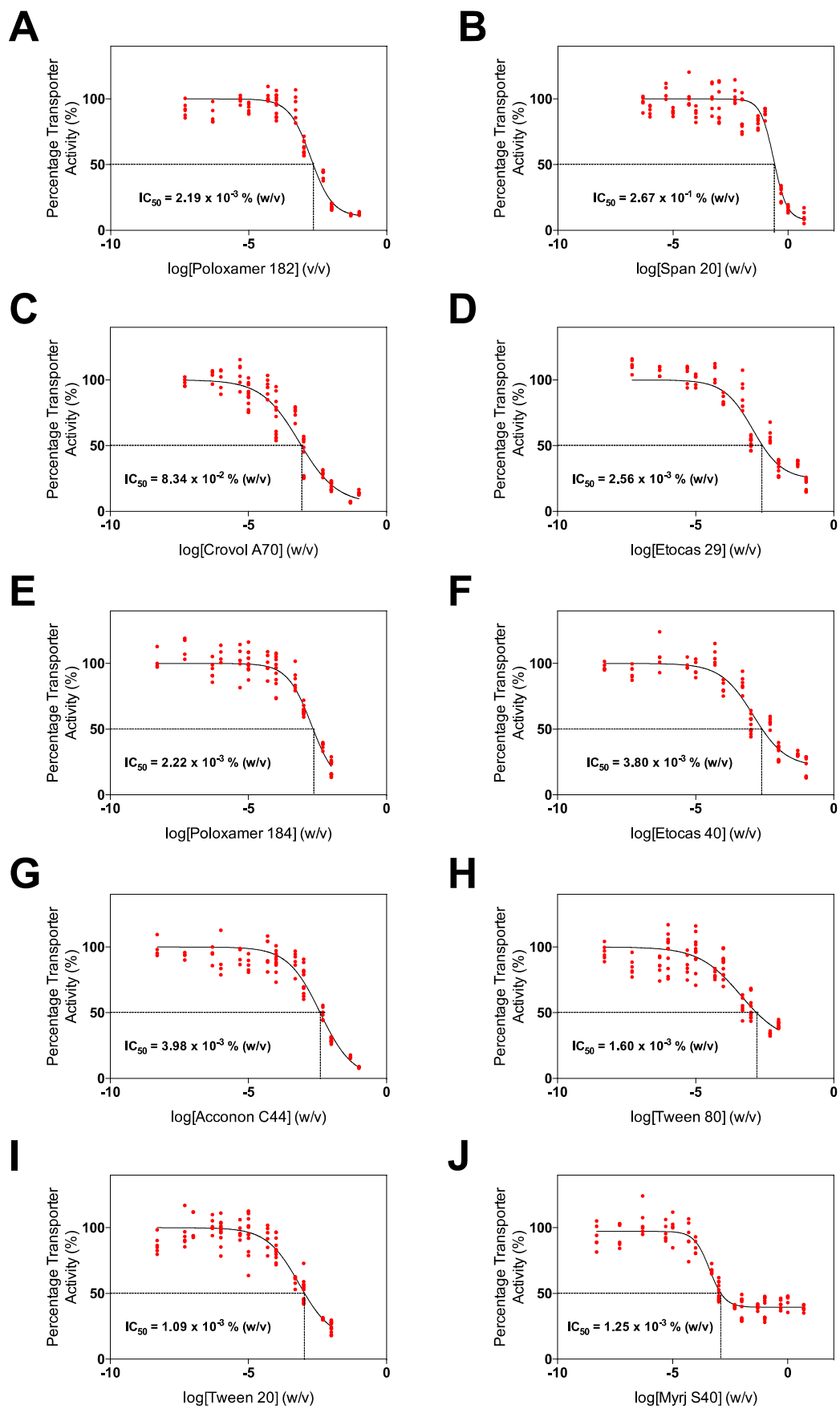
#### 4.6.1. Effects of Surfactants on Cellular Viability

In order to find acceptable doses of the surfactants to use on the cells, the mitochondrial activity of the Caco-2 monolayer was probed using the MTT assay. As all of the materials chosen for investigation are surfactants, they have a high propensity to interact with lipid membranes and therefore impart specific toxicities. Some materials such as the Etocas were tolerated well, at least as high as 0.1 % (w/v), whereas others were found to be toxic as low as 0.0001 % (w/v) for Brij CS-12, S-10 and Cetomacrogol 1000 (Figure A.1 of the Appendix). Despite the differences in nomenclature, the latter three compounds are closely related as PEGylated stearyl/cetostearyl ethers with varying lengths of the hydrophilic regions, and collectively these form the most toxic of the series tested. Morphological examination using light microscopy revealed that the cause of toxicity as damage ranged from altered cellular morphology, to monolayer fragmentation and, in the higher concentrations of some

excipients, complete removal of the monolayer (results not shown). Of the materials tested, Arlatone TV, Myrj S40, NatraGem S-140, Acconon C44 and Span 20 displayed distinctive 'step up' signature in a concentration dependent manner, indicating an apparent propagation in mitochondrial activity, previously attributed to efflux inhibition, presumably ABCB1, which results in higher intracellular accumulation of MTT and subsequent increase in formazan production in the mitochondria of the treated cells. However, these upward inflections were often able to mask certain toxicities and are therefore difficult to interpret, and monolayers were fragile during screening of some excipients in higher doses indicated to be non-toxic by MTT. Once more, the MTT toxicology assay was supplemented with visual confirmation of monolayer integrity using a working knowledge of the cell line.

#### 4.6.2. Effects of the Surfactants on ABCB1- and ABCC2-Mediated Efflux

In order to examine the underlying structural relationship between surfactants and efflux inhibition, a broad range of compounds encompassing different HLB values, molecular weights and structural composition were screened. The results are presented in Figure 4.13. Of the 24 tested, 12 yielded data from which  $IC_{50}$  values could be determined for ABCB1 inhibition with over 95 % confidence (Figure 4.13) with the remaining excipients correlating with linear regression and therefore showing no efflux activity (data not shown). Only Etocas 29 and 40 gave confident inhibition against ABCC2 (16.2  $\mu$ M and 12.9  $\mu$ M). Against ABCB1, the excipients gave the rank order poloxamer 335, poloxamer 407, Myrj S-40, Crovol A-70, poloxamer 184, poloxamer 182, Etocas 40, Tween 20, Etocas 29, Tween 80, Acconon C-44 and Span 20. Of all the excipients, Span gave by far the highest  $IC_{50}$ , with an unprecedented value of 7.7 mM (Table 4.6). This  $IC_{50}$  curve is very steep, occurring within the higher concentrations that were toxic to most materials. Excluding Span 20, the remaining excipients had  $IC_{50}$  values of 26.5  $\mu$ M or below. The excipients with the lowest values, poloxamers 335 and 407, showed  $IC_{50}$  values of 0.63 and 0.71  $\mu$ M (Table 4.6), exceeding that of VER (4.08  $\mu$ M) and CsA (1.16  $\mu$ M) (Table 4.1). Of the materials to give the 'step up' MTT signature, only Arlatone TV and NatraGem S140 failed to give corresponding  $IC_{50}$  curves against ABCB1, possibly due to the higher levels of toxicity of these materials occurring before inhibition could occur.



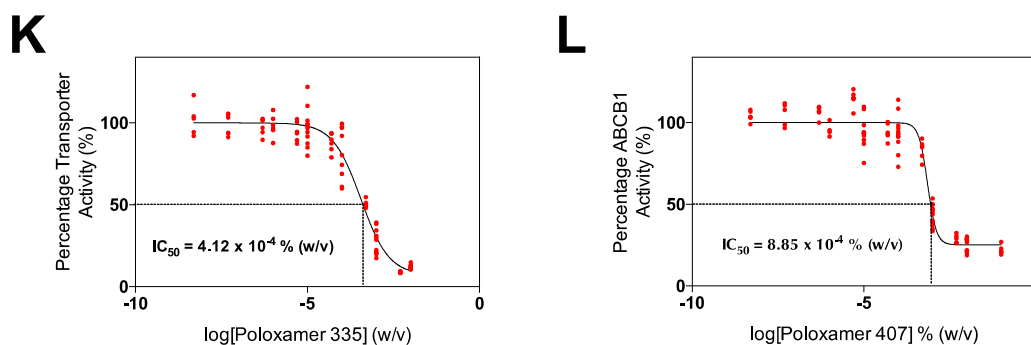


Figure 4.13. Percentage inhibition curves of various surfactants against ABCB1 showing A) Poloxamer 182, B) Span 20, C) Crovol A70, D) Etocas 29, E) Poloxamer 184, F) Etocas 40, G) Acconon C44, H) Tween 80, I) Tween 20, J) Myrj S40, K) Poloxamer 407 and L) Poloxamer 335. Sigmoidal curves were constructed from 4 different passage numbers on confluent Caco-2 monolayers grown on 96 well plates for 5-7 days and are shown pooled from a minimum of 4 replicates per concentration. Data presented as a function of overall R-123 or CDF (CDFDA) uptake for ABCB1 and ABCC2 respectively with initial conditions of 2.5  $\mu$ M extracellular tracer dye per well, with excipient-free control wells set to 100 % transporter activity.

Despite the inherent biological effects of excipients being well established, supporting kinetic data in the literature is difficult to find. Tween 80 has been shown to have an  $IC_{50}$  of 152  $\mu$ M for inhibition against P-gp using *MDR1* overexpressing mouse lymphocytes (P388/mdr) using R-123 as a substrate (Bogman et al., 2003). The results of the present study, 12.67  $\mu$ M (Table 4.6), is much lower than the previously reported value and may be attributed to the low membrane partitioning of P388/mdr cells by Tween 80 which could be cell type specific. However, the same study also gave the  $IC_{50}$  value for poloxamer 181, with a HLB of 3, as 0.01 % (w/v). The lowest HLB value of a poloxamer that we tested, P182, has a HLB of 7, and we determined an  $IC_{50}$  of 0.00219 % (w/v), which is within this range. As in our study, the group raised no significance modulation in the presence of P188 to either ABCB1 or ABCC2.

The mechanism of action of these materials against ABCB1 is most likely a multi-faceted process involving, amongst others, ATP depletion by the inhibition of ATPase (Batrakova et al., 2001, Batrakova and Kabanov, 2008) and/or membrane fluidisation (Hugger et al., 2002a, Lo, 2003). Membrane fluidisation is a fundamental factor in efflux inhibition due to the sensitivity of ABC transporters to their microenvironment (Sinicrope et al., 1992), in particular P-gp ATPase activity (Regev et al., 1999). Using porcine kidney epithelial cells overexpressing P-gp, MRP1 and MRP2, a similar study has examined Pluronic P85, similar in HLB to poloxamers 184 and 335 used in our study, as an efflux inhibitor (Batrakova et

al., 2004). The degree of ATPase inhibition was observed in the order MRP1 < MRP2 << P-gp, attributed to conformation changes of the transporter via membrane fluidisation and/or steric hindrance of drug-binding sites by P85 side chains. Batrakova *et al* suggest that MRP structures may be more robust and resilient to alterations in fluidisation, and also that the differences in the overall structures between P-gp and the MRP isoforms may also play a significant role by having a binding site which is inaccessible to the long side chains of the poloxamers (Batrakova et al., 2004). Evers *et al* could not find any correlation between P-gp and MRP inhibition using Pluronic L61 on MDCKII transfected cell lines (Evers et al., 2000). If this structural explanation is correct for transporter-specific excipient inhibition, it could explain why only two of our excipients yielded sufficient inhibition data to give an IC<sub>50</sub> value, the castor oil derivatives.

Previous literature has also noted the efficacy of the polyethoxylated castor oils against ABCC2. Cremophor EL and Cremophor RH (equivalent to Etocas 35 and Etocas 40, respectively) has been shown to decrease ABCC2-mediated transport on MDCKII-ABCC2 cells (Hanke et al., 2010). The same study also showed that Tween 80 also interrupted ABCC2 transport, but only at higher concentrations, and only after 5 hours of assay time (Hanke et al., 2010). In another study using SF9 membrane vesicles overexpressing MRP2, Cremophor EL and Cremophor RH was able to inhibit MRP2-mediated transport of scutellarin (Li et al., 2013a). In contrast to the study conducted herein, the study by Li *et al* also found that poloxamer 188, poloxamer 407 and Capmul MCM also inhibited ABCC2-mediated transport, but only after 4 hours incubation (Li et al., 2013a). A subsequent study found that the inhibition of ABCC2 by the polyethoxylated castor oils has been shown to be concentration-dependent (Li et al., 2014a). However, the distinction between excipients which inhibit ABCB1 and those which inhibit ABCC2 remains unclear.

Table 4.6. Physical properties and IC<sub>50</sub> values of the tested excipients. Molecular weight values were either obtained from the manufacturer or estimated from the structures, as given in the parentheses below. All other values were determined experimentally.

<i>Excipient</i>		<i>Physical Properties</i>			<i>IC<sub>50</sub> (μM)</i>			
		<i>HLB</i> <sup>•</sup>	<i>MW</i>	<i>State</i>	<i>Average</i>	<i>Upper</i>	<i>Lower</i>	
Capmul PG-12	Propylene Glycol Monolaurate	5	246 <sup>§</sup>	Liquid	-	-	-	
Capmul MCM	Medium Chain Mono- and Diglycerides	5.5	218 <sup>§</sup>	Liquid	-	-	-	
Capmul MCM C8	Glyceryl Monocaprylate	5.5	202 <sup>§</sup>	Liquid	-	-	-	
Capmul PG-8	Propylene Glycol Monocaprylate	6	258 <sup>§</sup>	Liquid	-	-	-	
Poloxamer 182	Poly(ethylene) Poly(propylene) Glycol	7.0	2500 <sup>•</sup>	Liquid	8.57	10.62	7.35	(Fig. 4.13a)
Span 20	Sorbitan Monolaurate	8.6	346 <sup>•</sup>	Liquid	7725.45	9793.18	6250.69	(Fig. 4.13b)
Arlatone TV	PEG 40 Sorbitan Peroleate	9.0	3508 <sup>§</sup>	Liquid	-	-	-	
Crovol A-70	PEG 60 Almond Glyceride	10.0	3251 <sup>§</sup>	Liquid	2.56	3.51	1.92	(Fig. 4.13c)
Etocas 29	PEG 29 Castor Oil	11.7	2202 <sup>§</sup>	Liquid	12.00	17.87	8.84	(Fig. 4.13d)
Brij S-10	PEG 10 Stearyl Ether	12.4	710 <sup>§</sup>	Waxy	-	-	-	
Poloxamer 184	Poly(ethylene) Poly(propylene) Glycol	13.0	2900 <sup>•</sup>	Liquid	7.64	10.11	5.95	(Fig. 4.13e)
Etocas 40	PEG 40 Castor Oil	13.0	2686 <sup>§</sup>	Liquid	9.55	14.45	6.62	(Fig. 4.13f)
Brij CS-12	PEG 12 Cetostearyl Ether	13.4	770 <sup>§</sup>	Waxy	-	-	-	
Acconon C-44	Lauroyl Macroglycerides	13.5	1500 <sup>•</sup>	Waxy	26.54	32.88	21.62	(Fig. 4.13g)
NatraGem S140	Polyglyceryl-4 Laurate/Sebacate	14.0	664/532 <sup>§</sup>	Liquid	-	-	-	
Acconon MC8-2	PEG 8 Caprylic/Capric Glycerides	14.5	350 <sup>•</sup>	Waxy	-	-	-	
Tween 80	PEG 80 Sorbitan Monolaurate	15.0	1310 <sup>•</sup>	Liquid	12.24	19.89	7.44	(Fig. 4.13h)
Cetomacrogol 1000	PEG 20 Cetostearyl Ether	15.7	1122 <sup>§</sup>	Waxy	-	-	-	
Tween 20	PEG 20 Sorbitan Monolaurate	16.7	1128 <sup>•</sup>	Liquid	9.65	12.76	7.41	(Fig. 4.13i)
Myrj S-40	PEG 40 Stearate	16.7	2044 <sup>§</sup>	Solid	6.13	8.84	4.62	(Fig. 4.13j)
Poloxamer 335	Poly(ethylene) Poly(propylene) Glycol	18.0	6500 <sup>•</sup>	Solid	0.63	0.75	0.53	(Fig. 4.13k)
Myrj S-100	PEG 100 Stearate	18.8	4684 <sup>§</sup>	Solid	-	-	-	
Poloxamer 407	Poly(ethylene) Poly(propylene) Glycol	22.0	12500 <sup>•</sup>	Solid	0.71	0.77	0.70	(Fig. 4.13l)
Poloxamer 188	Poly(ethylene) Poly(propylene) Glycol	29.0	8400 <sup>•</sup>	Solid	-	-	-	

<sup>•</sup>Determined by manufacturer

<sup>§</sup>Estimated from molecular weight

#### 4.6.3. The Effects of Surfactant Structure on Inhibition of ABCB1-Mediated Efflux

Using the HTS screening assay, 24 surfactants were screened for activity against the ABCB1 and ABCC2 efflux transporter systems, identifying 12 excipients as inhibitors of ABCB1. In order to elucidate the structure/function relationship between excipients and their efficacy, the molecular structures were examined in closer detail. It has previously been noted that the inhibitory effects of poloxamers against ABCB1 is heavily dependent upon the HLB of the molecules. In an comprehensive study, the block copolymers with intermediate propylene oxide blocks (30-60 units) with HLB values below 20 gave the optimum inhibition against P-gp in bovine brain microvessel endothelial cells (BBMECs) by increasing microviscosity of the lipid membrane and P-gp ATPase inhibition (Batrakova et al., 2003). Indeed, our findings are in agreement. Of the 5 poloxamers tested, only P188 showed no pharmacological activity against ABCB1 and was more hydrophilic than the other poloxamers with a HLB of 29. Yet, closer examination of Table 4.6 reveals substantial gaps in the list that cannot be explained using HLB alone.

Of the materials tested, the lowest molecular weight to be seen is Span 20, which has a comparatively high  $IC_{50}$  value. Tween 20, with a molecular weight of 1128 Da, has an  $IC_{50}$  value of 9.7  $\mu$ M, yet has a very similar molecular weight to Cetomacrogol 1000 (1122 Da) which had no effect on ABCB1-mediated efflux. For these materials, the separating factor appears to be the structural geometry. Tweens have central ring structure from which PEGylated moieties emanate, divided over 3 branches. For Cetomacrogol, the molecule is essentially split in two distinct regions, the hydrophobic part and the hydrophilic part in a linear fashion. As membrane interaction and subsequent fluidisation is the generally accepted mechanism of action, it can be expected that polarised linear chains represent a larger degree of steric hindrance during lipid partitioning compared to the compact geometry of Tween 20, through which membrane interactions can pivot around the hydrophobic ring system. Closely related to Cetomacrogol 1000, Brij CS-12 and Brij S-10 suffer the same fate. Myrj S-40 is also a linear chain, but appears to be able to interact with the membrane, and therefore inhibit, because of its more compact geometry with PEG 40 forming the hydrophilic element. In contrast, Myrj S-100 has no biological effect, most likely attributed to the extension of the linear chain by PEG 100 as the hydrophilic segment.

Interestingly, Arlatone TV has no inhibitory effect, yet possesses 6 branches structure emanating from a sorbitol backbone. In this case, the distribution of the PEGylation appears inadequate (an average of 6.6 repeat units per branch) to counter the bulk of the molecule.

#### 4.6.4. Conclusions of *In Vitro* Kinetic Screening using the HTS Method

The central aim of this chapter was to identify a number of excipients that could be incorporated into an oral dosage formulation. In order to do this, the following objectives were met:

- Kinetic data relating to the established inhibitors of the ABCB1 and ABCC2 efflux transporter systems was obtained in order to establish the functionality of these transporters on the Caco-2 cell line.
- A broad range of excipients were screened using the HTS assay for activity against ABCB1- and ABCC2-mediated transport, with a number of inhibitors found that could be used in oral dosage formulations.
- Non-specific mechanisms not related to efflux inhibition were carefully considered and excluded from the data, such as membrane damage and toxicology.

Using the HTS assay developed in the previous chapter, the established inhibitors of the efflux transporters gave  $IC_{50}$  values that were similar to that of published values, confirming the functional activity of the ABCB1 and ABCC2 transporters on the Caco-2 cell line and establishing the assay within the framework of existing literature. A large and diverse number of excipients were then screened for inhibition activity against the ABCB1 and ABCC2 transporter systems. This identified 12 excipients that are inhibitors of ABCB1 and 2 that are inhibitors of ABCC2. Care and attention was taken to identify mechanisms that were not transporter related such as toxicology, excipient-induced membrane damage and fluorescent probe quenching by surfactant encapsulation.

Of all of the excipients screened, surfactants with intermediate HLB values that were small and linear or larger and branched showed high efficacy. It is of interest to note that the data presented in this study puts a number of  $IC_{50}$  values for the excipients within the *micromolar* range. In this respect, Crovol A70, poloxamer 335 and poloxamer 407 have efficacy that exceeds VER ( $IC_{50}$  4.08), whilst P335 and P407 exceed that of CsA ( $IC_{50}$  1.16).

In terms of physiological relevance, these data need to be examined in the context of oral dosage forms. Poloxamers are typically not used to the high concentrations seen by binders or disintegrants for example, and their role is typically as coatings or emulsifiers. However, according to the Excipient Handbook, poloxamers may appear up to 10 % of a tablet (Rowe et al., 2009). Assuming a 500 mg tablet taken with accepted 250 mL of water, the materials with the lowest  $IC_{50}$  values in our dataset, the poloxamers 335 and 407, would only need to be present as 1.0 and 2.2 mg, respectively, if taken on an empty stomach. As such, the data obtained in this chapter offers a selection of materials that can be incorporated into oral dosage formulations for potential efflux inhibition *in vivo*.

## **Chapter 5**

### The Design and Manufacture of Orally Disintegrating Tablets with Enhanced Delivery Capability

## 5. The Design and Manufacture of Orally Disintegrating Tablets with Enhanced Delivery Capability

### 5.1. Chapter Aim and Objectives

The work presented in Chapter 4 characterised a diverse range of excipients in order to elucidate their biological effects against the ABCB1 and ABCC2 efflux transporter systems. This provides a working toolbox for the design and production of tablets with the potential to realise enhanced delivery of drugs which are prone to efflux. Therefore, the aim of the following work was to produce two orally disintegrating tablet (ODT) formulations with disintegration times conforming to *United States Pharmacopoeia* at or below 30 seconds (McLaughlin et al., 2009), utilising the excipient kinetic data obtained using the HTS screening assay of the previous chapter in order to achieve the potential for enhanced oral bioavailability. The work presented in the following chapter was conducted entirely during industrial placement at the Colorcon Dartford facility.

### 5.2. Tablet Design Overview

The ODTs chosen for formulation were a 295 mg 'low-dose' formulation, and a 793 mg 'high-dose' formulation. The high-throughput screening assay produced two clear lead candidate excipients, poloxamer 335 and poloxamer 407 with  $IC_{50}$  values of  $4.12 \times 10^{-4}$  % (w/v) and  $8.85 \times 10^{-4}$  % (w/v), respectively. Poloxamer 407 was chosen as the material for incorporation into the ODTs as a micronised version of the same polymer previously used in the high-throughput screening assay in the previous chapter.

This tablet development phase required two assumptions. The first is that the tablet must contain an excessive quantity of biologically active material. As such, the content of each tablet was chosen to be 10 % (w/w) as a surplus quantity to ensure a good drug: excipient ratio in the final diluted solution for *in vitro* uptake studies, delivering 28.6 mg and 79.3 mg of poloxamer 407 respectively for low-dose and high-dose tablets, both in excess of the 2.2 mg theoretical amount required.

The second assumption in the tablet design was a drug substitution. For this developmental phase, paracetamol (acetaminophen, APAP) was chosen as the active pharmaceutical ingredient (API) as a relatively non-toxic model drug. Fundamentally, one

of the objectives in the project was to produce a tablet with enhanced delivery, requiring not just biologically active excipients to exploit, but also a drug with poor uptake such that there is ample potential for improvement. APAP is neither an ABCB1 or ABCC2 substrate, and is able to traverse the cell membrane rapidly ( $P_{app}$  23.7-100  $\times 10^{-6}$  cm s<sup>-1</sup> (Irvine et al., 1999, Yamashita et al., 2000)), meaning that the impact of efflux transporters is likely to be negligible. Furthermore, APAP has 80 % fraction absorbed in humans (Irvine et al., 1999). The inclusion of APAP was entirely as a model compound to represent high-dose drug and to determine the impact of inclusion of P407 on the formulation of high-dose ODTs. The second model compound to be tested was atorvastatin (ATV). This drug has an efflux ratio of seven on the Caco-2 model (Wu et al., 2000), indicating excess efflux transport primarily by P-gp (Wu et al., 2000, Hochman et al., 2004, Li et al., 2011a), but with lesser contributions from the MRP2 and BCRP transporter systems (Li et al., 2011a). ATV tablets typically have 10, 20, 40 or 80 mg loading. Based on the differences in the typical dosage of the two model APIs, the high-dose formulation was intended to closely resemble a typical APAP tablet with ~ 40 % drug loading. The second formulation, the low-dose, was chosen as a typical sized ATV tablet to be converted at the advanced phase of the tablet development. The remaining excipients and the grades chosen are presented in Table 5.1.

Table 5.1. List of excipient selected for ODT development.

<i>Tablet Constituent</i>	<i>Type Chosen</i>	<i>Purpose</i>
Granulated Paracetamol	Compap™ PVP3	API
Ethyl Cellulose	Ethocel™ 7 FP	Binder
Microcrystalline Cellulose	Avicel® PH102	Disintegrant
Mannitol	Mannogem® 2028	Dilutant/Sweetener
Crospovidone	Kollidon® CL-F	Superdisintegrant
Efflux Modifier	Poloxamer 407	ABCB1 Inhibitor
Partially Pregelatinised Maize Starch	Starch 1500®	Multipurpose Binder/Filler

### 5.3. Design of Experiments: Screening Round 1

In order to explore the response of different combinations of the excipients MCC, mannitol and Starch 1500, a design of experiments approach was taken to design a set of experiments with varying concentrations of each material for both high and low-dose materials, with 40 % and 70 % excipient content, respectively. The JMP 12 DoE software proposed 10 formulations out of a potential 225 (Table 5.2). These formulations were then made into tablets by direct compression at 1 metric ton.

Table 5.2. Low-dose and high-dose formulation compositions indicated by the first round of DoE mapping using JMP 12 DoE software to optimise MCC, Starch 1500 and mannitol content within the ODT formulation.

#### Low-dose - 11 % Drug – 295 mg

##### 70% MCC/Starch 1500/Mannitol

<i>Excipient</i>	<i>Composition, % (w/w)</i>									
	<i>F1</i>	<i>F2</i>	<i>F3</i>	<i>F4</i>	<i>F5</i>	<i>F6</i>	<i>F7</i>	<i>F8</i>	<i>F9</i>	<i>F10</i>
Starch 1500	0.0	30.0	25.0	10.0	30.0	30.0	20.0	0.0	25.0	20.0
MCC	30.0	30.0	25.0	25.0	0.0	30.0	20.0	30.0	10.0	20.0
Mannitol	40.0	10.0	20.0	35.0	40.0	10.0	30.0	40.0	35.0	30.0
Ethocel 7 FP Premium	2.5	2.5	2.5	2.5	2.5	2.5	2.5	2.5	2.5	2.5
Poloxamer 407	10.0	10.0	10.0	10.0	10.0	10.0	10.0	10.0	10.0	10.0
Crospovidone	5.0	5.0	5.0	5.0	5.0	5.0	5.0	5.0	5.0	5.0
Glycerol Behenate	1.5	1.5	1.5	1.5	1.5	1.5	1.5	1.5	1.5	1.5
APAP	11.0	11.0	11.0	11.0	11.0	11.0	11.0	11.0	11.0	11.0
<b>Total</b>	100.0									

#### High-dose - 41 % Drug – 795 mg

##### 40% MCC/Starch 1500/Mannitol

<i>Excipient</i>	<i>Composition, % (w/w)</i>									
	<i>F1</i>	<i>F2</i>	<i>F3</i>	<i>F4</i>	<i>F5</i>	<i>F6</i>	<i>F7</i>	<i>F8</i>	<i>F9</i>	<i>F10</i>
Starch 1500	20.0	2.5	16.7	9.2	19.0	2.5	15.8	19.0	17.4	15.8
MCC	0.0	15.0	4.4	11.9	15.0	15.0	8.8	15.0	11.9	8.8
Mannitol	20.0	22.5	19.0	19.0	6.0	22.5	15.4	6.0	10.7	15.4
Ethocel 7 FP Premium	2.5	2.5	2.5	2.5	2.5	2.5	2.5	2.5	2.5	2.5
Poloxamer 407	10.0	10.0	10.0	10.0	10.0	10.0	10.0	10.0	10.0	10.0
Crospovidone	5.0	5.0	5.0	5.0	5.0	5.0	5.0	5.0	5.0	5.0
Glycerol Behenate	1.5	1.5	1.5	1.5	1.5	1.5	1.5	1.5	1.5	1.5
APAP	41.0	41.0	41.0	41.0	41.0	41.0	41.0	41.0	41.0	41.0
<b>Total</b>	100.0									

### 5.3.1. Tablet Description

Low-dose tablets were made to 295 mg in a 10 mm die to normal convex geometry. High-dose tablets were made to 793 mg flat-faced 13 mm die in order to accommodate the larger powder volume. Both tablet types appeared smooth and glossy.

### 5.3.2. Physical Characterisation

The hardness and disintegration information for both tablet formulations is presented in Figure 5.1. For the low-dose formulations, hardness was 5.9- 11.2 kp and disintegration times were 103-291 s (Figure 5.1a). For high-dose tablets, hardness was greater than the low-dose at 11.3 – 17.3 kp with disintegration times of 88-150 s (Figure 5.1b). Paracetamol is known for its poor compressibility, which results in poor hardness and a tendency to cap, a process that results in the separation of the crown from the tablet (Krycer et al., 1982), owing to the monoclinic crystal structure, which results in reduced plastic deformation. As such, unprocessed paracetamol is not used for direct compression, which limits its usefulness. An effective strategy to address this is to mix the paracetamol with polyvinylpyrrolidone (PVP), a binder which is able to undergo plastic deformation (Ayenew et al., 2012). When paracetamol is processed with PVP, this additive is able to influence the crystal habit of paracetamol. The action of PVP in habit modification is twofold; first, PVP interacts with paracetamol in the aqueous solution via hydrogen bonding (Horn and Ditter, 1982, Garekani et al., 2003), secondly, PVP is a strong inhibitor of crystal growth by direct adsorption onto the surface of the growing crystal (Ziller and Rupprecht, 1988). In a study examining the different grades of PVP, it was found that the effectiveness of additives, judged by the change in paracetamol crystal habit and the delay in crystal formation, was found to follow the molecular weight in the order PVP 50000 > PVP 10000 > PVP 2000 (Garekani et al., 2000b). Used in direct compression, the paracetamol particles produced by crystallisation in the presence of 0.5 % PVP 10, 000 or PVP 50, 000 produced hard tablets without capping (Garekani et al., 2000a). These particles consisted of multiple agglomerated microcrystals, which could fragment under pressure, allowing the opportunity for multiple fresh surfaces for enhanced interparticulate bonding. Indeed, the compacts produced in the presence of PVP exhibited lower elastic recoveries compared to untreated paracetamol (Garekani et al., 2000a). The APAP used in the current study is

Compap™ PVP3 which has been coprocessed with 3 % (w/w) PVP to aid compressibility. As such, both the low-dose and high-dose tablet formulations have good hardness.

Plastic disk inserts, permitted for use with disintegrating equipment according to the USP, were found to stick to the tablets high in Starch 1500, and they were subsequently omitted. Of all of the low-dose formulations tested, F1, F4, F5, F8, F9 and F10 had disintegration times conforming to the *European Pharmacopeia* limit of 180 seconds for uncoated tablets (*European Pharmacopeia*, 2009), but no formulations displayed disintegration times conforming to the *United States Pharmacopeia* limit of 30 seconds (McLaughlin et al., 2009). Interestingly, the fastest disintegration time was seen for low-dose F5, which contained high Starch 1500 and no MCC. This formulation also had the lowest hardness (5.9 kp). A strong correlation between hardness and disintegration has been demonstrated using uncoated caffeine tablets, whereby hardness was able to govern the all stages of drug dissolution (Kitazawa et al., 1975). Moreover, at low hardness, a larger pore network is likely to exist within the tablet to aid water ingress, which has an important impact upon disintegration time (Shangraw et al., 1980). Therefore, the lower hardness of F5 is likely a contributing factor in this faster disintegration time due to the higher degree of porosity of the tablets, coupled with the ability of Starch 1500 to swell as a mechanism of disintegration. All high-dose tablets conformed to the *European Pharmacopeia* limits independent of the excipient composition (*European Pharmacopeia*, 2009).

In order to test the robustness of the tablet formulations, friability testing was conducted according to the *United States Pharmacopeia* (USP, 2013). Low-dose tablet friability (Table 5.3) was found to be negligible for all low-dose formulations ( $\leq 0.044$  %) and well within the 1 % limit recommended by the *United States Pharmacopeia* (USP, 2013). Friability for the high-dose tablets was higher than low-dose tablets, but no greater than 0.7 % (Table 5.3) and also conforms to the 1 % limit recommended by the *United States Pharmacopeia* (USP, 2013). For both low-dose and high-dose formulations, width, thickness and weight variation were found to be negligible (Table 5.3). Moreover, the results of the initial study give room for improvement for both low-dose and high-dose formulations.

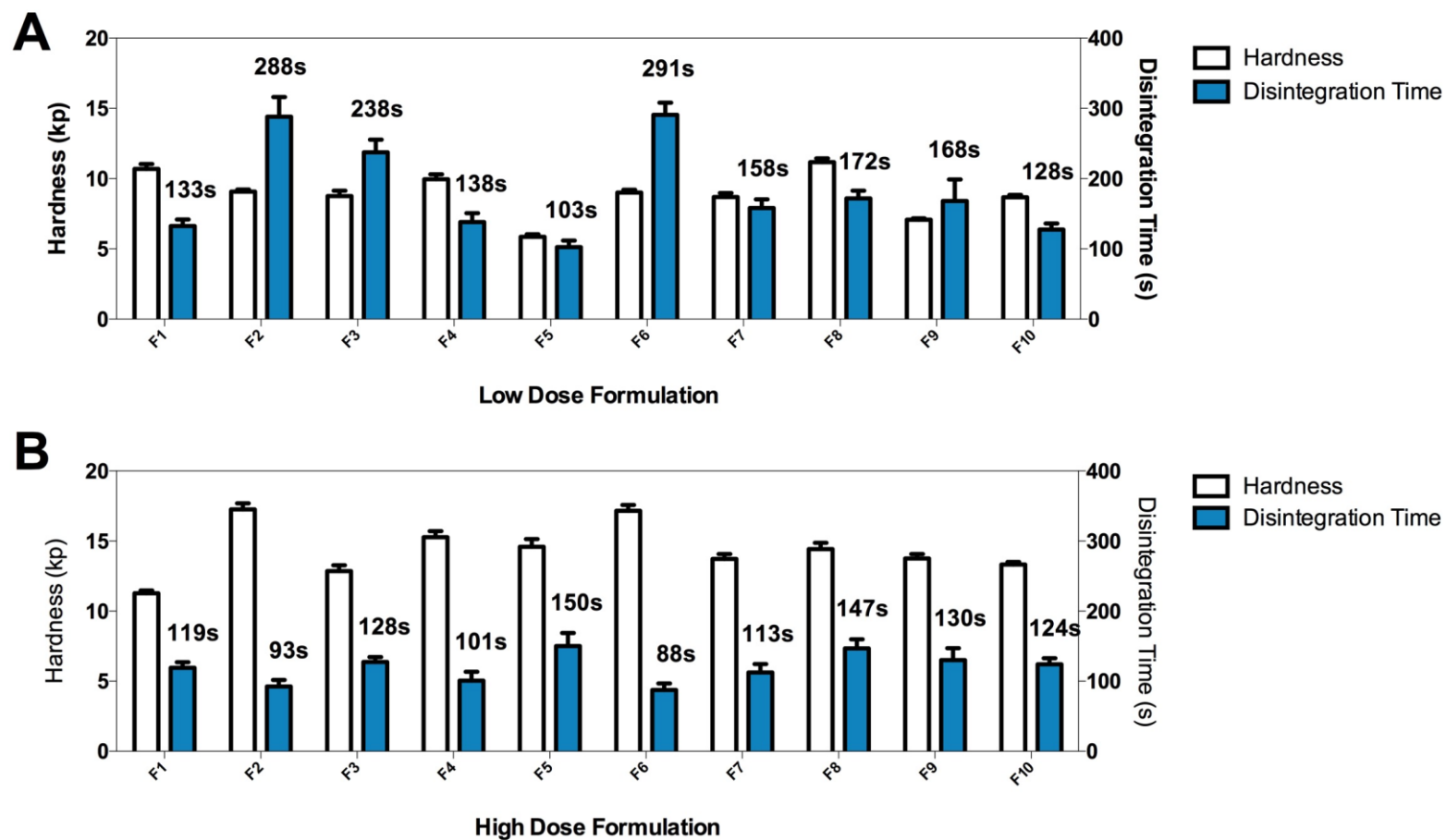


Figure 5.1. The results of the DoE screening approach, showing tablet hardness (clear bars) and disintegration time (blue bars) for A) low-dose and B) high-dose tablets. Whilst some low-dose formulations and all high-dose formulations were able to disintegrate in less than 3 minutes in accordance with the EP, no formulations conformed to the USP limit of 30 seconds. Data presented as mean  $\pm$  SD from  $n = 10$  tablets for hardness and 6 tablets for disintegration time.

Table 5.3. Remaining physical data from both high and low-dose APAP tablet. For all datasets,  $n = 10$  tablets.

<i>Formulation</i>	<i>Friability (%)</i>	<i>Width (mm)</i>	<i>Thickness (mm)</i>	<i>Weight (mg)</i>	
Low-dose	1	0.017	10.032 ± 0.023	4.076 ± 0.013	296.810 ± 0.737
	2	0.007	10.039 ± 0.009	4.181 ± 0.023	296.700 ± 0.799
	3	0.024	10.036 ± 0.007	4.172 ± 0.018	296.330 ± 0.738
	4	0.010	10.028 ± 0.004	4.120 ± 0.018	296.640 ± 1.125
	5	0.037	10.061 ± 0.009	4.207 ± 0.027	296.600 ± 0.720
	6	0.040	10.042 ± 0.018	4.183 ± 0.015	296.840 ± 0.570
	7	0.044	10.045 ± 0.012	4.159 ± 0.007	295.890 ± 0.713
	8	0.041	10.023 ± 0.007	4.068 ± 0.014	295.840 ± 0.560
	9	0.027	10.043 ± 0.008	4.178 ± 0.009	295.880 ± 0.661
	10	0.030	10.034 ± 0.005	4.155 ± 0.012	295.830 ± 0.499
High-dose	1	0.746	13.038 ± 0.021	5.362 ± 0.021	795.080 ± 0.975
	2	0.273	13.009 ± 0.007	5.268 ± 0.015	794.930 ± 1.608
	3	0.484	13.015 ± 0.005	5.315 ± 0.021	794.080 ± 0.588
	4	0.295	13.007 ± 0.009	5.318 ± 0.019	794.420 ± 1.030
	5	0.447	13.022 ± 0.004	5.374 ± 0.026	794.710 ± 1.007
	6	0.311	13.006 ± 0.007	5.280 ± 0.011	794.140 ± 0.961
	7	0.515	13.019 ± 0.006	5.348 ± 0.011	793.770 ± 0.860
	8	0.381	13.021 ± 0.009	5.381 ± 0.029	795.560 ± 0.977
	9	0.474	13.019 ± 0.012	5.378 ± 0.026	794.850 ± 0.546
	10	0.314	13.023 ± 0.015	5.340 ± 0.012	794.270 ± 0.589

### 5.3.3. Design of Experiments Interpretation of Excipient Composition

Using JMP 12 DoE software, the impact of Starch 1500, MCC and mannitol was examined in further detail using bivariate analysis. The data are presented in Figure 5.2 and Figure 5.3 for low-dose and high-dose formulations respectively. For the low-dose formulations, Starch 1500 decreased tablet strength, mannitol had little impact and MCC was able to improve tablet strength (Figure 5.2a). Of these, Starch 1500 and MCC correlated well, with  $r^2$  values of 0.60 and 0.80 respectively, moreover both of these excipients had a significant ( $p < 0.01$ ) impact upon tablet hardness (Table 5.4). For disintegration, Starch 1500 and MCC increased disintegration time whereas mannitol was able to decrease it (Figure 5.2b). The impact of mannitol had good correlation with the model ( $r^2 = 0.85$ ); furthermore mannitol was the only material to have a significant ( $p < 0.001$ ) impact upon disintegration for the low-dose formulations (Table 5.4). In agreement with the impact upon the low-dose formulations, Starch 1500 also decreased tablet strength of the high-dose formulations, mannitol had little impact and MCC was able to improve tablet strength (Figure 5.3a). Of these, Starch 1500 and MCC correlated well, with  $r^2$  values of 0.75 and 0.71 respectively, moreover both of these excipients had a significant ( $p < 0.01$ ) impact upon tablet strength (Table 5.5). Starch 1500 increased disintegration time, MCC had little impact whereas mannitol was able to decrease it (Figure 5.3b). Both Starch 1500 and mannitol correlated well in this model ( $r^2 = 0.77$  and  $0.79$  respectively), and the impact of both was significant ( $p < 0.001$ ) (Table 5.5).

Tablet hardness for both high and low formulations was shown to correlate well to an increase in MCC content (Figure 5.2a and Figure 5.3a). MCC is known to undergo a unique plastic deformation during compression that occurs through enhanced hydrogen bonding to adjacent MCC particles (Al-Khattawi and Mohammed, 2013), as opposed to conventional plastic deformation that occurs when compression is able to overcome the intermolecular forces of the material (Hess, 1978). This conglomerate hypothesis has been observed by measuring large amorphous regions in MCC by XRD and DSC (Al-Khattawi et al., 2014). In addition to increasing hardness, the low-dose tablets showed an increase in disintegration time with an increased level of MCC (Figure 5.2b), most likely attributed to the difficulty faced by the disintegrants in overcoming the binding forces of the tablet with increased strength. For the high-dose formulations, the impact of MCC on disintegration

was minimal ( $r^2 = 0$ ), suggesting the dominant role of the compressible form of APAP in determining the rate of disintegration (Figure 5.3b). Indeed, a common limitation of the compressible forms of paracetamol is poorer disintegration (Martinello et al., 2006).

For both high and low-dose APAP formulations, high Starch 1500 corresponded to poor tablet strength. Whilst the overall compressibility of Starch 1500 is good, the strength of the subsequent compacts is low. The reason for this is twofold: plastic deformation of Starch 1500 is a slow process, meaning quick compression is insufficient in producing strong interparticle bonds during plastic deformation, additionally the deformation is largely elastic (Rees and Rue, 1978). Furthermore, the disintegration time increased with the increased levels of Starch 1500, most likely attributed to the gel forming properties of the material. However, Starch 1500 is not intended as a stand-alone disintegrant and is recommended as part mixture of different excipients to complement disintegration by relying on the mechanism of swelling for its disintegration properties (Rojas and Kumar, 2012). Despite the absence of MCC in low-dose F5 (Table 5.2), Starch 1500 as the lone disintegrant gave the fastest disintegration time of the batch at 103 s (Figure 5.1), implying that the swelling mechanism was able to overcome the binding properties imparted by this tablet composition. Mannitol had no impact upon hardness for either formulation (Figure 5.2a and Figure 5.3a,  $r^2 > 0.05$ ). For both high and low formulations, increasing mannitol content led to a significant ( $p < 0.05$ ) decrease in disintegration time (Figure 5.2b and Figure 5.3b) likely attributed to the good wetting properties which facilitate the ingress of water to the crospovidone and so decreasing the disintegration time (Kubo and Mizobe, 1997).

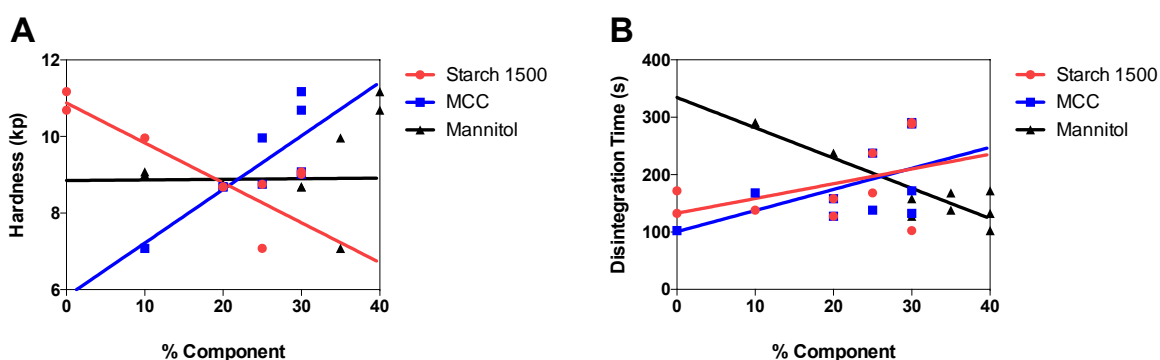


Figure 5.2. Design of experiments trace plots for low-dose formulations showing A) hardness and B) disintegration, showing the impact of Starch 1500 (red), MCC (blue) and mannitol (black).

Table 5.4. Summary of the model statistics on the impact of the test excipients on hardness and disintegration on the low-dose formulations from the first round of DoE screening.

	<i>Factor</i>	$r^2$	<i>F ratio</i>	<i>Prob &gt; F</i>
Hardness	Starch 1500	0.61	12.29	0.0080
	MCC	0.80	32.11	0.0005
	Mannitol	0.00	0.00	0.9742
Disintegration	Starch 1500	0.20	2.03	0.1925
	MCC	0.30	3.47	0.0996
	Mannitol	0.85	44.40	0.0002

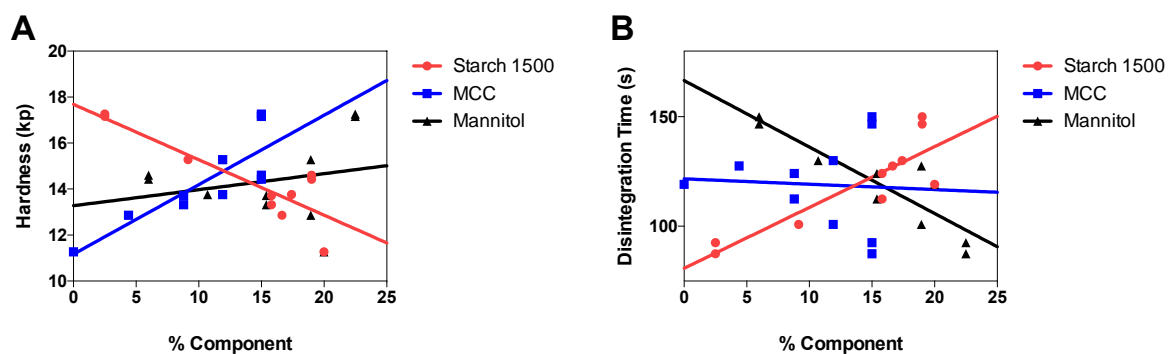


Figure 5.3. Design of experiments trace plots for high-dose formulations showing A) hardness and B) disintegration, showing the impact of Starch 1500 (red), MCC (blue) and mannitol (black).

Table 5.5. Summary of the model statistics on the impact of the test excipients on hardness and disintegration on the high-dose formulations from the first round of DoE screening.

	<i>Factor</i>	$r^2$	<i>F ratio</i>	<i>Prob &gt; F</i>
Hardness	Starch 1500	0.75	23.13	0.0012
	MCC	0.71	19.17	0.0024
	Mannitol	0.05	0.46	0.5161
Disintegration	Starch 1500	0.77	26.23	0.0009
	MCC	0.00	0.03	0.8697
	Mannitol	0.79	30.72	0.0005

## 5.4. Formulation Refinement

Having completed the first phase of tablet evaluation by evaluating the impact of filler composition, the other excipients were evaluated in order to improve disintegration time. From the DoE data presented Figure 5.1, the formulations with the fastest and slowest disintegration times (F5 and F6 for low-dose respectively, F6 and F5 for high-dose respectively) were selected as test platforms in order to examine the impact of the poloxamer 407, crospovidone and ethylcellulose content, as well as the grade of crospovidone used and finally the type of multi-purpose excipient.

### 5.4.1. Effects of Poloxamer 407 Content on Hardness and Disintegration

Poloxamer 407 was incorporated in excessive quantities from the start in order to understand the upper payload limits of biologically active material that each delivery vehicle can accommodate. However, the inadequate disintegration times above 30 seconds meant that this value needed to be revised. Therefore, the percentage poloxamer content was evaluated at 0-10 % of the tablet weight, with the results presented in (Figure 5.4). Increasing the poloxamer concentration from 0 % to 10 % weight within the tablets resulted in a general increase in hardness and disintegration time. For the low-dose F5 tablets, both hardness and disintegration increased as a function of P407 content in relation to the poloxamer-free control, with hardness becoming significant between 2 % and 10 % ( $p < 0.0001$ ) with an increase from 4.8 kp to 5.2 and 5.9 kp respectively. Disintegration times also increased from 56s to 103s for low-dose F5 over the concentration range tested, becoming significant ( $p < 0.0001$ ) at 10 % poloxamer content. For low-dose F6, a small but significant ( $p < 0.0001$ ) increase was seen in hardness when P407 was increased from 0 % to 2 % from 9.0 to 9.6 kp respectively, but this became non-significant ( $p > 0.05$ ) by 10 % poloxamer content indicating that this could be attributed to batch to batch variation. However, a massive increase in disintegration time was observed from 50s to 290s over the range tested, becoming significant ( $p < 0.0001$ ) at between 2% and 10 % poloxamer content. For the high-dose F5 formulation, hardness increased over the range tested from 10.4 kp at 0 % to 14.6 kp at 10 %, becoming significant ( $p < 0.0001$ ) at 2 % poloxamer content. Hardness also increased marginally, becoming significant ( $p < 0.05$ ) at 10 % poloxamer weight. For high-dose F6, the hardness increase became significant ( $p < 0.0001$ ) at 2 % poloxamer content, increasing from 12.2s to 17.2s over the range tested. Likewise, disintegration times

also increased from 39.2s to 88s over the range tested, becoming significant ( $p < 0.0001$ ) at 2 % poloxamer content.

Poloxamer 407 has previously been used in directly compressed tablets as a lubricant at 2 % (w/w) or less. In a study comparing micronised P407 to magnesium stearate, P407 gave similar ejection force data to that of magnesium stearate without decreasing tablet strength (Desai et al., 2007). In another study looking at the lubricant properties of 1-2 % P407, this material showed ejection forces less than that of magnesium stearate, but also increased disintegration times when used in conjunction with MCC as a binder and decreased slightly at 2 % P407 (Muzikova et al., 2012). Hardness followed a similar pattern; although this was not observed when spray dried lactose (Flowlac® 100) was used as a binder instead of MCC. The results presented in Figure 5.4 are different, as no significant ( $p > 0.05$ ) increase in hardness was observed between formulations with no P407 and those with 2 %.

In an additional study using the surfactant poloxamer 188 (similar in hydrophilicity to P407) in immediate release tablets, multivariate analysis revealed this excipient was able to act as a binder either directly or by increasing intragranular cohesion (Kaul et al., 2011). The increase in dissolution time seen for the immediate release tablets was attributed to the increase in hydrophilicity of the tablet retarding the wicking action of the disintegrant crospovidone, in addition to the overall binding effects of the poloxamer. Indeed, exchanging the crospovidone with croscarmellose sodium, a disintegrant with a higher swelling capacity than crospovidone, was able to counter the decrease in dissolution (Kaul et al., 2011). As crospovidone is dependent upon wicking for its action (Kornblum and Stoopak, 1973), this could explain how the addition of a hydrophilic material, P407, is able to significantly ( $p < 0.05$ ) increase the disintegration times of the tablets at 10 % (Figure 5.4). Furthermore, MCC is also a wicking agent (Al-Khattawi et al., 2014), and the same mechanism may explain the dramatic decrease in disintegration time from 290 s to 54 s for low-dose F6 containing 30 % (w/w) MCC when 10 % poloxamer is reduced to 2 % (Figure 5.4b). In contrast, low-dose F5 contains no MCC, but does have 30 % Starch 1500 (Table 5.2), which relies on swelling for its disintegration properties (Rojas and Kumar, 2012), and has a comparatively smaller reduction in disintegration time when P407 is reduced from 10 % to 2 % to 103 s to 61 s respectively (Figure 5.4a). Even at 2 % (w/w), the 295 mg low-dose

tablet delivers 5.9 mg of poloxamer 407, well in excess of the 2.2 mg required to exceed the  $IC_{50}$  value outlined in the previous chapter. Therefore, because of the improvement in disintegration time, 2 % P407 was chosen for the second round of DoE.

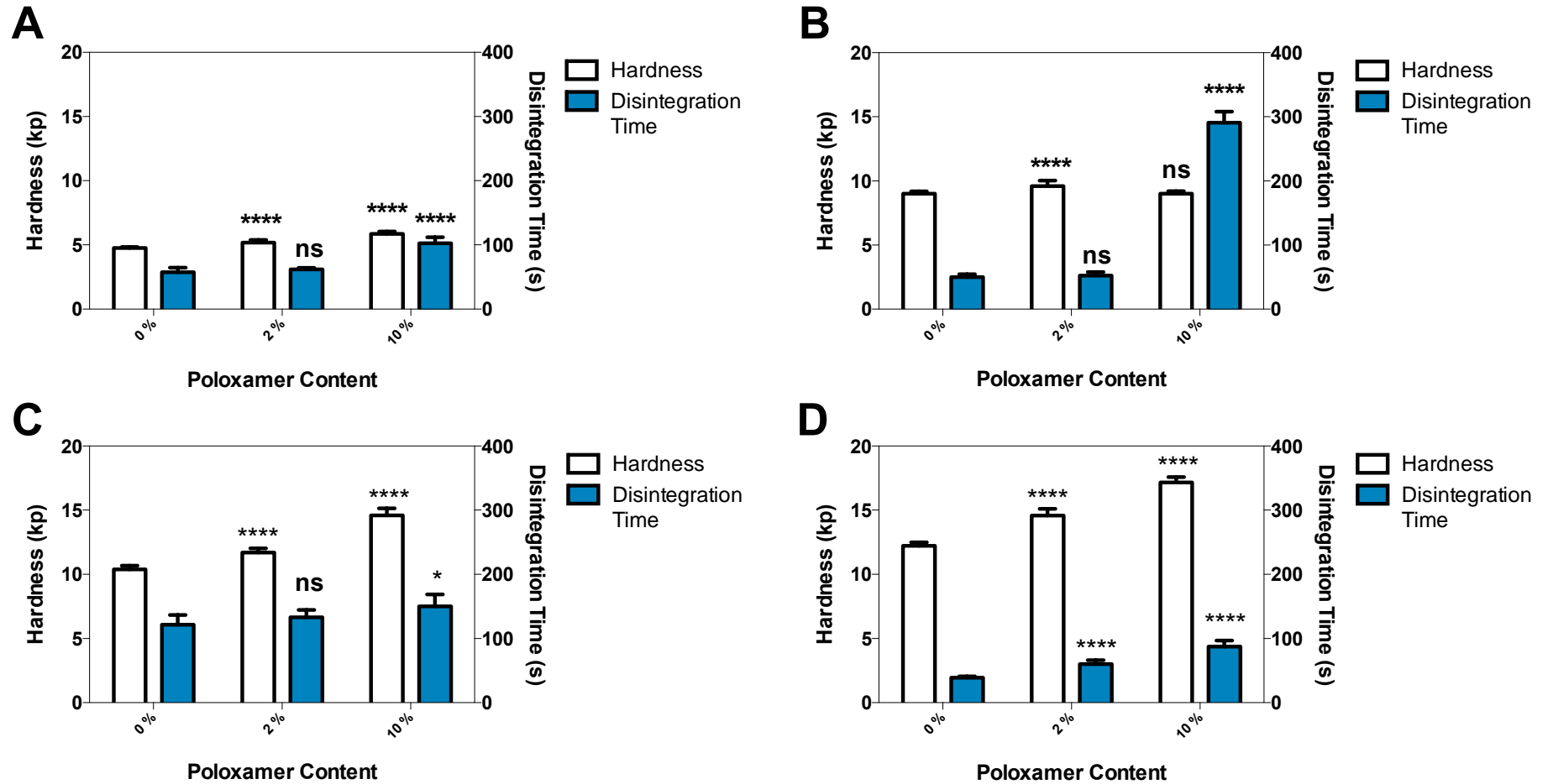


Figure 5.4. The impact of poloxamer 407 on A) low-dose F5, B) low-dose F6, C) high-dose F5 and D) high-dose F6, showing hardness (clear bars) and disintegration times (blue bars). Data presented as mean  $\pm$  SD from  $n = 10$  tablets for hardness and 6 tablets for disintegration time. Statistical significance was analysed using one-way ANOVA followed by Dunnett's *post hoc* test annotated as follows: ns ( $p > 0.05$ ); \* ( $p < 0.05$ ); \*\*\*\* ( $p < 0.0001$ ).

#### 5.4.2. Effects of Kollidon® Crospovidone Type on Hardness and Disintegration

Crospovidone is an insoluble polymer typically used as a superdisintegrant in ODT formulations (Figure 5.5). The manufacturer, BASF, offers a range of particle sizes to their product and these were evaluated for their impact on the tablet disintegration times. Kollidon® CL-F, with a particle size of 20-40  $\mu\text{m}$ , was initially selected for evaluation for the first round of DoE screening as an intermediate particle size that should display low levels of grittiness, thereby maintaining the aesthetics of a potentially marketable product. Kollidon® CL (particle size 110-130  $\mu\text{m}$ ), Kollidon® CL-SF (10-30  $\mu\text{m}$ ) and Kollidon® CL-M (3-10  $\mu\text{m}$ ) were also sourced as samples from BASF for evaluation.



Figure 5.5. The structural schematic of crospovidone.

The results of the superdisintegrant testing are presented in Figure 5.6. For both low-dose formulations, the CL-F, CL-SF and CL-M grades significantly increased hardness for all formulations ( $p < 0.001$ ) compared to the CL grade, most likely attributed to the higher compressibility of the smaller particle sizes. However, hardness appeared to plateau after the addition of the CL-F grade, and CL-F, CL-SF and CL-M all had similar hardness ( $p > 0.05$ ). The CL-F grade had a significant ( $p < 0.01$ ) reduction in disintegration time compared to the CL grade for low-dose F6, but had no significant ( $p > 0.05$ ) impact upon the disintegration times of low-dose F5 or both high-dose formulations compared to the CL grade. The CL-SF grade only showed a significant ( $p < 0.01$ ) decrease in disintegration time compared to CL for low-dose F6 and high-dose F6. The most profound impact upon disintegration time for all formulations was seen for tablets incorporating CL-M, with some formulations pushing over 10 minutes (Figure 5.6b and Figure 5.6c).

Crospovidone is more likely to allow water ingress via capillary action, known as wicking, by providing pores within the tablet network rather than swelling (Kornblum and Stoopak, 1973). By this action, the particle size of crospovidone is likely not the rate limiting factor in disintegration times as a smaller particle size is more likely to result in a better distribution within the tablet to offset the smaller particle sizes. However, the smaller particle size will lead to an increased compressibility, as seen in the significant ( $p < 0.0001$ ) increase in hardness of both low-dose tablets (Figure 5.6a and Figure 5.6b). However, the smaller particles of crospovidone do not have a consistent impact upon the high-dose formulations, indicating that the compressibility of the APAP at 70 % (w/w) is the dominant factor in these formulations (Figure 5.6c and Figure 5.6d).

In the development of ODTs containing sumatriptan succinate, Kollidon® CL-SF was chosen as the optimised formulation as it gave faster disintegration than Kollidon® CL as well as harder tablet at 5 % (w/w) (Sheshala et al., 2011). In a study comparing Kollidon® CL and Kollidon® CL-F in directly compressed tablets, the CL grade gave the shortest disintegration times, although the SF grade gave harder tablets (Zimmer et al., 2015). In another recent study, Kollidon® CL-SF and CL-F were compared in the development of orally disintegrating loratadine formulations, with no difference observed in disintegration times, although the CL-F grade gave harder tablets, in agreement with the data presented in Figure 5.6 (Amelian et al., 2015).

Due to the increase in hardness, a reduction or no change to disintegration times, coupled with the reduced grittiness of the grade owing to the smaller particle size, the CL-F grade was chosen for incorporation in all subsequent formulations. Further analysis of comparing CL-SF versus CL-F using high-dose F5 in later studies demonstrated a reduction in disintegration times (118 s and 134 s, respectively), and was the only formulation to display this reduction in disintegration time. However, CL-F was still carried forward in order to maintain commonality amongst the formulations as well as the aforementioned increase in hardness.

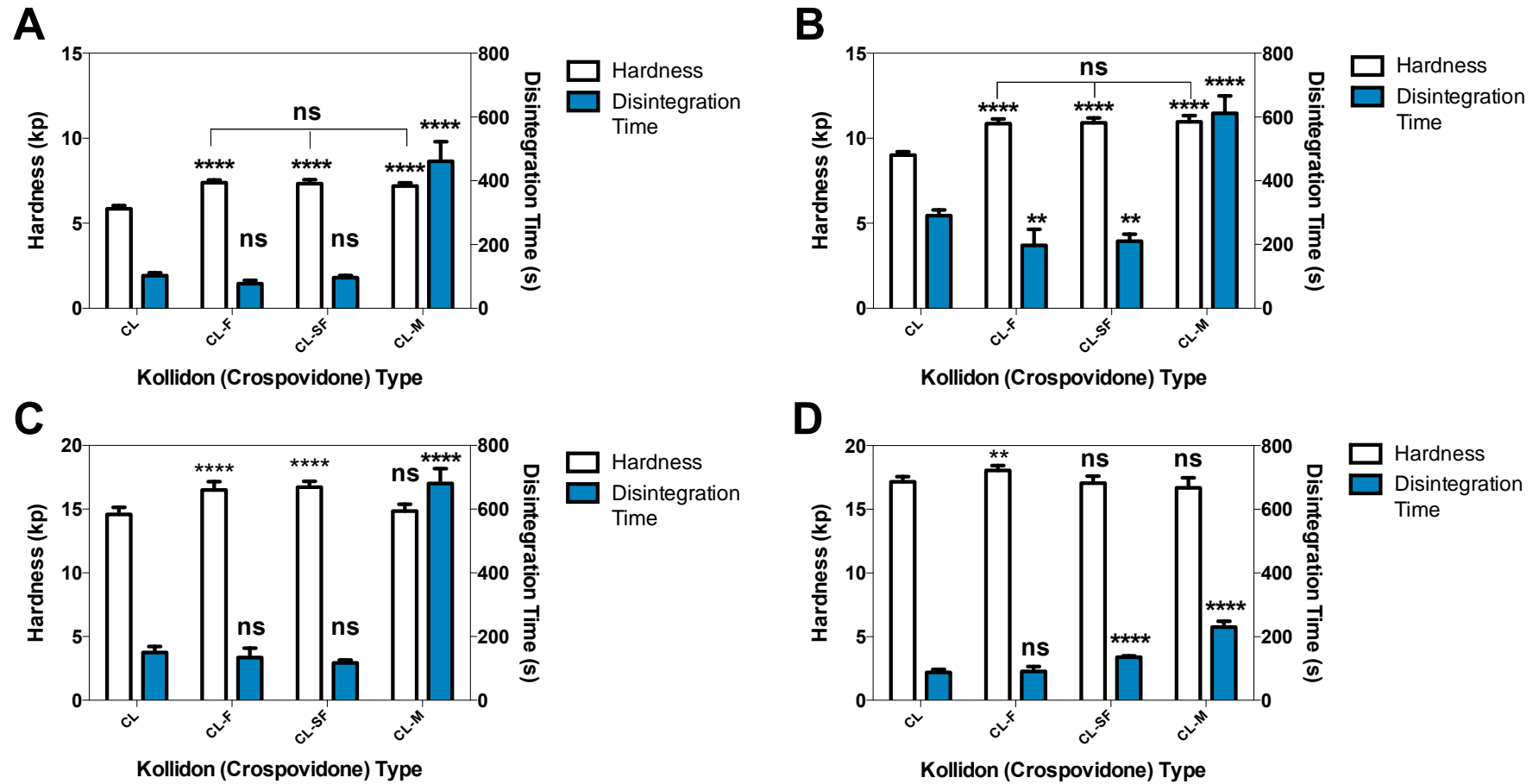


Figure 5.6. The impact changing the superdisintegrant type on A) low-dose F5, B) low-dose F6, C) high-dose F5 and D) high-dose F6, showing hardness (clear bars) and disintegration times (blue bars). Hardness and disintegration data shown as the mean from an  $n$  of 10 and 6 tablets respectively  $\pm$  SD. Statistical significance was analysed using one-way ANOVA followed by Dunnett's *post hoc* test annotated as follows: ns ( $p > 0.05$ ); \*\* ( $p < 0.01$ ); \*\*\*\* ( $p < 0.0001$ ).

#### 5.4.3. Effects of Kollidon® Crospovidone Concentration on Hardness and Disintegration

In addition to evaluating the type of crospovidone, the concentration of crospovidone was also examined up to 11 %, and the results are presented in Figure 5.7. In general, both low-dose F5 and F6 displayed both an increase in hardness and a decrease in disintegration time. For low-dose F5, a small but significant ( $p < 0.01$ ) decrease in hardness is observed at 8 % CL-F content, but this appears to be a product of batch-to-batch variation, becoming non-significant ( $p > 0.05$ ) again at 11 % CL-F content. Furthermore, low-dose F5 showed a small but significant decrease in disintegration time from 77 s to 61 s was observed at 8 % crospovidone content and above ( $p < 0.01$ ), although this does not appear to be dose dependent. For low-dose F6, hardness was increased, becoming significant ( $p < 0.0001$ ) at 11 % crospovidone. Only low-dose F6 responded well in terms of disintegration times, dropping significantly ( $p < 0.01$ ) from 198 s at 5 % crospovidone, to 137 s (at 8 %) and 92.5 (at 11 %). Both high-dose formulations responded little to increased crospovidone content, and neither exhibited a significant ( $p > 0.05$ ) impact upon disintegration, although high-dose F6 showed a significant ( $p < 0.0001$ ) decrease in hardness over the range tested (17.8 kp at 8 % crospovidone to 16.5 kp at 11% crospovidone content).

The decrease in disintegration time with increased crospovidone content is in general agreement with a previous study in which crospovidone was increased from 4 to 12 % without affecting disintegration time (Okuda et al., 2012). Only the low-dose F6 responded in a dose-dependent manner to increased superdisintegrant, which would supplement the poor tablet disintegration properties associated with a high MCC content indicated by the previous DoE study (Figure 5.2). Even with the decrease in disintegration time for low-dose F6 at 11 % crospovidone, this is still a much larger decrease in disintegration time than the equivalent low-dose F5 which did show a significant ( $p < 0.01$ ) decrease in disintegration time, but this did not appear dose dependent. For direct compression, crospovidone has been used at 2.5-8 % (w/w) (Okuda et al., 2012), 5 % (w/w) (Mishra et al., 2006) and 7 % (w/w) (Shu et al., 2002). As this material is expensive and takes up potential room within the tablet, other means were explored in order to bring disintegration times down to acceptable levels. Moreover, the poor disintegration is more likely attributed to the 10 % P407 blocking the wicking action of the crospovidone and MCC.

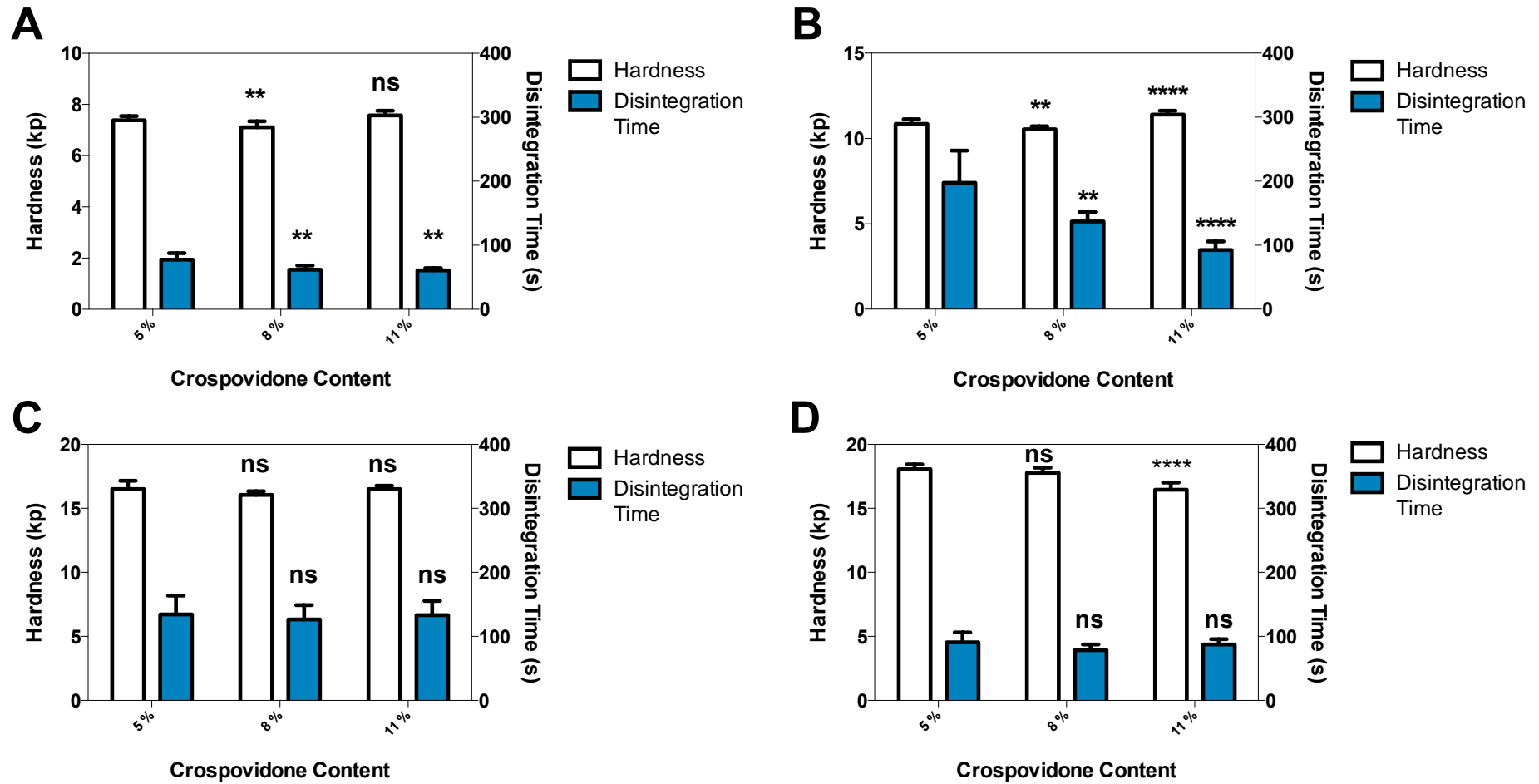


Figure 5.7. The impact changing concentration of the superdisintegrant, Kollidon CL-F, on A) low-dose F5, B) low-dose F6, C) high-dose F5 and D) high-dose F6, showing hardness (clear bars) and disintegration times (blue bars). Hardness and disintegration data shown as the mean from an  $n$  of 10 and 6 tablets respectively  $\pm$  SD. Statistical significance was analysed using one-way ANOVA followed by Dunnett's *post hoc* test annotated as follows: ns ( $p > 0.05$ ); \*\* ( $p < 0.01$ ); \*\*\*\*, ( $p < 0.0001$ ).

#### 5.4.4. Effects of Ethylcellulose Concentration on Hardness and Disintegration

Ethylcellulose is a hydrophobic polymer used in the role as a binder/filler (Figure 5.8). The role of this excipient has been evaluated in controlled release formulations of indometacin and theophylline, where the lower viscosity grades were able to produce harder tablets (Upadrashta et al., 1993). DOW produces ethylcellulose under the trade name ETHOCEL™, in grades 7 FP, 10 FP and 100 FP Premium corresponding to particle sizes 9.7, 6.1 and 41 μm. To maintain good compressibility, ETHOCEL 7 FP was chosen for incorporation as a binder for initial screening at 2.5 %, (w/w).



Figure 5.8. The schematic structure of ethylcellulose.

Due to poor disintegration times for both low-dose and high-dose formulations, the content of ethylcellulose was reevaluated for optimisation at 0-7.5 %, with the results presented in Figure 5.9. For all tablet formulations tested, a general increase in both hardness and disintegration time was observed. For both low-dose F5, an increase in hardness was seen over the range tested from 5.9 to 9.1 kp, becoming significant ( $p < 0.0001$ ) at 2.5 % ethylcellulose content versus the 0 % control, with a corresponding increase in disintegration time over the range tested from 48 s to 131 s, becoming significant at 2.5 % ethylcellulose content (Figure 5.9a). For low-dose F6, hardness increased from 9.3 to 12.7 kp over the range tested, becoming significant ( $p < 0.05$ ) at 2.5 % ethylcellulose content (Figure 5.9b). For high-dose F5, hardness increased over the range tested from 12.3 to 19.5 kp, becoming significant ( $p < 0.0001$ ) at 2.5 % ethylcellulose content, with disintegration increasing from 114 s to 180 s, becoming significant at 5 % ethylcellulose content (Figure 5.9c). Likewise, high-dose F5 showed an increase in hardness from 15.8 kp at 0 % ethylcellulose content to 19.7 kp at 10 %, becoming significant ( $p < 0.0001$ ) at 2.5 %

ethylcellulose content, with an increase in disintegration time over the range tested from 66 s to 119 s, becoming significant ( $p < 0.05$ ) at 2.5 % ethylcellulose content (Figure 5.9d).

Micronised ethylcellulose (particle size 5-10  $\mu\text{m}$ , roughly equivalent to 7 FP and 10 FP grades) has been used in orally disintegrating tablet formulations from 2.5-7.5 % (w/w), leading to a corresponding increase in hardness with a decrease in friability (Okuda et al., 2012) attributed to the increase in contact area between granules. Ethyl cellulose has been evaluated in controlled release formulation, where the lower viscosity grades were able to produce harder tablets (Upadrashta et al., 1993, Katikaneni et al., 1995b), indicating the better compressibility of the lower viscosity polymers. The mechanism of action of ethylcellulose compaction has been shown to be plastic deformation with a minor component of elasticity (Katikaneni et al., 1995a). However, the lower particle sizes have also been shown to lead to lower porosity (Upadrashta et al., 1994). Coupled with the insoluble nature of the polymer, this decrease in porosity is also likely to lead to a restriction in the access of water to the disintegrants, extending disintegration time. The results of testing ethylcellulose content in the present study are in agreement, as higher ethylcellulose content led to an increase in tablet hardness but also corresponded to an increase in disintegration time. Despite the advantages offered in hardness, the tablets appear to have adequate hardness without the addition of this excipient since disintegration is the primary focus. Therefore, this material was removed for the second round of DoE.

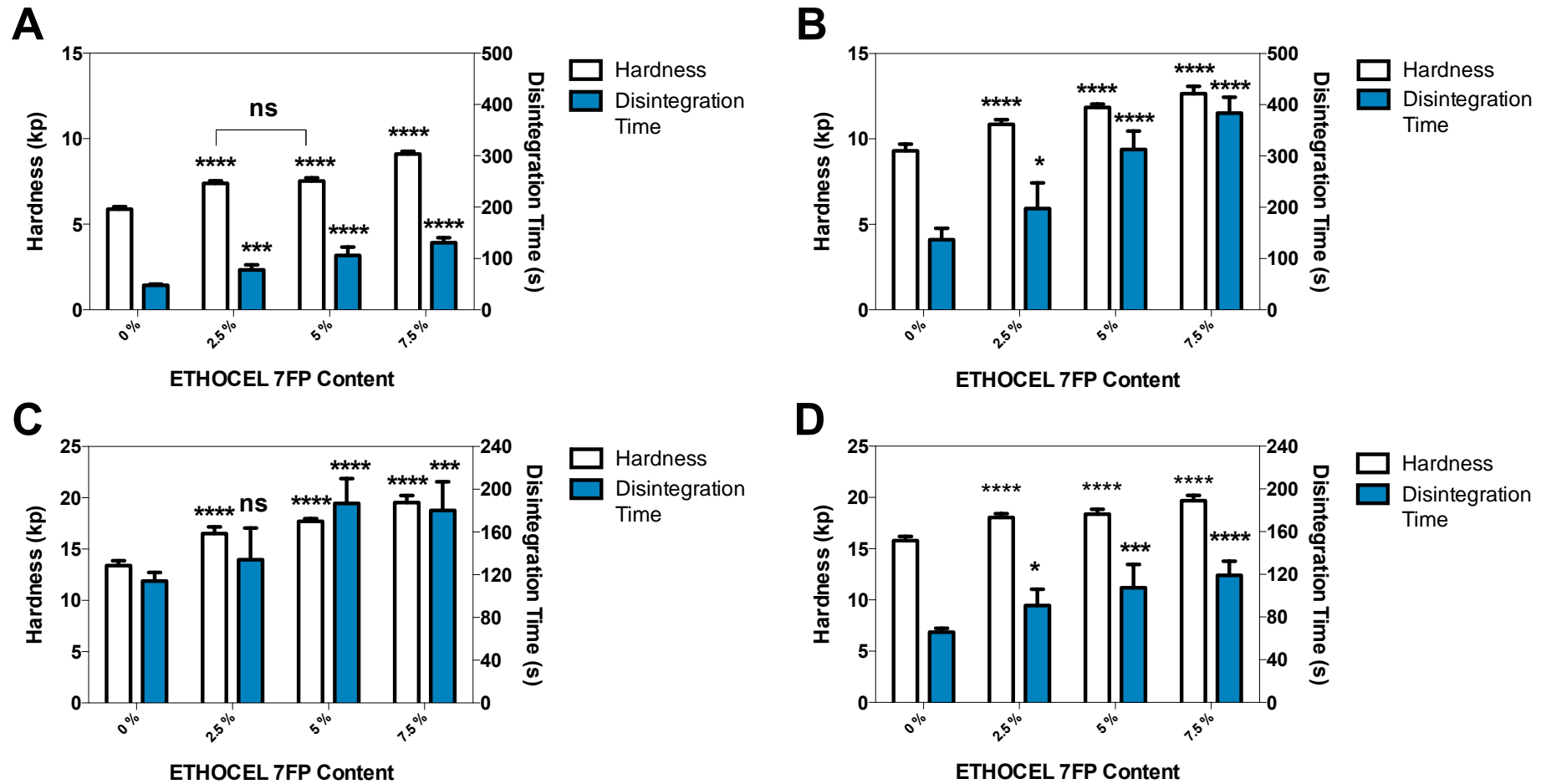


Figure 5.9 The impact of ETHOCEL 7 FP concentration on A) low-dose F5, B) low-dose F6, C) high-dose F5 and D) high-dose F6, showing hardness (clear bars) and disintegration times (blue bars). Hardness and disintegration data shown as the mean of  $n = 10$  and  $6$  tablets respectively  $\pm$  SD. Statistical significance was analysed using one-way ANOVA followed by Dunnett's *post hoc* test annotated as follows: ns ( $p > 0.05$ ); \* ( $p < 0.05$ ); \*\*\* ( $p < 0.001$ ); \*\*\*\* ( $p < 0.0001$ ).

#### 5.4.5. Effects of Binder Type and Further Optimisation

Having evaluated the composition of Starch 1500, MCC and mannitol, a second multipurpose excipient was evaluated as a replacement for Starch 1500 in the test formulations F5 and F6. Both Starch 1500 and StarCap 1500 are modified starches, but StarCap 1500 is a co-processed mixture of native starch and pregelatinised starch, which allows enhanced disintegration properties over Starch 1500. StarCap 1500 was therefore chosen for evaluation in order to address the poor disintegration times of the ODTs by utilising these superior disintegrating properties. The results of the evaluation are presented in Figure 5.10. Maintaining the 10 % P407 to make the results directly comparable to the previous Starch 1500 formulations, both low-dose formulations exhibited hardness that was significantly higher ( $p < 0.0001$ ), and disintegration times that were significantly lower ( $p < 0.001$ ) (Figure 5.10a and b). For both high-dose formulations, no significant ( $p > 0.05$ ) impact upon hardness was observed, although a decrease in disintegration time was observed for both formulations from 134 s to 82 s for high-dose F5 ( $p < 0.001$ ) and 91 s to 78 s for high-dose F6 ( $p > 0.05$ ) (Figure 5.10c and d). As such, StarCap 1500 was carried forward for subsequent formulations.

In order to explain the overall decrease in disintegration times and increased hardness using StarCap 1500, the differences between this material and Starch 1500 needs to be examined. Both StarCap 1500 and Starch 1500 have similar particle sizes (65 and 90  $\mu\text{m}$  respectively) so this cannot be used to explain the differences in hardness observed when StarCap 1500 is used. In terms of structural composition, native starch has poor binding properties but is an excellent disintegrant owing to the high amylose content, which is insoluble but swells upon contact with water. Conversely, fully gelatinised maize starch has excellent binding properties provided by the water-soluble amylopectin, but acts as a poor disintegrant. Starch 1500 is partially pregelatinised maize starch, combining intermediate properties of native and fully gelatinised maize starch. However, StarCap 1500 is a co-processed mixture of pregelatinised starch (essentially Starch 1500) and native starch, retaining more of the disintegrating properties of the latter. Additionally, Starch 1500 appears gel forming upon hydration, which most likely contradicts the wicking action of the superdisintegrant by impeding access of water. It is this reason that disks could not be used in conjunction with the disintegration testing equipment, as the tablets with high

Starch 1500 content ended up sticking. StarCap 1500 is a relatively new product to market so comparative data is difficult to find. When compared to Starch 1500, StarCap 1500 was shown to have quicker disintegration and tablet hardness in agreement with our study, with the additional advantage of having higher lubricant sensitivity (Mužíková and Eimerová, 2011).

Earlier data had shown that a P407 content of 2 % led to disintegration times comparable to 0 % P407 content (Figure 5.4). Initial screening was conducted at 10 % as an initial value, but this was always surplus to requirements and likely to change during later formulation development. StarCap 1500 in combination with 2 % P407 was examined and this led to a further reduction in disintegration time for all formulations (Figure 5.10) to 34 s and 30 s, respectively, for low-dose F5 and F6, and 61 s and 50 s for high-dose F5 and F6, significantly lower than the formulations containing Starch 1500 and 2 % P407 ( $p < 0.01$ ). Interestingly, low-dose F6 became the fastest low-dose formulation, despite previously the slowest. This change is also observed at 2 % P407 using Starch 1500 as a binder (Figure 5.10), indicating that the hydrophilic 10 % poloxamer was able to mask the properties of the disintegrants/superdisintegrants, as outlined in section 5.4.

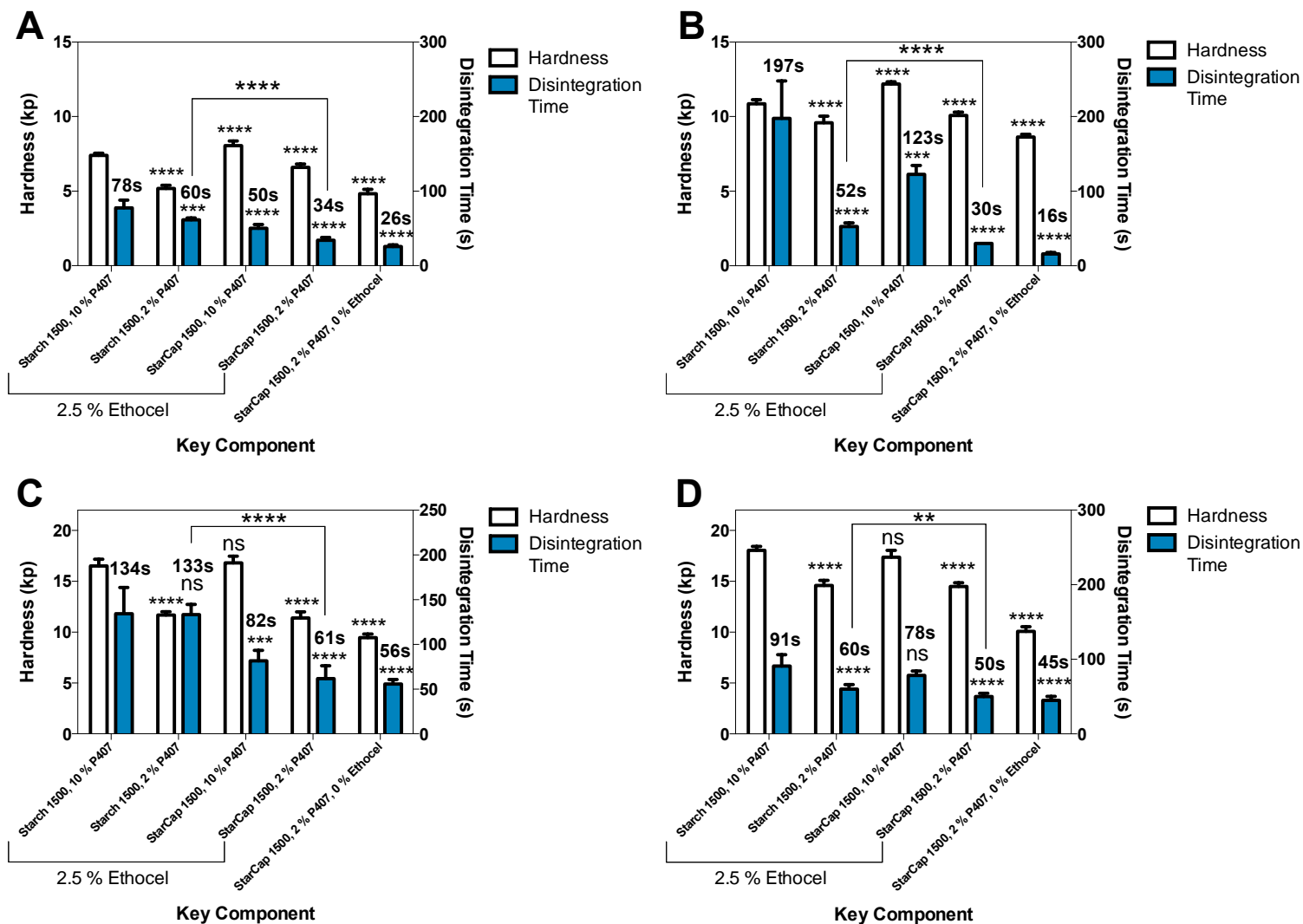


Figure 5.10. Summary of optimisation steps for A) low-dose F5, B) low-dose F6, C) high-dose F5 and D) high-dose F6, showing the conversion of the multipurpose binder, Starch 1500, to StarCap 1500, showing hardness (clear bars) and disintegration times (blue bars), in addition to optimising P407 to 2%. Hardness and disintegration data shown as the mean of  $n$  of 10 and 6 tablets respectively  $\pm$  SD with disintegration times annotated for clarity. Statistical significance was conducted by one-way ANOVA followed by Tukey's *post hoc* test. Statistical significance is annotated as follows: ns ( $p > 0.05$ ); \*\* ( $p < 0.01$ ); \*\*\*\* ( $p < 0.0001$ ).

## 5.5. Design of Experiments: Screening Round 2

The removal of ethylcellulose completely, coupled with the reduction in poloxamer content, produced ODTs with disintegration times of 16 and 45 seconds for the lead low-dose and high-dose tablets, respectively (Figure 5.10). As such, a second round of DoE screening was utilised to further refine the tablet composition by examining the impact of mannitol, MCC and StarCap 1500 on the ODT characteristics, with the latter taking the place of Starch 1500. For the low-dose, these materials now occupied 50.5 % of the tablet by weight, and the screening was set up in order to test 0-42 % of each excipient. From the previous round of DoE screening, it was found that mannitol was the only excipient to significantly ( $p < 0.05$ ) decrease disintegration time for both formulations (Table 5.4 and Table 5.5). For low-dose, disintegration time was less of a concern as the tablets were now disintegrating in less than 30 seconds. For the high-dose formulations, mannitol was screened using a higher percentage upper limit of 0-30 % (w/w), whereas MCC was examined at 0-20 % (w/w). As the impact of StarCap 1500 was unknown, it was tested in a slightly higher range of 0-23 % (w/w). From the screening outlined by JMP DoE software, 15 low-dose formulations and 14 high-dose formulations were suggested (Table 5.6).

### 5.5.1. Physical Characterisation

Hardness and disintegration data for the second round of the DoE screening is presented in Figure 5.11. The low-dose formulations produced tablets with a hardness value of 4.4- 11.9 kp, with disintegration times all of the low-dose formulations produced tablets with disintegration times of 16-29 s (Figure 5.11a). The high-dose formulations produced tablets with hardness values of 6.8-11.7 kp, although disintegration times were higher than low-dose at 36-78 s (Figure 5.11b). As such, all low-dose tablets conformed to both the *European Pharmacopeia* limit of 180 seconds for uncoated tablets (European Pharmacopeia, 2009) and to the *United States Pharmacopeia* limit of 30 seconds (McLaughlin et al., 2009). However, the high-dose tablets only conformed to the former and the 30-second target was never reached for these formulations (Figure 5.11b), with the lead high-dose formulations disintegrating at 37-38 s and 36 s seconds for F7/F8 and F13, respectively (formulations F7 and F8 are identical repeats).

Table 5.6. Low-dose and high-dose formulation compositions indicated by the second round of DoE mapping using JMP 12 DoE software to optimise MCC, Starch 1500 and mannitol content (indicating the key variables in red) within the ODT formulation.

Low-dose - 11 % Drug – 295 mg  
 80.5% MCC/StarCap 1500/Mannitol

Excipient	Composition, % (w/w)														
	F1	F2	F3	F4	F5	F6	F7	F8	F9	F10	F11	F12	F13	F14	F15
Mannitol	40.25	0.00	0.00	38.50	38.50	32.67	42.00	38.50	26.83	32.67	38.50	0.00	42.00	26.83	40.25
MCC	0.00	40.25	42.00	42.00	0.00	34.42	38.50	0.00	26.83	13.42	42.00	38.50	0.00	26.83	40.25
StarCap 1500	40.25	40.25	38.50	0.00	42.00	13.41	0.00	42.00	26.84	34.41	0.00	42.00	38.50	26.84	0.00
Poloxamer 407	2.00	2.00	2.00	2.00	2.00	2.00	2.00	2.00	2.00	2.00	2.00	2.00	2.00	2.00	2.00
Crospovidone	5.00	5.00	5.00	5.00	5.00	5.00	5.00	5.00	5.00	5.00	5.00	5.00	5.00	5.00	5.00
Glycerol Behenate	1.50	1.50	1.50	1.50	1.50	1.50	1.50	1.50	1.50	1.50	1.50	1.50	1.50	1.50	1.50
APAP	11.00	11.00	11.00	11.00	11.00	11.00	11.00	11.00	11.00	11.00	11.00	11.00	11.00	11.00	11.00
Total	100.00														

High-dose - 41 % Drug – 795 mg  
 50.5% MCC/StarCap 1500/Mannitol

Excipient	Composition, % (w/w)													
	F1	F2	F3	F4	F5	F6	F7	F8	F9	F10	F11	F12	F13	F14
Mannitol	30.00	28.75	27.50	30.00	23.75	17.50	30.00	30.00	23.75	26.88	15.63	7.50	18.75	7.50
MCC	10.00	0.00	0.00	0.00	10.00	10.00	20.00	20.00	10.00	15.00	15.00	20.00	20.00	20.00
StarCap 1500	10.50	21.75	23.00	20.50	16.75	23.00	0.50	0.50	16.75	8.62	19.87	23.00	11.75	23.00
Poloxamer 407	2.00	2.00	2.00	2.00	2.00	2.00	2.00	2.00	2.00	2.00	2.00	2.00	2.00	10.00
Crospovidone	5.00	5.00	5.00	5.00	5.00	5.00	5.00	5.00	5.00	5.00	5.00	5.00	5.00	5.00
Glycerol Behenate	1.50	1.50	1.50	1.50	1.50	1.50	1.50	1.50	1.50	1.50	1.50	1.50	1.50	1.50
APAP	41.00	41.00	41.00	41.00	41.00	41.00	41.00	41.00	41.00	41.00	41.00	41.00	41.00	41.00
Total	100.00													

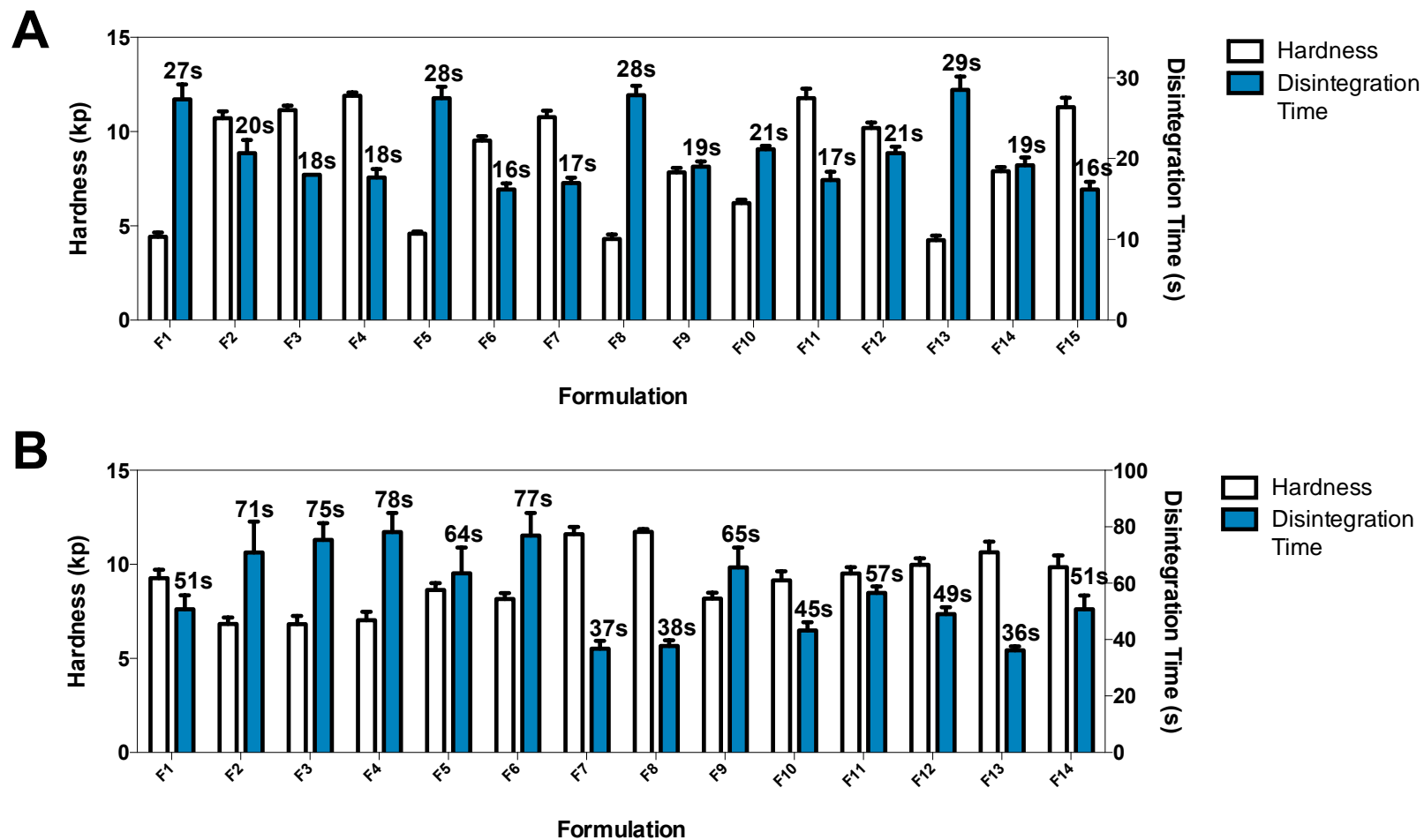


Figure 5.11. The results of the second round of DoE screening, showing tablet hardness (clear bars) and disintegration time (blue bars) for A) low-dose and B) high-dose tablets. Data presented as the mean of  $n = 10$  tablets for hardness and  $n = 6$  tablets for disintegration time  $\pm$  SD.

In order to test the robustness of the tablet formulations, friability testing was conducted according to the *United States Pharmacopeia* (USP, 2013), and the results are presented in Table 5.7. Low-dose tablet friability was found to be negligible for all low-dose formulations at 100 rotations ( $< 0.15\%$ ) and well with the 1% limit recommended by the *United States Pharmacopeia* (USP, 2013). Even using accelerated friability conditions of 500 revolutions, friability never exceeded 0.65% for all low-dose formulations. High-dose friability was higher than low-dose tablets (Table 5.7) and only formulations F7, F8, F10, F12 and F14 conformed to the recommended 1% limit recommended by the *United States Pharmacopeia* (USP, 2013).

Table 5.7. Results of friability testing of the low-dose and high-dose formulations following the second round of DoE screening, showing the percentage loss of tablet mass after 100 rotations and 400 rotations.

Formulation	Friability (%)		
	100 rpm	500 rpm	
Low-dose	1	0.10	0.54
	2	0.00	0.09
	3	0.06	0.16
	4	0.07	0.10
	5	0.08	0.40
	6	0.06	0.09
	7	0.05	0.10
	8	0.09	0.35
	9	0.08	0.21
	10	0.02	0.23
	11	0.15	0.16
	12	0.00	0.17
	13	0.13	0.65
	14	0.08	0.42
	15	0.07	0.10
High-dose	1	1.35	5.30
	2	1.82	6.66
	3	1.96	7.54
	4	1.75	6.51
	5	1.36	5.38
	6	1.32	4.99
	7	0.86	4.09
	8	0.86	3.45
	9	1.44	5.65
	10	1.04	3.99
	11	1.28	5.10
	12	0.91	2.78
	13	1.10	4.89
	14	1.06	4.18

### 5.5.2. Design of Experiments Interpretation of Data

With the formulations part optimised by the reduction in poloxamer content and the removal of ethylcellulose, a second round of screening was conducted in order to refine the tablets further, with the examination of StarCap 1500 in place of Starch 1500. The bivariate analysis of the second round of screening is presented in Figure 5.12 and Figure 5.13.

For the low-dose formulations, StarCap 1500 and mannitol decreased tablet strength whilst MCC was able to improve it (Figure 5.12a). Furthermore, MCC had almost perfect correlation with tablet strength ( $r^2 = 0.98$ ) (Table 5.8). For disintegration, higher StarCap 1500 content increased disintegration time, whereas MCC decreased it (Figure 5.12b). These effects were both significant ( $p < 0.05$ ), but the impact of mannitol was insignificant ( $p > 0.05$ ) on tablet disintegration (Table 5.8). For the high-dose formulations, StarCap 1500 and MCC led to a significant ( $p < 0.05$ ) decrease and increase respectively in tablet strength (Figure 5.13b), with MCC showing a particularly good fit to the model with  $r^2 = 0.98$  (Table 5.9). The impact of mannitol on high-dose hardness was insignificant ( $p > 0.05$ ). For high-dose formulations, higher StarCap 1500 content increased disintegration time, whereas MCC decreased it (Figure 5.13b), with  $r^2$  values of 0.55 and 0.75 respectively (Table 5.9). Mannitol once more correlated extremely poorly with disintegration time ( $r^2 = 0.01$ ), and neither was the impact significant ( $p > 0.05$ ).

For both formulations, the increased quantity of MCC led to an increase in hardness most likely attributed to its ability to undergo a unique plastic deformation during compression that occurs through enhanced hydrogen bonding to adjacent MCC particles (Al-Khattawi and Mohammed, 2013), as was also apparent for the first round of DoE screening (Figure 5.2a and Figure 5.3a). During the first round of DoE, MCC had no correlation with disintegration times with  $r^2$  values of 0.3 and 0.0 respectively for low-dose and high-dose formulations (Table 5.4 and Table 5.5). For the second round of DoE, MCC now correlated well for both formulations ( $r^2 \geq 0.85$ ), with decreasing disintegration times confirming the data presented in Figure 5.6 that poloxamer 407 was able to block the wicking action of the disintegrants when used at 10 % (w/w) (Kaul et al., 2011), allowing the wicking action of MCC to become a dominant factor. For both formulations, StarCap 1500 led to a decrease in hardness and an increase in disintegration time (Figure 5.12b and Figure 5.13b). Although

an improvement over Starch 1500, the plastic deformation of starch is a slow process meaning quick compression is insufficient in producing strong interparticle bonds during plastic deformation, and the deformation is largely elastic (Rees and Rue, 1978). The increased disintegration time associated with this material most likely corresponds to gel forming of the material upon hydration. Mannitol had no impact upon hardness for either formulation (Figure 5.12a and Figure 5.13a,  $r^2 > 0.05$ ). For both low-dose and high-dose formulations, increasing mannitol content had no impact ( $p < 0.05$ ) upon disintegration time (Figure 5.12b and Figure 5.13b). This is unlike the first round of DoE where mannitol significantly ( $p < 0.05$ ) decreased disintegration times for both formulations (Figure 5.2a and Figure 5.3a). As this was attributed to the wetting properties of the material (Kubo and Mizobe, 1997), removing the ethylcellulose and decreasing the poloxamer content down to 2 % (w/w) has likely achieved optimum wettability beyond that which mannitol is capable of achieving.

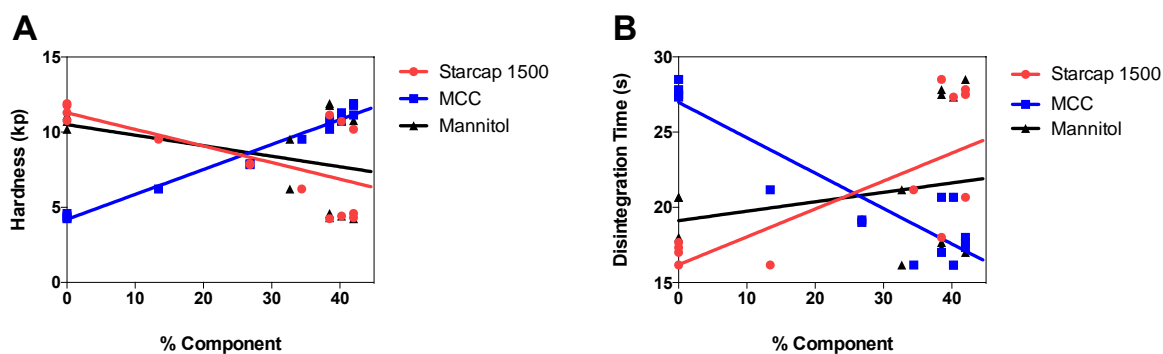


Figure 5.12. Design of experiments trace plots for low-dose formulations showing A) hardness and B) disintegration, showing the impact of StarCap 1500 (red), MCC (blue) and mannitol (black).

Table 5.8. Summary of the model statistics on the impact of the test excipients on hardness and disintegration on the low-dose formulations from the second round of DoE screening.

	<i>Factor</i>	$r^2$	<i>F ratio</i>	<i>Prob &gt; F</i>
Hardness	StarCap 1500	0.43	9.87	0.0078
	MCC	0.98	544.34	0.0001
	Mannitol	0.14	2.08	0.1725
Disintegration	Starch 1500	0.53	14.46	0.0022
	MCC	0.85	71.97	0.0001
	Mannitol	0.05	0.65	0.4342

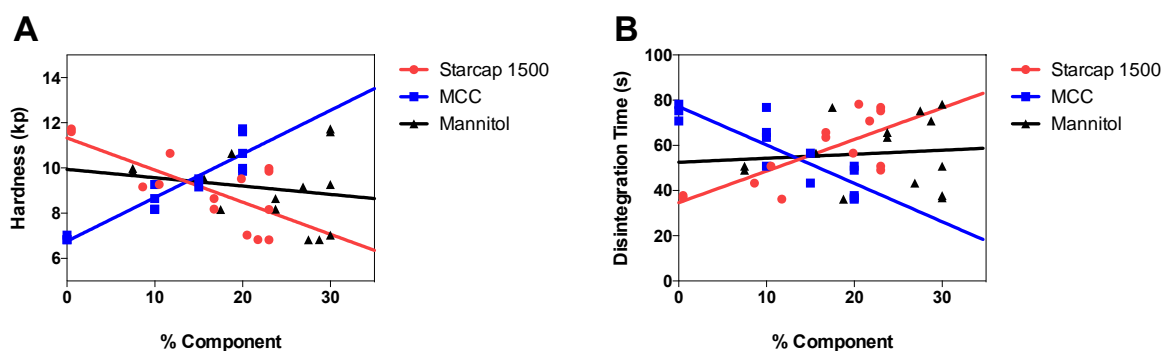


Figure 5.13. Design of experiments trace plots for high-dose formulations showing A) hardness and B) disintegration, showing the impact of StarCap 1500 (red), MCC (blue) and mannitol (black).

Table 5.9. Summary of the model statistics on the impact of the test excipients on hardness and disintegration on the high-dose formulations from the second round of DoE screening.

	<i>Factor</i>	$r^2$	<i>F ratio</i>	<i>Prob &gt; F</i>
Hardness	StarCap 1500	0.51	12.38	0.0042
	MCC	0.87	79.46	0.0001
	Mannitol	0.03	0.43	0.5264
Disintegration	StarCap 1500	0.55	14.51	0.0025
	MCC	0.75	36.04	0.0001
	Mannitol	0.01	0.11	0.7486

In general, all low-dose formulations at this stage of development could be classed as a potential marketable product; disintegration time is below 30 seconds, and hardness and friability data is within usable limits in order to withstand the stress of further unit processing, such as film coating and packaging. For the high-dose tablets, the decision was made to stop development after the second round of screening and pursue the low-dose

formulations for rotary press production. At the most advanced level of development, the lead formulation high-dose tablets, F13 had a disintegration time of 36 s and a hardness value of 10.7 kp (Figure 5.11b).

### 5.6. Scale-up Manufacture using the Rotary Tablet Press

Scale-up is an essential part of the transformation of a formula to a viable commercial product in the pharmaceutical industry. This phase can identify problems in the process such as unreproducible compressibility and lack of uniformity that may be problematic in the larger production cycle. In order to test the scale-up capability of the tablets, three formulations were selected for rotary trial using a Picolla multi-station press. The previous formulation F9, the theoretical centre point of the DoE design in which all excipients were at the same content, was modified according to Table 5.10. Formulation 1 is identical to the previous Formulation 9 from the second round of DoE (Table 5.6). This is accompanied by Formulation 2 containing 50 % more StarCap 1500 as a multipurpose binder and Formulation 3 containing 50 % more mannitol. The modified Formulation 2 (F2) and Formulation 3 (F3) were chosen to assess the impact of the multipurpose binder on the automated tableting press and to boost the concentration of mannitol to increase the potential palatability of the dosage formulation, respectively.

Table 5.10. The composition of the final formulations chosen for production of the Picolla rotary tablet press indicating the key variables (red).

<i>Excipient</i>	<i>Composition, % (w/w)</i>		
	<i>F1</i>	<i>F2</i>	<i>F3</i>
Mannitol	26.83	26.83	33.54
MCC	26.83	13.42	33.54
StarCap 1500	26.84	40.26	13.42
Poloxamer 407	2.00	2.00	2.00
Crospovidone	5.00	5.00	5.00
Glycerol Behenate	1.50	1.50	1.50
APAP	11.00	11.00	11.00

### 5.6.1. Physical Characterisation

The formations shown in Table 5.10 were first produced via manual compression on the Atlas A5 in order to compare single and rotary press data. The results are presented in Figure 5.14. Compared to F1, which has a hardness value of 7.9 kp, F2 and F3 have significantly ( $p > 0.0001$ ) different hardness values of 5.4 kp and 9.4 kp, respectively. Interestingly, disintegration times have the opposite effect, F1 showed a disintegration time of 19s, which increased to 23s for F2, and decreased to 16s for F3.

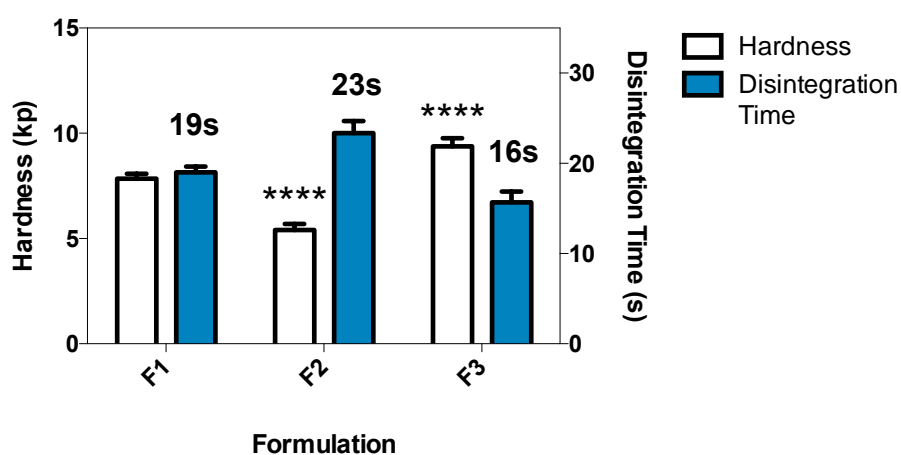


Figure 5.14. The formulations shown in Table 5.10 made by direct compression, showing tablet hardness (clear bars) and disintegration time (blue bars). Data presented as mean  $\pm$  SD from  $n = 10$  tablets for hardness and 6 tablets for disintegration time  $\pm$  SD. Statistical significance was calculated using one-way ANOVA with Dunnett's *post hoc* test, annotated as follows: \*\*\*\* ( $p < 0.0001$ ).

The 10-station rotary press was equipped with 5 convex 10 mm die, with the remaining stations fitted with a blank die to reduce overall production rates. Of the die fitted, 4 were of normal convex curvature and one was equipped with an embossed Colorcon brand. The latter die was noticed to be of a different diameter during the first run, and was unable to correctly press embossed tablets. This impacted the main compression force of all of the stations since the computer interface takes an average reading over all 5 stations. Due to the limited availability of the equipment and the large amount of time it would take to replace the defective station, the remaining tablets were intentionally produced at 6, 12, 18 and 22 kN compression force, rather than the intended 5, 10, 15 and 20 kN. As such, the compression force was approximately 25 % higher accounting for the ineffective station.

The hardness and disintegration times for the tablets produced by the rotary press are presented in Figure 5.15. Over the compression range tested, the differences in hardness are statistically well defined. At each level of compression, F3 is statistically ( $p < 0.001$ ) harder than F1 at each compression level. For disintegration, F3 was significantly ( $p < 0.0001$ ) faster at disintegrating at 6 kN and 12 kN than F2 except at 18 kN ( $p > 0.05$ ), and significantly ( $p < 0.001$ ) slower at 23 kN. Compared to F1, F3 was significantly faster at disintegrating at 12 kN and 18 kN, but statistically similar at the remaining compression forces ( $p > 0.05$ ). In general, F3 had the fastest disintegration times at 6-18 kN with disintegration times of 9 s, 15 s and 28 s, respectively, but at the highest compression (23 kN), F2 disintegrated the quickest at 31 s.

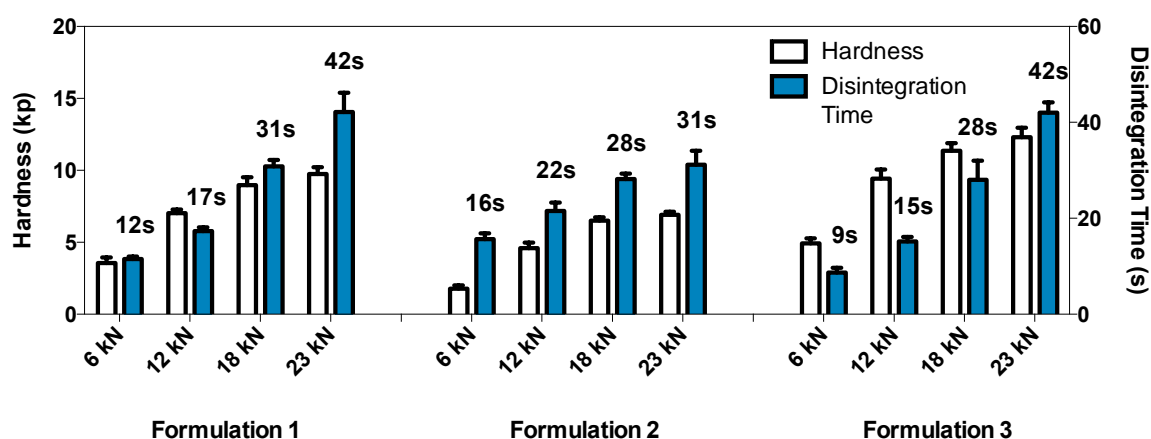


Figure 5.15. The results of the physical characterisation of tablets produced by the rotary tablet press, showing tablet hardness (clear bars) and disintegration time (blue bars). Data presented as the mean of  $n = 10$  tablets for hardness and  $n = 6$  tablets for disintegration time  $\pm$  SD.

For friability, all tablets were well within the 1 % limit recommended by the *United States Pharmacopeia* (USP, 2013) with values of 0.05-0.59 % loss, and substantial damage was only observed under accelerated friability stress conditions of 500 rotations (Table 5.11), although most tablet formulations still conformed at or close to the 1 % recommended limit under these conditions.

Table 5.11. The percentage weight loss of tablets produced by the rotary press, showing normal friability (100 rotations) and accelerated friability (500 rotations).

<i>Formulation</i>	<i>Compression (kN)</i>	<i>Friability (%)</i>	
		<i>100 rotations</i>	<i>500 rotations</i>
Formulation 1	6	0.29	1.79
	12	0.13	0.67
	18	0.13	0.65
	23	0.05	0.46
Formulation 2	6	0.59	4.58
	12	0.48	1.03
	18	0.14	0.83
	23	0.05	0.66
Formulation 3	6	0.13	1.06
	12	0.04	0.49
	18	0.10	0.49
	23	0.05	0.41

The rotary software has the added advantage of providing a plethora of information for the compression and ejection forces on each of the turret-fitted die, giving a greater interpretation of data than is possible on a single manual compression press. The impact of compression force on the physical characteristics of the tablets is presented in Figure 5.16.

The relationship between compression and ejection force is shown in Figure 5.16a. High ejection forces can result in tablet defects such as capping and lamination. The data shows that F3 has the highest ejection force of the formulation tested, followed by F1 and then F2, following the rank order of StarCap 1500 composition (F2>F1>F3), indicating that StarCap 1500 has superior lubricating properties to both mannitol and MCC. Starches have long been known to have lubricating properties (Jarosz and Parrott, 1984), and StarCap 1500 has been shown to increase sensitivity of the presence of the lubricant (Mužíková and Eimerová, 2011). The high lubricant sensitivity of starches is due to the compaction mechanism of plastic deformation (Jarosz and Parrott, 1984). In a study on a range of compressible powders, Starch 1500 and StarCap 1500 were shown to be highly plastic deforming (Li et al., 2013b).

The compactibility curves of the formulations are presented in Figure 5.16b. Hardness increases as a function of compression, however it can also be seen that hardness decreases

in the order  $F3 > F1 > F2$ . This rank order corresponds to the increasing concentrations of MCC in the formulations, and/or the decreasing StarCap 1500 content in agreement with the results of the second round of DoE screening (Figure 5.12).

Disintegration times as a function of compressibility are presented in Figure 5.16c. Disintegration time increases with increased compression, although interestingly F2 appears linear over the compression range tested suggesting that StarCap 1500, the main constituent material of F2, is able to maintain a wicking effect even after increased compression, whereas F2 had the lowest compression at 23 kN, both F1 and F3 had the fastest disintegration times at the remaining compression forces.

The effects of compression on friability are presented in Figure 5.16d. Friability decreases with increased compression force, and all formulations converged to almost 0 % friability at 23 kN. At low compression (5 kN), F3 shows the lowest percentage friability followed by F1 and F2, corresponding to a decrease in MCC content and/or an increase in StarCap 1500 content

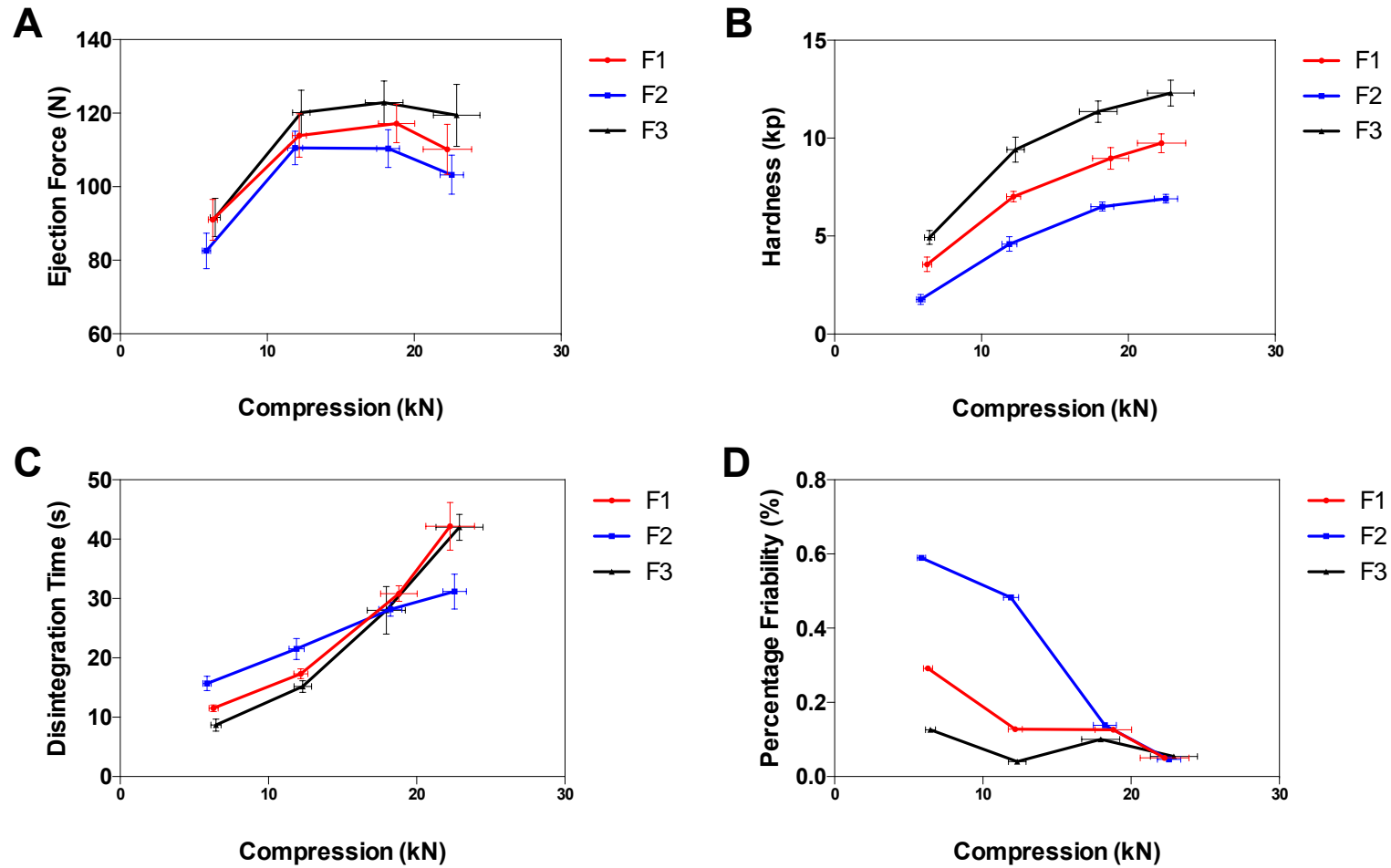


Figure 5.16. The results of the impact of compression force on range of physical tablet attributes, showing A) ejection force, B) hardness, C) disintegration time and D) friability. Data presented as the mean of  $n = 10$  tablets for hardness and friability and  $n = 6$  tablets for disintegration time  $\pm$  SD.

### 5.6.2. Weight Variation

Weight variation for tablets must conform to the following specifications according to the *United States Pharmacopeia* (USP, 2011):

- All 10 tablets tested must fall within  $\pm 15\%$  of the mean.
- RSD must be below 6 % of the mean.

Weight variation for all formulations is presented in Table 5.12. All formulations over a range of compressions, and the RSD did not exceed 1.8 % for all formulation.

Table 5.12. The weight variation data of tablets produced using the rotary press. Data presented from 10 tablets per formulation.

<i>Formulation</i>	<i>Compression (kN)</i>	<i>Average Weight (mg)</i>	<i>Standard Deviation</i>	<i>RSD (%)</i>
Formulation 1	6	296.48	2.78	0.94
	12	298.64	2.25	0.76
	18	300.72	3.77	1.25
	23	303.87	4.62	1.52
Formulation 2	6	301.13	2.77	0.92
	12	296.74	5.20	1.75
	18	303.24	2.83	0.93
	23	303.01	2.41	0.80
Formulation 3	6	293.24	2.60	0.89
	12	298.56	2.43	0.81
	18	301.16	3.34	1.11
	23	302.91	4.97	1.64

### 5.7. Evaluation of Over the Counter Orally Disintegrating Tablets

In order to compare the ODTs of APAP to known established products, three marketed formulations were tested in parallel to both the high and low-dose tablets. These were Nurofen® Meltlets, Calpol® SixPlus and Imodium instants® (Figure 5.17).



Figure 5.17. Marketed products used for comparative study, showing the biconcave shape of A) Calpol SixPlus and B) Nurofen Meltlets produced via direct compression and C) the flat faced, lyophilised Imodium Instants, and their respective unbroken blister packs.

Nurofen<sup>®</sup> Meltlets and Calpol<sup>®</sup> SixPlus tablets were both biconcave with rounded edges, whereas Imodium Instants<sup>®</sup> were small and flat faced (Figure 5.17). Both the Nurofen<sup>®</sup> Meltlets and Calpol<sup>®</sup> SixPlus tablets appear to be made by direct compression owing to the presence of magnesium stearate in the formulations. Imodium Instants are made via lyophilisation by pouring the mixture directly into blister packs. The OTC hardness and disintegration data is presented in Figure 5.18. The Nurofen<sup>®</sup> Meltlets and Calpol<sup>®</sup> SixPlus had hardness values of 6.1 kp and 5.3 kp, respectively, whereas the Instants were thin and fragile, and produced no detectable hardness value. The Meltlets had a disintegration time of 17.7s, and the Fastmelts has a disintegration time of 9.8s. For the Imodium Instants<sup>®</sup>, no disintegration time was recorded as the tablet dissolved instantly upon contact with water.

When compared to the lead low-dose and high-dose APAP formulations produced during the second round of DoE screening (low-dose F15 and high-dose F13 shown in Figure 5.11b), the marketed products display lower hardness values (Figure 5.18). For all three OTC products, the patient instructions state to break the foil lining of the blister pack prior to pushing the tablets out of the packet to prevent the tablet breaking. Therefore, the OTC

products demonstrate the feasibility of producing an ODT with excellent disintegration properties at the expense of poor hardness as this can be addressed with appropriate packaging. The current high-dose tablets developed in the present study are harder than the marketed OTCs for a similar drug loading – 250 mg paracetamol for Calpol® SixPlus (5.3 kp) and 325 mg paracetamol for the APAP high-dose formulations (10.7 kp).

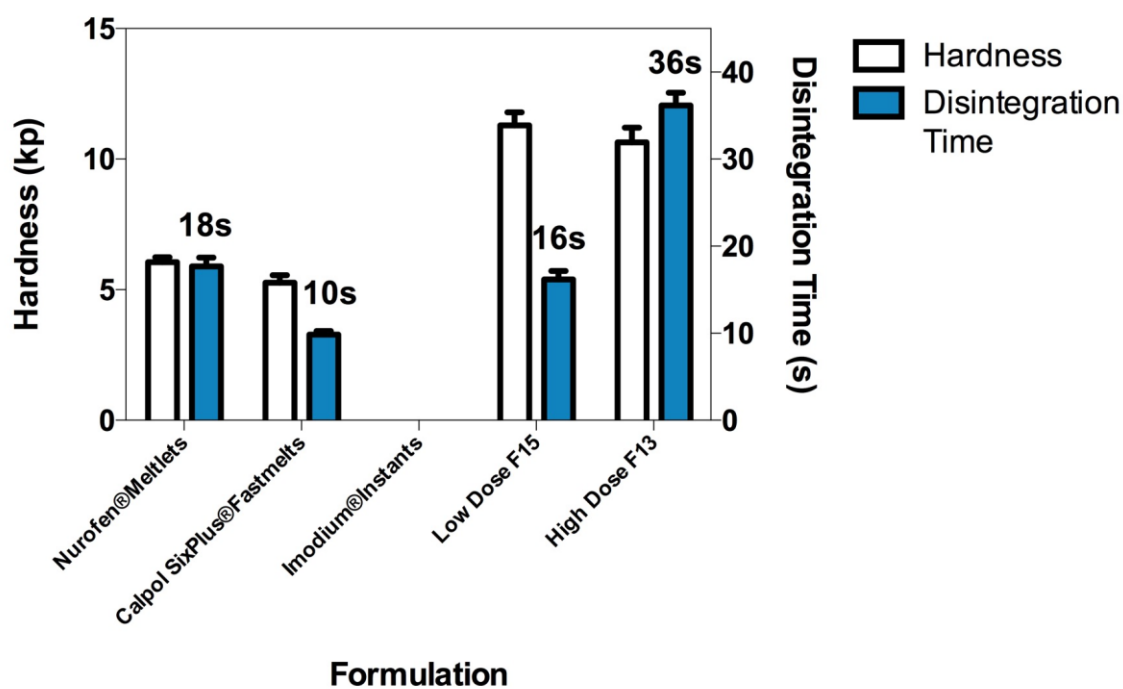


Figure 5.18 The hardness and disintegration times of OTC formulations. Data shown as the mean of  $n = 3$  tablets for disintegration and  $n = 3$  tablets for hardness,  $\pm$  SD. For Imodium® Instants, disintegration time was instantaneous upon contact with water. Likewise hardness was too low to be detected. OTC data is shown in comparison to the fastest disintegrating low-dose and high-dose tablets, F15 and F13 respectively, from the second round of DoE screening (shown in Figure 5.11) where data is presented as the mean of  $n = 6$  tablets for disintegration time  $n = 10$  tablets for hardness,  $\pm$  SD.

The lead formulation of the final development of the high-dose APAP after the second round of DoE screening, F13, had a disintegration time of 36 s and a hardness of 10.7 kp (Figure 5.18). The OTC Calpol® SixPlus, an ODT of identical weight to our high-dose tablets at 795 mg, and with comparable drug loading (325 mg for F13 and 250 mg for the Calpol® SixPlus), had a hardness of 5.3 kp with a disintegration time of 10 s (Figure 5.18), much faster than those which we were able to achieve. However, for the low-dose tablets, the rotary press provided a number of formulations with disintegration times less than 30 s. The rotary press Formulation 3 was able to disintegrate in 15 s when compressed at 12 kN,

with a hardness of 9.4 kp (Figure 5.15). Moreover, this same formulation provided tablets with disintegration times of 9 s when compressed at 5 kN, with a hardness of 4.9 kp similar in strength to that of Calpol® SixPlus.

### **5.8. Conclusions of Tablet Design and Manufacture**

The work in this chapter describes the development of two ODT formulations incorporating 2 % (w/w) poloxamer 407 as ABCB1 efflux transporter modulating excipient. At the end phase of development, tablets manufactured using a rotary tablet press had disintegration times below 30 seconds, conforming to *United States Pharmacopeia* specification. Any of these formulations, taken with a 250 mL glass of water on an empty stomach, are capable of delivering 5.9 mg of poloxamer 407 to give a final concentration of  $2.36 \times 10^{-3}$  % (w/v), or 2.7 times higher than the  $IC_{50}$ . All three of the final formulations made by rotary press conform to the *United States Pharmacopeia* specifications for disintegration in under 30 seconds at 12 kN compression, F2 and F3 also conform at 18 kN with F1 falling just outside this limit with a disintegration time of 31 seconds.

## **Chapter 6**

An Investigation into the Incorporation of Biologically-Active Surfactants into Ibuprofen Granule Coatings for the use in Directly Compressed ODTs

## 6. An Investigation into the Incorporation of Biologically-Active Surfactants into Ibuprofen Granule Coatings for the use in Directly Compressed

### 6.1. Introduction

In the previous chapter, ODT tablets were produced by direct compression containing 2 % (w/w) poloxamer 407, which was selected due to the high efficacy against the ABCB1 efflux transporter system. In order to widen the application of the excipients with inhibition properties found during screening in Chapter 4, a number of excipients were chosen for evaluation as constituents of granule coatings. Direct processing of drug particles by coatings have been used to improve the properties of the powders, such as improving flowability (Ehlers et al., 2009, Genina et al., 2010), or taste masking (Hamashita et al., 2007). Ibuprofen is known for its high degree of cohesion, resulting in poor flow properties as well as bad compaction (Rasenack and Müller, 2002), in addition to having a bitter taste (Gryczke et al., 2011). Therefore, ibuprofen is an excellent candidate for coating trials.

The aim of the work presented in this chapter was to evaluate the suitability of incorporating biologically active surfactants found to have kinetic activity against efflux transporters as coating agents alongside Kollicoat IR, and to study the impact of these coatings on the powder flow and the physical characteristics of the ODTs produced using the coated granules. The surfactants of interest were PEG 2000, poloxamer 407 (ABCB1  $IC_{50} = 8.85 \times 10^{-4}$ ), and Cremophor EL (PEG 40 Castor Oil) similar to the Etocas excipients that showed efficacy for both ABCB1 and ABCC2 (ABCB1  $IC_{50} = 3.80 \times 10^{-3}$ , ABCC2  $IC_{50} = 3.49 \times 10^{-3}$ ). Cremophor EL offered the additional challenge of being the only liquid used for formulation studies.

Kollicoat IR<sup>®</sup> is a polyvinyl alcohol-polyethylene glycol graft copolymer which has been specifically formulated for the purpose of tablet coating (Figure 6.1). As a non-ionic hydrophilic polymer, Kollicoat IR has the advantage of being equally soluble throughout the gastro-intestinal tract. This polymer has also been shown to reduce surface tension of water (Kolter et al., 2002).



Figure 6.1. The chemical structure of the polyvinyl alcohol-polyethylene glycol copolymer Kollicoat IR.

In order to evaluate the additional impact of surfactants in granule coatings, particles were made by wet granulation according to the composition of Table 6.1, and the resulting granules were then coated using Kollicoat IR or Kollicoat IR with 2 % (w/w) surfactant as outlined in Table 6.2.

Table 6.1. Formulation composition of ODTs used in coating trials.

<i>Excipient</i>	<i>Percentage Content (%)</i>	<i>Mass (g)</i>
Starch 1500	8.68	10.42
MCC	17.37	20.84
Mannitol	28.95	34.74
Crospovidone	4.50	5.40
Magnesium stearate	0.50	0.60
Ibuprofen	40.00	48.00
Total	100.00	120

Table 6.2. Nomenclature of Kollicoat IR dispersions.

<i>Coating dispersions</i>	<i>Name</i>
Uncoated	C0
10 % (w/v) Kollicoat IR	C1
10 % (w/v) Kollicoat IR + 2 % (w/v) PEG 2000	C2
10 % (w/v) Kollicoat IR + 2 % (w/v) Poloxamer 407	C3
10 % (w/v) Kollicoat IR + 2 % (w/v) Cremophor EL	C4

## 6.2. Evaluation of Flow Properties of Surfactant-Coated Granules

The flow properties of a powder during manufacturing can impact the quality of the finished product during pharmaceutical processing. Powder must flow easily and in a uniform manner to fill the die and to ensure uniformity of content and reproducibility within the tablet production cycle, as poor flow properties are associated with difficulties with filling and compression (Räsänen et al., 2003). Powder flow can be regarded as a multi-faceted process, influenced by particle size and size distribution, shape and moisture content, amongst others (Li et al., 2004). Due to this complexity, multiple methods of determining and classifying powder flowability have been developed as outlined in Table 6.3. As such, the coated granules were subjected a number of flowability tests, presented in Table 6.4.

Powder bulk density, defined as the ratio of mass of untapped powder over volume, and tapped density, the increase in bulk density after mechanical tapping, are simplistic measures of powder flow based on the intrinsic density of the powders (USP, 2012a). All coated granules showed significantly ( $p > 0.01$ ) higher bulk density measurements than that of the uncoated granules (C1), in addition, all coated granules showed a significantly ( $p > 0.001$ ) higher tapped density than that of the uncoated granules (Table 6.4). In contrast, the angle of repose showed no significant ( $p < 0.05$ ) difference between coated and uncoated granules (Table 6.4). However, these granules are categorically different according to this measure, with the granules made from formulation C2 showing 'excellent' flow properties, C3 and C1 showing 'good' flow properties, and C4 demonstrating 'fair' flow properties. According the Carr's Index data, only coating C3 containing 2 % poloxamer 407 showed any significant ( $p > 0.05$ ) difference compared to that of the uncoated granules. As a Carr's index value below 25 indicates excellent flow properties (Carr, 1965), all granules fall into the 'good' to 'excellent' category with the exception of C3 (Table 6.4). Likewise, C3 also showed a significant ( $p > 0.05$ ) increase according to the Hausner ratio, defined as the ratio between tapped and bulk density of powders, in relation to the other surfactant-coated granules. A Hausner ratio value below 1.25 indicates good powder flow characteristics (Abdullah and Geldart, 1999). As such, all granules demonstrated 'good' flowability with the exception of C3 which was characterised as 'fair' (Table 6.4). Granules coated with Cremophor EL (C4) showed the lowest values for both indicators out of all of the coatings tested.

As powder flow is a complicated process, many of the methods of determining the flow properties are subjective. In reflection of this, multiple methods were used to determine the flow properties of the coated and surfactant-coated granules. The angle of repose measures the internal friction or cohesion of the particles (Fahmy and Kassem, 2008), and according to this measure, formulation C4, containing Cremophor EL, showed the poorest flow properties of all the formulations tested, whereas Carr's index and the Hausner ratio determined C4 to have the best flow properties (Table 6.4). These latter two forms of measurement are based on the compressibility of the materials, whereby a higher coefficient of internal friction is associated with higher values (Chan and Page, 1997), whereas the angle of repose is based on the internal friction or cohesion of the particles (Fahmy and Kassem, 2008). The differences between the rank order of the granule flowability obtained from the angle of repose measure ( $C2 > C3 > C0 > C4$ ) versus Carr's Index and the Hausner ratio ( $C4 > C0 > C2 > C3$ ) are likely attributed to the subjective nature of the former. Despite its ease of use, the angle of repose is often considered as only a guide to powder flow characteristics, since it is subjective to the user and the initial experimental conditions, and is not an intrinsic property of the powder (Nagel and Peck, 2003). The angle of repose can vary depending upon the nature of the powder base which can influence cone morphology, and falling powder can add distortions in the cone peak (Taylor et al., 2000). As such, Carr's Index and the Hausner ratio are more widely considered as acceptable methods of measuring powder flowability. According to these two measures, granules coated with formulation C4 (Cremophor EL) showed the greatest flow properties. As the only liquid excipient tested amongst the three surfactants, Cremophor EL formed a visibly more viscous coating solution. In relation to the less viscous solutions of PEG 2000 and poloxamer 407, the coating containing Cremophor EL may have led to an increase in granule size. This could have led to a corresponding increase in flowability by overcoming the Van der Waals forces which restrict the flowability of smaller particles (Heim et al., 1999). In addition to particle size, the flowability of the granules is similar to the rank order of the moisture content for the surfactant-coated granules. Therefore, the poorer flowability of C2 and C3 compared to C4 and the uncoated powder is most likely attributed to the higher moisture content, which has been implicated in decreasing the flow properties by increasing interparticle interactions (Sun, 2016) and/or increasing the number of interactions by shortening the distance between particles (Coelho

and Harnby, 1978). Despite this, all powders showed appropriate flow properties and would perform well during pharmaceutical unit processing without arching in the hopper.

Table 6.3. The classification of powder flow based on angle of repose, Carr's Index and Hausner Ratio.

	<i>Angle of Repose (<math>\theta</math>)</i>	<i>Carr's Index (%)</i>	<i>Hausner Ratio</i>
Excellent	25-30	5-12	1.00-1.11
Good	31-35	12-16	1.12-1.18
Fair - aid not needed	36-40	18-21	1.19-1.25
Passable - may hang up	41-45	23-35	1.26-1.34
Poor - must agitate	46-66		1.35-1.45
Very Poor	56-65	33-38	1.46-1.59
Very, very poor	> 66	> 40	> 1.60

Table 6.4. The powder flow properties of the ODT formulations. Results are presented as mean  $\pm$  SD from  $n = 3$ , except moisture content.

<i>Coating solutions</i>	<i>Bulk density</i>	<i>Tapped density</i>	<i>Angle of repose (<math>\theta</math>)</i>	<i>Carr's index (%)</i>	<i>Hausner ratio</i>	<i>Moisture content (%)</i>
C0 – Uncoated	0.43 $\pm$ 0.01	0.49 $\pm$ 0.01	33.04 $\pm$ 1.50	12.24 $\pm$ 4.90	1.14 $\pm$ 0.06	7.20
C2 – 2 % (w/v) PEG 2000	0.49 $\pm$ 0.01	0.58 $\pm$ 0.02	30.62 $\pm$ 2.36	15.52 $\pm$ 5.00	1.18 $\pm$ 0.07	9.40
C3 – 2 % (w/v) Poloxamer 407	0.46 $\pm$ 0.01	0.60 $\pm$ 0.02	31.35 $\pm$ 0.44	23.33 $\pm$ 4.12	1.30 $\pm$ 0.07	10.50
C4 – 2 % (w/v) Cremophor EL	0.53 $\pm$ 0.00	0.58 $\pm$ 0.02	35.17 $\pm$ 0.61	8.62 $\pm$ 3.07	1.09 $\pm$ 0.04	8.10

### 6.3. Evaluation ODTs Produced using of Surfactant-Coated Granules

In order to evaluate the impact of the surfactant-coated granules on the ODT physical characteristics, the powders C2-C4 were compressed to form 500 mg tablets using 1 ton compression, and the tablet characteristics data is presented in Table 6.5. All surfactant-containing formulations showed a significantly ( $p < 0.05$ ) lower disintegration and hardness value compared to C1 (Kollicoat IR-only coating), alongside lower friability. Of the tablets made from the surfactant-coated granules, formulation C4 containing 2 % Cremophor EL showed the lowest friability at 2.19 %, followed by C3 (2 % poloxamer 407) and C2 (2 % PEG 2000) at 2.53 % and 3.62 %, respectively (Table 6.5). Between the surfactant-coated formulations, C4 produced the hardest tablets at 28.1 N, although hardness for all of these tablets was statistically similar ( $p > 0.05$ ). All formulations displayed disintegration times conforming to the *United States Pharmacopeia* limit of 30 seconds (McLaughlin et al., 2009, USP, 2013) (Table 6.5), with no significant ( $p > 0.05$ ) difference between all disintegration times.

The significantly lower disintegration times and hardness of the surfactant-containing formulations compared to the C1 (Kollicoat IR-only coated) formulations is most likely attributed to the higher compression forces used for C1 formulations (2 ton instead of 1 ton for C2-C4). This was used to address the poor hardness of a previous batch (data not shown) and likely contributed to an increase in tablet strength due to an increase in intramolecular bonds. Disintegration times for the surfactant-coated tablets were significantly ( $p < 0.05$ ) decreased under decreased compression attributed to the increase in the tablet porosity (Kitazawa et al., 1975), and partially due to the addition to the hydrophilic nature of the surfactants which increases wettability of the coating in comparison C1, which only contains Kollicoat IR. The acceptable levels of hardness for all tablet formulations is most likely attributed to the good compressibility of MCC, which is known to undergo a unique plastic deformation during compression that occurs through enhanced hydrogen bonding to adjacent MCC particles (Al-Khattawi and Mohammed, 2013). The formulation containing Cremophor EL (C4) showed lower friability and higher strength than the tablets made using the other formulations, which may be associated with the higher viscosity of this surfactant which aids the binding of the granules under compression (Gumaste et al., 2013).

Table 6.5. The physical properties of tablets produced from the coated powders C1 (compressed at 2 metric tons) and C2-C4 (compressed at 1 metric ton). Data presented  $\pm$  SD from  $n = 3$  tablets (aside from friability).

<i>Coating solutions</i>	<i>Friability (%)</i>	<i>Hardness (N)</i>	<i>Disintegration time (s)</i>
C1 – 10 % Kollicoat	0.807	81.76 $\pm$ 2.22	79.00 $\pm$ 6.56
C2 – 10 % Kollicoat + 2 % PEG 2000	3.624	24.13 $\pm$ 0.49	13.30 $\pm$ 1.53
C3 – 10 % Kollicoat + 2 % Poloxamer 407	2.525	27.30 $\pm$ 3.03	14.00 $\pm$ 1.73
C4 – 10 % Kollicoat + 2 % Cremophor EL	2.188	28.10 $\pm$ 3.92	13.67 $\pm$ 0.58

The application of surfactants in coatings has been the focus of a number of previous investigations. These studies are almost always directed towards the properties of the coating itself, rather than the holistic physical properties of the resulting tablets. Initial studies focused on the role of surfactants as plasticisers for tablet coatings, with one of the earliest studies focusing on the Tweens, where Tween 20 was shown to increase the hydrophilicity of the ethylcellulose coatings, with up to 60 % of this surfactant able to act as a plasticiser (Lindholm et al., 1986). Likewise, up to 20 % PEG 400 has been shown to decrease the glass transition temperature ( $T_g$ ) of HPMC free film coatings (Johnson et al., 1991). The same concentration of this polymer was shown to lower the  $T_g$  of Surelease® from 34.9 °C to 29 °C (Rohera and Parikh, 2002). In another study, up to 10% (w/w) Tween 80 and Span 80 were incorporated into the film-coating formulations. These surfactants increased the wettability of the tablets, shown by a decrease in the contact angle between the polymeric dispersion and the tablet surface. In addition, these surfactants decreased the  $T_g$  of the coatings shown by differential scanning calorimetry (DSC), indicating the polymer was able to emulsify the hydrophobic plasticiser tributyl citrate (TBC) (Felton et al., 2000). In a study looking at microporous membrane coatings for a water-soluble drug, PEG 4000 and Tween 80 were evaluated for their role in pore formation (Mishra and Mishra, 2010). In this study, PEG 4000 was found to be the most effective pore former followed by Tween 80, with PEG also acting as an effective plasticiser (Mishra and Mishra, 2010). In a more recent study examining the effects of the surfactant PEG 6000 added to HPMC as a coating for ibuprofen particles, PEG effectively reduced the agglomeration of the particles during coating when compared to HPMC alone (Miyadai et al., 2012). The results of the tablet studies herein demonstrate the addition of biologically active surfactants to granule coatings that can produce tablets with acceptable levels of hardness with disintegration times below 30 seconds.

#### 6.4. Uniformity of Content

Weight variation for tablets must conform to the following specifications according to the *United States Pharmacopeia* (USP, 2011). All 10 tablets tested must contain 85% - 115% of the drug content in comparison to the mean amount of Ibuprofen with an RSD below 6 % of the mean. The weight variation and content uniformity for all formulations is presented in Table 6.6. The highest weight variation was seen for uncoated tablets, although all conformed to the USP specifications. In addition, all tablets conformed to the content of uniformity.

Table 6.6. Content uniformity of tablets ( $n = 3$ ) produced from uncoated granules and granules coated with various dispersions (C1-C4).

<i>Tablet batch</i>	<i>Content uniformity (%)</i>	<i>% RSD</i>
C1 – Uncoated	98.80	2.78
C2 – 2 % (w/v) PEG 2000	99.39	2.21
C3 – 2 % (w/v) Poloxamer 407	99.12	2.21
C4 – 2 % (w/v) Cremophor EL	99.03	2.21

#### 6.5. Conclusion of the Investigation into Surfactant –Coated ODTs

This work demonstrated the feasibility of incorporating surfactants into granule coatings as an additional method of increasing the content of excipients with efflux inhibition properties within an ODT. The formulations containing these surfactants had flow properties ranging from ‘good’ to ‘excellent’ on the Carr’s Index and Hausner ratio scale, with the exception of coatings containing poloxamer 407, which was categorised as ‘fair’, most likely due to the higher water content of this coating. Cremophor EL demonstrated superior flow properties to that of uncoated granules, and produced tablets with lower friability and increased hardness compared to formulations containing PEG 2000 and poloxamer 407. All tablets made from the surfactant-coated granules showed disintegration times conforming to the USP, with disintegration times below 30 seconds with acceptable levels of hardness. The results of this study demonstrate the feasibility of incorporating biologically active surfactants into granule coatings for the use in making ODTs via direct compression, offering an additional supplementary method for potentially enhancing the delivery of drugs which are efflux substrates.

## Chapter 7

### Overall Conclusion

## 7. Overall Conclusions

Collectively, efflux transporters expressed on the apical membranes of intestinal epithelial cells are of interest from the pharmacodynamic and pharmacokinetic perspectives in anticipating the behaviour of a drug *in vivo*. The existing literature on the subject revealed an extensive yet disparate list of excipients that elicit an effect against the ABC efflux transporters, chiefly ABCB1. Such information is rarely quantified in the pharmacokinetic terms that could be of use to a formulation scientist wishing to increase the bioavailability of drugs that fall victim to efflux.

The aim of this thesis was to develop and validate a high-throughput screening assay to detect and quantify the effects of commonly used excipients against the ABCB1 and ABCC2 efflux transporter systems, and to utilise this knowledge to design and manufacture an oral dosage formulation with the capability to achieve enhanced delivery of drugs with poor oral bioavailability. In order to achieve this, a number of objectives were met:

- A novel HTS screening assay was developed and validated using the Caco-2 platform for the detection of commonly used excipients with a biological effect against ABCB1 and ABCC2. This assay had a turnaround time of less than 7 days.
- Unique modelling techniques were used in order to display the inhibition data synonymous with drug-drug interactions (DDIs). For the first time a number of  $IC_{50}$  values are presented which quantifies this data on par with established inhibitors of efflux.
- Finally, having identified poloxamer 407 as one of the most efficacious excipients at inhibiting ABCB1-mediated efflux using the HTS assay, a DoE approach was applied to the design and manufacture of ODTs incorporating quantities of this excipient that could exceed the calculated  $IC_{50}$  value if the tablet was taken with a 250 mL glass of water.

Initially IND was evaluated as an efflux probe substrate using the Caco-2 platform grown in Transwell® inserts. This examination of the transport of IND indicated that the apparent permeability was higher in the BL-AP direction, indicating that the travel in the absorptive direction is influenced by the action of efflux transporters. Despite this, the efflux ratio between these directions of travel did not exceed 2, suggesting that this efflux is not a major barrier to the transport of IND. As such, the efflux ratios that we obtained leave the transport of IND in a state of contention. Over the course of the experiments examining the transport of IND through Caco-2 monolayers,  $P_{app}$  values between  $2.18\text{-}2.59 \times 10^{-5} \text{ cm s}^{-1}$  were recorded, suggesting this compound is highly permeable and therefore a poor candidate for an efflux probe.

Despite this, PEG 8000, POLYOX N-10 and poloxamer 407 were able to increase the permeability of IND, potentially by the inhibition of the efflux transporter ABCB1. The efficacy of PEG 400 requires further investigation since the increase in uptake did not appear to be concentration dependent and aside from P407, statistically significant increases in IND transport was only observed for the highest concentration of the other excipients, and only after 60 minutes.

Although a powerful screening tool, the Transwell® model suffers from slow growth rates that limit throughput. As such, a novel assay was developed using the Caco-2 platform grown in 96-well plates to achieve high-throughput screening (HTS) using the fluorescent dye rhodamine 123 (R-123) as a high-affinity ABCB1-mediated dye and 5(6)-carboxy-2',7'-dichlorofluorescein as the high affinity ABCC2 probe. This latter probe is unable to cross membranes of cells, so is added to transport media in diacetate form that is able to freely diffuse to the cytoplasm where it gets converted to the fluorescent species. The fluorescent nature of these probes allowed for rapid detection and quantification of the *in vitro* data.

This HTS assay was optimised to a 5-7 day cellular growth time, resulting in a net saving of time and growth media when compared to the Transwell® model. Using this optimised protocol, the non-ionic excipients Tween 20 and Tween 80 were tested for their biological effect against the ABCB1 transporter below their cytotoxic concentrations. The results of this study validated the HTS platform against existing literature examining the biological effects of surfactants.

The data from the HTS assay was modelled using the kinetic approach by examining the amount of excipients required to reduce transporter activity by 50 % - the IC<sub>50</sub> value. This allowed the efficacy of excipients to be compared to that of the other excipients to achieve a rank order, particularly against established inhibitors, whilst also providing a theoretical excipient content that must come from the tablet dosage form.

In order to establish the functional activity of the transporters in the cell line, established inhibitors of the efflux transporters were tested in conjunction with the fluorescent probes in order to obtain their IC<sub>50</sub> values. Both ABCB1 and ABCC2 follow a dose-dependent response allowing the GraphPad Prism software to plot non-linear regression curves through the data points in order to obtain IC<sub>50</sub> to 95 % confidence. The inhibitors of ABCB1, verapamil (VER) and ciclosporin (CsA), give IC<sub>50</sub> values of 4.08 and 1.16  $\mu$ M, respectively, with the ABCC2 inhibitors indometacin (IND) and probenecid (PBD) giving IC<sub>50</sub> values of 38.08 and 68.08  $\mu$ M respectively. This confirmed the functional activity of both ABCB1 and ABCC2 on the Caco-2 cell line.

Having shown some efficacy during the previous Transwell® screening, PEGs of various molecular weights were re-examined using the HTS assay. Over the concentration range tested, none of the PEGs had a significant impact upon the intracellular accumulation of either fluorescent probes, suggesting no inhibition properties of these excipients. In contrast, poloxamers and Tweens were found to be highly efficacious against ABCB1-mediated efflux. Both of the Tweens (Tween 20 and 80) and 4 out of the 5 poloxamers tested yielded data from which IC<sub>50</sub> values could be determined for ABCB1 inhibition with over 95 % confidence. In order to expand on the study of poloxamers and Tweens, additional surfactants were obtained, incorporating a wider range of HLB values from lipophilic molecules of 4.5 to hydrophilic molecules at 29. These excipients were specifically chosen for variations in structure and molecular weights. These materials were evaluated for inhibitory effects against ABCB1 and ABCC2 transport using the HTS assay.

Of the 24 surfactants tested, IC<sub>50</sub> values could be determined for ABCB1 inhibition (with over 95 % confidence) for 12 surfactants. However, only Etocas 29 and 40 gave confident inhibition against ABCC2 (16.2  $\mu$ M and 12.9  $\mu$ M). Against ABCB1, the excipients gave the rank order poloxamer 335, poloxamer 407, Crovol A-70, Myrj S-40, poloxamer 184,

poloxamer 182, Etocas 40, Tween 20, Etocas 29, Tween 80, Acconon C-44 and Span 20. The excipients with the lowest value (greatest efficacy), poloxamer 335 and poloxamer 407, showed  $IC_{50}$  values of 0.63 and 0.71  $\mu\text{M}$ , which exceeded that of VER (4.08  $\mu\text{M}$ ) and CsA (1.16  $\mu\text{M}$ ). The highest efficacy was seen for short linear or larger branched molecules, both with intermediate HLB values.

The high-throughput screening assay produced two clear lead candidate excipients, poloxamer 335 and poloxamer 407, with  $IC_{50}$  values of  $4.12 \times 10^{-4}$  % (w/v) and  $8.85 \times 10^{-4}$  % (w/v), respectively. Poloxamer 407 was chosen as the material for the development of the ODT formulations using the Colorcon micronised version of the same polymer. This excipient was incorporated within the low-dose (295 mg) and high-dose (795 mg) APAP ODT formulations at 10 % (w/w).

In order to explore the response of the different combinations of the excipients MCC, mannitol and Starch 1500, a design of experiments approach was taken to design a set of experiments with varying concentrations of each material for both high and low-dose materials, with 40 % and 70 % excipient content, respectively. Using bivariate analysis, Starch 1500 decreased tablet strength, mannitol had little impact and MCC was able to improve tablet strength. Of these, Starch 1500 and MCC correlated well, with  $r^2$  values of 0.60 and 0.80, respectively; moreover both of these excipients had a significant ( $p < 0.01$ ) impact upon tablet strength. For disintegration, Starch 1500 and MCC increased disintegration time, whereas mannitol was able to decrease it. The impact of mannitol had good correlation with the model ( $r^2 = 0.85$ ); furthermore mannitol was the only material to have a significant ( $p < 0.001$ ) impact upon disintegration for the low-dose formulations. For the high-dose tablet formulations, Starch 1500 and MCC correlated well with tablet hardness, with  $r^2$  values of 0.75 and 0.71 respectively, and both had a significant ( $p < 0.01$ ) impact upon tablet strength. Starch 1500 increased disintegration time, MCC had little impact, whereas mannitol was able to decrease it. Both Starch 1500 and mannitol correlated well in this model ( $r^2 = 0.77$  and 0.79 respectively), and the impact of both was significant ( $p < 0.001$ ).

Both ODT formulations were then refined by the removal of ethylcellulose completely, the poloxamer content lowered to 2 % (w/w) and the modified starch, Starch 1500, was

exchanged for StarCap 1500, which has better disintegration properties. The net result was ODTs with disintegration times of 16 s and 45 s for the lead low-dose and high-dose tablets, respectively. A second round of DoE screening was used to examine the interplay between mannitol, MCC and StarCap 1500 on tablet hardness and disintegration.

For the low-dose formulations, StarCap 1500 and mannitol decreased tablet strength, whilst MCC was able to improve it. Additionally, MCC had almost perfect correlation with tablet strength ( $r^2 = 0.98$ ), and both MCC and StarCap 1500 had a significant ( $p < 0.05$ ) impact upon the response. For disintegration, higher StarCap 1500 content increased disintegration time, whereas MCC decreased it. These effects were both significant ( $p < 0.05$ ), but the impact of mannitol was insignificant ( $p > 0.05$ ) on tablet disintegration. For the high-dose formulations, StarCap 1500 and MCC led to a significant ( $p < 0.05$ ) decrease and increase respectively in tablet strength, with MCC showing a particularly good fit to the model with  $r^2 = 0.98$ . Mannitol had an insignificant ( $p > 0.05$ ) impact on high-dose hardness. For high-dose disintegration, higher StarCap 1500 content increased disintegration time, whereas MCC decreased it, with  $r^2$  values of 0.55 and 0.75, respectively. Mannitol correlated extremely poorly with disintegration time ( $r^2 = 0.01$ ), and neither was the impact significant ( $p > 0.05$ ).

From the second round of DoE screening, the low-dose formulation F9 was chosen for rotary press trial on the Picolla multi-station rotary tablet press in order to test the feasibility of the high-throughput manufacture of the designed dosage formulation. This formulation was chosen as the theoretical centre point of the DoE study e.g. equal composition of each excipient. Two additional variations were produced of this formulation: one contained 50 % more StarCap 1500 as a multipurpose binder and the second contained 50 % more mannitol.

Tablets produced using a rotary tablet press had disintegration times between 9-43 s over a range of compressions (6-23 kN), providing tablets that conformed to both the *European Pharmacopeia* and *United States Pharmacopeia*. Any of these formulations, taken with a 250 mL glass of water on an empty stomach, are capable of delivering 5.9 mg of poloxamer 407 to give a final concentration of  $2.36 \times 10^{-3}$  % (w/v), or 2.7 times higher than the  $IC_{50}$ .

In addition to incorporating poloxamer 407 directly into the formulation used to make ODTs by direct compression, the impact of surfactants upon granule coatings was also investigated. Coated ibuprofen granules were prepared using 10 % (w/v) Kollicoat IR solution alone or with the addition of 2 % (w/v) PEG 2000, poloxamer 407 or Cremophor EL. The Carr's index and Hausner ratio values indicated that granules coated with the solution containing 2 % (w/v) Cremophor EL had 'excellent' flow properties, with the flow properties of the uncoated granules and the granules coated with the additional 2 % (w/v) PEG 2000 being classified as 'good', and those coated in 2 % (w/v) poloxamer 407 being considered 'passable'. The ODTs made from these granules by direct compression showed disintegration times below 30 seconds, conforming the *United States Pharmacopeia*.

As such, the work of this thesis describes the development of a novel HTS assay for the detection of excipients with inhibitory properties against ABCB1 and ABCC2 that was harnessed to provide a shortlist of materials that could be incorporated into ODTs. This was then coupled with a DoE approach for producing ODT formulations with potentially enhanced delivery capability. Efflux transporters such as ABCB1 and ABCC2 expressed on the apical membranes of intestinal epithelial cells represent a formidable barrier to the efficient oral delivery of a plethora of drugs. Therefore, the integrated approach undertaken in this thesis provides a novel tablet design process that could provide formulation scientists with a method to improve the oral bioavailability of drugs that are efflux substrates.

Whilst investigating the biological effects of commonly used excipients, this thesis generated a series of  $IC_{50}$  values in order to demonstrate how much of each material would be required to reduce transporter activity by 50 %. Whilst excipient  $IC_{50}$  values remain elusive in literature, one parameter remains absent from the literature entirely: the inhibition constant ( $K_i$ ). This value indicates the potency of the inhibitor. By generating a series of Michaelis-Menten saturation curves (the initial rate of reaction,  $v$ , against the substrate concentration) in the presence of increasing inhibitor concentrations, double reciprocal Lineweaver-Burk plots can then be produced. From these, the change in  $K_m$  and  $V_{max}$  values at each inhibitor concentration (indicated by the x-axis and y-axis intercept respectively) compared to the non-treated control could then be used to elucidate if the

mode of inhibition is competitive, non-competitive or uncompetitive. Furthermore, plotting  $1/v$  against the inhibitor concentration at each concentration of substrate (a Dixon plot) gives a series of intersecting lines, and where they intercept gives the negative  $K_i$  value.

During the tablet development phase, paracetamol (APAP) was used as the model drug due to the safety concerns regarding the use of atorvastatin (ATV) in a commercial lab. Future work should focus on the conversion of these APAP tablets to ATV, and subsequently the reassessment of those tablets in terms of hardness, disintegration and friability which may have been altered by the presence of a different drug. Finally, the tablets were designed and manufactured to contain a surplus quantity of the biologically-active poloxamer 407 for the purpose of potentially inhibiting ABCB1-mediated transport of ATV *in vivo*. It would be of great value to demonstrate the efficacy of these tablets using the *in vitro* Transwell model in order to establish the statistically significant increase in ATV apical to basolateral transport across these monolayers when compared to tablets containing ATV without the poloxamer. This would provide the proof of concept of incorporating biologically-active excipients into oral dosage formulations to inhibit efflux-mediated drug transport, and validating the concept of the work behind this thesis.

## 8. References

- ABDULLAH, E. & GELDART, D. 1999. The use of bulk density measurements as flowability indicators. *Powder Technology*, 102, 151-165.
- ACHARYA, K. R., BHATTACHARYA, S. & MOULIK, S. 1997. Salt effects on surfactant aggregation and dye-micelle complexation. *Indian Journal of Chemistry. Sect. A: Inorganic, Physical, Theoretical & Analytical*, 36, 137-143.
- AHMED, I. S. & HASSAN, M. 2007. In vitro and in vivo evaluation of a fast-disintegrating lyophilized dry emulsion tablet containing griseofulvin. *European Journal of Pharmaceutical Sciences*, 32, 58-68.
- AL-KHATTAWI, A., IYIRE, A., DENNISON, T., DAHMASH, E., J BAILEY, C., SMITH, J., RUE, P. & MOHAMMED, A. R. 2014. Systematic screening of compressed ODT excipients: cellulosic versus non-cellulosic. *Current Drug Delivery*, 11, 486-500.
- AL-KHATTAWI, A. & MOHAMMED, A. R. 2013. Compressed orally disintegrating tablets: excipients evolution and formulation strategies. *Expert Opinion on Drug Delivery*, 10, 651-663.
- AL-MOHIZEA, A. M., ZAWANEH, F., ALAM, M. A., AL-JENOABI, F. I. & EL-MAGHRABY, G. M. 2014. Effect of pharmaceutical excipients on the permeability of P-glycoprotein substrate. *Journal of Drug Delivery Science and Technology*, 24, 491-495.
- AL-NASASSRAH, M. A., PODCZECK, F. & NEWTON, J. M. 1998. The effect of an increase in chain length on the mechanical properties of polyethylene glycols. *European Journal of Pharmaceutics and Biopharmaceutics*, 46, 31-38.
- ALAKHOV, V. Y., MOSKALEVA, E. Y., BATRAKOVA, E. V. & KABANOV, A. V. 1996. Hypersensitization of multidrug resistant human ovarian carcinoma cells by pluronic P85 block copolymer. *Bioconjugate Chemistry*, 7, 209-216.
- ALCANTARA, L. M., KIM, J., MORAES, C. B., FRANCO, C. H., FRANZOI, K. D., LEE, S., FREITAS-JUNIOR, L. H. & AYONG, L. S. 2013. Chemosensitization potential of P-glycoprotein inhibitors in malaria parasites. *Experimental Parasitology*.
- ALEXANDRIDIS, P., HOLZWARTH, J. F. & HATTON, T. A. 1994. Micellization of poly (ethylene oxide)-poly (propylene oxide)-poly (ethylene oxide) triblock copolymers in aqueous solutions: thermodynamics of copolymer association. *Macromolecules*, 27, 2414-2425.
- ALLER, S. G., YU, J., WARD, A., WENG, Y., CHITTABOINA, S., ZHUO, R., HARRELL, P. M., TRINH, Y. T., ZHANG, Q. & URBATSCH, I. L. 2009. Structure of P-glycoprotein reveals a molecular basis for poly-specific drug binding. *Science*, 323, 1718-1722.
- AMELIAN, A., SZEKALSKA, M., WILCZEWSKA, A. Z., BASA, A. & WINNICKA, K. 2015. Preparation and characterization of orally disintegrating loratadine tablets manufactured with co-processed mixtures. *Acta Poloniae Pharmaceutica*, 73, 453-460.
- AMELIAN, A. & WINNICKA, K. 2012. Effect of the type of disintegrant on the characteristics of orally disintegrating tablets manufactured using new ready-to-

- use excipients (Ludiflash® or Parteck®) by direct compression method. *African Journal of Pharmacy and Pharmacology*, 6, 2359-2367.
- AMIDON, G. L., SINKO, P. J. & FLEISHER, D. 1988. Estimating human oral fraction dose absorbed: a correlation using rat intestinal membrane permeability for passive and carrier-mediated compounds. *Pharmaceutical Research*, 5, 651-654.
- AMRUTKAR, J., PAWAR, S., NAKATH, P., KHAN, S. & YEOLE, P. 2007. Comparative evaluation of disintegrants by formulating famotidine dispersible tablets. *The Indian Pharmacist*, 6, 85-89.
- ANDERBERG, E. K., NYSTRÖM, C. & ARTURSSON, P. 1992. Epithelial transport of drugs in cell culture. VII: Effects of pharmaceutical surfactant excipients and bile acids on transepithelial permeability in monolayers of human intestinal epithelial (Caco-2) cells. *Journal of pharmaceutical sciences*, 81, 879-887.
- ANDERLE, P., NIEDERER, E., RUBAS, W., HILGENDORF, C., SPAHN-LANGGUTH, H., WUNDERLI-AlLENSPACH, H., MERKLE, H. P. & LANGGUTH, P. 1998. P-glycoprotein (P-gp) mediated efflux in Caco-2 cell monolayers: The influence of culturing conditions and drug exposure on P-gp expression levels. *Journal of Pharmaceutical Sciences*, 87, 757-762.
- ANNAERT, P. P. & BROUWER, K. L. 2005. Assessment of drug interactions in hepatobiliary transport using rhodamine 123 in sandwich-cultured rat hepatocytes. *Drug Metabolism and Disposition*, 33, 388-394.
- ARTURSSON, P., UNGELL, A.-L. & LÖFROTH, J.-E. 1993a. Selective paracellular permeability in two models of intestinal absorption: cultured monolayers of human intestinal epithelial cells and rat intestinal segments. *Pharmaceutical Research*, 10, 1123-1129.
- ARTURSSON, P., UNGELL, A. L. & LÖFROTH, J. E. 1993b. Selective paracellular permeability in two models of intestinal absorption: cultured monolayers of human intestinal epithelial cells and rat intestinal segments. *Pharmaceutical Research*, 10, 1123-1129.
- AUNGST, B. J. 2012. Absorption enhancers: applications and advances. *The AAPS Journal*, 14, 10-18.
- AYENEW, Z., PAUDEL, A. & VAN DEN MOOTER, G. 2012. Can compression induce demixing in amorphous solid dispersions? A case study of naproxen-PVP K25. *European Journal of Pharmaceutics and Biopharmaceutics*, 81, 207-213.
- BANAN, A., FARHADI, A., FIELDS, J., ZHANG, L., SHAIKH, M. & KESHAVARZIAN, A. 2003. The  $\delta$ -isoform of protein kinase C causes inducible nitric-oxide synthase and nitric oxide up-regulation: Key mechanism for oxidant-induced carbonylation, nitration, and disassembly of the microtubule cytoskeleton and hyperpermeability of barrier of intestinal epithelia. *Journal of Pharmacology and Experimental Therapeutics*, 305, 482-494.
- BARTHE, L., BESSOUET, M., WOODLEY, J. & HOUIN, G. 1998. The improved everted gut sac: a simple method to study intestinal P-glycoprotein. *International Journal of Pharmaceutics*, 173, 255-258.
- BARTHE, L., WOODLEY, J. & HOUIN, G. 1999. Gastrointestinal absorption of drugs: methods and studies. *Fundamental & Clinical Pharmacology*, 13, 154-168.
- BATRAKOVA, E. V. & KABANOV, A. V. 2008. Pluronic block copolymers: evolution of drug delivery concept from inert nanocarriers to biological response modifiers. *Journal of Controlled Release*, 130, 98-106.

- BATRAKOVA, E. V., LI, S., ALAKHOV, V. Y., MILLER, D. W. & KABANOV, A. V. 2003. Optimal structure requirements for pluronic block copolymers in modifying P-glycoprotein drug efflux transporter activity in bovine brain microvessel endothelial cells. *Journal of Pharmacology and Experimental Therapeutics*, 304, 845-854.
- BATRAKOVA, E. V., LI, S., LI, Y., ALAKHOV, V. Y. & KABANOV, A. V. 2004. Effect of pluronic P85 on ATPase activity of drug efflux transporters. *Pharmaceutical Research*, 21, 2226-2233.
- BATRAKOVA, E. V., LI, S., VINOGRADOV, S. V., ALAKHOV, V. Y., MILLER, D. W. & KABANOV, A. V. 2001. Mechanism of pluronic effect on P-glycoprotein efflux system in blood-brain barrier: contributions of energy depletion and membrane fluidization. *Journal of Pharmacology and Experimental Therapeutics*, 299, 483-493.
- BENET, L. Z., KROETZ, D., SHEINER, L., HARDMAN, J. & LIMBIRD, L. 1996. Pharmacokinetics: the dynamics of drug absorption, distribution, metabolism, and elimination. *Goodman and Gilman's The Pharmacological Basis of Therapeutics*, 3-27.
- BOGMAN, K., ERNE-BRAND, F., ALSENZ, J. & DREWE, J. 2003. The role of surfactants in the reversal of active transport mediated by multidrug resistance proteins. *Journal of Pharmaceutical Sciences*, 92, 1250-1261.
- BOURRE, L., THIBAUT, S., BRIFFAUD, A., LAJAT, Y. & PATRICE, T. 2002. Potential efficacy of a delta 5-aminolevulinic acid thermosetting gel formulation for use in photodynamic therapy of lesions of the gastrointestinal tract. *Pharmacological Research*, 45, 159-165.
- BUCKINGHAM, L. E., BALASUBRAMANIAN, M., EMANUELE, R. M., CLODFELTER, K. E. & COON, J. S. 1995. Comparison of solutol HS 15, Cremophor EL and novel ethoxylated fatty acid surfactants as multidrug resistance modification agents. *International Journal of Cancer*, 62, 436-442.
- BURDOCK, G. A. 2007. Safety assessment of hydroxypropyl methylcellulose as a food ingredient. *Food and Chemical Toxicology*, 45, 2341-2351.
- BURTON, P., CONRADI, R., HILGERS, A. & HO, N. 1993. Evidence for a polarized efflux system for peptides in the apical membrane of Caco-2 cells. *Biochemical and Biophysical Research Communications*, 190, 760-766.
- CALLAGHAN, R., BERRIDGE, G., FERRY, D. R. & HIGGINS, C. F. 1997. The functional purification of P-glycoprotein is dependent on maintenance of a lipid-protein interface. *Biochimica et Biophysica Acta (BBA) - Biomembranes*, 1328, 109-124.
- CAO, X., GIBBS, S. T., FANG, L., MILLER, H. A., LANDOWSKI, C. P., SHIN, H.-C., LENNERNAS, H., ZHONG, Y., AMIDON, G. L. & LAWRENCE, X. Y. 2006. Why is it challenging to predict intestinal drug absorption and oral bioavailability in human using rat model. *Pharmaceutical Research*, 23, 1675-1686.
- CARDARELLI, C. O., AKSENTIJEVICH, I., PASTAN, I. & GOTTESMAN, M. M. 1995. Differential effects of P-glycoprotein inhibitors on NIH3T3 cells transfected with wild-type (G185) or mutant (V185) multidrug transporters. *Cancer Research*, 55, 1086-1091.
- CARO, I., BOULENC, X., ROUSSET, M., MEUNIER, V., BOURRIÉ, M., JULIAN, B., JOYEUX, H., ROQUES, C., BERGER, Y. & ZWEIBAUM, A. 1995. Characterisation

- of a newly isolated Caco-2 clone (TC-7), as a model of transport processes and biotransformation of drugs. *International Journal of Pharmaceutics*, 116, 147-158.
- CARR, R. L. 1965. Evaluating flow properties of solids. *Chemical Engineering*.
- CARRASCO-POZO, C., MORALES, P. & GOTTELAND, M. 2013. Polyphenols Protect the Epithelial Barrier Function of Caco-2 Cells Exposed to Indomethacin through the Modulation of Occludin and Zonula Occludens-1 Expression. *Journal of Agricultural and Food Chemistry*, 61, 5291-5297.
- CARRENO-GOMEZ, B. & DUNCAN, R. 2002. Compositions with enhanced oral bioavailability. Google Patents.
- CHAN, L. C. Y. & PAGE, N. W. 1997. Particle fractal and load effects on internal friction in powders. *Powder Technology*, 90, 259-266.
- CHANG, R.-K., XIAODI, G., BURNSIDE, B. A. & COUCH, R. A. 2000. Fast-dissolving tablets. *Pharmaceutical Technology*, 24, 52-58.
- CHIOU, W. L. & BARVE, A. 1998. Linear correlation of the fraction of oral dose absorbed of 64 drugs between humans and rats. *Pharmaceutical Research*, 15, 1792-1795.
- CHIOU, W. L., JEONG, H. Y., CHUNG, S. M. & WU, T. C. 2000. Evaluation of using dog as an animal model to study the fraction of oral dose absorbed of 43 drugs in humans. *Pharmaceutical Research*, 17, 135-140.
- CHO, M. J., THOMPSON, D. P., CRAMER, C. T., VIDMAR, T. J. & SCIESZKA, J. F. 1989. The Madin Darby canine kidney (MDCK) epithelial cell monolayer as a model cellular transport barrier. *Pharmaceutical Research*, 6, 71-77.
- CHRESTA, C., ARRIOLA, E. & HICKMAN, J. 1996. Apoptosis and cancer chemotherapy. *Behring Institute Mitteilungen*, 232-240.
- COELHO, M. & HARNBY, N. 1978. Moisture bonding in powders. *Powder Technology*, 20, 201-205.
- COLE, S., BHARDWAJ, G., GERLACH, J., MACKIE, J., GRANT, C., ALMQUIST, K., STEWART, A., KURZ, E., DUNCAN, A. & DEELEY, R. 1992. Overexpression of a transporter gene in a multidrug-resistant human lung cancer cell line. *The AAPS Journal*, 258, 1650-1650.
- COLLNOT, E.-M., BALDES, C., WEMPE, M. F., HYATT, J., NAVARRO, L., EDGAR, K. J., SCHAEFER, U. F. & LEHR, C.-M. 2006. Influence of vitamin E TPGS poly (ethylene glycol) chain length on apical efflux transporters in Caco-2 cell monolayers. *Journal of Controlled Release*, 111, 35-40.
- COLOMBO, F., ARMSTRONG, C., DUAN, J. & RIOUX, N. 2012. A high throughput in vitro mrp2 assay to predict in vivo biliary excretion. *Xenobiotica*, 42, 157-163.
- COON, J. S., KNUDSON, W., CLODFELTER, K., LU, B. & WEINSTEIN, R. S. 1991. Solutol HS 15, nontoxic polyoxyethylene esters of 12-hydroxystearic acid, reverses multidrug resistance. *Cancer Research*, 51, 897-902.
- CORNAIRE, G., WOODLEY, J., HERMANN, P., CLOAREC, A., ARELLANO, C. & HOUIN, G. 2004. Impact of excipients on the absorption of P-glycoprotein substrates in vitro and in vivo. *International Journal of Pharmaceutics*, 278, 119-131.
- COWMAN, A. F. 1991. The p-glycoprotein homologs of plasmodium falciparum: are they involved in chloroquine resistance? *Parasitology Today*, 7, 70-76.
- CUI, D. M., XU, Q. W., GU, S. X., SHI, J. L. & CHE, X. M. 2009. PAMAM-drug complex for delivering anticancer drug across blood-brain barrier in-vitro and in-vivo. *African Journal of Pharmacy and Pharmacology*, 3, 227-233.

- D'EMANUELE, A., JEVPRASEPHANT, R., PENNY, J. & ATTWOOD, D. 2004. The use of a dendrimer-propranolol prodrug to bypass efflux transporters and enhance oral bioavailability. *Journal of Controlled Release*, 95, 447-453.
- DAHAN, A. & AMIDON, G. L. 2010. MRP2 mediated drug-drug interaction: indomethacin increases sulfasalazine absorption in the small intestine, potentially decreasing its colonic targeting. *International Journal of Pharmaceutics*, 386, 216-220.
- DALE, O., HOFFER, C., SHEFFELS, P. & KHARASCH, E. D. 2002. Disposition of nasal, intravenous, and oral methadone in healthy volunteers. *Clinical Pharmacology & Therapeutics*, 72, 536-45.
- DAOUD, R., KAST, C., GROS, P. & GEORGES, E. 2000. Rhodamine 123 binds to multiple sites in the multidrug resistance protein (MRP1). *Biochemistry*, 39, 15344-15352.
- DESAI, D., ZIA, H. & QUADIR, A. 2007. Evaluation of selected micronized poloxamers as tablet lubricants. *Drug Delivery*, 14, 413-426.
- DESAI, P. V., RAUB, T. J. & BLANCO, M. J. 2012. How hydrogen bonds impact P-glycoprotein transport and permeability. *Bioorganic & Medicinal Chemistry Letters*.
- DIMITRIJEVIC, D., SHAW, A. J. & FLORENCE, A. T. 2000. Effects of some non-ionic surfactants on transepithelial permeability in Caco-2 cells. *Journal of Pharmacy and Pharmacology*, 52, 157-162.
- DINGE, A. & NAGARSENKER, M. 2008. Formulation and evaluation of fast dissolving films for delivery of triclosan to the oral cavity. *AAPS PharmSciTech*, 9, 349-356.
- DINTAMAN, J. M. & SILVERMAN, J. A. 1999. Inhibition of P-glycoprotein by D- $\alpha$ -tocopheryl polyethylene glycol 1000 succinate (TPGS). *Pharmaceutical Research*, 16, 1550-1556.
- DOLUISIO, J. T., BILLUPS, N. F., DITTERT, L. W., SUGITA, E. T. & SWINTOSKY, J. V. 1969. Drug absorption I: An in situ rat gut technique yielding realistic absorption rates. *Journal of Pharmaceutical Sciences*, 58, 1196-1200.
- DOW 2000. Using METHOCEL Cellulose Ethers for Controlled Release of Drugs in Hydrophilic Matrix Systems.
- DOW 2002. METHOCEL Cellulose Ethers in Aqueous Systems for Tablet Coating.
- DOYLE, L. A., YANG, W. D., ABRUZZO, L. V., KROGMANN, T., GAO, Y. M., RISHI, A. K. & ROSS, D. D. 1998. A multidrug resistance transporter from human MCF-7 breast cancer cells. *Proceedings of the National Academy of Sciences of the United States of America*, 95, 15665-15670.
- DUDEJA, P. K., ANDERSON, K. M., HARRIS, J. S., BUCKINGHAM, L. & COON, J. S. 1995. Reversal of Multidrug-Resistance Phenotype by Surfactants: Relationship to Membrane Lipid Fluidity. *Archives of Biochemistry and Biophysics*, 319, 309-315.
- EHLERS, H., RÄIKKÖNEN, H., ANTIKAINEN, O., HEINÄMÄKI, J. & YLIRUUSI, J. 2009. Improving flow properties of ibuprofen by fluidized bed particle thin-coating. *International Journal of Pharmaceutics*, 368, 165-170.
- EL-SAYED, M., RHODES, C. A., GINSKI, M. & GHANDEHARI, H. 2003. Transport mechanism(s) of poly (amidoamine) dendrimers across Caco-2 cell monolayers. *International Journal of Pharmaceutics*, 265, 151-157.

- EL-SHEIKH, A. A., VAN DEN HEUVEL, J. J., KOENDERINK, J. B. & RUSSEL, F. G. 2007. Interaction of nonsteroidal anti-inflammatory drugs with multidrug resistance protein (MRP) 2/ABCC2-and MRP4/ABCC4-mediated methotrexate transport. *Journal of Pharmacology and Experimental Therapeutics*, 320, 229-235.
- ELGINDY, N. A., SAMAHA, M. W. & ELMARADNY, H. A. 1988. EVALUATION OF BINDER ACTIVITIES ON THE PHYSICAL-PROPERTIES AND COMPRESSION CHARACTERISTICS OF GRANULES PREPARED BY 2 DIFFERENT MODES. *Drug Development and Industrial Pharmacy*, 14, 977-1005.
- ELSHAER, A., HANSON, P. & MOHAMMED, A. R. 2014. A novel concentration dependent amino acid ion pair strategy to mediate drug permeation using indomethacin as a model insoluble drug. *European Journal of Pharmaceutical Sciences*, 62, 124-131.
- ENGLUND, G., RORSMAN, F., RÖNNBLUM, A., KARLBOM, U., LAZOROVA, L., GRÅSJÖ, J., KINDMARK, A. & ARTURSSON, P. 2006. Regional levels of drug transporters along the human intestinal tract: co-expression of ABC and SLC transporters and comparison with Caco-2 cells. *European Journal of Pharmaceutical Sciences*, 29, 269-277.
- EUROPEAN PHARMACOPEIA 2009. Version 6.5.
- EVERS, R., KOOL, M., SMITH, A., VAN DEEMTER, L., DE HAAS, M. & BORST, P. 2000. Inhibitory effect of the reversal agents V-104, GF120918 and Pluronic L61 on MDR1 Pgp-, MRP1-and MRP2-mediated transport. *British Journal of Cancer*, 83, 366.
- EYTAN, G. D., REGEV, R., OREN, G., HURWITZ, C. D. & ASSARAF, Y. G. 1997. Efficiency of P-glycoprotein-Mediated Exclusion of Rhodamine Dyes from Multidrug-Resistant Cells is Determined by their Passive Transmembrane Movement Rate. *European Journal of Biochemistry*, 248, 104-112.
- FAASSEN, F., VOGEL, G., SPANINGS, H. & VROMANS, H. 2003. Caco-2 permeability, P-glycoprotein transport ratios and brain penetration of heterocyclic drugs. *International Journal of Pharmaceutics*, 263, 113-122.
- FAGERHOLM, U. & LENNERNÄS, H. 1995. Experimental estimation of the effective unstirred water layer thickness in the human jejunum, and its importance in oral drug absorption. *European Journal of Pharmaceutical Sciences*, 3, 247-253.
- FAHMY, R. H. & KASSEM, M. A. 2008. Enhancement of famotidine dissolution rate through liquisolid tablets formulation: in vitro and in vivo evaluation. *European Journal of Pharmaceutics and Biopharmaceutics*, 69, 993-1003.
- FATTINGER, K., BENOWITZ, N., JONES, R. & VEROTTA, D. 2000. Nasal mucosal versus gastrointestinal absorption of nasally administered cocaine. *European Journal of Clinical Pharmacology*, 56, 305-310.
- FELDMAN, M. & BARNETT, C. 1991. Fasting gastric pH and its relationship to true hypochlorhydria in humans. *Digestive Diseases and Sciences*, 36, 866-869.
- FELLER, N., BROXTERMAN, H., WÄHRER, D. & PINEDO, H. 1995. ATP-dependent efflux of calcein by the multidrug resistance protein (MRP): no inhibition by intracellular glutathione depletion. *FEBS Letters*, 368, 385-388.
- FELTON, L. A., AUSTIN-FORBES, T. & MOORE, T. A. 2000. Influence of surfactants in aqueous-based polymeric dispersions on the thermomechanical and adhesive properties of acrylic films. *Drug Development and Industrial Pharmacy*, 26, 205-210.

- FÖGER, F., MALAIVIJITNOND, S., WANNAPRASERT, T., HUCK, C., BERNKOP-SCHNÜRCH, A. & WERLE, M. 2008. Effect of a thiolated polymer on oral paclitaxel absorption and tumor growth in rats. *Journal of Drug Targeting*, 16, 149-155.
- FÖRSTER, F., VOLZ, A. & FRICKER, G. 2008. Compound profiling for ABCC2 (MRP2) using a fluorescent microplate assay system. *European Journal of Pharmaceutics and Biopharmaceutics*, 69, 396-403.
- FORSTER, S., THUMSER, A. E., HOOD, S. R. & PLANT, N. 2012. Characterization of rhodamine-123 as a tracer dye for use in in vitro drug transport assays. *PLoS One*, 7, e33253.
- GABOR, F., FILLAFER, C., NEUTSCH, L., RATZINGER, G. & WIRTH, M. 2010. Improving oral delivery. *Drug Delivery*. Springer.
- GARCIA-RUIZ, C., MARI, M., COLELL, A., MORALES, A., CABALLERO, F., MONTERO, J., TERRONES, O., BASAÑEZ, G. & FERNÁNDEZ-CHECA, J. C. 2009. Mitochondrial cholesterol in health and disease. *Histology and Histopathology*, 24, 117-132.
- GAREKANI, H. A., FORD, J. L., RUBINSTEIN, M. H. & RAJABI-SIAHBOOMI, A. R. 2000a. Highly compressible paracetamol - II. Compression properties. *International Journal of Pharmaceutics*, 208, 101-110.
- GAREKANI, H. A., FORD, J. L., RUBINSTEIN, M. H. & RAJABI-SIAHBOOMI, A. R. 2000b. Highly compressible paracetamol: I: crystallization and characterization. *International Journal of Pharmaceutics*, 208, 87-99.
- GAREKANI, H. A., SADEGHI, F. & GHAZI, A. 2003. Increasing the aqueous solubility of acetaminophen in the presence of polyvinylpyrrolidone and investigation of the mechanisms involved. *Drug Development and Industrial Pharmacy*, 29, 173-179.
- GAUSH, C. R., HARD, W. L. & SMITH, T. F. 1966. Characterization of an established line of canine kidney cells (MDCK). *Experimental Biology and Medicine*, 122, 931-935.
- GENEIDI, A. S., ADEL, M. S. & SHEHATA, E. 1981. PREPARATION AND IN-VITRO DISSOLUTION CHARACTERISTICS OF VARIOUS FAST RELEASE SOLID DISPERSIONS OF GLIBENCLAMIDE. *Canadian Journal of Pharmaceutical Sciences*, 15, 78-80.
- GENINA, N., RÄIKKÖNEN, H., EHLERS, H., HEINÄMÄKI, J., VESKI, P. & YLIRUUSI, J. 2010. Thin-coating as an alternative approach to improve flow properties of ibuprofen powder. *International Journal of Pharmaceutics*, 387, 65-70.
- GIBBONS, S., OLUWATUYI, M. & KAATZ, G. W. 2003. A novel inhibitor of multidrug efflux pumps in *Staphylococcus aureus*. *Journal of Antimicrobial Chemotherapy*, 51, 13-17.
- GO, V. 1976. Measurement of gastric functions during digestion of ordinary solid meals in man. *Gastroenterology*, 70, 203-210.
- GOLDBERG, D. S., GHANDEHARI, H. & SWAAN, P. W. 2010. Cellular entry of G3. 5 poly (amido amine) dendrimers by clathrin-and dynamin-dependent endocytosis promotes tight junctional opening in intestinal epithelia. *Pharmaceutical Research*, 27, 1547-1557.

- GOLDBERG, H., LING, V., WONG, P. Y. & SKORECKI, K. 1988. Reduced cyclosporin accumulation in multidrug-resistant cells. *Biochemical and Biophysical Research Communications*, 152, 552-558.
- GOOLE, J., LINDLEY, D. J., ROTH, W., CARL, S. M., AMIGHI, K., KAUFFMANN, J. M. & KNIPP, G. T. 2010. The effects of excipients on transporter mediated absorption. *International Journal of Pharmaceutics*, 393, 17-31.
- GRABOVAC, V., LAFFLEUR, F. & BERNKOP-SCHNÜRCH, A. 2015. Thiomers: Influence of molecular mass and thiol group content of poly (acrylic acid) on efflux pump inhibition. *International Journal of Pharmaceutics*, 493, 374-379.
- GREINDL, M., FOEGER, F., HOMBACH, J. & BERNKOP-SCHNÜRCH, A. 2009. In vivo evaluation of thiolated poly(acrylic acid) as a drug absorption modulator for MRP2 efflux pump substrates. *European Journal of Pharmaceutics and Biopharmaceutics*, 72, 561-566.
- GRÈS, M.-C., JULIAN, B., BOURRIÉ, M., MEUNIER, V., ROQUES, C., BERGER, M., BOULENC, X., BERGER, Y. & FABRE, G. 1998. Correlation between oral drug absorption in humans, and apparent drug permeability in TC-7 cells, a human epithelial intestinal cell line: comparison with the parental Caco-2 cell line. *Pharmaceutical Research*, 15, 726-733.
- GRIFFIN, W. C. 1946. Classification of surface-active agents by "HLB". *J Soc Cosmetic Chemists*, 1, 311-326.
- GRIMM, S. W., EINOLF, H. J., HALL, S. D., HE, K., LIM, H.-K., LING, K.-H. J., LU, C., NOMEIR, A. A., SEIBERT, E. & SKORDOS, K. W. 2009. The conduct of in vitro studies to address time-dependent inhibition of drug-metabolizing enzymes: a perspective of the pharmaceutical research and manufacturers of America. *Drug Metabolism and Disposition*, 37, 1355-1370.
- GRYCZKE, A., SCHMINKE, S., MANIRUZZAMAN, M., BECK, J. & DOUROUMIS, D. 2011. Development and evaluation of orally disintegrating tablets (ODTs) containing Ibuprofen granules prepared by hot melt extrusion. *Colloids and Surfaces B: Biointerfaces*, 86, 275-284.
- GUAN, Y., HUANG, J., ZUO, L., XU, J., SI, L., QIU, J. & LI, G. 2011. Effect of Pluronic P123 and F127 Block Copolymer on P-glycoprotein Transport and CYP3A Metabolism. *Archives of Pharmacal Research*, 34, 1719-1728.
- GUMASTE, S. G., DALRYMPLE, D. M. & SERAJUDDIN, A. T. M. 2013. Development of Solid SEDDS, V: Compaction and Drug Release Properties of Tablets Prepared by Adsorbing Lipid-Based Formulations onto NeusilinA (R) US2. *Pharmaceutical Research*, 30, 3186-3199.
- HAMASHITA, T., NAKAGAWA, Y., AKETO, T. & WATANO, S. 2007. Granulation of core particles suitable for film coating by agitation fluidized Bed I. Optimum formulation for core particles and development of a novel friability test method. *Chemical & Pharmaceutical Bulletin*, 55, 1169-1174.
- HAN, H.-K. & LEE, H.-K. 2011. Improved effectiveness of biochanin A as a P-gp inhibitor in solid dispersion. *Die Pharmazie-An International Journal of Pharmaceutical Sciences*, 66, 710-715.
- HANKE, U., MAY, K., ROZEHNAL, V., NAGEL, S., SIEGMUND, W. & WEITSCHIES, W. 2010. Commonly used nonionic surfactants interact differently with the human efflux transporters ABCB1 (p-glycoprotein) and ABCC2 (MRP2). *European Journal of Pharmaceutics and Biopharmaceutics*, 76, 260-268.

- HEADING, R. C., NIMMO, J., PRESCOTT, L. & TOTHILL, P. 1973. The dependence of paracetamol absorption on the rate of gastric emptying. *British Journal of Pharmacology*, 47, 415-421.
- HEIM, L.-O., BLUM, J., PREUSS, M. & BUTT, H.-J. 1999. Adhesion and friction forces between spherical micrometer-sized particles. *Physical Review Letters*, 83, 3328.
- HELLINGER, É., BAKK, M. L., PÓCZA, P., TIHANYI, K. & VASTAG, M. 2010. Drug penetration model of vinblastine-treated Caco-2 cultures. *European Journal of Pharmaceutical Sciences*, 41, 96-106.
- HEREDI-SZABO, K., KIS, E., MOLNAR, E., GYORFI, A. & KRAJCSI, P. 2008. Characterization of 5 (6)-carboxy-2,'7'-dichlorofluorescein transport by MRP2 and utilization of this substrate as a fluorescent surrogate for LTC4. *Journal of Biomolecular Screening*.
- HESS, H. 1978. Tablets under the microscope. *Pharmaceutical Technology*, 2, 38-57.
- HIROHASHI, T., SUZUKI, H. & SUGIYAMA, Y. 1999. Characterization of the transport properties of cloned rat multidrug resistance-associated protein 3 (MRP3). *Journal of Biological Chemistry*, 274, 15181-15185.
- HIROHASHI, T., SUZUKI, H., TAKIKAWA, H. & SUGIYAMA, Y. 2000. ATP-dependent transport of bile salts by rat multidrug resistance-associated protein 3 (Mrp3). *Journal of Biological Chemistry*, 275, 2905-2910.
- HITCHCOCK, S. A., ORR, S. T. M., RIPP, S. L., BALLARD, T. E., HENDERSON, J. L., SCOTT, D. O., OBACH, R. S., SUN, H. & KALGUTKAR, A. S. 2012. Structural Modifications that Alter the P-Glycoprotein Efflux Properties of Compounds. *Journal of Medicinal Chemistry*, 55, 4877-4895.
- HOCHMAN, J. H., PUDVAH, N., QIU, J., YAMAZAKI, M., TANG, C., LIN, J. H. & PRUEKSARITANONT, T. 2004. Interactions of human P-glycoprotein with simvastatin, simvastatin acid, and atorvastatin. *Pharmaceutical Research*, 21, 1686-1691.
- HOLLÓ, Z., HOMOLYA, L., HEGEDÜS, T. & SARKADI, B. 1996. Transport properties of the multidrug resistance-associated protein (MRP) in human tumour cells. *FEBS Letters*, 383, 99-104.
- HONJO, Y., HRYCYNA, C. A., YAN, Q.-W., MEDINA-PÉREZ, W. Y., ROBEY, R. W., VAN DE LAAR, A., LITMAN, T., DEAN, M. & BATES, S. E. 2001. Acquired mutations in the MXR/BCRP/ABCP gene alter substrate specificity in MXR/BCRP/ABCP-overexpressing cells. *Cancer Research*, 61, 6635-6639.
- HORN, D. & DITTER, W. 1982. CHROMATOGRAPHIC STUDY OF INTERACTIONS BETWEEN POLYVINYLPIRROLIDONE AND DRUGS. *Journal of Pharmaceutical Sciences*, 71, 1021-1026.
- HU, M., LI, Y., DAVITT, C. M., HUANG, S.-M., THUMMEL, K., PENMAN, B. W. & CRESPI, C. L. 1999. Transport and metabolic characterization of Caco-2 cells expressing CYP3A4 and CYP3A4 plus oxidoreductase. *Pharmaceutical Research*, 16, 1352-1359.
- HUANG, K. T., CHEN, Y. H. & WALKER, A. M. 2004. Inaccuracies in MTS assays: major distorting effects of medium, serum albumin, and fatty acids. *Biotechniques*, 37, 406, 408, 410-2.
- HUANG, S. M., TEMPLE, R., THROCKMORTON, D. & LESKO, L. 2007. Drug interaction studies: study design, data analysis, and implications for dosing and labeling. *Clinical Pharmacology & Therapeutics*, 81, 298-304.

- HUBBARD, D., ENDA, M., BOND, T., MOGHADDAM, S. P. H., CONARTON, J., SCAIFE, C., VOLCKMANN, E. & GHANDEHARI, H. 2015. Transepithelial Transport of PAMAM Dendrimers Across Isolated Human Intestinal Tissue. *Molecular Pharmaceutics*, 12, 4099-4107.
- HUGGER, E. D., AUDUS, K. L. & BORCHARDT, R. T. 2002a. Effects of poly (ethylene glycol) on efflux transporter activity in Caco-2 cell monolayers. *Journal of pharmaceutical sciences*, 91, 1980-1990.
- HUGGER, E. D., NOVAK, B. L., BURTON, P. S., AUDUS, K. L. & BORCHARDT, R. T. 2002b. A comparison of commonly used polyethoxylated pharmaceutical excipients on their ability to inhibit P-glycoprotein activity in vitro. *Journal of Pharmaceutical Sciences*, 91, 1991-2002.
- HUGHES, J. & CROWE, A. 2010. Inhibition of P-glycoprotein-mediated efflux of digoxin and its metabolites by macrolide antibiotics. *Journal of Pharmacological Sciences*, 113, 315-324.
- INÁCIO, Â. S., MESQUITA, K. A., BAPTISTA, M., RAMALHO-SANTOS, J., VAZ, W. L. & VIEIRA, O. V. 2011. In vitro surfactant structure-toxicity relationships: implications for surfactant use in sexually transmitted infection prophylaxis and contraception. *PLoS One*, 6, e19850.
- IRVINE, J. D., TAKAHASHI, L., LOCKHART, K., CHEONG, J., TOLAN, J. W., SELICK, H. & GROVE, J. R. 1999. MDCK (Madin–Darby canine kidney) cells: a tool for membrane permeability screening. *Journal of Pharmaceutical Sciences*, 88, 28-33.
- ISHIKAWA, T., MUKAI, B., SHIRAIISHI, S., UTOGUCHI, N., FUJI, M., MATSUMOTO, M. & WATANABE, Y. 2001. Preparation of rapidly disintegrating tablet using new types of microcrystalline cellulose (PH-M series) and low substituted-hydroxypropylcellulose or spherical sugar granules by direct compression method. *Chemical and Pharmaceutical Bulletin*, 49, 134-139.
- JAROSZ, P. J. & PARROTT, E. L. 1984. Effect of lubricants on tensile strengths of tablets. *Drug Development and Industrial Pharmacy*, 10, 259-273.
- JOHNSON, B. M., CHARMAN, W. N. & PORTER, C. J. 2002a. An in vitro examination of the impact of polyethylene glycol 400, pluronic P85, and vitamin E dα-tocopheryl polyethylene glycol 1000 succinate on P-glycoprotein efflux and enterocyte-based metabolism in excised rat intestine. *AAPS Pharmsci*, 4, 193-205.
- JOHNSON, B. M., CHARMAN, W. N. & PORTER, C. J. H. 2002b. An in vitro examination of the impact of polyethylene glycol 400, pluronic P85, and vitamin E dα-tocopheryl polyethylene glycol 1000 succinate on P-glycoprotein efflux and enterocyte-based metabolism in excised rat intestine. *The AAPS Journal*, 4, 193-205.
- JOHNSON, K., HATHAWAY, R., LEUNG, P. & FRANZ, R. 1991. Effect of triacetin and polyethylene glycol 400 on some physical properties of hydroxypropyl methylcellulose free films. *International Journal of Pharmaceutics*, 73, 197-208.
- JONKER, J. W., SMIT, J. W., BRINKHUIS, R. F., MALIEPAARD, M., BEIJNEN, J. H., SCHELLENS, J. H. M. & SCHINKEL, A. H. 2000. Role of breast cancer resistance protein in the bioavailability and fetal penetration of topotecan. *Journal of the National Cancer Institute*, 92, 1651-1656.
- JULIANO, R. L. & LING, V. 1976. A surface glycoprotein modulating drug permeability in Chinese hamster ovary cell mutants. *Biochimica et Biophysica Acta (BBA)-Biomembranes*, 455, 152-162.

- KABANOV, A. V., BATRAKOVA, E. V. & ALAKHOV, V. Y. 2002. Pluronic((R)) block copolymers for overcoming drug resistance in cancer. *Advanced Drug Delivery Reviews*, 54, 759-779.
- KARARLI, T. T. 1995. Comparison of the gastrointestinal anatomy, physiology, and biochemistry of humans and commonly used laboratory animals. *Biopharmaceutics & Drug Disposition*, 16, 351-380.
- KATIKANENI, P., UPADRASHTA, S., ROWLINGS, C., NEAU, S. & HILEMAN, G. 1995a. Consolidation of ethylcellulose: effect of particle size, press speed, and lubricants. *International Journal of Pharmaceutics*, 117, 13-21.
- KATIKANENI, P. R., UPADRASHTA, S. M., NEAU, S. H. & MITRA, A. K. 1995b. Ethylcellulose matrix controlled release tablets of a water-soluble drug. *International Journal of Pharmaceutics*, 123, 119-125.
- KAUFMAN, S. & KAYE, M. 1979. Effect of ethanol upon gastric emptying. *Gut*, 20, 688-692.
- KAUL, G., HUANG, J., CHATLAPALLI, R., GHOSH, K. & NAGI, A. 2011. Quality-by-design case study: investigation of the role of poloxamer in immediate-release tablets by experimental design and multivariate data analysis. *AAPS PharmSciTech*, 12, 1064-1076.
- KEEFE, D. L., YEE, Y.-G. & KATES, R. E. 1981. Verapamil protein binding in patients and in normal subjects. *Clinical Pharmacology & Therapeutics*, 29, 21-26.
- KHAN, S., ELSHAER, A., RAHMAN, A. S., HANSON, P., PERRIE, Y. & MOHAMMED, A. R. 2011. Genomic evaluation during permeability of indomethacin and its solid dispersion. *Journal of Drug Targeting*, 19, 615-623.
- KIM, J.-S., MITCHELL, S., KIJEK, P., TSUME, Y., HILFINGER, J. & AMIDON, G. L. 2006. The suitability of an in situ perfusion model for permeability determinations: utility for BCS class I biowaiver requests. *Molecular Pharmaceutics*, 3, 686-694.
- KITAZAWA, S., JOHNNO, I., ITO, Y., TERAMURA, S. & OKADA, J. 1975. Effects of hardness on disintegration time and dissolution rate of uncoated caffeine tablets. *Journal of Pharmacy and Pharmacology*, 27, 765-770.
- KLEPSCH, F. & ECKER, G. F. 2010. Impact of the Recent Mouse P-Glycoprotein Structure for Structure-Based Ligand Design. *Molecular Informatics*, 29, 276-286.
- KOLTER, K., GOTSCHKE, M. & SCHNEIDER, T. 2002. Physicochemical characterization of Kollicoat IR®. *BASF ExAct*, 8, 2-3.
- KOMAROV, P. G., SHTIL, A. A., BUCKINGHAM, L. E., BALASUBRAMANIAN, M., PIRANER, O., EMANUELE, R. M., RONINSON, I. B. & COON, J. S. 1996. Inhibition of cytarabine-induced MDR1 (P-glycoprotein) gene activation in human tumor cells by fatty acid-polyethylene glycol-fatty acid diesters, novel inhibitors of P-glycoprotein function. *International Journal of Cancer*, 68, 245-250.
- KOOL, M., VAN DER LINDEN, M., DE HAAS, M., SCHEFFER, G. L., DE VREE, J. M. L., SMITH, A. J., JANSEN, G., PETERS, G. J., PONNE, N. & SCHEPER, R. J. 1999. MRP3, an organic anion transporter able to transport anti-cancer drugs. *Proceedings of the National Academy of Sciences*, 96, 6914-6919.
- KORNBLUM, S. S. & STOOPAK, S. B. 1973. New Tablet Disintegrating Agent - Crosslinked Polvinylpyrrolidone. *Journal of Pharmaceutical Sciences*, 62, 43-49.
- KRUIJTZER, C. M. F., BEIJNEN, J. H., ROSING, H., HUININK, W. W. T., SCHOT, M., JEWELL, R. C., PAUL, E. M. & SCHELLENS, J. H. M. 2002. Increased oral

- bioavailability of topotecan in combination with the breast cancer resistance protein and P-glycoprotein inhibitor GF120918. *Journal of Clinical Oncology*, 20, 2943-2950.
- KRYCER, I., POPE, D. G. & HERSEY, J. A. 1982. The prediction of paracetamol capping tendencies. *Journal of Pharmacy and Pharmacology*, 34, 802-804.
- KUBO, H. & MIZOBE, M. 1997. Improvement of dissolution rate and oral bioavailability of a sparingly water-soluble drug, (+/-)-5- 2-(2-naphthalenylmethyl)-5-benzoxazolyl -methyl -2,4-thiazolid inedione, in co-ground mixture with D-mannitol. *Biological & Pharmaceutical Bulletin*, 20, 460-463.
- LAHDENPÄÄ, E., NISKANEN, M. & YLIRUUSI, J. 1997. Crushing strength, disintegration time and weight variation of tablets compressed from three Avicel® PH grades and their mixtures. *European Journal of Pharmaceutics and Biopharmaceutics*, 43, 315-322.
- LAM, F. C., LIU, R., LU, P., SHAPIRO, A. B., RENOIR, J. M., SHAROM, F. J. & REINER, P. B. 2001.  $\beta$ -Amyloid efflux mediated by p-glycoprotein. *Journal of Neurochemistry*, 76, 1121-1128.
- LAMPRECHT, A. & BENOIT, J.-P. 2006. Etoposide nanocarriers suppress glioma cell growth by intracellular drug delivery and simultaneous P-glycoprotein inhibition. *Journal of Controlled Release*, 112, 208-213.
- LE FERREC, E., CHESNE, C., ARTUSSON, P., BRAYDEN, D., FABRE, G., GIRES, P., GUILLOU, F., ROUSSET, M., RUBAS, W. & SCARINO, M. L. 2001. In Vitro Models of the Intestinal Barrier. *ATLA*, 29, 649-668.
- LENNERNÄS, H. 1997. Human jejunal effective permeability and its correlation with preclinical drug absorption models. *Journal of Pharmacy and Pharmacology*, 49, 627-638.
- LENNERNÄS, H., AHRENSTEDT, Ö., HÄLLGREN, R., KNUTSON, L., RYDE, M. & PAALZOW, L. K. 1992. Regional jejunal perfusion, a new in vivo approach to study oral drug absorption in man. *Pharmaceutical Research*, 9, 1243-1251.
- LENTZ, K. A., POLLI, J. W., WRING, S. A., HUMPHREYS, J. E. & POLLI, J. E. 2000. Influence of passive permeability on apparent P-glycoprotein kinetics. *Pharmaceutical Research*, 17, 1456-1460.
- LI-BLATTER, X., NERVI, P. & SEELIG, A. 2009. Detergents as intrinsic P-glycoprotein substrates and inhibitors. *Biochimica et Biophysica Acta (BBA)-Biomembranes*, 1788, 2335-2344.
- LI, J., VOLPE, D. A., WANG, Y., ZHANG, W., BODE, C., OWEN, A. & HIDALGO, I. J. 2011a. Use of transporter knockdown Caco-2 cells to investigate the in vitro efflux of statin drugs. *Drug Metabolism and Disposition*, 39, 1196-1202.
- LI, L., YI, T. & LAM, C. W.-K. 2014a. Inhibition of human efflux transporter ABCC2 (MRP2) by self-emulsifying drug delivery system: influences of concentration and combination of excipients. *Journal of Pharmacy & Pharmaceutical Sciences*, 17, 447-460.
- LI, L., YI, T. & LAM, C. W. K. 2013a. Interactions between human multidrug resistance related protein (MRP2; ABCC2) and excipients commonly used in self-emulsifying drug delivery systems (SEDDS). *International Journal of Pharmaceutics*, 447, 192-198.
- LI, L., YI, T. & LAM, C. W. K. 2014b. Inhibition of Human Efflux Transporter ABCC2 (MRP2) by Self-emulsifying Drug Delivery System: Influences of Concentration

- and Combination of Excipients. *Journal of Pharmacy and Pharmaceutical Sciences*, 17, 447-460.
- LI, M., SI, L., PAN, H., RABBA, A. K., YAN, F., QIU, J. & LI, G. 2011b. Excipients enhance intestinal absorption of ganciclovir by P-gp inhibition: Assessed in vitro by everted gut sac and in situ by improved intestinal perfusion. *International Journal of Pharmaceutics*, 403, 37-45.
- LI, Q., RUDOLPH, V., WEIGL, B. & EARL, A. 2004. Interparticle van der Waals force in powder flowability and compactibility. *International Journal of Pharmaceutics*, 280, 77-93.
- LI, X. H., ZHAO, L. J., RUAN, K. P., FENG, Y. & RUAN, K. F. 2013b. The application of factor analysis to evaluate deforming behaviors of directly compressed powders. *Powder Technology*, 247, 47-54.
- LIN, Y., SHEN, Q., KATSUMI, H., OKADA, N., FUJITA, T., JIANG, X. & YAMAMOTO, A. 2007. Effects of Labrasol and other pharmaceutical excipients on the intestinal transport and absorption of rhodamine123, a P-glycoprotein substrate, in rats. *Biological and Pharmaceutical Bulletin*, 30, 1301-1307.
- LINDHARDT, K. & BECHGAARD, E. 2003. Sodium glycocholate transport across Caco-2 cell monolayers, and the enhancement of mannitol transport relative to transepithelial electrical resistance. *International Journal of Pharmaceutics*, 252, 181-186.
- LINDHOLM, T., LINDHOLM, B. Å., NISKANEN, M. & KOSKINIEMI, J. 1986. Polysorbate 20 as a drug release regulator in ethyl cellulose film coatings. *Journal of Pharmacy and Pharmacology*, 38, 686-688.
- LING, V. 1987. Multidrug Resistance and P-Glycoprotein Expression. *Annals of the New York Academy of Sciences*, 507, 7-8.
- LIPINSKI, C. A., LOMBARDO, F., DOMINY, B. W. & FEENEY, P. J. 1997. Experimental and computational approaches to estimate solubility and permeability in drug discovery and development settings. *Advanced Drug Delivery Reviews*, 23, 3-25.
- LIU, Y. J. & CHIU, G. N. C. 2013. Dual-Functionalized PAMAM Dendrimers with Improved P-Glycoprotein Inhibition and Tight Junction Modulating Effect. *Biomacromolecules*, 14, 4226-4235.
- LO, Y.-L. 2003. Relationships between the hydrophilic-lipophilic balance values of pharmaceutical excipients and their multidrug resistance modulating effect in Caco-2 cells and rat intestines. *Journal of Controlled Release*, 90, 37-48.
- LÖBENBERG, R. & AMIDON, G. L. 2000. Modern bioavailability, bioequivalence and biopharmaceutics classification system. New scientific approaches to international regulatory standards. *European Journal of Pharmaceutics and Biopharmaceutics*, 50, 3-12.
- LÖSCHER, W. & POTSCHKA, H. 2005. Drug resistance in brain diseases and the role of drug efflux transporters. *Nature Reviews Neuroscience*, 6, 591-602.
- LOZOYA-AGULLO, I., ZUR, M., WOLK, O., BEIG, A., GONZÁLEZ-ÁLVAREZ, I., GONZÁLEZ-ÁLVAREZ, M., MERINO-SANJUÁN, M., BERMEJO, M. & DAHAN, A. 2015. In-situ intestinal rat perfusions for human F abs prediction and BCS permeability class determination: investigation of the single-pass vs. the Doluisio experimental approaches. *International Journal of Pharmaceutics*, 480, 1-7.

- MA, Q., HAN, Y. C., CHEN, C., CAO, Y. N., WANG, S. L., SHEN, W. W., ZHANG, H. Y., LI, Y. Z., VAN DONGEN, M. A., HE, B., YU, M. M., XU, L., HOLL, M. M. B., LIU, G., ZHANG, Q. & QI, R. 2015. Oral Absorption Enhancement of Probucol by PEGylated G5 PAMAM Dendrimer Modified Nanoliposomes. *Molecular Pharmaceutics*, 12, 665-674.
- MAHMUD, T., RAFI, S. S., SCOTT, D. L., WRIGGLESWORTH, J. M. & BJARNASON, I. 1996. Nonsteroidal antiinflammatory drugs and uncoupling of mitochondrial oxidative phosphorylation. *Arthritis & Rheumatism*, 39, 1998-2003.
- MANDAGERE, A. K., THOMPSON, T. N. & HWANG, K.-K. 2002. Graphical model for estimating oral bioavailability of drugs in humans and other species from their Caco-2 permeability and in vitro liver enzyme metabolic stability rates. *Journal of Medicinal Chemistry*, 45, 304-311.
- MARTINELLO, T., KANEKO, T. M., VELASCO, M. V. R., TAQUEDA, M. E. S. & CONSIGLIERI, V. O. 2006. Optimization of poorly compactable drug tablets manufactured by direct compression using the mixture experimental design. *International Journal of Pharmaceutics*, 322, 87-95.
- MATSSON, P., PEDERSEN, J. M., NORINDER, U., BERGSTRÖM, C. A. S. & ARTURSSON, P. 2009. Identification of novel specific and general inhibitors of the three major human ATP-binding cassette transporters P-gp, BCRP and MRP2 among registered drugs. *Pharmaceutical Research*, 26, 1816-1831.
- MCLAUGHLIN, R., BANBURY, S. & CROWLEY, K. 2009. Orally disintegrating tablets: the effect of recent FDA guidance on ODT technologies and applications. *Pharmaceutical Technology*, 2009.
- MEASE, K., SANE, R., PODILA, L. & TAUB, M. E. 2012. Differential selectivity of efflux transporter inhibitors in Caco-2 and MDCK-MDR1 monolayers: A strategy to assess the interaction of a new chemical entity with P-gp, BCRP, and MRP2. *Journal of Pharmaceutical Sciences*, 101, 1888-1897.
- MEHUYS, E., REMON, J. P., KORST, A., VAN BORTEL, L., MOLS, R., AUGUSTIJNS, P., PORTER, C. & VERVAET, C. 2005. Human bioavailability of propranolol from a matrix-in-cylinder system with a HPMC-Gelucire® core. *Journal of Controlled Release*, 107, 523-536.
- MILLER, D. W., BATRAKOVA, E. V., WALTNER, T. O., ALAKHOV, V. Y. & KABANOV, A. V. 1997. Interactions of pluronic block copolymers with brain microvessel endothelial cells: evidence of two potential pathways for drug absorption. *Bioconjugate Chemistry*, 8, 649-657.
- MILNE, C.-P. & BRUSS, J. B. 2008. The economics of pediatric formulation development for off-patent drugs. *Clinical Therapeutics*, 30, 2133-2145.
- MISHRA, D. N., BINDAL, M., SINGH, S. K. & VIJAYA KUMAR, S. G. 2006. Spray dried excipient base: a novel technique for the formulation of orally disintegrating tablets. *Chemical and Pharmaceutical Bulletin*, 54, 99-102.
- MISHRA, M. & MISHRA, B. 2010. Design and evaluation of microporous membrane coated matrix tablets for a highly water soluble drug. *Chemical and Pharmaceutical Bulletin*, 58, 995-1000.
- MITREVEJ, A., SINCHAIPANID, N. & FAROONGSARNG, D. 1996. Spray-dried rice starch: comparative evaluation of direct compression fillers. *Drug Development and Industrial Pharmacy*, 22, 587-594.

- MIYADAI, N., HIGASHI, K., MORIBE, K. & YAMAMOTO, K. 2012. Optimization and characterization of direct coating for ibuprofen particles using a composite fluidized bed. *Advanced Powder Technology*, 23, 40-45.
- MIZUNO, N., NIWA, T., YOTSUMOTO, Y. & SUGIYAMA, Y. 2003. Impact of drug transporter studies on drug discovery and development. *Pharmacological Reviews*, 55, 425-461.
- MOTTINO, A. D., HOFFMAN, T., JENNES, L. & VORE, M. 2000. Expression and localization of multidrug resistant protein mrp2 in rat small intestine. *Journal of Pharmacology and Experimental Therapeutics*, 293, 717-723.
- MUŽÍKOVÁ, J. & EIMEROVÁ, I. 2011. A study of the compaction process and the properties of tablets made of a new co-processed starch excipient. *Drug Development and Industrial Pharmacy*, 37, 576-582.
- MUZIKOVA, J., VYHLIDALOVA, B. & PEKAREK, T. 2012. A study of micronized poloxamers as lubricants in direct compression of tablets. *Acta Poloniae Pharmaceutica*, 70, 1087-1096.
- MUZÍKOVÁ, J., VYHLÍDALOVÁ, B. & PEKÁREK, T. 2012. A study of micronized poloxamers as lubricants in direct compression of tablets. *Acta Poloniae Pharmaceutica*, 70, 1087-1096.
- NAGEL, K. M. & PECK, G. E. 2003. Investigating the effects of excipients on the powder flow characteristics of theophylline anhydrous powder formulations. *Drug Development and Industrial Pharmacy*, 29, 277-287.
- NAIL, S. L. & GATLIN, L. A. 1993. Freeze drying: principles and practice. *Pharmaceutical Dosage Forms: Parenteral Medications*, 2, 163-233.
- NAITO, M. & TSURUO, T. 1989. Competitive-inhibition by verapamil of atp-dependent high-affinity vincristine binding to the plasma-membrane of multidrug-resistant k562 cells without calcium-ion involvement. *Cancer Research*, 49, 1452-1455.
- NIMMO, W., HEADING, R., WILSON, J., TOTHILL, P. & PRESCOTT, L. 1975. Inhibition of gastric emptying and drug absorption by narcotic analgesics. *British Journal of Clinical Pharmacology*, 2, 509-513.
- ODA, M., SAITOH, H., KOBAYASHI, M. & AUNGST, B. J. 2004.  $\beta$ -Cyclodextrin as a suitable solubilizing agent for in situ absorption study of poorly water-soluble drugs. *International Journal of Pharmaceutics*, 280, 95-102.
- OKHAMAFE, A. O. & YORK, P. 1985. Interaction Phenomena in some Aqueous-Based Tablet Coating Polymer Systems. *Pharmaceutical Research*, 2, 19-23.
- OKUDA, Y., IRISAWA, Y., OKIMOTO, K., OSAWA, T. & YAMASHITA, S. 2012. Further improvement of orally disintegrating tablets using micronized ethylcellulose. *International Journal of Pharmaceutics*, 423, 351-359.
- PALM, K., STENBERG, P., LUTHMAN, K. & ARTURSSON, P. 1997. Polar molecular surface properties predict the intestinal absorption of drugs in humans. *Pharmaceutical Research*, 14, 568-571.
- PAN, B. F., DUTT, A. & NELSON, J. A. 1994. Enhanced transepithelial flux of cimetidine by madin-darby canine kidney-cells overexpressing human p-glycoprotein. *Journal of Pharmacology and Experimental Therapeutics*, 270, 1-7.
- PASTAN, I., GOTTESMAN, M. M., UEDA, K., LOVELACE, E., RUTHERFORD, A. V. & WILLINGHAM, M. C. 1988. A retrovirus carrying an MDR1 cDNA confers multidrug resistance and polarized expression of P-glycoprotein in MDCK cells. *Proceedings of the National Academy of Sciences*, 85, 4486-4490.

- PATIST, A., BHAGWAT, S., PENFIELD, K., AIKENS, P. & SHAH, D. 2000. On the measurement of critical micelle concentrations of pure and technical-grade nonionic surfactants. *Journal of Surfactants and Detergents*, 3, 53-58.
- PAULI-MAGNUS, C., VON RICHTER, O., BURK, O., ZIEGLER, A., METTANG, T., EICHELBAUM, M. & FROMM, M. F. 2000. Characterization of the major metabolites of verapamil as substrates and inhibitors of P-glycoprotein. *Journal of Pharmacology and Experimental Therapeutics*, 293, 376-382.
- PENG, K.-C., CLUZEAUD, F., BENS, M., VAN HUYEN, J.-P. D., WIOLAND, M. A., LACAVER, R. & VANDEWALLE, A. 1999. Tissue and cell distribution of the multidrug resistance-associated protein (MRP) in mouse intestine and kidney. *Journal of Histochemistry & Cytochemistry*, 47, 757-767.
- PERLOFF, M. D., MOLTKE, L. L. & GREENBLATT, D. J. 2002. Fexofenadine Transport in Caco-2 Cells: Inhibition with Verapamil and Ritonavir. *The Journal of Clinical Pharmacology*, 42, 1269-1274.
- PERLOFF, M. D., STÖRMER, E., VON MOLTKE, L. L. & GREENBLATT, D. J. 2003. Rapid assessment of P-glycoprotein inhibition and induction in vitro. *Pharmaceutical Research*, 20, 1177-1183.
- POLLI, J. W., WRING, S. A., HUMPHREYS, J. E., HUANG, L., MORGAN, J. B., WEBSTER, L. O. & SERABJIT-SINGH, C. S. 2001. Rational use of in vitro P-glycoprotein assays in drug discovery. *Journal of Pharmacology and Experimental Therapeutics*, 299, 620-628.
- POND, S. M. & TOZER, T. N. 1984. First-pass elimination basic concepts and clinical consequences. *Clinical Pharmacokinetics*, 9, 1-25.
- POOLE, K. 2005. Efflux-mediated antimicrobial resistance. *Journal of Antimicrobial Chemotherapy*, 56, 20-51.
- POYHIA, R., SEPPALA, T., OLKKOLA, K. & KALSO, E. 1992. The pharmacokinetics and metabolism of oxycodone after intramuscular and oral administration to healthy subjects. *British Journal of Clinical Pharmacology*, 33, 617-621.
- POYHIA, R., VAINIO, A. & KALSO, E. 1993. A review of oxycodones clinical pharmacokinetics and pharmacodynamics. *Journal of Pain and Symptom Management*, 8, 63-67.
- PRIME-CHAPMAN, H. M., FEARN, R. A., COOPER, A. E., MOORE, V. & HIRST, B. H. 2004. Differential multidrug resistance-associated protein 1 through 6 isoform expression and function in human intestinal epithelial Caco-2 cells. *Journal of Pharmacology and Experimental Therapeutics*, 311, 476-484.
- PROFIT, L., EAGLING, V. A. & BACK, D. J. 1999. Modulation of P-glycoprotein function in human lymphocytes and Caco-2 cell monolayers by HIV-1 protease inhibitors. *Aids*, 13, 1623-1627.
- QUADIR, A. & KOLTER, K. 2006. A comparative study of current superdisintegrants. *Pharmaceutical Technology*.
- RAINSFORD, K. & WILLIS, C. 1982. Relationship of gastric mucosal damage induced in pigs by antiinflammatory drugs to their effects on prostaglandin production. *Digestive Diseases and Sciences*, 27, 624-635.
- RÄSÄNEN, E., ANTIKAINEN, O. & YLIRUUSI, J. 2003. A new method to predict flowability using a microscale fluid bed. *Aaps Pharmscitech*, 4, 418-424.
- RASENACK, N. & MÜLLER, B. W. 2002. Ibuprofen crystals with optimized properties. *International Journal of Pharmaceutics*, 245, 9-24.

- RAUB, T. J. 2006. P-glycoprotein recognition of substrates and circumvention through rational drug design. *Molecular Pharmaceutics*, 3, 3-25.
- RAUTIO, J., HUMPHREYS, J. E., WEBSTER, L. O., BALAKRISHNAN, A., KEOGH, J. P., KUNTA, J. R., SERABJIT-SINGH, C. J. & POLLI, J. W. 2006. In vitro p-glycoprotein inhibition assays for assessment of clinical drug interaction potential of new drug candidates: a recommendation for probe substrates. *Drug Metabolism and Disposition*, 34, 786-792.
- RAVIV, Y., POLLARD, H., BRUGGEMANN, E., PASTAN, I. & GOTTESMAN, M. 1990. Photosensitized labeling of a functional multidrug transporter in living drug-resistant tumor cells. *Journal of Biological Chemistry*, 265, 3975-3980.
- REES, J. & RUE, P. 1978. Time-dependent deformation of some direct compression excipients. *Journal of Pharmacy and Pharmacology*, 30, 601-607.
- REGE, B. D., KAO, J. P. Y. & POLLI, J. E. 2002. Effects of nonionic surfactants on membrane transporters in Caco-2 cell monolayers. *European Journal of Pharmaceutical Sciences*, 16, 237-246.
- REGE, B. D., YU, L. X., HUSSAIN, A. S. & POLLI, J. E. 2001. Effect of common excipients on Caco-2 transport of low-permeability drugs. *Journal of Pharmaceutical Sciences*, 90, 1776-1786.
- REGEV, R., ASSARAF, Y. G. & EYTAN, G. D. 1999. Membrane fluidization by ether, other anesthetics, and certain agents abolishes P-glycoprotein ATPase activity and modulates efflux from multidrug-resistant cells. *European Journal of Biochemistry*, 259, 18-24.
- RIAD, L. E. & SAWCHUK, R. J. 1991. Effect of polyethylene glycol 400 on the intestinal permeability of carbamazepine in the rabbit. *Pharmaceutical Research*, 8, 491-497.
- RICHARDSON, J., SCALERA, V. & SIMMONS, N. 1981. Identification of two strains of MDCK cells which resemble separate nephron tubule segments. *Biochimica et Biophysica Acta (BBA)-General Subjects*, 673, 26-36.
- ROHERA, B. D. & PARIKH, N. H. 2002. Influence of type and level of water-soluble additives on drug release and surface and mechanical properties of Surelease® films. *Pharmaceutical Development and Technology*, 7, 421-432.
- ROJAS, J. & KUMAR, V. 2012. Evaluation of the disintegration properties of microcrystalline cellulose II and commercial disintegrants. *Die Pharmazie-An International Journal of Pharmaceutical Sciences*, 67, 500-506.
- ROOHINEJAD, S., MIDDENDORF, D., BURRITT, D. J., BINDRICH, U., EVERETT, D. W. & OEY, I. 2014. Capacity of natural  $\beta$ -carotene loaded microemulsion to protect Caco-2 cells from oxidative damage caused by exposure to H<sub>2</sub>O<sub>2</sub>. *Food Research International*, 66, 469-477.
- ROWE, R. C., SHESKEY, P. J. & QUINN, M. E. 2009. Handbook of Pharmaceutical Excipients. *Pharmaceutical Press*, 6th Edition.
- SACHS-BARRABLE, K., THAMBOO, A., LEE, S. D. & WASAN, K. M. 2007. Lipid excipients Peceol and Gelucire 44/14 decrease P-glycoprotein mediated efflux of rhodamine 123 partially due to modifying P-glycoprotein protein expression within Caco-2 cells. *Journal of Pharmacy & Pharmaceutical Sciences*, 10, 319-31.
- SADEKAR, S., THIAGARAJAN, G., BARTLETT, K., HUBBARD, D., RAY, A., MCGILL, L. D. & GHANDEHARI, H. 2013. Poly(amido amine) dendrimers as absorption enhancers for oral delivery of camptothecin. *International Journal of Pharmaceutics*, 456, 175-185.

- SAMPAIO, J. L., MORENO, M. J. & VAZ, W. L. C. 2005. Kinetics and thermodynamics of association of a fluorescent lysophospholipid derivative with lipid bilayers in liquid-ordered and liquid-disordered phases. *Biophysical Journal*, 88, 4064-4071.
- SANDRI, G., BONFERONI, M. C., ROSSI, S., FERRARI, F., GIBIN, S., ZAMBITO, Y., DI COLO, G. & CAMELLA, C. 2007. Nanoparticles based on N-trimethylchitosan: evaluation of absorption properties using in vitro (Caco-2 cells) and ex vivo (excised rat jejunum) models. *European Journal of Pharmaceutics and Biopharmaceutics*, 65, 68-77.
- SASTRY, S. V., NYSHADHAM, J. R. & FIX, J. A. 2000. Recent technological advances in oral drug delivery—a review. *Pharmaceutical Science & Technology Today*, 3, 138-145.
- SÄWE, J. 1986. High-dose morphine and methadone in cancer patients. *Clinical Pharmacokinetics*, 11, 87-106.
- SCHUETZ, E. G., YASUDA, K., ARIMORI, K. & SCHUETZ, J. D. 1998. HumanMDR1 and Mousemdr1a P-Glycoprotein Alter the Cellular Retention and Disposition of Erythromycin, but Not of Retinoic Acid or Benzo(a)pyrene. *Archives of Biochemistry and Biophysics*, 350, 340-347.
- SEAGER, H. 1998. Drug-delivery products and the zydys fast-dissolving dosage form\*. *Journal of Pharmacy and Pharmacology*, 50, 375-382.
- SHANGRAW, R., MITREVEJ, A. & SHAH, M. 1980. A new era of tablet disintegrants. *Pharmaceutical Technology*, 4, 49-57.
- SHAPIRO, A. B., FOX, K., LAM, P. & LING, V. 1999. Stimulation of P-glycoprotein-mediated drug transport by prazosin and progesterone. *European Journal of Biochemistry*, 259, 841-850.
- SHAPIRO, A. B. & LING, V. 1997. Positively cooperative sites for drug transport by P-glycoprotein with distinct drug specificities. *European Journal of Biochemistry*, 250, 130-137.
- SHEN, Q., LIN, Y., HANDA, T., DOI, M., SUGIE, M., WAKAYAMA, K., OKADA, N., FUJITA, T. & YAMAMOTO, A. 2006. Modulation of intestinal P-glycoprotein function by polyethylene glycols and their derivatives by in vitro transport and in situ absorption studies. *International Journal of Pharmaceutics*, 313, 49-56.
- SHESHALA, R., KHAN, N. & DARWIS, Y. 2011. Formulation and optimization of orally disintegrating tablets of sumatriptan succinate. *Chemical and Pharmaceutical Bulletin*, 59, 920-928.
- SHIMADA, T., YAMAZAKI, H., MIMURA, M., INUI, Y. & GUENGERICH, F. P. 1994. Interindividual variations in human liver cytochrome P-450 enzymes involved in the oxidation of drugs, carcinogens and toxic chemicals: studies with liver microsomes of 30 Japanese and 30 Caucasians. *Journal of Pharmacology and Experimental Therapeutics*, 270, 414-423.
- SHONO, Y., NISHIHARA, H., MATSUDA, Y., FURUKAWA, S., OKADA, N., FUJITA, T. & YAMAMOTO, A. 2004. Modulation of intestinal P-glycoprotein function by cremophor EL and other surfactants by an in vitro diffusion chamber method using the isolated rat intestinal membranes. *Journal of Pharmaceutical Sciences*, 93, 877-885.
- SHU, T., SUZUKI, H., HIRONAKA, K. & ITO, K. 2002. Studies of rapidly disintegrating tablets in the oral cavity using co-ground mixtures of mannitol with crospovidone. *Chemical and Pharmaceutical Bulletin*, 50, 193-198.

- SINICROPE, F. A., DUDEJA, P., BISSONNETTE, B., SAFA, A. & BRASITUS, T. 1992. Modulation of P-glycoprotein-mediated drug transport by alterations in lipid fluidity of rat liver canalicular membrane vesicles. *Journal of Biological Chemistry*, 267, 24995-25002.
- SLATER, L. M., SWEET, P., STUPECKY, M., WETZEL, M. W. & GUPTA, S. 1986. Cyclosporine-A Corrects Daunorubicin Resistance in Ehrlich-Ascites-Carcinoma. *British Journal of Cancer*, 54, 235-238.
- STEPHENS, R., O'NEILL, C., WARHURST, A., CARLSON, G., ROWLAND, M. & WARHURST, G. 2001. Kinetic profiling of P-glycoprotein-mediated drug efflux in rat and human intestinal epithelia. *Journal of Pharmacology and Experimental Therapeutics*, 296, 584-591.
- STÖRMER, E., PERLOFF, M. D., VON MOLTKE, L. L. & GREENBLATT, D. J. 2001. Methadone inhibits rhodamine123 transport in Caco-2 cells. *Drug Metabolism and Disposition*, 29, 954-956.
- STRICKLEY, R. G. 2004. Solubilizing excipients in oral and injectable formulations. *Pharmaceutical Research*, 21, 201-230.
- SUN, C. C. 2016. Quantifying effects of moisture content on flow properties of microcrystalline cellulose using a ring shear tester. *Powder Technology*, 289, 104-108.
- TAIPALENSUU, J., TÖRNBLM, H., LINDBERG, G., EINARSSON, C., SJÖQVIST, F., MELHUS, H., GARBERG, P., SJÖSTRÖM, B., LUNDGREN, B. & ARTURSSON, P. 2001. Correlation of gene expression of ten drug efflux proteins of the ATP-binding cassette transporter family in normal human jejunum and in human intestinal epithelial Caco-2 cell monolayers. *Journal of Pharmacology and Experimental Therapeutics*, 299, 164-170.
- TAMAI, I. & SAFA, A. R. 1991. Azidopine noncompetitively interacts with vinblastine and cyclosporin A binding to P-glycoprotein in multidrug resistant cells. *Journal of Biological Chemistry*, 266, 16796-16800.
- TANG, A. S., CHIKHALE, P. J., SHAH, P. K. & BORCHARDT, R. T. 1993. Utilization of a human intestinal epithelial cell culture system (Caco-2) for evaluating cytoprotective agents. *Pharmaceutical Research*, 10, 1620-1626.
- TAPIERO, H., MUNCK, J.-N., FOURCADE, A. & LAMPIDIS, T. J. 1984. Cross-resistance to rhodamine 123 in adriamycin-and daunorubicin-resistant Friend leukemia cell variants. *Cancer Research*, 44, 5544-5549.
- TAYLOR, M. K., GINSBURG, J., HICKEY, A. J. & GHEYAS, F. 2000. Composite method to quantify powder flow as a screening method in early tablet or capsule formulation development. *AAPS PharmSciTech*, 1, 20-30.
- TEOW, H. M., ZHOU, Z. Y., NAJLAH, M., YUSOF, S. R., ABBOTT, N. J. & D'EMANUELE, A. 2013. Delivery of paclitaxel across cellular barriers using a dendrimer-based nanocarrier. *International Journal of Pharmaceutics*, 441, 701-711.
- TIBERG, F., MALMSTEN, M., LINSE, P. & LINDMAN, B. 1991. Kinetic and equilibrium aspects of block copolymer adsorption. *Langmuir*, 7, 2723-2730.
- TOMPKINS, L., LYNCH, C., HAIDAR, S., POLLI, J. & WANG, H. 2010. Effects of commonly used excipients on the expression of CYP3A4 in colon and liver cells. *Pharmaceutical Research*, 27, 1703-1712.

- TROUTMAN, M. D. & THAKKER, D. R. 2003. Efflux ratio cannot assess P-glycoprotein-mediated attenuation of absorptive transport: asymmetric effect of P-glycoprotein on absorptive and secretory transport across Caco-2 cell monolayers. *Pharmaceutical Research*, 20, 1200-1209.
- TSURUO, T., IIDA, H., TSUKAGOSHI, S. & SAKURAI, Y. 1981. Overcoming of vincristine resistance in P388 leukemia in vivo and in vitro through enhanced cytotoxicity of vincristine and vinblastine by verapamil. *Cancer Research*, 41, 1967-1972.
- UEDA, K., CARDARELLI, C., GOTTESMAN, M. M. & PASTAN, I. 1987. Expression of a full-length cDNA for the human "MDR1" gene confers resistance to colchicine, doxorubicin, and vinblastine. *Proceedings of the National Academy of Sciences*, 84, 3004-3008.
- UJHELYI, Z., FENYVESI, F., VÁRADI, J., FEHÉR, P., KISS, T., VESZELKA, S., DELI, M., VECSENYÉS, M. & BÁCSKAY, I. 2012. Evaluation of cytotoxicity of surfactants used in self-micro emulsifying drug delivery systems and their effects on paracellular transport in Caco-2 cell monolayer. *European Journal of Pharmaceutical Sciences*, 47, 564-573.
- UPADRASHTA, S. M., KATIKANENI, P. R., HILEMAN, G. A. & KESHARY, P. R. 1993. Direct compression controlled release tablets using ethylcellulose matrices. *Drug Development and Industrial Pharmacy*, 19, 449-460.
- UPADRASHTA, S. M., KATIKANENI, P. R., HILEMAN, G. A., NEAU, S. H. & ROWLINGS, C. E. 1994. Compressibility and compactibility properties of ethylcellulose. *International Journal of Pharmaceutics*, 112, 173-179.
- USMANI, M. T., SHOAIB, M. H., NASIRI, M. I., YOUSUF, R. I., ZAHEER, K. & AHMED, K. 2015. Development and Evaluation of Orally Disintegrating Tablets of Montelukast Sodium by Direct Compression Method. *Tropical Journal of Pharmaceutical Research*, 14, 1-6.
- USP 2011. United States Pharmacopeia, Chapter <905> UNIFORMITY OF DOSAGE UNITS.
- USP 2012a. United States Pharmacopeia, Chapter <616> BULK DENSITY AND TAPPED DENSITY OF POWDERS.
- USP 2012b. United States Pharmacopeia, Chapter <701> DISINTEGRATION.
- USP 2012c. United States Pharmacopeia, Chapter <1217> TABLET BREAKING FORCE.
- USP 2013. United States Pharmacopeia, Chapter <1216> TABLET FRIABILITY. p974.
- USSING, H. H. & ZERAHN, K. 1951. Active Transport of Sodium as the Source of Electric Current in the Short-circuited Isolated Frog Skin. *Acta Physiologica Scandinavica*, 23, 110-127.
- VAN AUBEL, R. A., HARTOG, A., BINDELS, R. J., VAN OS, C. H. & RUSSEL, F. G. 2000. Expression and immunolocalization of multidrug resistance protein 2 in rabbit small intestine. *European Journal of Pharmacology*, 400, 195-198.
- VAN ITALLIE, C. M., FANNING, A. S., BRIDGES, A. & ANDERSON, J. M. 2009. ZO-1 stabilizes the tight junction solute barrier through coupling to the perijunctional cytoskeleton. *Molecular Biology of the Cell*, 20, 3930-3940.
- VARMA, M. V. S. & PANCHAGNULA, R. 2005. Enhanced oral paclitaxel absorption with vitamin E-TPGS: Effect on solubility and permeability in vitro, in situ and in vivo. *European Journal of Pharmaceutical Sciences*, 25, 445-453.

- VELLONEN, K.-S., HONKAKOSKI, P. & URTTI, A. 2004. Substrates and inhibitors of efflux proteins interfere with the MTT assay in cells and may lead to underestimation of drug toxicity. *European Journal of Pharmaceutical Sciences*, 23, 181-188.
- WACHER, V. J., WU, C. Y. & BENET, L. Z. 1995. Overlapping substrate specificities and tissue distribution of cytochrome P450 3A and P-glycoprotein: Implications for drug delivery and activity in cancer chemotherapy. *Molecular Carcinogenesis*, 13, 129-134.
- WADE, A. & WELLER, P. J. 1994. *Handbook of pharmaceutical excipients*, Pharmaceutical Press.
- WAGER, T. T., CHANDRASEKARAN, R. Y., HOU, X., TROUTMAN, M. D., VERHOEST, P. R., VILLALOBOS, A. & WILL, Y. 2010. Defining desirable central nervous system drug space through the alignment of molecular properties, in vitro ADME, and safety attributes. *ACS Chemical Neuroscience*, 1, 420-434.
- WAGNER, M. C., RHODES, G., WANG, E., PRUTHI, V., ARIF, E., SALEEM, M. A., WEAN, S. E., GARG, P., VERMA, R. & HOLZMAN, L. B. 2008. Ischemic injury to kidney induces glomerular podocyte effacement and dissociation of slit diaphragm proteins Neph1 and ZO-1. *Journal of Biological Chemistry*, 283, 35579-35589.
- WALTER, E. & KISSEL, T. 1995. Heterogeneity in the human intestinal cell line Caco-2 leads to differences in transepithelial transport. *European Journal of Pharmaceutical Sciences*, 3, 215-230.
- WANG, E. J., CASCIANO, C. N., CLEMENT, R. P. & JOHNSON, W. W. 2001. Active transport of fluorescent P-glycoprotein substrates: Evaluation as markers and interaction with inhibitors. *Biochemical and Biophysical Research Communications*, 289, 580-585.
- WANG, Y., HAO, D., STEIN, W. D. & YANG, L. 2006. A kinetic study of Rhodamine123 pumping by P-glycoprotein. *Biochimica et Biophysica Acta (BBA)-Biomembranes*, 1758, 1671-1676.
- WATANABE, Y., KOIZUMI, K., ZAMA, Y., KIRIYAMA, M. & MATSUMOTO, Y. 1995. New compressed tablet rapidly disintegrating in saliva in the mouth using crystalline cellulose and a disintegrant. *Biological and Pharmaceutical Bulletin*, 18, 1308-1310.
- WESTERHOUT, J., VAN DE STEEG, E., GROSSOUW, D., ZEIJDNER, E. E., KRUL, C. A., VERWEI, M. & WORTELBOER, H. M. 2014. A new approach to predict human intestinal absorption using porcine intestinal tissue and biorelevant matrices. *European Journal of Pharmaceutical Sciences*, 63, 167-177.
- WILSON, G., HASSAN, I., DIX, C., WILLIAMSON, I., SHAH, R., MACKAY, M. & ARTURSSON, P. 1990. Transport and permeability properties of human Caco-2 cells: an in vitro model of the intestinal epithelial cell barrier. *Journal of Controlled Release*, 11, 25-40.
- WILSON, T. H. & WISEMAN, G. 1954. The use of sacs of everted small intestine for the study of the transference of substances from the mucosal to the serosal surface. *The Journal of Physiology*, 123, 116.
- WOODCOCK, D. M., JEFFERSON, S., LINSENMEYER, M. E., CROWTHER, P. J., CHOJNOWSKI, G. M., WILLIAMS, B. & BERTONCELLO, I. 1990. Reversal of

- the multidrug resistance phenotype with cremophor EL, a common vehicle for water-insoluble vitamins and drugs. *Cancer Research*, 50, 4199-4203.
- WU, X., WHITFIELD, L. R. & STEWART, B. H. 2000. Atorvastatin transport in the Caco-2 cell model: contributions of P-glycoprotein and the proton-monocarboxylic acid co-transporter. *Pharmaceutical Research*, 17, 209-215.
- XU, M., MOLENTO, M., BLACKHALL, W., RIBEIRO, P., BEECH, R. & PRICHARD, R. 1998. Ivermectin resistance in nematodes may be caused by alteration of P-glycoprotein homolog. *Molecular and Biochemical Parasitology*, 91, 327-335.
- YAMAGATA, T., KUSUHARA, H., MORISHITA, M., TAKAYAMA, K., BENAMEUR, H. & SUGIYAMA, Y. 2007a. Effect of excipients on breast cancer resistance protein substrate uptake activity. *Journal of Controlled Release*, 124, 1-5.
- YAMAGATA, T., KUSUHARA, H., MORISHITA, M., TAKAYAMA, K., BENAMEUR, H. & SUGIYAMA, Y. 2007b. Improvement of the oral drug absorption of topotecan through the inhibition of intestinal xenobiotic efflux transporter, breast cancer resistance protein, by excipients. *Drug Metabolism and Disposition*, 35, 1142-1148.
- YAMAGATA, T., MORISHITA, M., KUSUHARA, H., TAKAYAMA, K., BENAMEUR, H. & SUGIYAMA, Y. 2009. Characterization of the inhibition of breast cancer resistance protein-mediated efflux of mitoxantrone by pharmaceutical excipients. *International Journal of Pharmaceutics*, 370, 216-219.
- YAMASHITA, S., FURUBAYASHI, T., KATAOKA, M., SAKANE, T., SEZAKI, H. & TOKUDA, H. 2000. Optimized conditions for prediction of intestinal drug permeability using Caco-2 cells. *European Journal of Pharmaceutical Sciences*, 10, 195-204.
- YAMAZAKI, T., SATO, Y., HANAI, M., MOCHIMARU, J., TSUJINO, I., SAWADA, U. & HORIE, T. 2000. Non-ionic detergent Tween 80 modulates VP-16 resistance in classical multidrug resistant K562 cells via enhancement of VP-16 influx. *Cancer Letters*, 149, 153-161.
- YANG, S., LIU, J., CHEN, Y. & JIANG, J. 2012. Reversal effect of Tween-20 on multidrug resistance in tumor cells in vitro. *Biomedicine & Pharmacotherapy*, 66, 187-194.
- YEH, P.-Y., SMITH, P. L. & ELLENS, H. 1994. Effect of medium-chain glycerides on physiological properties of rabbit intestinal epithelium in vitro. *Pharmaceutical Research*, 11, 1148-1154.
- YU, L., BRIDGERS, A., POLLI, J., VICKERS, A., LONG, S., ROY, A., WINNIKE, R. & COFFIN, M. 1999. Vitamin E-TPGS increases absorption flux of an HIV protease inhibitor by enhancing its solubility and permeability<sup>1</sup>. *Pharmaceutical Research*, 16, 1812-1817.
- YUASA, H., MATSUDA, K. & WATANABE, J. 1993. Influence of anesthetic regimens on intestinal absorption in rats. *Pharmaceutical Research*, 10, 884-888.
- YUMOTO, R., MURAKAMI, T., NAKAMOTO, Y., HASEGAWA, R., NAGAI, J. & TAKANO, M. 1999. Transport of rhodamine 123, a P-glycoprotein substrate, across rat intestine and Caco-2 cell monolayers in the presence of cytochrome P-450 3A-related compounds. *Journal of Pharmacology and Experimental Therapeutics*, 289, 149-155.
- YUNG-CHI, C. & PRUSOFF, W. H. 1973. Relationship between the inhibition constant (K<sub>i</sub>) and the concentration of inhibitor which causes 50 per cent inhibition (I<sub>50</sub>) of an enzymatic reaction. *Biochemical Pharmacology*, 22, 3099-3108.

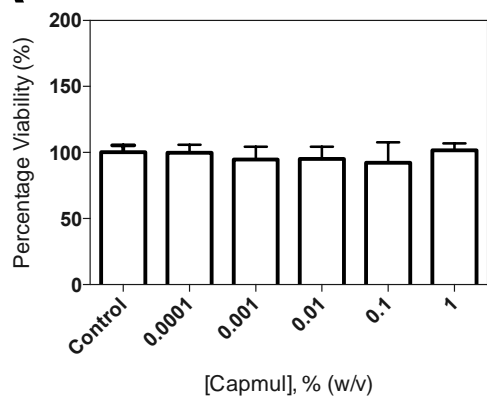
- YUNOMAE, K., ARIMA, H., HIRAYAMA, F. & UEKAMA, K. 2003. Involvement of cholesterol in the inhibitory effect of dimethyl- $\beta$ -cyclodextrin on P-glycoprotein and MRP2 function in Caco-2 cells. *FEBS Letters*, 536, 225-231.
- ZAMAN, G. J., VERSANTVOORT, C. H., SMIT, J. J., EIJDENS, E. W., DE HAAS, M., SMITH, A. J., BROXTERMAN, H. J., MULDER, N. H., DE VRIES, E. G. & BAAS, F. 1993. Analysis of the expression of MRP, the gene for a new putative transmembrane drug transporter, in human multidrug resistant lung cancer cell lines. *Cancer Research*, 53, 1747-1750.
- ZAMEK-GLISZCZYNSKI, M. J., XIONG, H., PATEL, N. J., TURNCLIFF, R. Z., POLLACK, G. M. & BROUWER, K. L. R. 2003. Pharmacokinetics of 5 (and 6)-carboxy-2',7'-dichlorofluorescein and its diacetate promoiety in the liver. *Journal of Pharmacology and Experimental Therapeutics*, 304, 801-809.
- ZHANG, Q.-Y., DUNBAR, D., OSTROWSKA, A., ZEISLOFT, S., YANG, J. & KAMINSKY, L. S. 1999. Characterization of human small intestinal cytochromes P-450. *Drug Metabolism and Disposition*, 27, 804-809.
- ZHAO, Y. H., LE, J., ABRAHAM, M. H., HERSEY, A., EDDERSHAW, P. J., LUSCOMBE, C. N., BOUTINA, D., BECK, G., SHERBORNE, B. & COOPER, I. 2001. Evaluation of human intestinal absorption data and subsequent derivation of a quantitative structure-activity relationship (QSAR) with the Abraham descriptors. *Journal of Pharmaceutical Sciences*, 90, 749-784.
- ZILLER, K. H. & RUPPRECHT, H. 1988. Control of Crystal-Growth in Drug Suspensions .1. Design of a Control Unit and Application to Acetaminophen Suspensions. *Drug Development and Industrial Pharmacy*, 14, 2341-2370.
- ZIMMER, L., KASPEREK, R. & POLESZAK, E. 2015. Dissolution properties and kinetic study of sulfadimidine and trimethoprim tablets containing four different superdisintegrants. *Acta Poloniae Pharmaceutica*, 72, 347-355.
- ZIMMERMANN, C., GUTMANN, H., HRUZ, P., GUTZWILLER, J. P., BEGLINGER, C. & DREWE, J. 2005. Mapping of multidrug resistance gene 1 and multidrug resistance-associated protein isoform 1 to 5 mRNA expression along the human intestinal tract. *Drug Metabolism and Disposition*, 33, 219-224.

**Appendix**

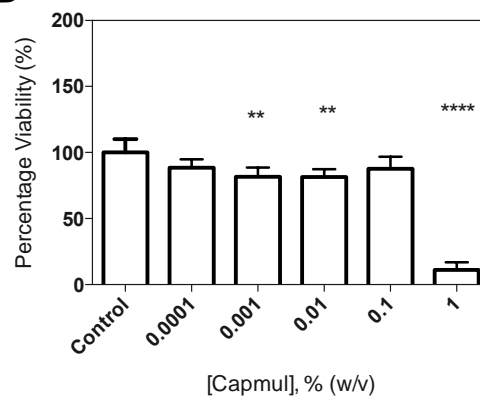
MTT Toxicology Data

Appendix – MTT Toxicology Data

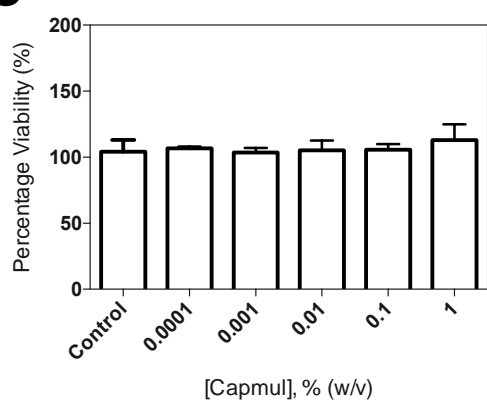
**A**



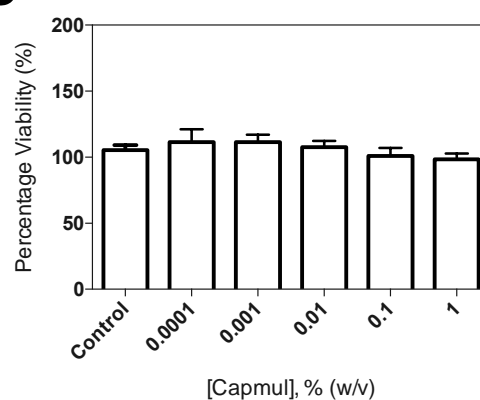
**B**



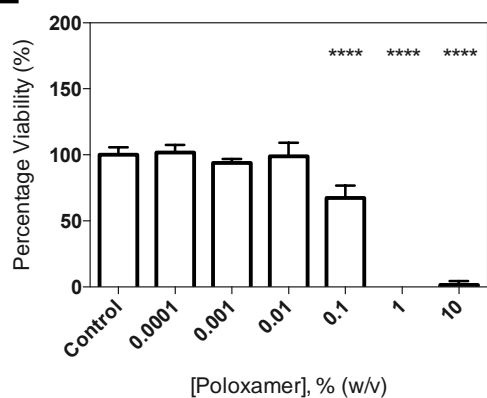
**C**



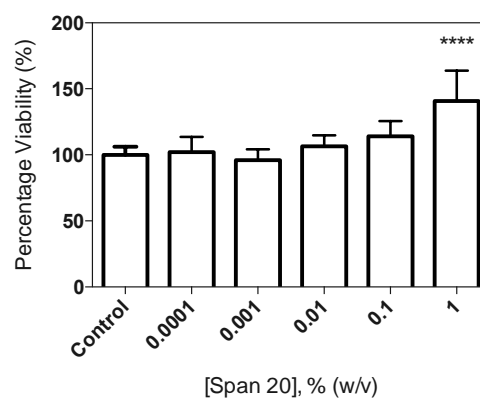
**D**



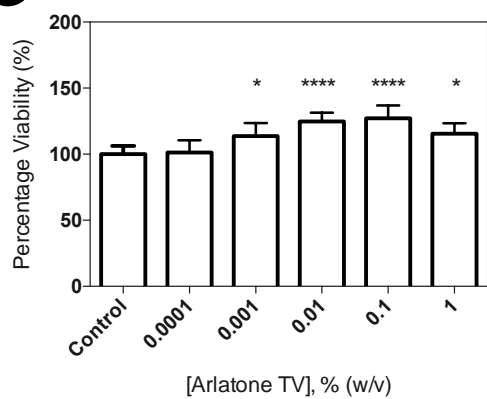
**E**



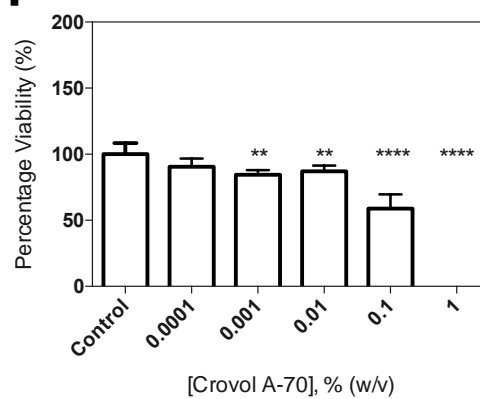
**F**

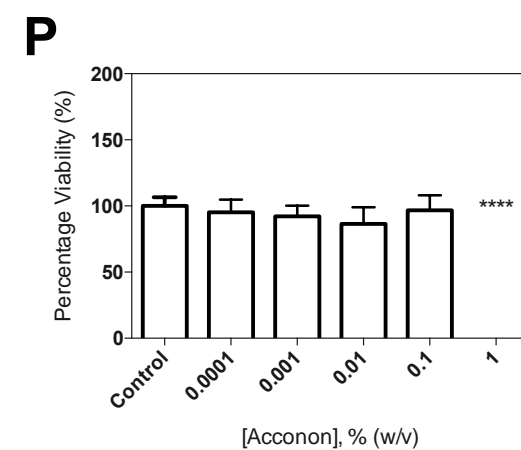
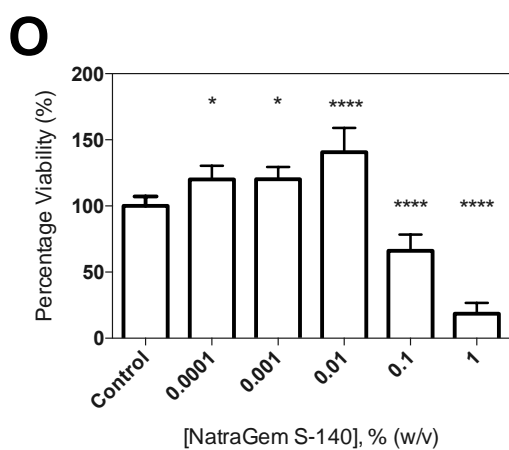
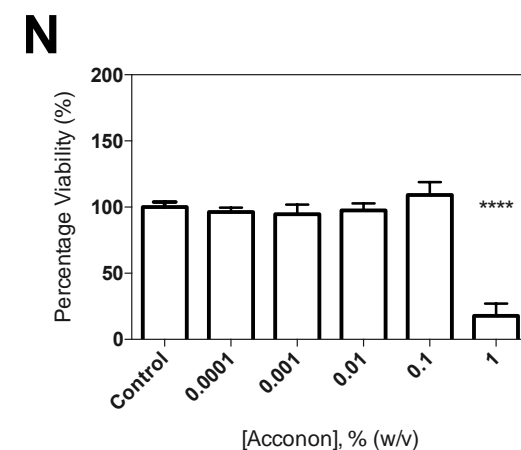
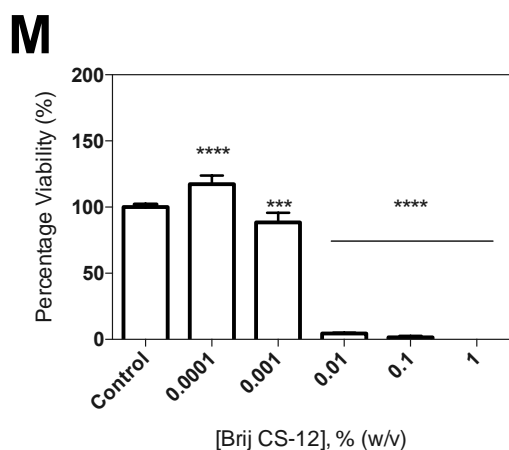
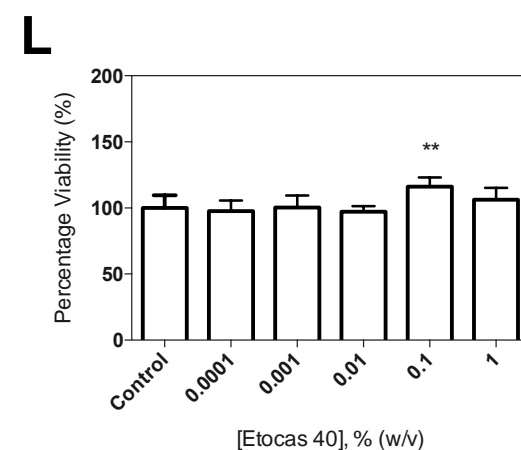
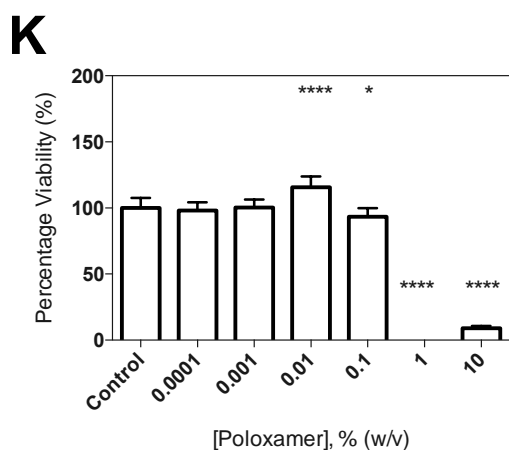
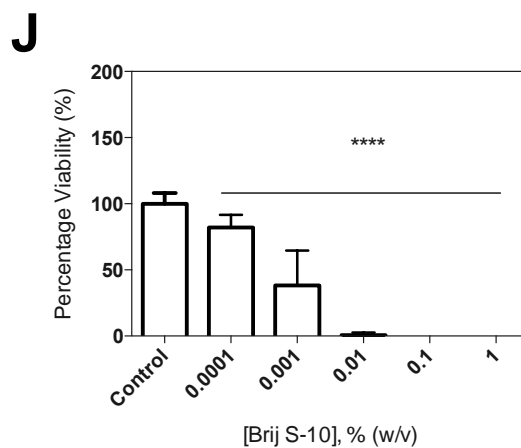
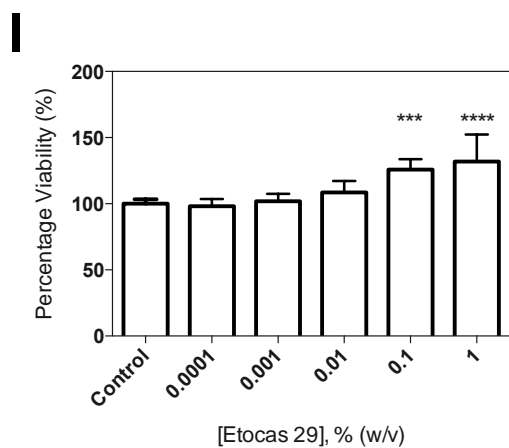


**G**



**H**





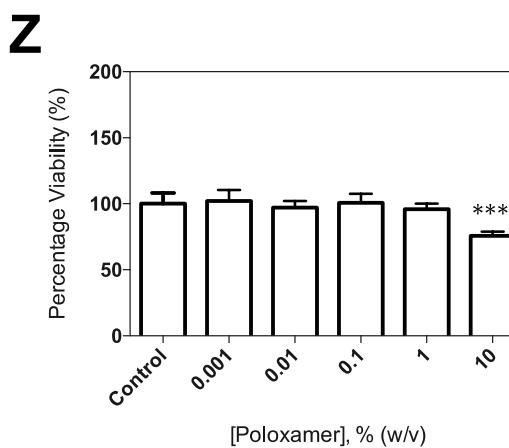
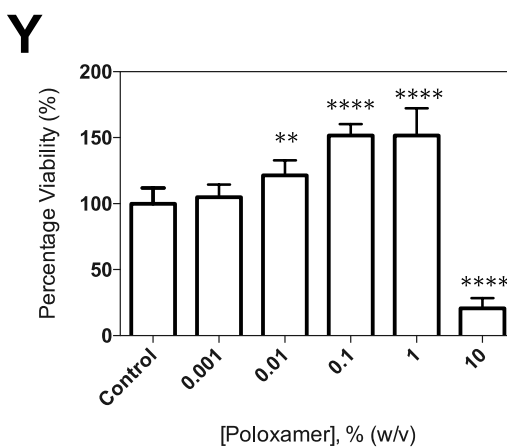
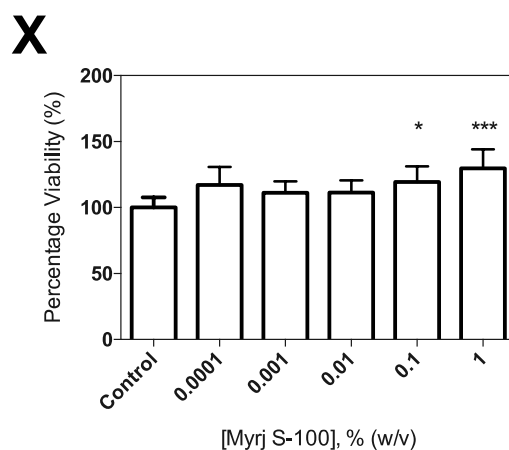
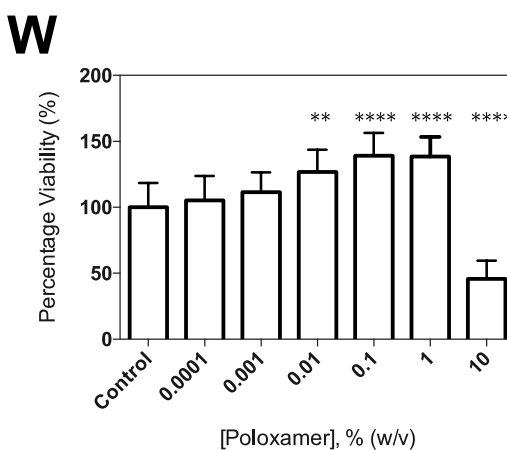
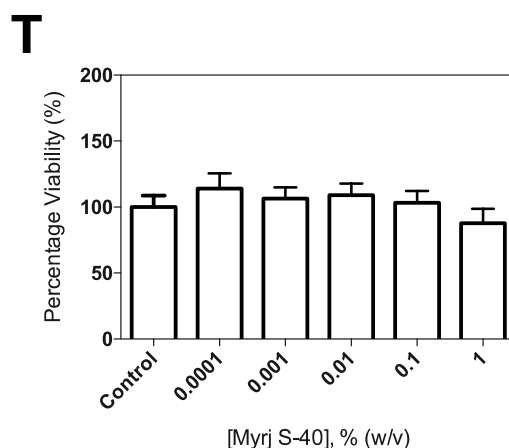
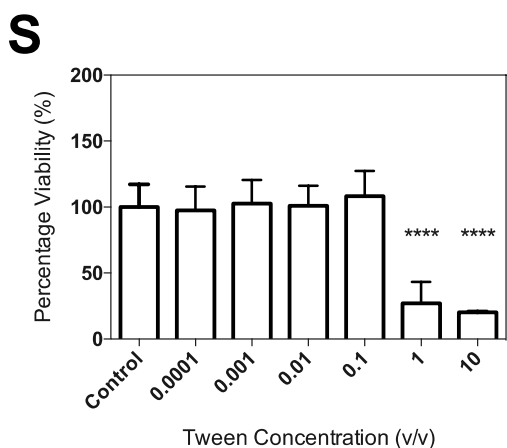
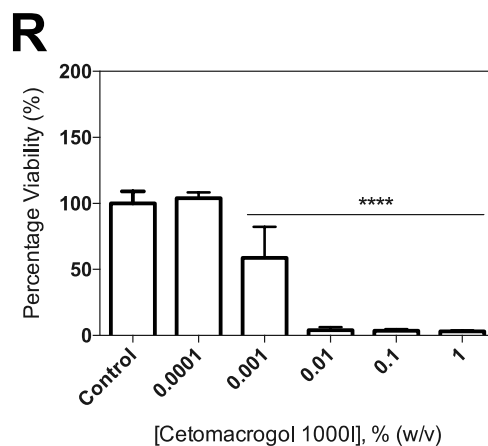
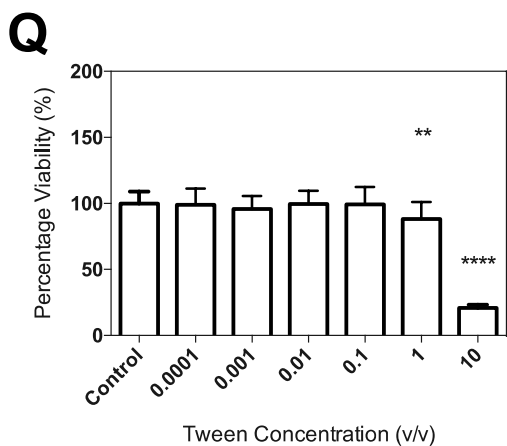


Figure A.1. The effects of the surfactants on cellular viability using the MTT toxicology assay, showing A) Capmul PG-8, B) Capmul MCM, C) Capmul MCM C8, D) Capmul PG-12, E) Poloxamer 182, F) Span 20, G) Arlatone TV, H) Crovol A-70, I) Etocas 29, J) Brij S-10, K) Poloxamer 184, L) Etocas 40, M) Brij CS-12, N) Acconon C-44, O) NatraGem S140, P) Acconon MC8-2, Q) Tween 80, R) Cetomacrogol 1000, S) Tween 20, T) Myrj S-40, W) Poloxamer 335, X) Myrj S-100, Y) Poloxamer 407, Z) Poloxamer 188. Caco-2 cells were grown for 5-7 days on 96-well plates prior to experimentation. Data presented as the mean value of at least 6 replicates  $\pm$  SD. Statistical significance was analysed using one-way ANOVA followed by Dunnett's *post hoc* test with variance as follows: \* ( $p < 0.05$ ); \*\* ( $p < 0.01$ ); \*\*\* ( $p < 0.001$ ); \*\*\*\* ( $p < 0.0001$ ).

---